A proteomic and genomic investigation into the role of lamin A in colorectal cancer cell motility

CLARE RUTH FOSTER

A proteomic and genomic investigation into the role of lamin A in colorectal cancer cell motility - Clare Ruth Foster

Lamins are type V intermediate filament proteins found at the nuclear envelope. Expression of lamin A in colorectal cancer (CRC) tumours is correlated with poor prognosis and expression of lamin A in CRC cell lines promotes greatly increased cell motility. The aim of this study was to identify proteins that promote cell motility in response to lamin A expression and to investigate lamin A regulated changes in gene/protein expression and cytoskeletal organisation that might underpin the increased cell motility.

The effects of lamin A expression were studied using quantitative proteomic and genomic methods using cells from the colorectal cancer cell line SW480 which had been transfected with GFP-lamin A (SW480/lamA) or GFP as a control (SW480/cntl). A biochemical fractionation technique was optimised for the preparation of cytoskeletal fractions which were analysed by 2D DIGE (2D difference in-gel electrophoresis) to reveal accurate and reproducible changes in the representation of proteins within the cytoskeleton in SW480/lamA cells compared to controls. The majority of proteins identified were either components of the actin/intermediate filament cytoskeleton, protein chaperones or translation initiation/elongation factors. Interestingly, tissue transglutaminase 2, a protein which modifies elements of the cytoskeleton and is associated with cancer progression, was highly over-represented in the cytoskeleton fraction of SW480/lamA cells.

Ingenuity Pathway Analysis was used to analyse genome-wide Affymetrix microarray analysis of SW480/cntl and SW480/lamA cell lines. A highly significant interaction network was identified which clustered together genes linked to cancer, cellular movement and cellular growth and proliferation. Epithelial markers such as *CDH1* were down-regulated and mesenchymal markers such as *FN1* were up-regulated in cells expressing GFP-lamin A, which suggested that lamin A over-expression may lead to an epithelial-mesenchymal transition (EMT). As A-type lamins are known to modulate downstream effects of TGFβ signalling, and TGFβ is an inducer of EMT, changes in genes involved in TGFβ signalling were investigated. Knockdown of lamin A using siRNA led to decreased expression of *TGFBI* and *SNAI2* followed by reduced cell motility.

The data suggest that expression of lamin A in CRC cells causes changes in the organisation of the actin cytoskeleton and in TGFβ signalling, potentially involving an epithelial to mesenchymal transition, leading to increased cell motility and an increased risk of death from cancer.

University of Durham

School of Biological and Biomedical Sciences

A proteomic and genomic investigation into the role of lamin A in colorectal cancer cell motility

Clare Ruth Foster

Thesis submitted for the degree of Doctor of Philosophy

February 2012

Table of Contents

Chapter Four - The effects of siRNA knockdown of lamin A on gene and protein expression and cell motility

Chapter Five – General Discussion

Table of Figures

Chapter One

Chapter Two

Chapter Three

Chapter Four

List of Tables

Chapter One

Chapter Two

Chapter Three

Chapter Four

Declaration

I declare that all experiments described herein are my own work and were carried out at the School of Biological and Biomedical Sciences, University of Durham, under the supervision of Professor C. J. Hutchison and Professor S.A. Przyborski. The 2DE and 2D DIGE experiments in Chapter 2 were carried out in conjunction with Miss. J. Robson and Dr. J. W. Simon, Proteomics Facility, University of Durham. The microarray dataset analysis in Chapter 3 was a collaboration with Dr. D. Swan, Newcastle University and the Q-PCR data in Chapter 3 was produced with the help of Miss. D. Battle, University of Durham. This thesis has been composed by myself. No material has been submitted previously for a degree at this or any other university. The copyright of this thesis rests with the author. No quotation from it should be published in any format, including electronic and the internet, without the author's prior written consent. All information derived from this thesis must be acknowledged appropriately.

Clare Foster

List of Publications based on this thesis

Foster, C.R., Przyborski, S.A., Wilson, R.G., and Hutchison, C.J. (2010). Lamins as cancer biomarkers. Biochem Soc Trans *38*, 297-300.

Foster, C.R., Robson, J.L., Simon, W.J., Twigg, J., Cruikshank, D., Wilson, R.G., and Hutchison, C.J. (2011). The role of Lamin A in cytoskeleton organization in colorectal cancer cells: A proteomic investigation. Nucleus *2*, 434-443.

Acknowledgements

I am very grateful for the funding from the J G W Patterson Foundation and the South Tees Hospitals NHS Foundation Trust which supported this study. This thesis is dedicated to the members of my family who have been affected by cancer, particularly Grandad Chivers and Auntie Jen, who died of cancer, and Grandad Parky who is currently fighting cancer.

I would like to thank my supervisor, Prof. Chris Hutchison for giving me the opportunity to study for a PhD and for his support and guidance throughout my studies. There are many different people who have also helped me to complete my PhD. I'd particularly like to thank Pam Ritchie for her invaluable help and expertise, Dr. Tom Cox for teaching me the basics when I first started and Dr. Naomi Willis for her help in the lab and for all the useful discussions about my project. I'd also like to thank Joanne Robson, Dr. Vanja Pekovic, Danni Battle and Dr. Dan Swan for teaching me various different techniques. In addition, I'm very grateful to Dr. Heike Grabsch at Leeds University for allowing me to do a project in her lab during one of my undergraduate vacations, and for giving me the confidence that I could do a PhD.

My husband Jona has been an amazing source of inspiration and encouragement. I'd like to thank him for looking after me so well during the final writing up period and for listening to me talking about lamins every day for the past four years. Special thanks too to Mum and Dad and all my family for the many ways in which they have supported me (and for always asking how my cells are getting on). Lastly, I would like to thank God for giving me strength and perseverance throughout my PhD.

"*From religion comes a man's purpose; from science, his power to achieve it. Sometimes people ask if religion and science are not opposed to one another. They are: in the sense that the thumb and fingers of my hand are opposed to one another. It is an opposition by means of which anything can be grasped."* – Sir William Henry Bragg

List of Abbreviations

µg	Microgram
µl	Microlitre
1D	One-dimensional
2D	Two-dimensional
2D-DIGE	Two-dimensional difference in-gel electrophoresis
2DE	Two-dimensional gel electrophoresis
5-FU	5-fluorouracil
AICR	American Institute for Cancer Research
AJCC	American Joint Committee on Cancer
AR	Amphiregulin
BAF	Barrier to autointegration factor
BCC	Basal cell carcinoma
BMP	Bone morphogenic protein
bp	Base pair
BRB	Blot rinse buffer
BRB/T	Blot Rinse Buffer + Tween-20
BSA	Bovine Serum Albumin
C-	Carboxy terminal
cDNA	Complementary DNA
CEA	Carcinoembryonic antigen
CHAPS	3-[(3-Cholamidopropyl)dimethylammonio]-1-propanesulphonate
CI	Confidence Interval
CIMP	CpG island methylator phenotype
CIN	Chromosomal Instability
CLASSICC	Conventional versus laparoscopic-assisted surgery in CRC
CpG	Cytosine-phosphate-guanine
CRC	Colorectal cancer
CSK	Cytoskeleton
CSK/T	Cytoskeleton buffer/Triton X100
C_T	Cycle threshold
Da	Daltons
ddH_2O	Double distilled water
DFS	Disease-free survival
Dig	Digestion buffer
Dig/Dnase	Digestion buffer/DNase
DMF	Dimethylformamide
DNA	Deoxyribonucleic acid
DNase	Deoxyribonuclease
DTT	Dithiothreitol

ECACC	European Collection of Cell Cultures
ECL	Enhanced Chemiluminescence
ECM	Extracellular matrix
EDTA	Ethylenediamine tetraacetic acid
EF-1γ	Eukaryotic translation elongation factor 1 gamma
EF-1δ	Eukaryotic translation elongation factor 1 delta
EF-Tu	Tu translation elongation factor, mitochondrial
EGFP	Enhanced Green Fluorescent Protein
EGFR	Epidermal Growth Factor Receptor
EGTA	Ethylene glycol tetraacetic acid
eIF2	Eukaryotic translation initiation factor 2
eIF2α	Eukaryotic translation initiation factor 2, subunit 1 alpha, 35kDa
eIF5A	Eukaryotic translation initiation factor 5A
EMT	Epithelial-mesenchymal transition
EPI	Epiregulin
ER	Endoplasmic reticulum
Ext	Extraction buffer
FAP	Familial Adenomatous Polyposis
FBS	Foetal Bovine Serum
FOBt	Faecal Occult Blood test
GCRMA	Guanine Cytosine Robust Multi-Array Analysis
GFP	Green Fluorescent Protein
GI	Gastrointestinal
GOI	Gene of interest
GTP	Guanosine triphosphate
HCC	Hepatocellular carcinoma
HCl	Hydrochloric Acid
HG U133	Human Genome U133 Genechip [Affymetrix]
HNPCC	Hereditary Non-polyposis Colorectal Cancer
HR	Hazard Ratio
HRP	Horseradish Peroxidase
Hsp	Heat shock protein
HUVEC	Human umbilical vein endothelial cells
IEF	Isoelectric focusing
IF	Intermediate Filament
iFOBt	Immunochemical Faecal Occult Blood test
INM	Inner Nuclear Membrane
IPA	Ingenuity Pathways Analysis
IPG	Immobilised pH gradient
KASH	Klarsicht/ANC-1/Syne homology
kb	Kilobase

kDa	Kilodalton
L-15	Leibovitz growth medium
LAP	Lamina Associated Polypeptide
LCC	Left-sided colon cancer
LEF	Lymphoid enhancer factor
LEM	LAP2, Emerin, MAN1
LINC	Linker of nucleoskeleton and cytoskeleton
LOH	Loss of Heterozygosity
M	Molar
mA	Milliamps
MAC	Modified Astler Coller system
MALDI-ToF-ToF	Matrix-assisted laser-desorption/ionization time-of-flight/time-of-flight
MAP	Mitogen-activated protein
MEF	Mouse embryonic fibroblasts
mg	Milligram
MIN	Microsatellite instability
ml	Millilitre
mM	Millimolar
MM	Mismatch
MMR	Mismatch Repair
MOWSE	Molecular Weight Search
MRC	Medical Research Council
mRNA	Messenger RNA
MS	Mass spectrometry
MSI	Microsatellite Instability
MTOC	Microtubule organising centre
N-	Amino terminal
N/CSK	Nucleo-/Cyto-skeleton
NCS	Newborn Calf Serum
NE	Nuclear Envelope
NEM	N-ethylmaleimide
NET	Nuclear envelope transmembrane protein
NHS	National Health Service
NLCS	Netherlands Cohort Study on Diet and Cancer
NLS	Nuclear Localisation Signal
NPC	Nuclear Pore Complex
NSAID	Non-steroidal anti-inflammatory drug
ONM	Outer nuclear membrane
OS	Overall survival
PBS	Phosphate Buffered Saline
PCR	Polymerase Chain Reaction

pI	Isoelectric point
PIPES	Piperazine-N,N'-bis(2-ethanesulphonic acid)
PM	Perfect Match
pRb	Retinoblastoma protein
Q-PCR	Quantitative Real-Time Polymerase Chain Reaction
RCC	Right-sided colon cancer
RHAMM	Receptor for hyaluronan mediated motility
RNA	Ribonucleic acid
RNase	Ribonuclease
rpm	Revolutions per minute
R-SMAD	Receptor-regulated SMAD
RT	Room temperature
SCC	Squamous cell carcinoma
SDS	Sodium Dodecyl Sulphate
SDS-PAGE	Sodium Dodecyl Sulphate - Polyacrylamide Gel Electrophoresis
SE	Standard error of the mean
SILAC	Stable isotope labelling with amino acids in cell culture
siRNA	Small interfering ribonucleic acid
SMAD	Mothers against decapentaplegic homologue
SUN	Sad1/UNC-84 homology
TCF	T cell factor
TEMED	N,N,N',N'-Tetramethylethylenediamine
TG2	Transglutaminase 2
TGFβ	Transforming growth factor, beta
TGFBI	Transforming growth factor, beta - induced
TGST	Testicular germ cell tumour
T_m	Melting temperature
TNM	Tumour-Node-Metastasis
TOF	Time of flight
TSG	Tumour suppressor gene
V	Volts
v/v	Volume/volume
Vh	Volt hours
w/v	Weight/volume
WCRF	World Cancer Research Fund

CHAPTER ONE
Introduction

1.1. Colorectal cancer

The word cancer originated with the Greek physician Hippocrates (460-370BC), who referred to tumours as *karkinos*, the Greek word for crab, which translates into Latin as *cancer*. Hippocrates believed that cancer was caused by an excess of black bile, and this belief was commonplace for over a thousand years. It was subsequently thought that cancer was caused by abnormalities in the lymphatic system, chromic irritation or trauma. In the past century there have been vast improvements in our knowledge of tumour development, which we now understand involves a series of genetic changes causing a normal cell to become cancerous. In their seminal paper, Hanahan and Weinberg described the six hallmarks of cancer that describe the properties of most, if not all, malignant cells: self-sufficiency in growth signals, insensitivity to anti-growth signals, tissue invasion and metastasis, limitless replicative potential, sustained angiogenesis and the evasion of apoptosis (Hanahan and Weinberg, 2000). In 2011, Hanahan and Weinberg added two further hallmarks to this list: the preprogramming of energy metabolism and the evasion of immune destruction (Hanahan and Weinberg, 2011).

Worldwide, the most commonly diagnosed cancers are lung cancer (1.61 million cases), breast cancer (1.38 million cases) and colorectal cancer (CRC) (1.23 million cases) (Ferlay et al., 2010b). CRC is the second most common cancer in females and the third most common cancer in males. Men are more likely to develop CRC than women; the overall sex ratio of the age standardised rates is 1.4:1 (Ferlay et al., 2010b). Incidence rates vary in different countries, with 60% of CRC occurring in developed regions, and countries that have experienced a rise in prosperity, such as Japan, have shown increased rates of CRC (Key, 2002). The highest rates of CRC are in Western Europe and Australia/New Zealand, and the lowest rates are in Africa (excluding Southern Africa) and South-Central Asia (Figure 1.1) (Ferlay et al., 2010b).

CRC is the fourth most common cause of cancer deaths worldwide. Mortality rates are generally lower in women compared to men and are highest in Central and Eastern Europe (20.3 per 100,000 males and 12.1 per 100,000 females) and lowest in Middle Africa (3.5 per 100,000 males and 2.7 per 100,000 females) (Ferlay et al., 2010b). In the UK, deaths from

CRC decreased between 1995-2008 from 27.5 to 21.9 per 100,000 population in men and 18.8 to 14.4 per 100,000 population in women (Bray et al., 2002; Ferlay et al., 2010a). 5 year survival in England increased from 44.8% (males) and 46.6% (females) in 1990-1994 to 51.8% (males and females combined) in 2000-2002 (Sant et al., 2003; Verdecchia et al., 2007). The increased survival rates are thought to be due to improvements in treatment, diagnosis and knowledge of cancer genetics (Sant et al., 2003; Schurer and Kanavos, 2010; Sengupta et al., 2008). Rates of CRC survival vary across England, with a 6% difference between areas with the highest and lowest 5 year survival rates, compared to only a 3% range for breast cancer, which may be due to differences in service delivery, stage at diagnosis, communication issues or cultural differences (Charatan, 2004).

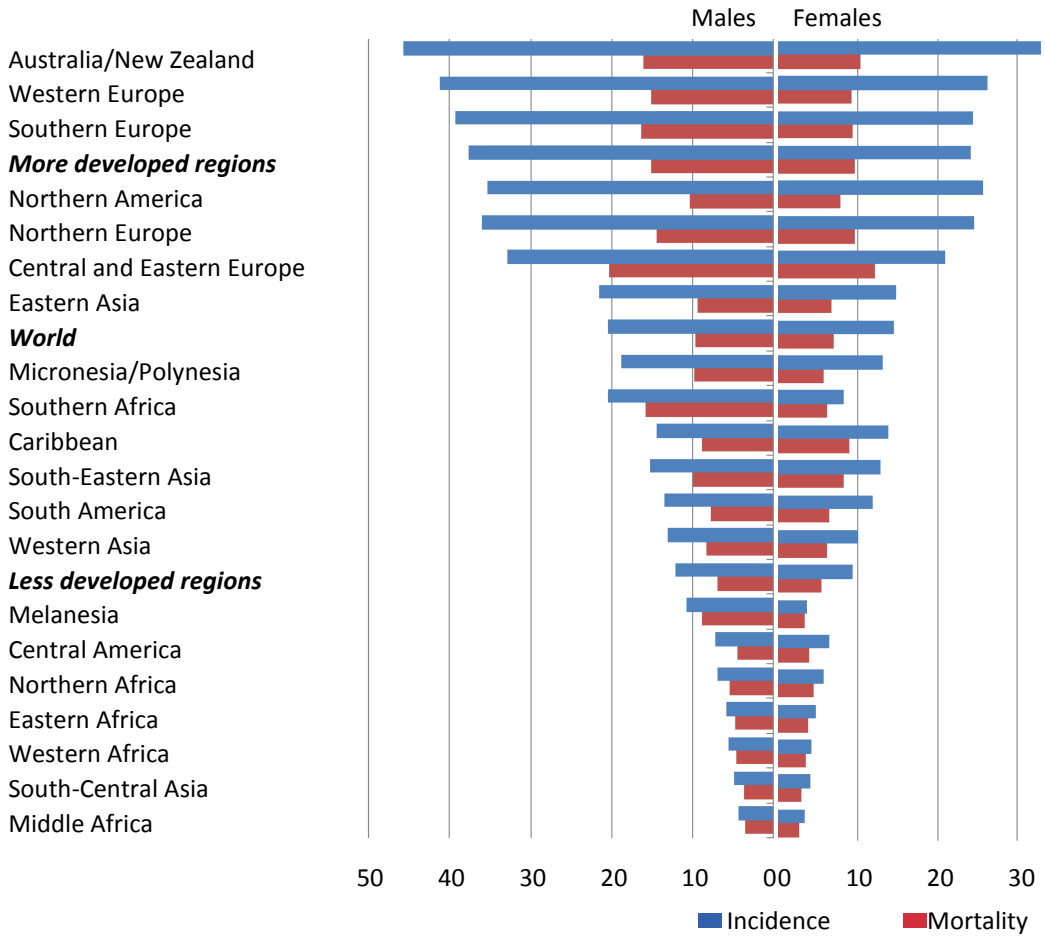

Figure 1.1: Estimated age-standardised incidence and mortality rates (per 100,000 population) for CRC (adapted from Ferlay et al., 2010b)

1.1.1. Hereditary CRC

CRC exists in a sporadic form and in inherited forms such as familial adenomatous polyposis (FAP), hereditary nonpolyposis CRC (HNPCC) and hamartomatous polyposis syndromes. Sporadic CRC accounts for approximately 75% of all CRC cases and mostly arises in those

aged 60 years or above as it is the result of accumulation of genetic alterations. Young-onset CRC is usually linked to familial syndromes and genetic predisposition. The lifetime risk of those over 50 with no personal or family history of CRC is 5-6%; in those with first/second degree relatives with CRC, this can increase to 20%; and in those with hereditary CRC syndromes the lifetime risk is 80-100% (Rustgi, 2007).

HNPCC, also known as Lynch syndrome, is an autosomal dominant condition which causes 2-5% of CRCs and is a genetically heterogeneous disease (Fearon, 2011). Patients have germline mutations in DNA mismatch repair (MMR) genes, with the majority of known HNPCC mutations being found in the genes *MSH2* and *MLH1.* Tumours from HNPCC patients also often contain alterations in microsatellite sequences, a condition known as microsatellite instability (MSI). There is a more rapid transition from adenomatous lesion to carcinoma compared to sporadic cancers, as affected cells accumulate mutations swiftly due to the impaired DNA repair mechanism. HNPCC patients have an 80% lifetime risk of developing CRC, and have often developed tumours by the age of 40. HNPCC also increases the risk of other cancers such as gastric, ovarian, endometrial, renal and hepatobiliary cancers.

FAP is also an autosomal dominant syndrome which causes 0.5-1% of CRCs and affects approximately 1 in 10,000 births (Fearon, 2011; Lipton and Tomlinson, 2006; Rustgi, 2007). Germline mutations in *APC*, typically frameshift or nonsense mutations, lead to premature truncation of protein synthesis. FAP is characterised by hundreds to thousands of adenomas in the colon and rectum which usually start to appear in the patient's second decade of life. It is almost certain that one of the polyps will transform into CRC by the time the patient reaches the age of 40. Hence, endoscopic screening from the age of 10 is recommended, and typical treatment for FAP involves the removal of the colon.

Other conditions which increase CRC risk include hamartomatous polyposis syndromes, comprising a number of different syndromes which predispose the patient to developing hamartomatous polyps, ulcerative colitis and Crohn's disease.

1.1.2. Risk Factors

Many cases of CRC are caused by environmental factors, and incidence rates could decrease if changes were made to diet and lifestyle (WCRF/AICR, 2007). A recent World Cancer Research Fund/American Institute for Cancer Research (WCRF/AICR) continuous update report examined the effects of diet and physical activity on CRC risk, based on a systematic

review of over 1000 papers (Norat, 2010; WCRF/AICR, 2011). They reported that there is 'convincing' evidence that regular physical activity and consumption of food containing dietary fibre decrease the risk of colon cancer, and that consumption of red and processed meat, excess body fatness, abdominal fatness and the factors that lead to greater adult attained height, or its consequences, increase the risk of CRC (Norat, 2010; WCRF/AICR, 2011). The evidence also showed that it was 'probable' that foods containing garlic, milk and calcium decrease the risk of CRC.

1.1.2.1. Factors that decrease the risk of CRC

There is strong evidence that physical activity reduces the risk of colon cancer, however there is no conclusive evidence for an effect of physical activity on rectal cancer (Norat, 2010; WCRF/AICR, 2011). The mechanisms by which physical activity decreases the risk of colon cancer are currently unknown. However, several ideas have been suggested, involving gut transit time, immune function, chronic inflammation, levels of insulin and insulin-like growth factors, genetics and obesity (Harriss et al., 2007).

The finding that fibre intake decreases CRC risk was first shown in the 1970s (Burkitt, 1971). There are a number of theories which may explain the protective effect of dietary fibre. It is thought that the physical properties of fibre may be important including its absorption of water as it passes through the digestive system. Also, the fermentation of fibre by the colonic microflora can produce butyrate, which is known to stimulate apoptosis (Avivi-Green et al., 2000; Hague et al., 1993).

It is probable that consumption of foods containing garlic reduces the risk of CRC (Norat, 2010; WCRF/AICR, 2011). Garlic contains allyl sulphur compounds, which can protect against cancer via a number of different mechanisms, including inhibition of carcinogen-induced DNA adduct formation, blocking cellular growth, proliferation and angiogenesis, inducing differentiation and apoptosis and enhancing carcinogen-detoxifying enzymes (Ngo et al., 2007). Garlic also contains kaempferol, selenium, vitamins A and C, arginine and fructooligosaccharides which protect against cancer (Ngo et al., 2007). It is also probable that milk and calcium consumption reduces the risk of CRC (Norat, 2010; WCRF/AICR, 2011). Calcium sequesters CRC-promoting bile acids in the colon and can induce differentiation, increase apoptosis and decrease proliferation of epithelial cells (Bernstein et al., 2005; Lupton et al., 1996; Whitfield et al., 1995).

Other factors which may reduce the risk of CRC include non-steroidal anti-inflammatory drugs (NSAIDs), hormone replacement therapy and estrogen.

1.1.2.2. Factors that increase the risk of CRC

There are many potential CRC risk factors including consumption of red/processed meat and alcohol, body and abdominal fatness, adult attained height, smoking, infectious agents, radiation, industrial chemicals, some medications and unsaturated fat. Some of the risk factors with the most convincing evidence are discussed below.

There are several mechanisms by which consumption of red and processed meat may lead to CRC. High temperatures used during cooking of meat can result in the formation of heterocyclic amines, which are potent carcinogens (Sugimura et al., 2004). Processed meat, often defined as meat preserved by smoking, curing, salting or adding preservatives, often contains large amounts of salt, nitrite and nitrates. Degradation products of amino acids can react with nitrite and nitrate, forming *N*-nitroso compounds. Haem iron in the diet can also increase the amount of carcinogenic *N*-nitroso compounds and can lead to the production of free radicals (Cross et al., 2003; Nelson, 2001).

High body and abdominal fatness increase the risk of CRC. Body fatness is commonly measured using the body mass index (BMI), however this is a crude measure of obesity and the pattern of fat distribution is thought to be more important in some circumstances. Abdominal fatness, measured by the waist circumference and/or waist to hip ratio, in particular increases insulin resistance (Despres, 1993), which can lead to increased insulin production and an increased risk of colon cancer (Trevisan et al., 2001). Obesity in general stimulates the inflammatory response which can lead to cancer, as the adipose tissue of obese individuals recruits macrophages, which secrete pro-inflammatory signal molecules and cytokines (Fantuzzi, 2005).

Adult attained height is associated with risk of several different cancers, with taller people being at increased risk (Gunnell et al., 2001). Height may act as a biomarker for another exposure, since it is dependent on many factors, including genetic influences, childhood diet/health/mental well being, the timing of puberty, circulating hormone levels and prenatal environmental factors (Gunnell et al., 2001). Height may also affect cancer risk as it is possible that the larger the number of cells in a body, the higher the chance of malignant transformation (Albanes and Winick, 1988).

There is also convincing evidence that consumption of alcohol increases risk of CRC in males, and it probably also increases risk in females (Norat, 2010; WCRF/AICR, 2011). This may be due to higher alcohol consumption in men compared to women, differences in choices of drink, hormone-related differences in alcohol metabolism or susceptibility to alcohol. Ethanol is carcinogenic as it can inhibit DNA methylation, interact with retinoid metabolites and produce toxic metabolites such as acetaldehyde (Seitz and Stickel, 2007).

The link between smoking and lung cancer is well known. An association between CRC and smoking has been disputed, but a recent systematic review showed that both past and current smokers have increased risk of CRC (Liang et al., 2009). Cigarette smoke contains at least 80 mutagenic carcinogens and is a source of oxidative stress. Smoking can increase tumour growth by inducing angiogenesis and suppressing cell-mediated immunity (O'Byrne et al., 2000).

1.1.3. Anatomy of the colon and rectum

The colon is about 150cm long and it absorbs water and salts and propels unabsorbed faecal waste towards the rectum. It is divided into several different segments (Figure 1.2). The rectum is the terminal portion of the large intestine and serves as a temporary storage site for faeces. It is approximately 15 cm long.

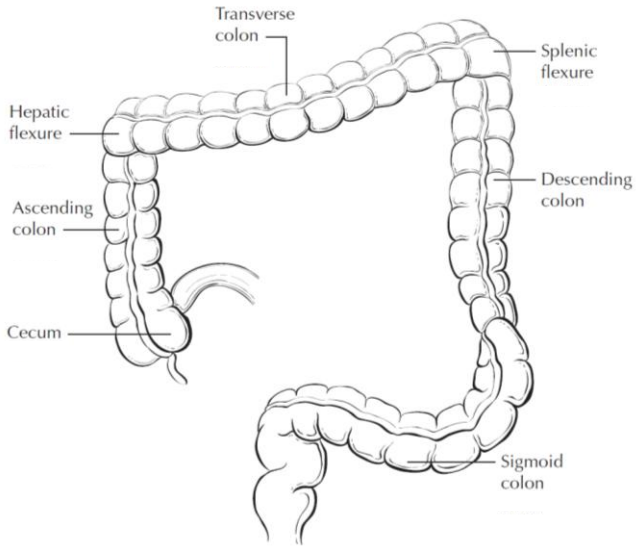

Figure 1.2: Anatomic subsites of the colon (Greene, 2002)

Cancers arising on the left and the right side of the colon have different biological and clinical properties (Benedix et al., 2010; Bufill, 1990). Right sided tumours arise proximal to the splenic flexure (caecum, ascending colon, transverse colon), and left sided tumours originate distal to the splenic flexure (descending colon, sigmoid colon, rectum) (Figure 1.2).

Since the 1980s, the percentage of right-sided colon cancers (RCC) has been increasing, and the percentage of left-sided (LCC) and sigmoid colon cancers has been decreasing (Jass, 1991; Levi et al., 1993; Meguid et al., 2008; Obrand and Gordon, 1998). The reason for this change is not known, although hypotheses include the effects of changes in screening, genetic/environmental epidemiology and an increasingly elderly population (Meguid et al., 2008). RCCs are more common in women than in men, can cause pain, bleeding and anaemia and have a worse prognosis than LCCs (Benedix et al., 2010; Meguid et al., 2008).

The intestinal wall comprises several layers (Figure 1.3): the mucosa (a simple columnar epithelium which forms millions of crypts), lamina propria (the basement membrane), muscularis mucosa (a thin layer of smooth muscle), submucosa (loose connective tissue), muscularis propria (containing circular and longitudinal smooth muscle), subserosa and serosa.

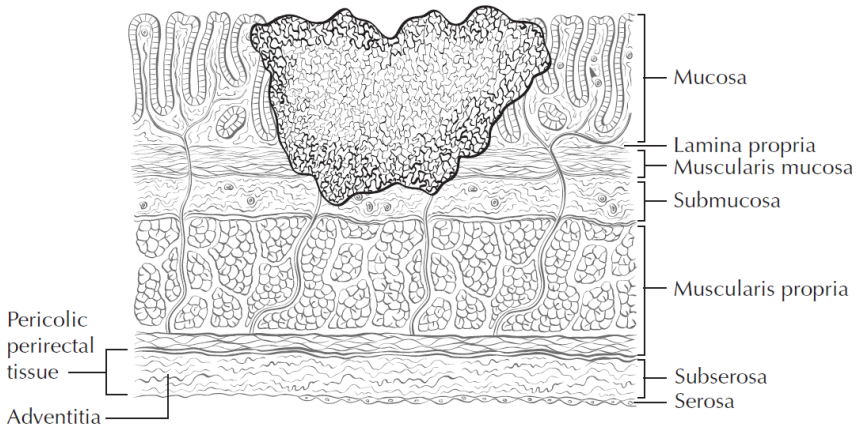

Figure 1.3: Layers of the colon showing a tumour invading the submucosa (Greene, 2002)

The mucosa consists of millions of crypts comprising goblet cells, columnar cells, endocrine cells and undifferentiated stem cells. Stem cells reside at the bottom of the crypt, where they can communicate with pericryptal myofibroblasts which are niche cells adjacent to the crypt (Figure 1.4). The stem cells are interspersed with $CD24^{+}$ cells, thought to be the colonic equivalent of Paneth cells in the small intestine, which express signals needed for stem cell maintenance in culture (Sato et al., 2011). Slightly higher up the crypt are the transit amplifying cells and committed progenitor cells. Cells undergo differentiation as they migrate from the base of the crypt towards the lumen. Epithelial cell turnover is rapid, and differentiated cells are shed at the surface of the colon.

Over 95% of CRCs are adenocarcinomas, which originate in the mucosa, usually from benign growths or adenoma. Types of adenocarcinomas include mucinous tumours and signet ring

tumours, which are relatively rare. Other types of CRC including carcinoids, sarcomas and lymphomas are rarer and are treated differently to adenocarcinomas and squamous cells cancers. CRC as discussed in this thesis refers to adenocarcinomas.

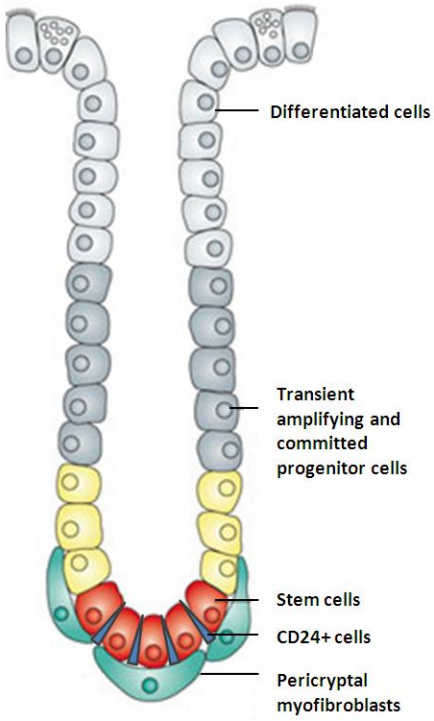

Figure 1.4: Anatomy of the colon crypt (adapted from Gatenby et al., 2010) – Stem cells and CD24+ cells at the base of the colonic crypt and differentiated cells at the top of the crypt are separated by transient amplifying/committed progenitor cells.

1.1.4. Carcinogenesis

In cancer, gene defects are either found in oncogenes, leading to increased or novel gene functions, or in tumour suppressor genes (TSGs), leading to loss of gene function. Both alleles of a TSG must be mutated for the gene to lose function – this is known as the two hit hypothesis (Knudson, 1971). Gene defects are found in many types of inherited and sporadic CRCs, although no germline oncogenic mutations have so far been discovered. Mutations in a small number of TSGs are found in many CRC cases.

Carcinogenesis in the colon occurs when the balance between proliferation, differentiation, migration and apoptosis is lost, leading to hyperproliferation. Genetic alterations leading to CRC arise incrementally and occur stochastically, but accumulate in a non-random order. The classic model of colon cancer (Figure 1.5) shows a stepwise progression from adenoma to carcinoma (Fearon and Vogelstein, 1990).

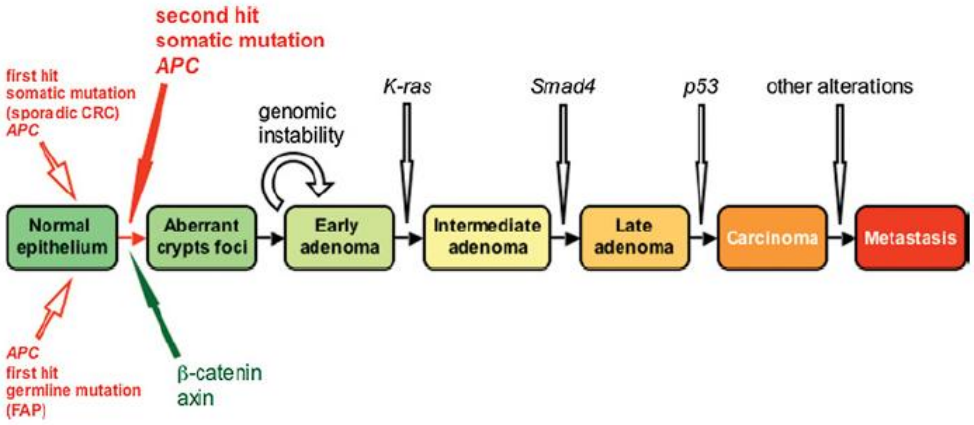

Figure 1.5: Genetic model of colorectal carcinogenesis, adapted from Fearon and Vogelstein, 1990 (Pinto and Clevers, 2005) - Stepwise progression of CRC requires mutations in Wnt signalling pathway components for tumour initiation. Epigenetic events and mutations in genes such as *K-ras* and *Smad4* are required for progression towards malignancy.

The type of cells from which CRCs arise is still disputed. Some favour a 'top down' model in which tumours arise from dysplastic cells on the surface of the crypt and grow down into the crypt (Shih et al., 2001), whereas others prefer a 'bottom up' model in which tumours start in the stem cells at the base of the crypt (Preston et al., 2003). The presence of cancer stem cells (CSCs) has been reported in several subtypes of cancer, including colon (O'Brien et al., 2007), breast (Al-Hajj et al., 2003) and brain (Singh et al., 2004). The CSC model describes a hierarchical system in which only a small population of cancer cells, namely the CSCs, are able to initiate and maintain tumour growth. This contrasts with the stochastic theory in which every cancer cell is capable of initiating a tumour (Dick, 2003). CSCs maintain their aggressive properties as they are capable of self-renewal and differentiation (Dick, 2003).

The classic model of CRC suggests that there are two main molecular pathways in CRC: chromosomal instability (CIN) and microsatellite instability (MIN), which have different pathological features. These pathways are also known as the 'gatekeeper' (CIN) and the 'caretaker' (MIN) pathways (Kinzler and Vogelstein, 1996). CIN/gatekeeper pathway cancers account for most sporadic and FAP CRCs. The tumours contain chromosomal abnormalities including aneuploidy, inactivation of tumour suppressor genes (TSG) and loss of heterozygosity (LOH). This pathway features the disruption of genes that encode proteins which regulate growth such as *APC*, *p53* and *KRAS.* MIN is involved in around 10-15% of sporadic CRCs and in most HNPCC cancers. These cancers demonstrate genetic or epigenetic abnormalities in DNA mismatch repair genes such as *MMR* genes. Alongside

mutations of the genes in the CIN pathway, mutations are found in genes such as *TGFβIIR*, *IGF2R* and *BAX* (Weitz et al., 2005).

Some CRCs exhibit epigenetic changes, in addition to or instead of genetic abnormalities. An important epigenetic mechanism for CRC is widespread CpG island methylation, known as the CpG island methylator phenotype (CIMP) which involves hypermethylation of many tumour suppressor genes such as the MMR gene *MLH1* (Curtin et al., 2011; Toyota, 1999). CIMP occurs in around 20-40% of CRCs and most cases of sporadic MIN feature CIMP silencing of *MLH1* (Toyota, 1999).

Vogelstein's classic model of colon cancer (Figure 1.5) has been recently revised (Issa, 2008) to account for epigenetic changes and the finding that some CRCs exhibit neither CIN nor MIN (Georgiades et al., 1999). The new model (Figure 1.6) comprises three distinct pathways which display different clinicopathological features.

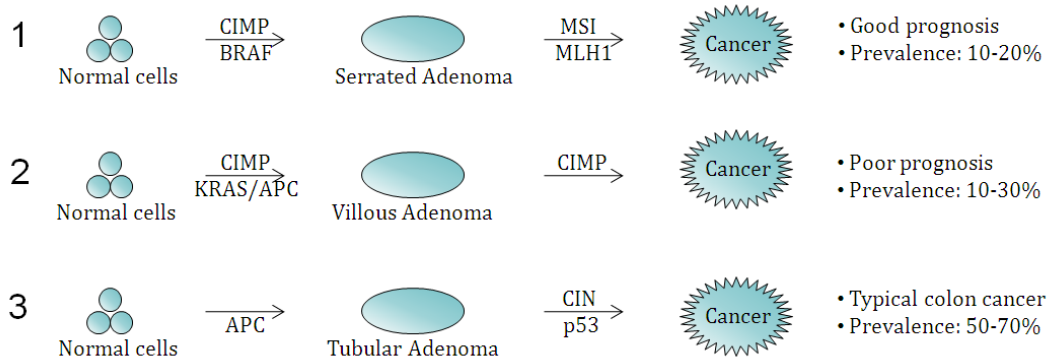

Figure 1.6: Multiple pathways to CRC – adapted from Issa, 2008 - Sporadic CRC arises from at least three separate pathways. Pathway 2 is very heterogeneous and may arise from serrated as well as villous adenomas. It is not known whether or not the different pathways can originate in identical cells.

Cancers arising from different pathways exhibit different prognoses and different responses to treatment. MSI tumours with no *BRAF* mutations have good prognoses whereas CIMP tumours with no MSI have poor prognoses (Issa, 2008). In the future, it may be possible to have a system of personalised therapy based on the molecular profile of the tumour; however the methods of detection of genetic/epigenetic alterations will have to be vastly improved before this can become a reality.

1.1.4.1. APC and the canonical Wnt signalling pathway

After the discovery that germline mutations in *APC* lead to FAP (Groden et al., 1991; Kinzler et al., 1991), somatic mutations in *APC* were shown to occur often in sporadic CRC (Powell

et al., 1992). 70-80% of sporadic CRCs contain inactivating *APC* mutations, most of which cause premature truncation of the APC protein. *APC* mutations are an early event in adenoma development (Powell et al., 1992). Mutations in other Wnt pathway components, such as *CTNNB1* (encoding β-catenin) (Sparks et al., 1998), *AXIN1 and AXIN2* (Salahshor and Woodgett, 2005) and *TCF4* (Fukushima et al., 2001), are sometimes found in CRCs which lack APC mutations.

APC is a negative regulator of Wnt signalling, as it can regulate the intracellular levels of β-catenin (Munemitsu et al., 1995). In the absence of Wnt signalling, APC binds the scaffold protein Axin, promoting phosphorylation of β-catenin by casein kinase 1 and GSK3β. This targets β-catenin for ubiquitination and proteosomal degradation.

In the canonical Wnt signalling pathway, when Wnt ligands are present, they interact with Frizzled and LRP5/6 co-receptor, inhibiting GSK3β and Axin. The APC-Axin complex is therefore disrupted and β-catenin cannot be marked for destruction. β-catenin then enters the nucleus, where is interacts with TCF/LEF transcription factors. This allows expression of Wnt target genes such as the proto-oncogenes *CMYC* and *cyclin D1*, growth factors such as *FGF9* and *FGF20* and Wnt pathway feedback regulators such as *AXIN2* and *Dickkopf-1*. When *APC* is inactivated in cancer, β-catenin is no longer targeted for destruction, mimicking the constitutive activation of Wnt signalling. β-catenin can then complex with TCF/LEF transcription factors, turning on expression of Wnt target genes.

Wnt/β-catenin signalling controls homeostasis of the crypt axis in the colon (Batlle et al., 2002; van de Wetering et al., 2002). The TCF-4/β-catenin complex functions as a switch controlling proliferation versus differentiation. Proliferating crypt cells in normal tissue express genes known to be TCF-4/β-catenin target genes in CRC cells, whereas normal differentiated cells express genes repressed by TCF-4/β-catenin. There is also a gradient of β-catenin expression in the nucleus, which is low in cells at the base of the crypt, and high in cells at the top of the crypt (van de Wetering et al., 2002).

1.1.4.2. Other genes involved in CRC carcinogenesis

In a typical cancer it is thought that there are approximately 80 DNA mutations that alter amino acids, fewer than fifteen of which are likely to drive the initiation, progression or maintenance of the tumour (Wood et al., 2007). There are a small number of genes which are commonly mutated in CRC, known as ‘gene mountains’ and a much larger number of

genes which are mutated in a small proportion of tumours, known as 'gene hills'. Here, I discuss the genes which are most commonly mutated in CRC.

KRAS, which encodes a member of the Ras family of small G proteins, is mutated in many cancers. Somatic mutations in *KRAS* are found in approximately 40% of CRCs and occur later in the development of CRCs than *APC* mutations (Fearon, 2011). Around 10% of <1cm adenomas contain *KRAS* mutations, compared to 50-60% of >1cm adenomas (Vogelstein et al., 1988). Somatic mutations in *PIK3CA*, the gene encoding the catalytic p110α subunit of PI3K, are found in 15-30% of CRCs (Samuels et al., 2004; Wood et al., 2007), leading to activation of *PIK3CA* activity (Carson et al., 2008). 20% of CRCs have somatic mutations inactivating *FBXW7*, a gene which encodes an F-box protein which regulates levels of cyclin E, c-Myc, c-Jun and Notch (Tan et al., 2008). This may therefore result in aberrant regulation of many different oncogenic proteins and pathways.

p53 regulates genes which encode proteins with roles in promoting apoptosis, regulating cell cycle checkpoints and restricting angiogenesis. 75% of CRCs show LOH at 17p, the location of the p53 gene (Vogelstein et al., 1988). In the majority of tumours with 17p LOH, the other p53 allele is somatically mutated. Most p53 mutations are missense mutations, and some are nonsense and frameshift mutations (Fearon, 2011). As most adenomas lack mutations in p53 or 17p LOH, loss of p53 function is thought to be a late development in the adenoma-carcinoma transition (Baker et al., 1990).

Other somatic mutations affect components of the TGFβ pathway. Over 70% of CRCs have LOH of 18q, which contains the genes for SMAD2 and SMAD4 (Vogelstein et al., 1988). 10-15% of CRCs contain inactivating mutations in *SMAD4*, 5% of CRCs contain mutations in *SMAD2* and 5% contain mutations in *SMAD3* (Fearon, 2011; Wood et al., 2007). 25% of CRCs and more than 90% of MSI-high CRCs contain an inactivating mutation in *TGFβIIR*, which encodes the TGFβ type II receptor (Markowitz et al., 1995).

1.1.5. Screening

The aim of CRC screening is to detect cancer at an early stage when treatment is most effective. National screening programmes were introduced in England and Scotland between 2007 and 2010. Currently, individuals in England aged 60-74 and in Scotland aged 50-74 are invited to take a Faecal Occult Blood test (FOBt) every two years, and people aged 75+ can request a test kit. The FOBt is able to detect small amounts of blood in the stool. If the test is positive, patients are invited for further investigation, usually a colonoscopy. A

colonoscopy is used to diagnose CRC and polyps, which if present can be removed for further testing. The NHS is currently reviewing the evidence for the immunochemical FOBt (iFOBt), which can quantify the amount of blood present in a sample, and only identifies blood from the bowel.

FOB screening is known to reduce the risk of dying from CRC (Scholefield et al., 2002) and a systematic review of four randomised control trials (Hardcastle et al., 1996; Kewenter et al., 1994; Kronborg et al., 1996; Mandel et al., 1993), showed a 16% reduction in CRC mortality in populations offered screening and a 23% reduction in those actually screened (Towler et al., 1998).

In April 2011, it was announced that the NHS bowel cancer screening programme would introduce flexible sigmoidoscopy screening over the next few years for those aged 55 and over. This procedure involves a visual examination of the rectum and sigmoid colon, in which two-thirds of CRC are located, using an endoscope. A recent study showed that flexible sigmoidoscopy screening reduces CRC incidence by 33% and mortality by 43% and that 489 people need to be screened to prevent one CRC death (Atkin et al., 2010).

1.1.6. Classification

The classification of cancer patients into different stages is used for several reasons: to give an indication of prognosis, to aid in planning the most effective course of treatment, to help evaluate the results of treatment and to facilitate information exchange and research into cancer. There are numerous staging systems in use for CRC but there is currently no general consensus on which system is the most appropriate for use.

1.1.6.1. Dukes staging and modifications

The earliest attempt at classification of CRC was the staging system of Cuthbert Dukes (Dukes, 1932). This consisted of three categories based on the extent of spread of the carcinoma and the involvement of local lymph nodes:

A Carcinoma is limited to the wall of the rectum, no extension into extrarectal tissues, no metastases in lymph nodes

B Carcinoma has spread by direct continuity to the extrarectal tissues, no invasion of the regional lymph nodes

C Metastases present in the regional lymph nodes

The Dukes system was based on observations of rectal cancers, however it was suggested that the system may be applied to all intestinal carcinomas (Dukes, 1932). Dukes stage C was later subdivided into C1 if only the regional lymph nodes contained metastases and C2 if the apical lymph nodes contained metastases (Dukes, 1949; Dukes and Bussey, 1958).

In 1949, the system was modified by Kirklin to include cancers of the colon (Kirklin et al., 1949). Kirklin modified stage A to indicate tumours limited to the mucosa, and subdivided stage B into B1 (tumours extending into the muscularis propria) and B2 (tumours penetrating the muscularis propria). Stage C remained a single, non-divided stage.

Later, in 1954, Astler and Coller extended Kirklin's classification by separating Dukes C into C1 (tumour limited to the wall with positive lymph nodes) and C2 (tumour extending through all layers with positive lymph nodes) (Astler and Coller, 1954). Confusingly, these categories are not the same as Dukes' C1 and C2 categories. The Astler and Coller system was further refined by Gunderson and Sosin in 1974, adding B3 (lesions adherent to/invading adjacent organs) and stage C3 (gross nodal disease with extension and invasion of adjacent organs) (Gunderson and Sosin, 1974). The system encompassing the modifications of the Dukes system described by Kirklin, Astler, Coller, Gunderson and Sosin is known at the Modified Astler Coller system (MAC).

In 1967, Turnbull added a later stage to the Dukes classification, designated stage D, for patients with distant metastases or invasion of adjacent organs (Turnbull et al., 1967). Newland then further modified the system to include stages D1 (local tumour remaining after resection) and D2 (distant metastases) (Newland et al., 1981).

The multitude of different modified Dukes classifications has led to difficulty comparing patients, especially given that authors often do not specify which system they are using (Raraty and Winstanley, 1998).

1.1.6.2. TNM staging

The American Joint Committee on Cancer (AJCC) system of classification for CRC uses the TNM (tumour-node-metastasis) system and is now in its seventh edition (Edge, 2009). TNM staging is widely used worldwide and is being continually improved based on new data (Gospodarowicz et al., 2004). The most recent edition of this staging system describes a total of nine stages for CRC (I, IIA, IIB, IIC, IIIA, IIIB, IIIC, IVA and IVB; Table 1.1). Patients are stratified using the depth of tumour penetration (T), number of positive lymph nodes (N) and extent of distant metastasis (M) (Table 1.2).

The TNM system is more detailed than the Dukes system, and takes into account more features of the cancer, which means patients can be compared more precisely. The TNM system can be used for preoperative clinical assessments, whereas Dukes staging is based on pathological findings following surgery (Dukes and Bussey, 1958; Eschrich et al., 2005). However, the Dukes system is still popular due to its simplicity.

1.1.6.3. Molecular staging and prognostic biomarkers

Dukes staging is very effective at predicting prognosis for those with stage A and D tumours. However, all the staging systems described above are limited in discriminating prognosis of intermediate stage patients (Dukes B and C). Molecular staging, based on the gene expression profile of the tumour, may be more effective in predicting long-term survival rates. For example, a cDNA classifier, based on microarray data from 43 genes, was 90% accurate (93% sensitivity and 84% specificity) at predicting 36-month overall survival of Dukes stage B and C patients. This was significantly better than Dukes staging ($p = 0.0378$) and discriminated patients into significantly different groups by survival time ($p < 0.001$) (Eschrich et al., 2005). Consequently, molecular staging may be a useful technique to be applied in future. It would be beneficial to improve or create new staging systems as further prognostic factors are discovered, to allow clinicians to more accurately predict patient prognosis.

A prognostic biomarker is a parameter that can be used to predict patient survival. As patients with tumours which are histologically identical can have different prognoses and different responses to chemotherapy, molecular biomarkers which more accurately predict patient survival would be invaluable for patient management. There are several features of colon cancer that may be useful as prognostic markers, including expression of lamin A, preoperative CEA (carcinoembryonic antigen) levels, MSI status, LOH at chromosome18q, expression of thymidylate synthase, p53 or Ki-67 and the presence of lymphovascular or perineural invasion (Allegra et al., 2003; Gill et al., 2004; Quah et al., 2008; Tejpar, 2007; Willis et al., 2008). However, none of these markers is yet recommended for use in a clinical setting (Zlobec and Lugli, 2008).

Predictive biomarkers are used to discern patients that would benefit from adjuvant chemotherapy. Prognostic biomarkers do not necessarily also function as predictive biomarkers, for example the correlation between p53 expression and benefit of adjuvant chemotherapy is controversial (Ahnen, 1999; Allegra et al., 2003).

Stage	T	N	M	Dukes	MAC
0	Tis	N0	M0	-	-
I	T1	N0	M0	A	A
	T2	N0	M0	A	B1
IIA	T3	N0	M0	B	B2
IIB	T4a	N0	M0	B	B2
IIC	T4b	N0	M0	B	B3
IIIA	T1-T2	N1/N1c	M0	C	C1
	T1	N2a	M0	C	C1
IIIB	T3-T4a	N1/N1c	M0	C	C2
	T2-T3	N2a	M0	C	C1/2
	T1-T2	N2b	M0	C	C1
IIIC	T4a	N2a	M0	C	C2
	T3-T4a	N2b	M0	C	C2
	T4b	N1-N2	M0	C	C3
IVA	Any T	Any N	M1a	-	-
IVB	Any T	Any N	M1b	-	-

Table 1.1: Comparison of staging systems (Edge, 2009)

Primary Tumour (T)	
T0	No evidence of primary tumour
Tis	Carcinoma in situ: intraepithelial or invasion of lamina propria
T1	Tumour invades submucosa
T	Tumour invades muscularis propria
T3	Tumour invades through the muscularis propria into pericolorectal tissues
T4a	Tumour penetrates to the surface of the visceral peritoneum
T4b	Tumour directly invades or is adherent to other organs or structures
TX	Primary tumour cannot be assessed
Regional Lymph Nodes (N)	
N0	No regional lymph node metastasis
N1	Metastasis in 1-3 regional lymph nodes
N1a	Metastasis in 1 regional lymph node
N1b	Metastasis in 2-3 regional lymph nodes
N1c	Tumour deposit(s) in the subserosa, mesentery or nonperitonealised pericolic or perirectal tissues without regional nodal metastasis
N2	Metastasis in 4 or more regional lymph nodes
N2a	Metastasis in 4-6 regional lymph nodes
N2b	Metastasis in 7 or more regional lymph nodes
Distant Metastasis (M)	
M0	No distant metastasis
M1	Distant metastasis
M1a	Metastasis confined to 1 organ/site (e.g. liver, lung, ovary or non-regional node)
M1b	Metastases in more than 1 organ/site or the peritoneum

Table 1.2: Definitions of T, N and M in AJCC staging system (7th edition) (Edge, 2009)

However, LOH at chromosome 18q in microsatellite-stable cancers and mutation of the gene for the type II receptor for TGFβ in MIN cancers can act as both prognostic biomarkers and predictive markers of the benefit of adjuvant chemotherapy for stage III colon cancer (Watanabe et al., 2004).

1.1.7. Treatment

Surgical resection with curative intent is the main form of treatment for Stage I-III CRC, usually through traditional open surgery, though laparoscopic resection is also increasingly being used (Schurer and Kanavos, 2010). Laparoscopic surgery has many advantages over open surgery, including faster recovery, fewer systemic and wound complications and less pain (Noel et al., 2007). However, the MRC CLASICC (conventional versus laparoscopic-assisted surgery in CRC) trial found that there was no difference in overall survival (OS) or disease-free survival (DFS) for CRC patients treated by laparoscopic or open surgery (Jayne et al., 2010). During surgery, it is important that lymph nodes are removed and identified, to reduce the chance of local recurrence from tumour in lymph nodes, and to aid patient management post-surgery. The larger the number of lymph nodes examined, the better the accuracy of staging, the more likely it is that patients are classified as node-positive and the higher the long-term survival rates. However, there is currently no consensus on the optimum number of nodes that should be removed.

Some patients are offered adjuvant therapy following surgery, most commonly chemotherapy. For patients with Stage III colon cancer, adjuvant treatment such as 5-FU (5-Fluorouracil) based adjuvant chemotherapy with oxaliplatin is known to improve DFS and OS (Andre et al., 2009). Stage I and II patients are often cured by surgery alone, with 5-year survival rates of 75-95%. However, it is important to be able to stratify stage II patients by risk, as some of these patients have similar relapse rates to stage III patients, and would benefit from adjuvant treatment. Adjuvant chemotherapy after surgical resection of the primary tumour increases survival by approximately 10% for patients with Stage III tumours, and by 4% for patients with Stage II tumours (Midgley et al., 2009).

Use of post-operative chemotherapy for those with Stage II colon cancer is controversial. For patients who have been cured by surgical resection, chemotherapy is unnecessary and dangerous and should be avoided. Stage II tumours are heterogeneous and range from those with very early penetration into the bowel wall to aggressive tumours with involvement of adjacent organs. It has been suggested that Stage II patients with high risk features such as obstruction, perforation, inadequate lymph node sampling or T4 disease

should be considered for adjuvant chemotherapy, dependent on their age and co-morbidities (Figueredo et al., 2008). It is widely accepted that further high-risk features need to be identified which can aid in selecting patients who would benefit from chemotherapy and that more effective, less toxic therapies need to be found (Figueredo et al., 2008). There are a number of possible ways of identifying patients with high-risk features, including clinicopathologic characteristics, molecular biomarkers and genomic, proteomic or metabolomic profiling (Section 1.1.6.3).

1.2. Lamins

1.2.1. The nuclear envelope

Lamins are type V intermediate filament proteins that bind together to form a filamentous meshwork encompassing the nucleoplasmic side of the nuclear envelope (NE). Lamins are also present in the nuclear matrix (see Section 1.2.4.3). The NE separates the nucleus from the cytoplasm in eukaryotic cells and is composed of an outer nuclear membrane (ONM) and an inner nuclear membrane (INM), which are fused at the site of nuclear pore complexes (NPCs). The ONM is continuous with the endoplasmic reticulum (ER) and is studded with ribosomes, whereas the INM is distinct from the ER and contains nuclear envelope transmembrane proteins (NETs) such as the lamina-associated polypeptides (LAPs) (Schirmer et al., 2003; Senior and Gerace, 1988) (Figure 1.7). NPCs control the exchange of components between the nucleus and the cytoplasm.

The lamina was first discovered as a detergent and salt resistant component of the nucleus (Dwyer and Blobel, 1976; Pappas, 1956). Three genes are known to encode lamin proteins in human somatic cells: *LMNA,* encoding the A-type lamins and *LMNB1* and *LMNB2,* encoding the B type lamins. A-type lamins (A, AΔ10, C and C2) are alternatively spliced products of *LMNA* (Lin and Worman, 1993; Machiels et al., 1996). Lamins A and C are identical for the first 566 amino acids, following which lamin C lacks exons 11 and 12 and part of exon 10. Lamin C has 6 unique C terminal amino acids and lamin A has an extra 98 amino acids at the C terminus. As its name suggests, lamin AΔ10 lacks exon 10 (Machiels et al., 1996). Lamin A (70kDa) and lamin C (65kDa) are expressed in most differentiated cells (Broers et al., 1997) whereas lamin C2 is expressed only in the germline (Furukawa et al., 1994). Lamin AΔ10 is expressed in some tumour cell lines and normal cells (Machiels et al., 1996).

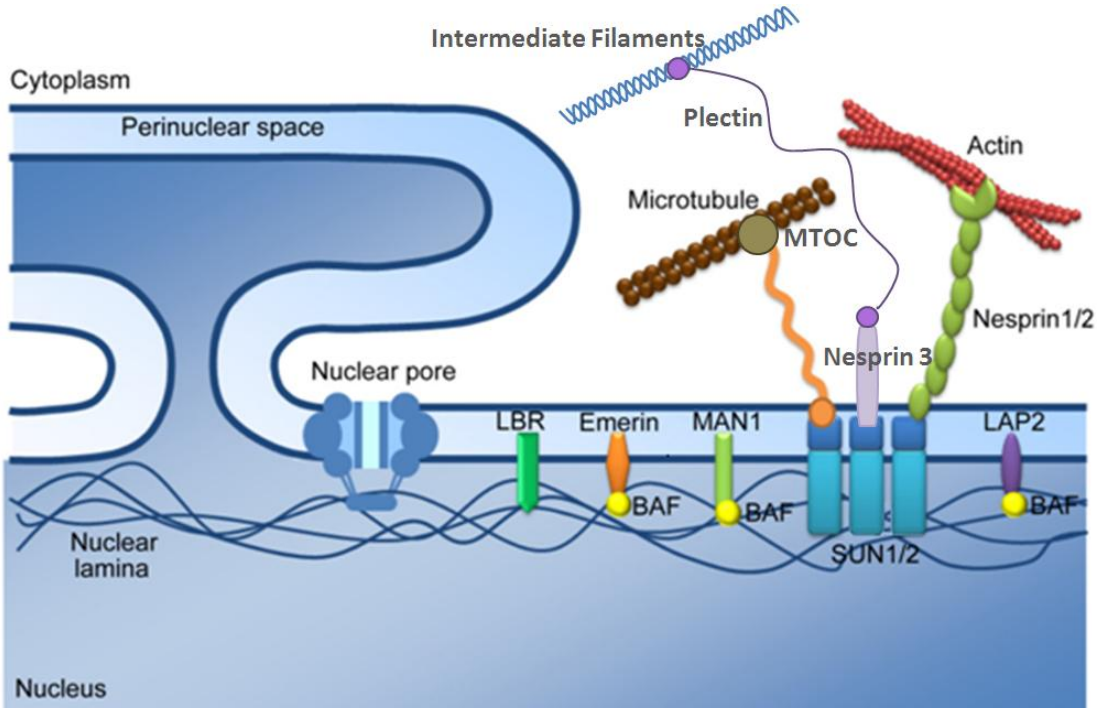

Figure 1.7: The nuclear envelope (adapted from Chi et al, 2009) - The nuclear envelope contains nuclear pore complexes and NETs such as LBR, emerin, MAN1 and LAP2. The nuclear lamina encompasses the nucleoplasmic side of the nuclear envelope.

B-type lamins, encoded by *LMNB1* (lamin B1) (Lin and Worman, 1995) and *LMNB2* (lamin B2 and B3) (Biamonti et al., 1992; Furukawa and Hotta, 1993; Hoger et al., 1990) are essential for cell survival (Harborth et al., 2001). Lamins B1 (67kDa) and B2 (68kDa) are expressed in most cells, although lamin B2 is more ubiquitous than lamin B1 (Broers et al., 1997). Lamin B3 is only expressed in spermatocytes (Furukawa and Hotta, 1993). Gene targeting of lamin A in mouse models has shown that only B-type lamins are necessary for embryonic development, but A-type lamins are necessary for post-natal survival (Sullivan et al., 1999).

1.2.2. Structure of lamins

Lamin proteins have a tripartite structure typical of intermediate filament proteins (Fisher et al., 1986; McKeon et al., 1986). They consist of a globular NH_2-terminal head domain, a central coiled-coil α-helical rod domain and a globular COOH-terminal tail domain. The central rod domain contains four α-helical subsegments (coils 1A, 1B, 2A and 2B) separated by short linker regions (L1, L12 and L2) (Conway and Parry, 1990).

However, there are also some differences between IF proteins and lamins. The head domain is shorter than in other IF proteins (Fisher et al., 1986) and lamins contain a 42 amino acid long insertion within coil 1B of the rod domain. The tail domain contains a

nuclear localisation signal (NLS) (Fisher et al., 1986; Loewinger and McKeon, 1988). A CaaX motif (where C represents cysteine, a represents any aliphatic residue and X represents any amino acid) is present in the tail domain of lamin A and B-type lamins, but not in lamin C, and is the site of posttranslational modifications (Fisher et al., 1986; Kitten and Nigg, 1991; McKeon et al., 1986; Vorburger et al., 1989).

1.2.3. Assembly and post-translational modification of lamins

Initially, lamins form parallel dimers via their coiled-coil domains. Two lamin dimers then associate in a polar 'head to tail' formation, in which the N- and C- terminal ends overlap by 2-4nm (Aebi et al., 1986), following which they form antiparallel out of register associations (Strelkov et al., 2004; Stuurman et al., 1998). Both the head and tail domains of lamins contain cyclin dependent kinase 1 (CDK1) target sequences, and phosphorylation of these sequences is correlated with disassembly of lamin filaments during mitosis (Peter et al., 1991; Peter et al., 1990; Ward and Kirschner, 1990). Phosphorylation of additional sequences in the head and tail domains may allow the correct assembly of lamin filaments (Collas et al., 1997; Stuurman, 1997).

For lamin A and B-type lamins to be correctly localised at the INM, their COOH-terminal cysteine residues must undergo isoprenylation and methylation. Firstly, a 15-carbon farnesyl isoprenoid is added to the cysteine of the CaaX box, before the aaX sequence is removed and the cysteine is methylated. B type lamins also require LAP2β for their correct assembly into the nuclear lamina (Furukawa and Kondo, 1998; Yang et al., 1997).

Once at the INM, lamin A undergoes further post-translational modifications, to progress from prelamin A to mature lamin A. The last 15 amino acids of prelamin A are cleaved by the zinc metalloproteinase Zmpste24, resulting in the loss of the isoprenylated cysteine residue (Bergo et al., 2002; Pendas et al., 2002).

1.2.4. The role of lamins in the control of nuclear and cellular architecture

Lamins anchor NETs at the INM. A-type and B-type lamins often, but not always, bind to different NETs, for example A-type lamins bind emerin (Clements et al., 2000) and B-type lamins bind LAP2β (Furukawa and Kondo, 1998). Emerin interacts with MAN1 (Mansharamani and Wilson, 2005) and emerin, LAP2β and MAN1 bind to BAF (barrier to autointegration factor) (Furukawa, 1999; Lee et al., 2001; Mansharamani and Wilson, 2005; Shumaker et al., 2001). Complexes of lamins and NETs are important for organising

peripheral chromatin, organising the cytoskeleton and anchoring nuclear pore complexes within the nuclear envelope. These processes are discussed in more detail in the following sections.

1.2.4.1. The role of lamins in DNA binding and regulation of gene expression

A network of lamins and lamin-binding proteins are involved in tethering chromatin to the nuclear envelope. A-type lamins can directly bind DNA (Stierle et al., 2003) however it is thought that most interactions between DNA and lamins occur indirectly, through lamin binding proteins. Both A-type lamins and the lamin-binding LEM (LAP2, Emerin, MAN) domain proteins bind BAF, which can bind DNA (Holaska et al., 2003; Zheng et al., 2000). BAF is involved in higher order chromatin structure, nuclear assembly and gene regulation (Haraguchi et al., 2001; Holaska et al., 2003; Segura-Totten et al., 2002). Lamins may play a role in organising heterochromatin, as some laminopathies and *LMNA* null nuclei show a dramatic loss of heterochromatin (Goldman et al., 2004; Scaffidi and Misteli, 2005; Sullivan et al., 1999).

The nuclear lamina is thought to play a role in regulation of gene expression, particularly in the repression of genes. It has recently been shown that there are over 1,300 sites of interaction between the genome and the lamina, known as lamina-associated domains (Guelen et al., 2008), which typically display low gene expression levels. Artificial tethering of genes to the lamina can also lead to repression of gene expression (Reddy et al., 2008). Furthermore, A-type lamins can bind a number of transcriptional repressors including hypophosphorylated Rb (Mancini et al., 1994; Ozaki et al., 1994), BAF (Holaska et al., 2003) and SREBP1a and 1c (Lloyd et al., 2002) .

1.2.4.2. Lamin function in the control of nuclear size and shape

Most cells contain round or oval nuclei, but some specialised or diseased cells display altered nuclear shape. Abnormally shaped nuclei are often seen in cells with reduced lamin expression and in laminopathies (Capell and Collins, 2006; Liu et al., 2000; Sullivan et al., 1999) and depletion of lamins leads to reduced nuclear size (Jenkins et al., 1993). Changes in nuclear shape can affect the rigidity of the nucleus and/or gene expression, and it has been suggested that these effects may be due to changes in lamin proteins (Webster et al., 2009).

1.2.4.3. Lamins and the nuclear matrix

A homologue of the cytoplasmic cytoskeleton, known as the nuclear matrix or nucleoskeleton, is present in the nucleus (Rando et al., 2000) and is thought to contain A-type lamins, actin, myosin and spectrin-repeat proteins (Broers et al., 2005; Pederson and Aebi, 2005; Pestic-Dragovich et al., 2000; Young and Kothary, 2005). Many aspects of the nuclear matrix are not yet fully understood and its function as a structural, force-bearing structure is disputed (Misteli, 2007; Pederson, 2000).

The suggestion that actin is present in the nucleus was once controversial, but now actin is known to be involved in several nuclear processes such as chromatin remodelling and gene splicing (Rando et al., 2000). Many papers have convincingly detected actin in the nucleus (Rando et al., 2000) and all isoforms of actin contain nuclear export sequences (Wada et al., 1998). In the nucleus, phalloidin stainable F-actin filaments are not present, which may be due to the geometry of the interchromatin space (Pederson and Aebi, 2002). Instead, 80% of actin is free and 20% is found as oligomers or short polymers (McDonald et al., 2006).

Actin binds both A- and B-type lamins (Fairley et al., 1999; Sasseville and Langelier, 1998; Simon et al., 2010). Lamin A tails also contain a unique actin binding domain in residues 564-608 and they are capable of bundling F-actin *in vitro* (Simon et al., 2010). It is thought that lamins may suppress formation of F-actin in the nucleus through regulating actin polymers or sequestering G-actin, as nuclei of Drosophila muscle cells that lack the A-type lamin contain phalloidin-stainable fibres (Schulze et al., 2009; Simon et al., 2010).

1.2.4.4. LINC complexes and the cytoskeleton

It has recently been shown that the cytoskeleton is connected to the nucleus through LINC (linker of nucleoskeleton and cytoskeleton) complexes, formed through binding of KASH (Klarsicht/ANC-1/Syne homology) domain proteins such as nesprins to SUN (Sad1 and UNC-84 homology) domain proteins (Starr and Han, 2003). The physical connection between the cytoskeleton and the nucleus is important for force transmission, cell migration and nuclear positioning. SUN1 and SUN2 bind to A-type lamins at the INM and interact with nesprins in the perinuclear space (Crisp et al., 2006; Haque et al., 2006; Padmakumar et al., 2005). Some nesprin isoforms bind lamin A and/or C (Libotte et al., 2005; Mislow et al., 2002) and A-type lamins are necessary for nesprin-2 localisation at the nuclear envelope (Libotte et al., 2005).

Nesprins can connect to all three of the major components of the cytoskeleton. Nesprins-1 and -2 giant isoforms bind to actin (Padmakumar et al., 2004; Zhen et al., 2002) and nesprin-1 is thought to be an actin bundling protein (Padmakumar et al., 2004). Nesprins-1,-2 and -4 can connect to microtubules through interacting with kinesin and/or dynein (Fan and Beck, 2004; Roux et al., 2009; Schneider et al., 2011) whilst nesprin-3 associates with the IF cytoskeleton via plectin (Wilhelmsen et al., 2005). The lamin binding protein emerin also interacts with nesprins (Mislow et al., 2002; Wheeler et al., 2007) and nuclear and cytoplasmic actin (Fairley et al., 1999; Lattanzi et al., 2003) and it increases F-actin filament assembly by binding to and stabilising the pointed ends of F-actin (Holaska et al., 2004).

Another recent discovery is that thick actin filament bundles organised into an 'actin cap' are located above the apical surface of the nucleus in some cells (Khatau et al., 2009; Khatau et al., 2010). Khatau *et al.* showed that the actin cap is connected to the NE through LINC complexes, plays a role in controlling nuclear shape and is structurally and functionally distinct from conventional actin fibres at the basal and dorsal surfaces of cells. The actin cap was lost in most *LMNA*$^{-/-}$ cells but no disorganisation of basal stress fibres was observed.

LMNA$^{-/-}$ MEFs contain mislocalised LINC complex proteins (Crisp et al., 2006; Libotte et al., 2005). These cells also have a lack of mechanical stiffness and disturbed actin, tubulin and vimentin-based filaments (Broers et al., 2004; Lammerding et al., 2004). Fibroblasts with disrupted LINC complexes have a loss of cellular mechanical stiffness similar to that in fibroblasts lacking A-type lamins (Stewart-Hutchinson et al., 2008), which demonstrates the importance of LINC complexes in the mechanical properties of the cell.

1.2.5. Lamin expression and cell motility

Several studies have shown that lamin A/C deficiency in mouse embryonic fibroblasts (MEFs) results in reduced cell migration and this is thought to be caused by deficient nuclear-CSK organisation and/or reduced CSK stiffness (Houben et al., 2009; Lee et al., 2007). *LMNA*$^{-/-}$ MEFs displayed softening of the cytoplasm (Lee et al., 2007) and loss of nuclear reorientation during cell migration (Houben et al., 2009). Depletion of A-type lamins and/or emerin leads to deficient microtubule organising centre (MTOC) polarisation (Hale et al., 2008; Lee et al., 2007) and detachment of the MTOC from the nucleus (Hale et al., 2008; Houben et al., 2009; Lee et al., 2007; Salpingidou et al., 2007). It is important to note that A-type lamin deficiency or mutation does not always lead to reduced cell motility (Emerson et al., 2009; Hale et al., 2008; Lu et al., 2009)

The link between A-type lamins and cell motility has also been studied in cancer cells. Previous work in our laboratory has shown that expression of lamin A in colon carcinoma promotes increased cell motility (Willis et al., 2008). In wounding assays, wound closure was seven times faster in cells transfected with GFP–lamin A compared with control cells transfected with GFP alone. Lamin A was shown to control a pathway in which up-regulated expression of T plastin, an actin bundling protein, led to down-regulated expression of the cell adhesion molecule E-cadherin, resulting in increased cell motility. Loss of E-cadherin and expression of plastins are often hallmarks of tumours, correlating with invasive and metastatic behaviour (Foran et al., 2006; Perl et al., 1998). The findings of Willis *et al.* may reveal a function of lamin A as a regulator of a pathway involving actin dynamics, cell adhesion and cell motility. It is possible that lamin A expression controls the reorganization of the cytoskeleton through its association with LINC complexes, causing alterations in cell migration.

1.2.6. Lamins as a marker of colonic stem cells

Our group has previously investigated A-type lamin expression in colonic crypts using immunohistochemistry (Figure 1.8). Strong lamin A/C expression was found in differentiated cells, whereas no A-type lamin expression was found in the proliferative region (Willis et al., 2008). Serial crypt sections revealed reciprocal expression of lamin A/C and the DNA replication protein PCNA (proliferating-cell nuclear antigen) at the crypt base. The cells in the putative stem cell niche were positive for lamin A, but not lamin C, revealing lamin A as a putative marker of colonic stem cells.

1.3. Lamins and disease

1.3.1. Laminopathies

Abnormal structure or processing of *LMNA* lead to a wide range of degenerative diseases termed laminopathies (Broers et al., 2006). *LMNA* is one of the most highly mutated genes in the genome; to date over 200 different *LMNA* mutations have been discovered. Primary laminopathies are caused by mutations in *LMNA*, whereas secondary laminopathies are caused by mutations in *FACE-1*, which is involved in posttranslational processing of prelamin A.

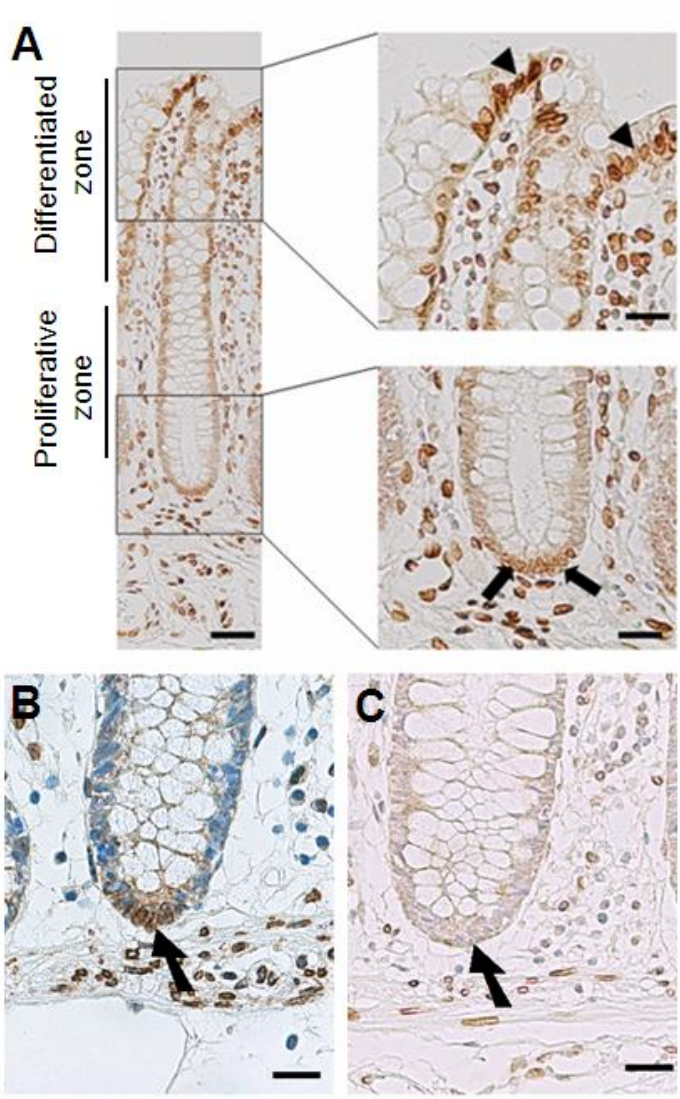

Figure 1.8: A-type lamin expression in the colonic crypt (Willis et al., 2008)

A Thin sections of normal colon stained with JoL2 (anti-lamin A/C), counterstained with Mayers Haemalum. Arrowheads show differentiated epithelium cells and arrows indicate the putative stem cell niche. Scale bars = 150 μm (left-hand panel) & 50 μm (right-hand panels).

B, C Serial sections of normal colonic epithelium immunohistochemically stained with 133A2 (anti-lamin A) (**B**) and RaLC (anti-lamin C) (**C**). Arrowheads indicate functional differentiated cells and arrows indicate cells within the proposed stem cell niche. Scale bars = 50 μm.

Some laminopathies affect specific tissues, i.e. striated muscles, peripheral nerves or adipose tissue. Others affect two or more tissue types, and some laminopathies cause premature ageing syndromes, such as progeria.

1.3.2. Lamins and cancer

Many of the cell processes that lamins are involved in are implicated in tumour progression, such as control of nuclear architecture, regulation of gene expression, apoptosis, senescence and chromatin organization and segregation (Broers et al., 2006). Therefore the effects of alterations of lamin expression or localization in tumour cells are particularly complex. As discussed above, A type lamins bind to a number of LEM domain proteins - LAP2α, MAN1 and emerin - which regulate growth regulators and can therefore be components of cancer pathways. Mutant emerin results in nuclear accumulation of β-catenin and fibroblasts null for emerin show autostimulatory growth (Markiewicz et al., 2006). LAP2α and A-type lamins have been shown to anchor unphosphorylated pRb, a growth suppressor, in the nucleus (Markiewicz et al., 2002). MAN1 antagonises TGFβ signalling by binding to Smad2 and Smad3 (Lin et al., 2005).

The TGFβ superfamily contains TGFβs, bone morphogenic proteins (BMPs) and activins, which are known to regulate development, differentiation and homeostasis. The role of TGFβ in cancer was initially thought to be in the suppression of tumours (Markowitz and Roberts, 1996), but it was later also found to have oncogenic activities (Wakefield and Roberts, 2002). In colon cancer, the function of TGFβ depends on the differentiation stage of the tumour, as it inhibits proliferation in the early stage of cancer and stimulates invasion at later stages of tumour progression (Hsu et al., 1994; Schroy et al., 1990).

The canonical TGFβ signalling pathway is inherently simple, comprising three TGFβ-receptors (TβR-I, -II and –III) and three latent transcription factors (Smad2, 3 and 4). TGFβ stimulates responsive cells by binding TβR-III, which presents TGFβ to TβR-II. TβR-II then activates TβR-I, which phosphorylates Smads 2 and 3. Smads 2 and 3 subsequently associate with Smad4, and the Smad2/3/4 complex translocates to the nucleus where it can interact with transcriptional regulators to induce or repress TGFβ target genes. There are also numerous Smad-independent pathways in which TGFβ-signalling can occur. TGFβ is known to inhibit NFκB and to stimulate MAP kinases, small GTPases, protein tyrosine kinases and PI3K/AKT (Derynck and Zhang, 2003; Tian et al., 2011).

A-type lamins are known to modulate responses to TGFβ signalling in mesenchymal cells (Van Berlo et al., 2005). Van Berlo *et al.* showed that A-type lamins regulate the phosphorylation and de-phosphorylation of R-SMADs (receptor-regulated SMADs) and that A-type lamins are essential for inhibition of proliferation by TGFβ. MAN1, a lamin A-interacting protein, is also known to regulate TGFβ signalling through binding to R-SMADs (Lin et al., 2005; Osada et al., 2003).

1.3.2.1. Lamins as diagnostic biomarkers

Numerous studies have tried to elucidate the relationship between lamin expression and cancer subtype by investigating the changes in lamin expression in malignant cells and tissue sections. Expression levels of lamins are often but not always aberrant in tumours.

As B-type lamins are necessary for cell survival (Harborth et al., 2001), at least one B-type lamin is always present in a malignant cell. Abnormal expression levels are present in some tumour subtypes: expression is usually found to be reduced (Broers et al., 1993; Moss et al., 1999), but increased lamin B1 expression has also been shown in prostate cancer and in hepatocellular carcinoma (HCC) (Coradeghini et al., 2006; Lim et al., 2002; Sun et al., 2010). The presence of B-type lamins in most normal and tumour cells renders them poor diagnostic biomarkers for many cancer subtypes. However, lamin B1 has the potential to be used as a diagnostic biomarker to detect HCC from an early stage, as it is overexpressed in early and late stage HCC when compared to non-malignant controls ($p < 0.0001$). Lamin B1 mRNA was present in plasma of HCC patients and was found to detect early stage HCCs with a sensitivity of 76% and a specificity of 82% (Sun et al., 2010).

As with B-type lamins, there is no simple overall pattern of A-type lamin expression in cancer and frequently no consistent patterns are observed between cancer subtypes. Many studies show lamin A/C to be downregulated in tumour cells (Broers et al., 1993; Moss et al., 1999; Venables et al., 2001), but expression is also frequently positive or upregulated (Broers et al., 1993; Hudson et al., 2007; Tilli et al., 2003). Often expression levels can vary dramatically even within cancer subtypes, for example in colorectal and basal cell carcinomas, A-type lamin expression can be positive (Tilli et al., 2003; Venables et al., 2001; Willis et al., 2008), reduced (Moss et al., 1999; Venables et al., 2001) or negative (Moss et al., 1999; Venables et al., 2001; Willis et al., 2008) in tumour tissue.

The presence of variable A-type lamin expression in most tumour subtypes suggests that in most cases, A-type lamins may not be useful as diagnostic biomarkers. Nevertheless, cell

type-specific lamin A expression may be valuable as a diagnostic biomarker for detecting some cancers such as skin cancer. In non-cancerous skin, lamin A is not expressed in basal layers of the epidermis. However, in the apparently normal epidermis covering squamous cell carcinoma (SCC) and basal cell carcinoma (BCC), lamin A was found to be present in the basal layer (Tilli et al., 2003).

Lamin A/C has been shown to aberrantly localise to the cytoplasm in some lung carcinomas, colon adenoma and adenocarcinoma, pancreatic and gastric cancers (Broers et al., 1993; Moss et al., 1999; Willis et al., 2008) whilst lamin B1 was localised to the cytoplasm in some colon and lung cancers (Moss et al., 1999). Lamin C was localised to the nucleolus in BCC and adrenal cortex carcinoma (Tilli et al., 2003; Vaughan et al., 2001; Venables et al., 2001). A number of studies have shown that lamins are present in the nucleoplasm and nuclear matrix in addition to the nuclear envelope in non-tumour cells (Fricker et al., 1997; Goldman et al., 1992; Moir et al., 1994). Therefore, the detection of lamins in the cytoplasm is more likely to function as a diagnostic marker than the detection of lamin C in the nucleolus.

Research into the use of lamins as cancer biomarkers is still at an early stage and none are yet being used clinically. A and B-type lamins have limited use as diagnostic biomarkers in many cancers, due to their variable expression between and within cancer subtypes and the presence of at least one B-type lamin in every tumour and normal cell.

1.3.2.2. Lamins as markers of tumour proliferation

Proliferating epithelial cells contain low levels of A-type lamins (Broers et al., 1997) and overexpression of A-type lamin expression has been shown to inhibit cell proliferation (Ivorra et al., 2006). However, data on the relationship between A-type lamins and proliferation in cancer cells is currently inconclusive. In BCC, highly proliferative cells were negative for expression of lamin A, whereas slow growing tumours were negative for expression of lamin C (Venables et al., 2001). Ki67 and lamin A/C expression were found to be mutually exclusive in about 80% of Hodgkin's disease cells (Jansen et al., 1997). However, co-expression of lamin A and Ki-67 was found in 56% of proliferating SCC cells and in 62% of proliferating BCC tumour cells (Tilli et al., 2003). It appears that too little is known about the patterns of A-type lamin expression in proliferating tumour cells for it to be used as a marker for cell proliferation.

1.3.2.3. Lamins as markers of tumour differentiation

In non-cancerous tissue, A-type lamins are generally only expressed in differentiated cells (Broers et al., 1997; Rober et al., 1989) and lamin B1 has been shown to be reduced in some differentiated cells (Broers et al., 1997; Machiels et al., 1997). The link between B-type lamin expression and differentiation appears to vary with tumour subtype. B-type lamins were expressed in testicular germ cell tumours (TGCTs) regardless of the degree of differentiation (Machiels et al., 1997) whilst well differentiated SCCs showed reduced expression of lamins B1 and B2 compared to poorly differentiated tumours (Oguchi et al., 2002). The presence of A-type lamins is often used to demarcate differentiated tumour cells. Down-regulation of A-type lamins in poorly differentiated tumours has been shown in many tumour subtypes such as SCC (Oguchi et al., 2002) and gastric carcinoma (Wu et al., 2009b). A study into TGCTs (Machiels et al., 1997) showed that differentiated non-seminomas were positive for lamins A/C, only lamin C was expressed in embryonal carcinoma (EC), and poorly differentiated seminomas were negative for lamins A/C. It is understood that in general, the poorer the differentiation of tumour cells, the worse the prognosis. More work needs to be carried out to assess the potential for expression of lamin A/C to act as a prognostic biomarker by defining the degree of differentiation of tumour cells.

1.3.3 The effect of A-type lamin expression on cancer prognosis

The link between cancer prognosis and A-type lamin expression is complex. Some studies point to a lack of lamin A/C expression as a sign of poor prognosis. CpG island promoter hypermethylation, which silences *LMNA* and leads to loss of lamin A/C expression in nodal diffuse large B-cell lymphoma, has been correlated with a decrease in overall survival (P=0.0005) (Agrelo et al., 2005). Moreover, a recent study has revealed that patients with gastric carcinoma cells containing down-regulated lamin A/C expression have poorer prognosis compared with those expressing lamin A/C (P=0.034) and that lamin A/C expression is an independent prognostic factor (Wu et al., 2009a).

However, in colorectal cancer, Willis *et al.* discovered that patients with CRC tumours expressing lamin A/C were almost twice as likely to die from the cancer compared with clinicopathologically identical patients with tumours showing negative expression of lamin A/C (Hazard ratio [HR] 1.85; 95% confidence interval [C.I.] 1.16–2.97, p=0.005) (Willis et al., 2008). A-type lamins are therefore potential biomarkers of poor prognosis in CRC. It has been suggested that the poorer prognosis of CRC patients with lamin A expressing tumours

may be linked to the discovery that lamin A is a marker of colonic stem cells (Willis et al., 2008) as cancer cells with characteristics of stem cells may be more aggressive (O'Brien et al., 2007).

The results described above suggest that the effect of A-type lamin expression on cancer prognosis, and hence their use as prognostic biomarkers, may depend greatly on the subtype of cancer involved.

1.4 Thesis aims and overview

The central aim of this thesis was to further elucidate the mechanisms by which overexpression of lamin A in CRC cells causes increased cell motility, leading to a poor prognosis for patients. I sought to use quantitative proteomic and genomic techniques to assess the effect of lamin A expression on gene and protein expression and on the organisation of the cytoskeleton. The effects of lamin A expression were studied using cells from the colorectal cancer cell line SW480 which had been transfected with GFP-laminA (SW480/lamA) or GFP as a control (SW480/cntl).

Chapter 2 describes the optimisation of a biochemical fractionation protocol in order to isolate cytoskeletal fractions. 2D DIGE was then used to analyse the effect of overexpression of lamin A on the representation of proteins within the cytoskeleton of CRC cells. 64 protein spots showed highly reproducible changes in representation and 29 of these spots were identified using mass spectrometry. The majority of proteins fell into three distinct categories and these proteins were either components of the actin and intermediate filament cytoskeleton, protein chaperones or translation initiation and elongation factors. Most interestingly, tissue transglutaminase 2, a protein associated with cancer progression which is known to crosslink elements of the cytoskeleton, was highly over-represented in the cytoskeleton fraction of SW480/lamA cells. The results suggested that changed protein cross-linking and folding in SW480/lamA cells may lead to changes in the organisation of the cytoskeleton, accounting for the increased cell motility.

In Chapter 3, the data from a genome-wide Affymetrix microarray study comparing SW480/lamA cells with control cells were analysed using Ingenuity Pathways Analysis (IPA). Interaction networks showing known literature-curated interactions were produced. The most highly significant network produced by IPA clustered together molecules linked to cancer, cellular movement and cellular growth and proliferation. Epithelial markers such as *CDH1* were down-regulated and mesenchymal markers such as *FN1* were up-regulated in

SW480/lamA cells, which suggested that lamin A over-expression may lead to an epithelial-mesenchymal transition. Further analysis of the dataset using IPA revealed that there was a statistically significant overlap between IPA lists of genes linked to EMT and the microarray dataset.

Chapter 4 explores the effects of siRNA knockdown of lamin A in SW480/lamA cells. Transfection of si-lamin A resulted in a reduction of endogenous lamin A expression by over 95% and a reduction of GFP-lamin A expression by over 50% by 120 hours after transfection. Cells transfected with si-lamin A were less motile than control cells, confirming that upregulation of lamin A in CRC cells causes increased cell motility. As A-type lamins are known to modulate downstream effects of TGFβ signalling, and TGFβ is an inducer of EMT, changes in genes involved in TGFβ signalling were investigated. Knockdown of lamin A using siRNA showed that reduced cell motility was preceded by decreased expression of *TGFBI* and *SNAI2*. Therefore, expression of lamin A in CRC cells may cause increased cell motility cause through changes in TGFβ signalling, potentially involving an epithelial to mesenchymal transition.

CHAPTER TWO
The effects of over-expression of lamin A on cytoskeleton organisation in CRC cells

2.1. Introduction

The aim of this study was to further understand the mechanisms behind the finding that SW480 CRC cells over-expressing lamin A exhibit increased cell motility (Willis et al., 2008). Willis *et al.* used wounding assays to investigate cell motility, and discovered that wound closure was seven times faster in cells transfected with GFP–lamin A compared with control cells transfected with GFP alone, when the percentage reduction in wound closure was measured over 12 hours. Expression of GFP-lamin A was found to cause up-regulation of the actin bundling protein T-plastin, and down-regulation of the cell adhesion molecule E-cadherin. Loss of E-cadherin and increased expression of plastins are often hallmarks of tumours, correlating with invasive and metastatic behaviour (Foran et al., 2006; Perl et al., 1998). These findings suggest that lamin A regulates a pathway involving actin dynamics, cell adhesion and cell motility.

The nucleus is known to be connected to the cytoskeleton through LINC complexes, formed through binding of KASH domain proteins such as nesprins to SUN domain proteins (Starr and Han, 2003). SUN1 and SUN2 bind to A-type lamins at the INM and interact with nesprins in the perinuclear space (Crisp et al., 2006; Haque et al., 2006; Padmakumar et al., 2005). Nesprins can bind A-type lamins (Libotte et al., 2005; Mislow et al., 2002), actin (Padmakumar et al., 2004; Zhen et al., 2002), plectin (Wilhelmsen et al., 2005), kinesin and dynein (Fan and Beck, 2004; Roux et al., 2009; Schneider et al., 2011). This provides a pathway by which signals can travel between the outside of the cell and the nucleus. Lamin A expression may therefore control the reorganisation of the cytoskeleton through its association with LINC complexes, causing alterations in cell migration.

In addition to the link between A-type lamins and cell motility, there is a link between A-type lamin expression in CRC cells and patient survival. Patients with CRC tumours expressing A-type lamins were found to be almost twice as likely to die from their disease compared with clinicopathologically identical patients whose tumours were negative for expression of A-type lamins (Hazard ratio [HR] 1.85; 95% confidence interval [C.I.] 1.16–

2.97, p=0.005) (Willis et al., 2008). A-type lamins are therefore potential biomarkers for poor prognosis in CRC.

The aim of this study was to investigate changes induced in the organisation of the cytoskeleton when lamin A is over-expressed in colon carcinoma cells. To do this, I used the model system that was used by Willis *et al.* The SW480 cell line was originally derived from a Broders' grade 4, Dukes B primary colon adenocarcinoma taken from a 50 year old Caucasian male (Leibovitz et al., 1976). SW480 cells, which express endogenously low levels of lamin A were stably transfected with DNA constructs encoding either EGFP-lamin A (SW480/lamA) or EGFP (SW480/cntl) (Willis et al., 2008). SW480/cntl cells maintain low expression levels of lamin A, whereas SW480/lamA cells express both higher levels of endogenous lamin A and GFP-lamin A.

In this study, the cytoskeleton was isolated using a biochemical fractionation method and subsequently 2D DIGE (2 dimensional difference in gel electrophoresis) was used to assess differences in protein expression. Elucidating the processes by which lamin A expression causes increased cell motility may help us to understand the finding that colorectal cancer patients expressing A-type lamins in the tumour are twice as likely to die.

2.2. Materials and Methods

2.2.1. General chemicals and materials

All chemicals and reagents used in this project were purchased from Sigma-Aldrich (Poole, UK), BDH Ltd. (VWR International Ltd., Leicestershire, UK) or Melford Laboratories Ltd. (Suffolk, UK) unless otherwise stated. All chemicals were Molecular Biology grade, except those from BDH, which were AnalaR® analytical grade.

2.2.2. Mammalian cell culture

Cell culture was performed in a containment level 2 tissue culture laboratory using strict aseptic techniques. All plasticware was supplied by Greiner Bio-One Ltd. (Gloucestershire, UK).

2.2.2.1. Cell lines

Cells used were from the colon carcinoma cell line SW480, kindly supplied by Dr. Naomi Willis, originally obtained from the European Collection of Cell Cultures (ECACC, Salisbury, Wiltshire, UK). This cell line was originally derived from a Broders' grade 4, Dukes B primary colon adenocarcinoma taken from a 50 year old Caucasian male (Leibovitz et al., 1976). Cells had been stably transfected with DNA constructs encoding either EGFP-lamin A (SW480/lamA) or EGFP (SW480/cntl) (Willis et al., 2008). EGFP-lamin A full length was a gift from Dr M Izumi, Institute of Physical and Chemical Research, Saitama, Japan.

2.2.2.2. Subculture

Cells were cultured in L-15 (Leibovitz) medium with 2mM Glutamine (Invitrogen), supplemented with 100 units/ml penicillin and 100µg/ml streptomycin (Invitrogen), and 10% foetal bovine serum (FBS) lot 057K3395. Cultures were grown in 75cm^2 flasks, maintained at 37^{o}C in a humidified environment without CO_2.

Once cells had reached 70% confluency, they were washed with Versene [137mM NaCl, 2.7mM KCl, 8mM Na_2HPO_4, 1.5mM KH_2PO_4, 1.5mM EDTA pH 7.4] and detached from the flask with Versene containing 10% (v/v) trypsin at 37^{o}C in a humidified atmosphere for 4 minutes. They were then neutralised with medium and centrifuged (Eppendorf 5810R) at 200g for 5 minutes. Supernatants were removed and cells were resuspended in medium and seeded into new flasks. SW480/cntl cells were split 1:2-1:4 and SW480/lamA cells were split 1:4-1:6.

2.2.2.3. Cryopreservation

Cells were harvested and pelleted by centrifugation as described above. The supernatant was removed, cells were resuspended in 4ml phosphate buffered saline (PBS) and centrifuged (Eppendorf 5810R) at 200g for 5 minutes. The supernatant was removed and cells were resuspended in 90% (v/v) supplemented L-15 medium (Invitrogen) and 10% (v/v) dimethylsulphoxide (DMSO), added drop-wise. Cells were transferred to cryovials and placed in a Nalgene™ Cryo 1^{o}C Freezing Container which was kept at -80^{o}C for several days before being transferred to a -150^{o}C freezer for long-term storage.

To re-establish cell cultures, cells were thawed at 37^{o}C and re-suspended in 4ml L-15 medium (Invitrogen). Cells were then centrifuged (Eppendorf 5810R) at 200g for 5 minutes. The supernatant was removed and cell pellets were resuspended in 2ml medium before being transferred to T-25 cell culture flasks. In subsequent passages, some cells were transferred to T-75 flasks and some were cryopreserved to replenish stores of stock cells.

2.2.2.4. Cell counting

Cell suspensions were applied to the chambers of an Improved Neubauer haemocytometer. A light microscope (Zeiss Telaval 31) was used to view the cells. Cells in the four corner squares were counted, excluding cells that touched the upper and left hand side edges of the squares. The mean number of cells per square was calculated, and this number was multiplied by $1.0x10^4$ to give the number of cells per ml.

2.2.3. Biochemical fractionation

2.2.3.1. Initial protocol

The cytoskeletal extraction protocol was modified from a protocol to extract the nuclear matrix (Dyer et al., 1997). Cells were grown to 70% confluency before being washed in versene, trypsinised and centrifuged as described in Section 2.2.2. Cells were resuspended and washed in PBS before centrifugation at 200g for 5 minutes (Eppendorf 5810R). For storage, cell pellets were snap frozen in liquid nitrogen and stored in a -80^{o}C freezer.

A sequential extraction was performed involving ice-cold buffers to produce four insoluble pellets and four supernatants (Table 2.1). 10µl protease inhibitor cocktail (Sigma) and 0.1ml of 100mM DTT were added freshly to every 1ml of each buffer. After each extraction step, soluble and insoluble fractions were separated by centrifugation (Sigma centrifuge) at 1200g (4,000RPM) for 5 minutes at 4^{o}C.

Table 2.1: Buffers used in biochemical fractionation

Buffer name	Buffer abbreviation	Buffer composition
Cytoskeleton buffer	CSK	10mM PIPES (piperazine-N,N′-bis(2-ethanesulphonic acid)) pH6.8, 10mM KCl, 300mM sucrose, 3mM $MgCl_2$, 1mM EGTA pH8.0
Cytoskeleton buffer/ Triton X	CSK/T	10mM PIPES (piperazine-N,N′-bis(2-ethanesulphonic acid)) pH6.8, 10mM KCl, 300mM sucrose, 3mM $MgCl_2$, 1mM EGTA pH8.0, **0.5% (v/v) Triton X-100**
Digestion buffer	Dig	10mM PIPES (piperazine-N,N′-bis(2-ethanesulphonic acid)) pH6.8, **50mM NaCl**, 300mM sucrose, 3mM $MgCl_2$, 1mM EGTA pH8.0
Digestion buffer/DNase	Dig/DNase	10mM PIPES (piperazine-N,N′-bis(2-ethanesulphonic acid)) pH6.8, **50mM NaCl**, 300mM sucrose, 3mM $MgCl_2$, 1mM EGTA pH8.0, **500 units/ml DNase I**
Extraction buffer	Ext	10mM PIPES (piperazine-N,N′-bis(2-ethanesulphonic acid)) pH6.8, **250mM ammonium sulphate,** 300mM sucrose, 3mM $MgCl_2$, 1mM EGTA pH8.0

Briefly, cell pellets were thawed at 37°C, resuspended in 800µl CSK buffer and split into 4 equal samples of 200µl. Samples were then centrifuged. The supernatants were collected into one tube, labelled S1 and one pellet was labelled P1. P1 and S1 were kept on ice until the end of the procedure. The remaining 3 pellets were then resuspended in 200µl CSK/T buffer and incubated for 5 min on ice. After centrifugation, all 3 supernatants were transferred into a tube labelled S2 and one pellet was kept and labelled P2. Both were kept on ice until the end of the procedure. Two pellets were then resuspended in 200µl Dig buffer, centrifuged, and the supernatants discarded before the pellets were resuspended in 200µl Dig/DNase and incubated for 20min at room temperature. Samples were then centrifuged, supernatants were transferred into tube S3, one pellet was labelled P3 and both were kept on ice. The last sample was extracted with 200µl Ext buffer, incubated for 5 min on ice and centrifuged. The supernatant was removed and labelled S4 and the pellet was labelled P4.

Pellets were then incubated with 125µl ice-cold hypotonic buffer [10mM Tris-HCl pH7.4, 10mM KCl, 3mM $MgCl_2$, 0.1% (v/v) Triton X-100] plus 2µl DNase (5 units/µl) and 2µl protease inhibitor cocktail for 10 min on ice. 125µl 2x sample buffer [125mM Tris-HCl pH 6.8, 2% (v/v) sodium dodecyl sulphate (SDS), 2mM dithiothreitol (DTT), 20% (v/v) glycerol, 5% (v/v) β-mercaptoethanol and 0.25% (w/v) bromophenol blue] was then added to each

pellet tube, heated for 3min at 95^{o}C and centrifuged for 30 seconds at 13000g in a bench top centrifuge (VWR).

50µl 5x sample buffer [312.5mM Tris-HCl pH 6.8, 5% (v/v) SDS, 5mM DTT, 50% (v/v) glycerol, 12.5% (v/v) β-mercaptoethanol and 0.625% (w/v) bromophenol blue] was added to each supernatant tube, heated for 3 min at 95^{o}C and centrifuged for 30 seconds at 13000g in a bench top centrifuge (VWR).

All samples were snap frozen in liquid nitrogen and stored in a -80^{o}C freezer.

2.2.3.2. Final protocol

The reasons for the changes made to the protocol are discussed in the results section of this chapter.

SW480/lamA and SW480/cntl cells were grown to the desired confluency (40%, 70% or 100% as described in the appropriate results section) before being washed in versene, trypsinised, counted and centrifuged as described above. Cells were resuspended and washed in 4ml PBS before centrifugation (Eppendorf 5810R) at 200g for 10 minutes.

A sequential extraction (see Figure 2.1) was performed involving the ice-cold buffers described in Table 2.1 to produce four insoluble pellets and four supernatants. 10µl protease inhibitor cocktail and 100µl of 0.4M N-ethylmaleimide (NEM) were added freshly to every 1ml of each buffer. After each extraction step, soluble and insoluble fractions were separated by centrifugation at 1200g for 5 minutes at 4^{o}C (Sigma centrifuge).

Fractionation of both SW480/lamA and SW480/cntl cells was carried out simultaneously. In brief, an appropriate volume of CSK buffer was added to cell pellets so that 820µl of CSK buffer could be removed from each pellet tube for the biochemical fractionation procedure, with both tubes containing the same number of cells. Each sample was then split into 4 aliquots of 200µl and the tubes were centrifuged. The supernatants were collected into one tube, labelled S1. One pellet was labelled P1. After each step, the labelled pellets and supernatants were snap frozen in liquid nitrogen until the end of the procedure. The remaining 3 pellets were then resuspended in 200µl CSK/T buffer and incubated for 5 min on ice. After centrifugation, all 3 supernatants were transferred into a tube labelled S2 and one pellet was kept and labelled P2. The two remaining pellets were then resuspended in 200µl Dig buffer, centrifuged, and the supernatants discarded before the pellets were resuspended in 200µl Dig/DNase and incubated for 20min at room temperature. Samples were then centrifuged, supernatants were transferred into tube S3

and one pellet was labelled P3. The last sample was extracted with 200µl Ext buffer, incubated for 5 min on ice and centrifuged. The supernatant was removed and labelled S4 and the pellet was labelled P4.

Pellets were then thawed and incubated with 86µl ice-cold hypotonic buffer [10mM Tris-HCl pH7.4, 10mM KCl, 3mM MgCl2, 0.1% (v/v) Triton X-100] plus 2µl DNase (5 units/µl), 10 µl 0.4M NEM and 2µl protease inhibitor cocktail for 10 min on ice. Each P1 was homogenised with a Dounce homogeniser to extract the proteins using 10 gentle strokes of the pestle. 5µl was removed from each sample in order to calculate protein concentration. 95µl 2x sample buffer [125mM Tris-HCl pH 6.8, 2% (v/v) SDS, 2mM DTT, 20% (v/v) glycerol, 5% (v/v) β-mercaptoethanol and 0.25% (w/v) bromophenol blue] was then added to each pellet and all pellet samples were heated for 3min at 95^{o}C and centrifuged for 30 seconds at 13000g in a bench top centrifuge (VWR).

Supernatants were thawed and 5µl was removed from each sample in order to calculate protein concentration. Samples were incubated with 50µl 5x sample buffer [312.5mM Tris-HCl pH 6.8, 5% (v/v) SDS, 5mM DTT, 50% (v/v) glycerol, 12.5% (v/v) β-mercaptoethanol and 0.625% (w/v) bromophenol blue], heated for 3 min at 95^{o}C and centrifuged for 30 seconds at 13000g in a bench top centrifuge (VWR).

All samples were snap frozen in liquid nitrogen and stored in a -80^{o}C freezer.

2.2.4. Preparation of whole cell extracts

Cells grown in T-75 cell culture flasks were washed in versene, trypsinised and centrifuged as described in Section 2.2.2. Cells were resuspended and washed in 4ml PBS before centrifugation at 200g for 10 minutes (Eppendorf 5810R). After the supernatant was removed, cells were snap frozen in liquid nitrogen and stored at -80^{o}C. When required, cell pellets were thawed, resuspended in 500µl hypotonic buffer [10mM Tris-HCl pH7.4, 10mM KCl, 3mM $MgCl_2$, 0.1% (v/v) Triton X-100] plus 2µl DNase (5 units/µl), 2µl protease inhibitor cocktail, 50µl 0.4M NEM and incubated on ice for 10 minutes. 5µl of each sample was removed in order to calculate protein concentration. 500µl 2x sample buffer [125mM Tris-HCl pH 6.8, 2% (v/v) SDS, 2mM DTT, 20% (v/v) glycerol, 5% (v/v) β-mercaptoethanol and 0.25% (w/v) bromophenol blue] was then added to each sample and tubes were heated to 95^{o}C for 3 minutes then centrifuged for a minute at 13000g in a bench top centrifuge (VWR).

Figure 2.1 Biochemical Fractionation Protocol

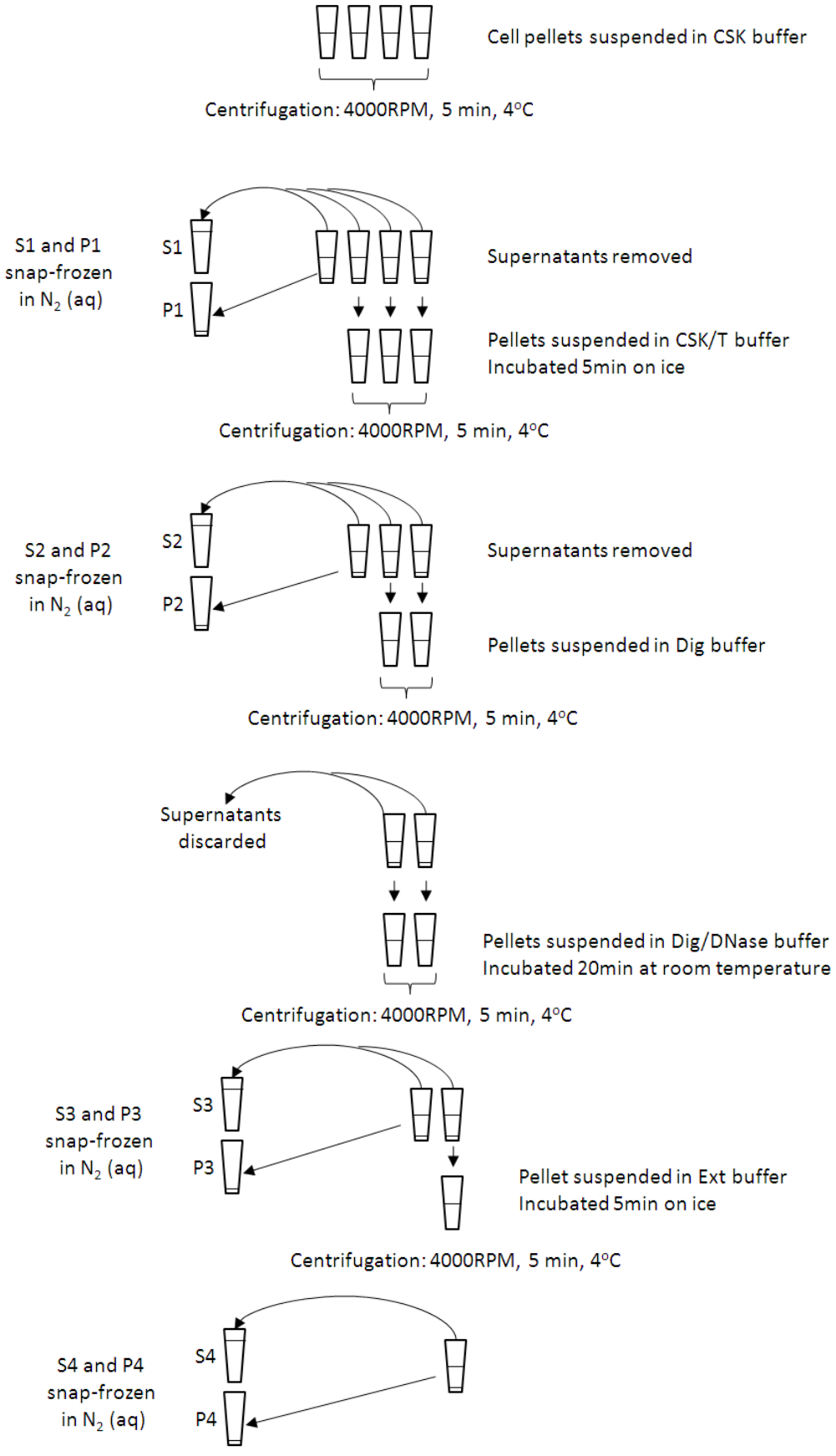

2.2.5. One-dimensional SDS-PAGE

One-dimensional SDS-PAGE was performed following the procedure of Laemmli (Laemmli, 1970) to separate proteins according to their molecular weights (M_r). Gels were cast using the Mini-Protean Electrophoresis System (BioRad). Firstly, a 1mm thick resolving gel was formed containing either 10% or 12% (v/v) poly-acrylamide [10/12% (v/v) ProSieve® 50 acrylamide gel solution (Cambrex BioScience Wokingham, Ltd., UK), 375mM Tris-HCl pH 8.8, 0.1% (w/v) SDS, 0.05% (w/v) ammonium persulphate (Fisher Biosciences) and 0.04% (v/v) TEMED (N,N,N',N'-Tetramethylethylenediamine). Butan-1-ol was pipetted onto the top of the gel solution to ensure the top of the gel was flat. After the gel had set, the butan-1-ol was poured off. The stacking gel solution was prepared, as for the resolving gel but containing 5% (w/v) acrylamide, 125mM Tris-HCl pH 6.8 and 0.1% (v/v) TEMED. The resolving gel solution was added to the top of the resolving gel and a Teflon comb was inserted to form wells.

Gels were submerged in Tank buffer [25mM Tris pH 8.3, 192mM Glycine, 0.1% (v/v) SDS] and protein samples prepared for SDS-PAGE (Section 2.2.4) were added to wells, with an equal concentration of protein added to each well. 10µl of protein ladder - PageRuler™ Prestained Protein Ladder Plus (Fermentas) or Prestained SDS-PAGE Standards (BioRad) - was used for visualising molecular weights of proteins and to demonstrate transfer of proteins onto nitrocellulose membranes.

Table 2.2: Composition of one-dimensional SDS-PAGE gels

	Final concentration	
	Resolving Gel	**Stacking Gel**
ProSieve® 50 acrylamide gel solution	10% or 12% (v/v)	5%
Tris-HCl pH 8.8	375mM	-
Tris-HCl pH 6.8	-	125mM
SDS	0.1% (w/v)	0.1% (w/v)
Ammonium persulphate	0.05% (w/v)	0.05% (w/v)
TEMED	0.04% (v/v)	0.1% (v/v)

SDS-PAGE was performed at 100V, 40mAmp for approximately 2 hours, until the samples had migrated to the bottom of the resolving gel. Proteins were then visualised using Coomassie Brilliant Blue (Section 2.2.7.5) or immunoblotting as described below.

2.2.5.1. Immunoblotting

Proteins separated by SDS-PAGE were transferred from the gel onto nitrocellulose membrane (Protran®, grade BA85, Schleicher and Schuell Bioscience Inc., Keene, NH) in Transfer buffer [25mM Tris-HCl pH 9.2, 192mM Glycine, 0.1% (v/v) SDS, 20% (v/v) methanol] at 30V, 25mAmp for 16 hours at 4^{o}C.

Membranes were washed in 2x Blot Rinse buffer [10mM Tris pH7.4, 150mM NaCl, 1mM EDTA] containing 0.1% (v/v) Tween-20® (BRB/T) on an orbital shaker. Blocking was performed in Blocking buffer (BRB/T + 4% (w/v) non-fat dry milk) for 1.5 hours at room temperature on an orbital shaker. Membranes were incubated with primary antibody at room temperature for 1 hour on an orbital shaker. Primary antibody was diluted in BRB + 1% (v/v) NCS at concentrations detailed in Table 2.3. Membranes were then washed 3 times for 15min each time in 2XBRB/T on an orbital shaker before incubation with secondary antibody for 1hour at room temperature on an orbital shaker. Polyclonal HRP-conjugated secondary antibody (Stratech Scientific Limited, UK) was diluted in BRB + 1% (v/v) NCS 1:2000. After incubation, membranes were washed three times for 15min each time in 2XBRB/T on an orbital shaker.

500µl of enhanced chemiluminescence (ECL) reagent (Amersham Biosciences) was added to each membrane for 2 minutes. The chemiluminescence signal was detected using Hyperfilm™ ECL films (Amersham Biosciences) and a Compact X4 Automatic X-ray Film Processor (Xograph Imaging Systems Ltd., Gloucestershire, UK).

Table 2.3: Details of primary antibodies used in immunoblotting

Protein targeted/clone	Host Species	Dilution	Manufacturer/ Reference
Actin(AC-40)	Mouse	1:1000-1:2000	Sigma
α-tubulin	Mouse	1:1000	Sigma
Lamin A/C (JoL2)	Mouse	1:200	Dyer et al., 1997
Keratin 18	Mouse	1:1000	Oncogene
Vinculin (VIN-11-5)	Mouse	1:500	Sigma

2.2.6. Densitometry

Differences in protein expression as determined by immunoblotting were quantified using densitometry. Developed X-ray films were scanned in a Fujifilm Intelligent Dark Box II (Fujifilm Medical Systems, Edison, NJ) directed by Fujifilm Image Reader LAS-1000 Pro Ver.

2.11 software. Intensities were quantified using Image J (Rasband, W.S., ImageJ, U. S. National Institutes of Health, Bethesda, Maryland, USA, http://rsb.info.nih.gov/ij/, 1997-2009).

2.2.7. Proteomics

Equipment used for proteomic analysis was cleaned before use to remove keratins and other compounds that may interfere with proteomic analysis. All proteomic experiments were carried out in collaboration with Dr. J.W. Simon and Miss. J. Robson, Durham.

2.2.7.1. Protein sample preparation

2.2.7.1.1. Protein isolation

Biochemical fractionation was performed on SW480/lamA and SW480/cntl cell extracts in the procedure described in Section 2.2.3. However, instead of producing four pellets (P1-4) and four supernatants (S1-4) in each fractionation procedure, the sample was not split into four, and only P4 was produced. The supernatants were discarded. Each P4 was solubilised in 86µl lysis buffer [9M urea, 2M thiourea, 4% (w/v) CHAPS] plus 2µl protease inhibitor cocktail (Sigma), 2µl DNase (5 units/µl) and 10µl 0.4M NEM.

2.2.7.1.2. Acetone precipitation

Acetone precipitation is performed to remove any non-protein contaminants such as salt which may interfere with the 2D DIGE process. 1ml of ice-cold 80% (v/v) acetone was added to the cell pellet, which was then vortexed and incubated overnight at -20^{o}C before centrifugation at 15,000g for 10minutes at 4^{o}C in a bench top centrifuge (VWR). The supernatant was discarded and pellets were washed once more with ice-cold 80% (v/v) acetone before centrifugation at 15,000g for 10minutes at 4^{o}C. After the supernatant was removed, the pellet was air dried for 1 minute. The pellet was resuspended in 500µl Tris-urea labelling buffer [9M urea, 2M thiourea, 4% (w/v) CHAPS, 30mM Tris-HCl pH8.8] and vortexted for 1 hour. Samples were centrifuged for 10 minutes at 15,000g. All samples were stored at -20^{o}C for short-term and -80^{o}C for long-term storage.

2.2.7.1.3. Modified Bradford Assay

It is important to be able to accurately calculate protein concentration for 2D DIGE analysis so that identical amounts of protein can be added to each gel, to allow accurate comparisons.

The Bradford assay is a colorimetric assay which utilises the fact that Coomassie Brilliant Blue G-250 undergoes an absorbance shift from 465nm to 595nm when it binds to

proteins. An increase in absorbance at 595nm is proportional to the amount of Coomassie Brilliant Blue that has bound to proteins, and hence the protein concentration. The protein concentration of an unknown sample can be calculated by comparing its absorbance value to those of samples of known protein concentration. However, basic reagents present in samples prepared for 2D DIGE analysis, such as urea and carrier ampholytes, can interfere with the binding of Coomassie Brilliant Blue to proteins. A modified assay has therefore been developed in which dilute acid is added to protein samples at the start of the procedure, neutralising the sample (Ramagli and Rodriguez, 1985).

BSA (bovine serum albumin) standards in labelling buffer [9M urea, 2M thiourea, 4% (w/v) CHAPS, 30mM Tris-HCl pH8.8] ranging from 0-15µg were prepared from a stock solution of 1µg/µl and made up to a final volume of 15µl in ddH_2O. 2µl of protein samples in labelling buffer were also made up to a final volume of 15µl in ddH_2O water. To each sample, 10µl 0.1M HCl, 75µl ddH_2O water and 900µl of 25% (v/v) Protein Assay Dye Reagent Concentrate (BioRad) was added. Samples were vortexed and left to stand for 15min at room temperature. Absorbance at 595nm was measured using a spectrophotometer (Thistle Scientific, UK) and the concentrations of unknown protein samples were calculated using the absorbance values of the BSA standards.

2.2.7.2. Mini-format 1D SDS-PAGE

1D SDS-PAGE was performed as described in Section 2.2.5 using 12% gels, with 20µg protein added to each well.

2.2.7.3. Mini-format 2D SDS-PAGE

2.2.7.3.1. Protein loading by in-gel rehydration

7cm Immobiline™ Dry strips (GE Healthcare) were used with linear pH gradients of pH3-10 and pH4-7, as described in the results section. 125µl rehydration solution (50-100µg protein solubilised in 9M urea, 2M thiourea, 4% (w/v) CHAPS, 1% (w/v) DTT, 2% (v/v) IPG (immobilised pH gradient) buffer pH 3-10 or 4-7 (GE Healthcare), 0.002% (w/v) bromophenol blue) was added to each groove of an Immobiline™ DryStrip reswelling tray (Amersham Biosciences). IPG strips were laid gel-side down on top of the rehydration solution, covered with 2ml paraffin oil and left to rehydrate overnight.

2.2.7.3.2. First dimension isoelectric focusing (IEF)

IEF separates proteins according to their isoelectric points (pI). Briefly, hydrated strips were rinsed with ddH_2O and placed gel side up on a Multiphor II Electophoresis System connected to an EPS 3501 XL Powers Supply (Amersham Biosciences) with the acidic end towards the anode. Electrode wicks were soaked with ddH_2O and laid across each end of the IPG strips, making contact with the gels. Electrodes were placed on top of the wicks and paraffin oil was poured onto the strips. IEF was performed with a circulating water bath (Grant Instruments Ltd., Cambridgeshire, UK) maintaining the ceramic cooling plate at 20^{o}C to ensure IPG strips did not overheat. The electrophoresis programmes used are detailed in Tables 2.4 and 2.5. The current was maintained at 50µA/strip and the power at 5W. The Volt hours determined the length of the IEF run, and time was always in excess.

Table 2.4: IEF programme (pH 3-10)

Step	Volts (V)	Volt hours (Vh)
1	200	10
2	3500	2800
3	3500	3700
Total		6510

Table 2.5: IEF programme (pH 4-7)

Step	Volts (V)	Volt hours (Vh)
1	200	10
2	3500	2800
3	3500	5200
Total		8010

2.2.7.3.3. IPG strip equilibration

During strip equilibration, proteins are prepared for electrophoresis in the second dimension through reduction by DTT and binding to SDS. Iodoacetamide is used to alkylate the proteins' thiol groups, in order to prevent their re-oxidation during electrophoresis.

IPG strips were rinsed with ddH_2O and incubated in 2ml equilibration buffer (6M urea, 30% (v/v) glycerol, 2% (w/v) SDS, 50mM Tris HCl pH 8.8, 0.002% (w/v) bromophenol blue) supplemented with 1% (w/v) DTT on an orbital shaker, at room temperature for 15minutes.

The DTT/equilibration buffer was poured off, and equilibration buffer supplemented with 4.8% (w/v) iodoacetamide was poured onto the strips. This incubation was also carried out in the equilibration tray on an orbital shaker, at room temperature for 15minutes.

2.2.7.3.4. Second dimension SDS-PAGE

SDS-PAGE was performed as described in Section 2.2.5 using 12% resolving gels, with the following modifications:

The space above the resolving gel was rinsed with ddH_2O and the rinsed IPG strip was placed on top of the resolving gel, in the place of a stacking gel. 5µl PageRuler™ Prestained Protein Ladder Plus (Fermentas, York, UK) was loaded onto a small square of filter paper, which was placed next to the alkaline end of the IPG strip. Water was removed with blotting paper, and agarose sealing solution (1% (w/v) low melting point agarose, 0.002% (w/v) bromophenol blue in tank buffer [25mM Tris pH 8.3, 192mM Glycine, 0.1% (v/v) SDS] was poured on top of the strip. Proteins were then visualised using Coomassie Brilliant Blue or silver staining (Section 2.2.7.5).

2.2.7.4. Large-format 2D SDS-PAGE

2.2.7.4.1. Gel casting

Plates were soaked in 1% (v/v) Decon™ overnight before use to remove any polyacrylamide or protein that may be attached. Plates were then rinsed in water, soaked in 1% (v/v) HCl for one hour, rinsed with water and allowed to air dry. Plates were wiped with 2-4ml of Bind-saline solution [80% (v/v) ethanol, 0.01% (v/v) PlusOne Bind-Silane (Amersham Biosciences), 0.2% (v/v) glacial acetic acid] so the gel would be immobilized onto the glass plate. An a2DE optimizer (Nextgen Sciences, Huntingdon, UK) was used to cast 10% homogenous large format gels with low fluorescence glass cassettes (260mm x 200mm x 1mm).

2.2.7.4.2. Reswelling IPG strips

24cm IPG strips (pH4-7) (Amersham Biosciences) were rehydrated in an Immobiline™ Dry Strip Re-swelling Tray (Amersham Biosciences). Rehydration solution (lysis buffer, 1% (w/v) DTT, 2% ampholytes pH4-7, 0.002% (w/v) bromophemol blue) in a final volume of 500µl was placed into grooves in the tray and the IPG strips were laid gel-side down on top of the solution. 3ml paraffin oil was added onto the top of each strip to prevent urea crystallization and evaporation and strips were left to re-swell overnight.

2.2.7.4.3. Protein loading using anodic cups

Rehydrated strips were placed on the EttanIPGphor manifold tray (Amersham Biosciences), with the gel side facing up and the basic end at the cathode. Electrode wicks (5 x 12mm) were soaked in water and blotted to remove excess liquid. The wicks were placed at either end of each IPG strip and electrodes were clipped on top of each wick. Anodic cups were placed on the anodic end of each strip. 70µl paraffin oil was placed in each cup to ensure no leaks were present and 70µl sample containing 200µg or 500µg protein was then pipetted underneath the oil into the cups. Paraffin oil was poured on top of the IPG strips.

2.2.7.4.4. First dimension IEF

IEF was performed as described in Section 2.2.7.3.2 but on an Ettan™ IPGphor™ Isoelectric Focusing System (Amersham Biosciences). The samples were run overnight to a total of 70kVh at 50µA per strip at 20°C using the programme outlined in Table 2.6.

Table 2.6: IEF programme settings

Step	Step Type	Time	Volts (V)
1	Gradient	10min	500
2	Gradient	1hr20min	1000
3	Gradient	1hr40min	4000
4	Step 'n' Hold	10hr	6500
5	Step 'n' Hold	60hr	1000

2.2.7.4.5. IPG strip equilibration

Strips were equilibrated as described in Section 2.2.7.3 but using 5ml of each buffer as opposed to 2ml.

2.2.7.4.6. Second dimension SDS-PAGE

An Ettan™ DALT*twelve* Large Format Vertical System (Amersham Biosciences) was used for second dimension SDS-PAGE. The butan-1-ol in the space above the resolving gel was washed away using ddH_2O and the IPG strips were placed carefully onto the gel. The water was removed by blotting and agarose sealing solution (1% (w/v) low melting point agarose, 0.002% (w/v) bromophenol blue in Tris-glycine SDS electrophoresis buffer) was poured onto the strips.

7.5 litres of tank buffer [25mM Tris pH 8.3, 192mM Glycine, 0.1% (v/v) SDS] was added to the lower reservoir of the tank and 2.5 litres of 2x tank buffer was added to the upper reservoir. Electrophoresis was carried out at 5W per gel for 30 minutes followed by 17W

per gel for 4 hours at 25°C. After electrophoresis, gels were imaged by staining with SYPRO Ruby (Section 2.2.7.5).

2.2.7.5. In-gel protein staining

2.2.7.5.1. Coomassie Brilliant Blue R-250

Gels containing proteins separated by SDS-PAGE were stained sequentially in three Coomassie Brilliant Blue solutions (see Table 2.7) to allow the gradual removal of background staining. Volumes used (100-500ml) were appropriate for the size of the gel. Solutions were heated in a microwave for 30 seconds before the gel was placed in the solution and left to incubate with on an orbital shaker overnight (solution 1) or for 1hr (solutions 2 and 3). Gels were then washed with Destain solution (67.5% (v/v) until the background of the gel was transparent, with the protein bands stained blue. Gels were visualised using a Fujifilm Intelligent Dark Box II (Fujifilm Medical Systems, Edison, NJ) directed by Fujifilm Image Reader LAS-1000 Pro Ver. 2.11 software.

Table 2.7: Composition of Coomassie Brilliant Blue solutions

Component	Coomassie Blue solution			Destain Solution
	1	2	3	
1.25% (w/v) Coomassie Brilliant Blue R-250 in ddH_2O	2%	0.25%	0.25%	-
Propan-2-ol	25%	10%	-	-
Glacial Acetic Acid	10%	10%	10%	10%
Glycerol	-	-	-	10%

2.2.7.5.2. PlusOne silver staining

Gels were fixed in 250ml fixing solution [40% (v/v) methanol, 10% (v/v) glacial acetic acid] twice for 15 minutes each. This was poured off and 250ml sensitising solution [30% (v/v) methanol, 6.8% (w/v) sodium acetate, 0.2% (w/v) sodium thiosulphate] was added and incubated for 30 minutes. Gels were washed in deionised water three times for ten minutes each, then were incubated in 250ml of 0.5% (w/v) silver nitrate for 20 minutes. After brief washing with deionised water, gels were incubated in 250ml developing solution [2.5% sodium carbonate, 0.008% (w/v) formaldehyde] for approximately 4 minutes or until spots were visible. To stop the reaction, gels were transferred to 250ml of 1.46% (w/v) EDTA and incubated for ten minutes. Finally gels were washed in deionised water three times for five minutes each wash. Images were taken with a Fujifilm Intelligent Dark Box II

(Fujifilm Medical Systems, Edison, NJ) directed by Fujifilm Image Reader LAS-1000 Pro Ver. 2.11 software.

2.2.7.5.3. SYPRO Ruby

Gels were fixed in 250ml fixing solution [40% (v/v) methanol, 10% (v/v) glacial acetic acid] twice for 30-60 minutes each and then incubated in SYPRO™ Ruby Protein Stain (Genomic Solutions Ltd., Huntingdon, UK) overnight in the dark. Gels were rinsed briefly with deionised water, then incubated twice in de-stain solution [10% (v/v) methanol, 6% (v/v) acetic acid) for 1-2hrs each. All steps were performed with gentle agitation. Images were taken by a Typhoon Variable Mode Imager (GE Healthcare/Amersham Biosciences).

2.2.7.6. 2-Dimensional Difference in-Gel Electrophoresis

2D DIGE enables a quantitative analysis of proteins from multiple samples to be compared on one 2D gel.

2.2.7.6.1. CyDye Labelling

Protein samples were prepared as described in Section 2.2.7.1. The pHs of the samples were adjusted to pH 8-9 if necessary with 1M NaOH. CyDye DIGE Fluor minimal dyes (GE Healthcare) that had been reconstituted with DMF (dimethylformamide) (≤0.005% H_2O, ≤99.8% pure) were used at a concentration of 0.04mM. For each sample, 1µl of Cy-5 dye was added to 50µg protein in 38µl Tris-urea labelling buffer. A pooled standard was prepared by mixing 50µg protein from each sample in a total volume of 380µl Tris-urea labelling buffer and adding 10µl Cy-3 dye. After addition of the CyDye, samples were mixed by vortexing and left on ice in the dark. To quench the reaction after exactly 30 minutes, 1µl of 10mM lysine was added to each individual sample and 10µl of 10mM lysine was added to the pooled sample. Samples were then mixed by vortexing and incubated on ice for 10 minutes.

A 1D SDS-PAGE gel (Section 2.2.5) was run to evaluate the labelling efficiency. Gels were visualized using a Typhoon Variable Mode Imager (GE Healthcare/Amersham Biosciences).

10µg of each Cy5-labelled sample was mixed with 10µg of Cy3-labelled pooled internal standard, 80µl ddH_2O water, 400µl (80% v/v) acetone and 5µl 1.5M Tris pH8.8. Samples were incubated for an hour at room temperature then centrifuged (VWR) for 10 minutes at 14,000g, at room temperature. The supernatant was removed and the pellets were air dried for 3 minutes. Samples were resuspended in lysis buffer supplemented with 1% (w/v) DTT and 2% (v/v) ampholytes (pH4-7) in a final volume of 70µl and vortexed for two hours.

2.2.7.6.2. Large-format 2DE of labelled protein samples

This was performed as described in Section 2.2.7.4; however gels were run overnight at a total of 4W. This was increased to 17W per gel in the morning until the dye front had reached the base of the gel.

2.2.7.6.3. DIGE gel imaging

CyDye labelled proteins were visualized by a Typhoon Variable Mode Imager (GE Healthcare/Amersham Biosciences). The machine was switched on 30minutes before use to warm up, and the scanning surface was cleaned using lint-free tissue, 70% (v/v) ethanol and ddH_2O.

Immediately after SDS-PAGE, gels were rinsed with ddH_2O, dried with tissue and scanned. Gels waiting to be scanned were kept in the dark. +3mm Gel Alignment Guides were used and gels were scanned at the +3mm focal plane whilst being pressed to prevent movement. Cy3 images were scanned using a 532nm laser and a 580nm BP 30 emission filter. Cy5 images were scanned using a 633nm laser and a 670nm BP 30 emission filter. Initial images were scanned at 500µm (pixel size) resolution and an appropriate photomultiplier tube voltage was chosen to avoid pixel saturation. Final images were acquired at 100µm (pixel size) resolution and were saved as .GEL files. Two images were produced per gel, and these were overlaid and saved as multi-channel dataset (.ds) files.

2.2.7.6.4. Image analysis

Only four replicates of SW480/lamA were used in the analysis as the principle components analysis showed that one of the replicates was anomalous. Gel images were processed using Progenesis Samespots (Nonlinear Dynamics, UK). Gel images were aligned in automatic model then checked manually. An Anova test was performed, and spots with a p-value of <0.05 and a power of >0.7 were chosen to be identified by mass spectrometry. This list of 64 spots was further reduced to a list of 29 spots which were confirmed by eye to be likely to contain sufficient protein for mass spectrometry analysis.

2.2.7.7. Mass spectrometry

Trypic digestion of proteins was performed on a ProGest Workstation (Genomic Solutions Ltd.) using a ProGest robot according to the ProGest long trypsin digestion protocol. Protein spots were removed from the gel and placed in a 96 well microtitre plate containing microscopic holes to allow positive liquid displacement during reagent changes. Gel plugs were equilibrated in 50µl of 50mM ammonium bicarbonate, reduced and

alkylated with 10mM DTT and 100mM iodoacetamide and destained and dessicated with acetonitrile.

50mM ammonium bicarbonate containing 5% (w/v) trypsin (Promega) was used to rehydrate the gel plugs and digest the proteins for 12 hours at 37^{o}C. Extraction of the proteins was performed with 50% (v/v) acetonitrile, 0.1% (v/v) trifluoroacetic acid into a final volume of 50µl. Peptide extracts were freeze-dried and resuspended in 10µl 0.1% (v/v) formic acid.

Matrix-assisted laser-desorption/ionization time-of-flight/time-of-flight (MALDI-ToF-ToF) mass spectrometry was performed on a 4800 Plus MALDI TOF/TOF Analyser (Applied Biosystems, Warrington, UK).

1µl of matrix solution [saturated α-cyano-4-hydroxy-cinnamic acid in 50% (v/v) acetonitrile, 0.1% (v/v) trifluoroacetic acid and 10mM ammonium acetate] was spotted onto the MALDI target. 1µl peptide solution was then added to each position and left to dry for 1 hour.

TOF-MS analysis was performed using automated data acquisition and processing with the Applied Biosystems 4000 series Explorer software (v3.5) using reflector mode, 1000 total laser shots per spectrum, the mass range 700-4000 m/z and a laser intensity of 3300V. Spectra were then noise-corrected, peak de-isotoped and internally calibrated using the trypsin autolysis peaks 842.5100 and 221.1046 m/z. The eight most abundant precursor ions per spectra then underwent fragmentation and MS-MS analysis using a 1kV CID fragmentation method, with 4000 laser shots per spectra and a laser intensity of 3800 over the mass range.

2.2.7.7.1. Protein Identification

GPS Explorer software (v3.6, Applied Biosciences) generated peak lists of ion masses from the MS and MS-MS spectra for each sample. Combined lists of MS and MS-MS data were matched to theoretical trypsin digests of proteins from the NCBInr database (www.ncbi.nlm.nih.gov) using the MASCOT software (v2.2, Matrix Science) at a mass accuracy of 50ppm. The search included the parameters: digestion enzyme trypsin, single missed cleavage allowed, variable modifications of carboxymethyl cystein and oxidized methionine and fragment ion tolerance of 0.2Da.

Results were ranked by the MOWSE score (Pappin et al., 1993) which uses the number of peptide matches, the number of fragment ion matches, the matching accuracy and a weighting for large peptide fragment matches.

2.2.8. Wounding assays

Differences in cell motility were measured using scratch wound assays. SW480/lamA and SW480/cntl cells were seeded at $7.5x10^5$ cells per well in a 12 well plate. Once cells reached 100% confluency, the cell media was removed and wounds were made using a 10µl pipette tip (Star Lab, UK). The cell media was changed two times to remove floating cells. The wound area was visualized using a live cell imaging phase contrast microscope (Zeiss) at X10 magnification. Images were captured every 15minutes for 24 hours in identical wound locations. Three wound locations were chosen per well.

The width of the wound at the start (0hr) and end (24hr) of the experiment was measured six times for each wound at 100µm intervals using Axiovision Rel. 4.8 (Zeiss). The mean distance the cells moved in 24hours was calculated and standard errors were calculated from the biological replicates. A paired student t-test was used to test for statistical significance.

2.3. Results

2.3.1. Confirmation that SW480/lamA cells contain higher levels of GFP-lamin A and endogenous lamin A than SW480/cntl cells

SW480/lamA and SW480/cntl cells are used as a model system to investigate the effect of lamin A expression on colorectal cancer cells (Willis et al., 2008). To confirm that the cells were still expressing the expected levels of lamin A, protein levels were analysed by immunoblotting and densitometry (Figure 2.2). SW480/lamA cells contained GFP-lamin A, lamin A and lamin C, whereas SW480 cells contained only lamin A and lamin C, as expected. Expression of endogenous lamin A was over 30% higher in the presence of GFP-lamin A. When the expression levels of both endogenous lamin A and GFP-lamin A were taken into account, SW480/cntl cells contained 65% less lamin A than SW480/lamA cells.

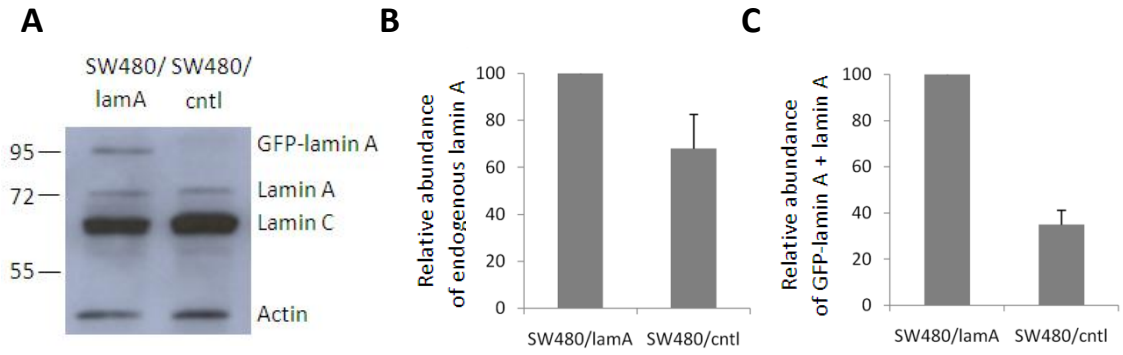

Figure 2.2: SW480/lamA cells contain higher levels of GFP-lamin A and endogenous lamin A than SW480/cntl cells

A Whole cell extracts of SW480/lamA and SW480/cntl cells were resolved on a 10% SDS-PAGE gel, transferred to nitrocellulose and probed with Jol2 (anti-lamin A/C) antibody. Actin antibody was used as a loading control.

B Densitometric analysis of endogenous lamin A expression in SW480/lamA cells relative to SW480/cntl cells. Images were taken with Fujifilm Intelligent Dark Box II and relative densities were measured with Image J software. Error bars represent standard errors.

C Densitometric analysis of GFP-lamin A plus endogenous lamin A expression in SW480/lamA cells relative to SW480/cntl cells, as above. Error bars represent standard errors.

2.3.2. Confirmation that SW480/lamA cells are more motile than SW480/cntl cells

Willis *et al.* demonstrated that SW480/lamA cells are more motile than SW480/cntl cells using scratch wounding assays (Willis et al., 2008). To confirm that SW480/lamA cells were still more motile than SW480/cntl cells, scratch wounding assays were performed. Cells were grown in 6-well plates and wounded with a 10µl pipette tip. The mean distance moved by cells in 24 hours was calculated from phase-contrast images. SW480/lamA cells were shown to be more motile than control cells (Figure 2.3). There was a statistically significant difference between the distance moved by SW480/lamA and SW480/cntl cells in 24 hours ($p<0.05$) using a paired t-test. SW480/lamA cells moved 20% further than SW480/cntl cells in 24 hours.

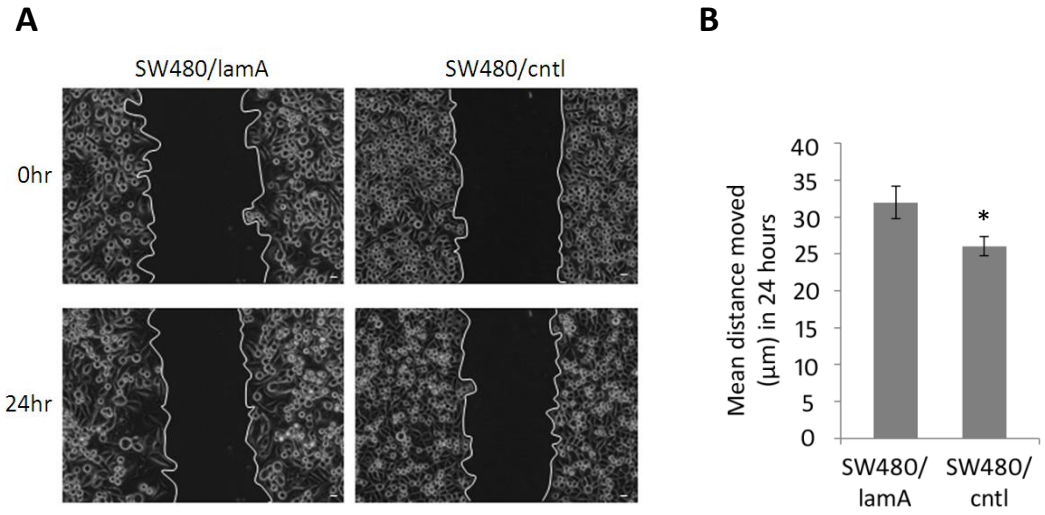

Figure 2.3: SW480/lamA cells are more motile than SW480/cntl cells

A Representative phase-contrast images of the start and end time points of the cell wounding assay. Cells were grown in 12-well plates and wounded with a 10µl pipette tip. Scale bars = 20µm.

B The mean distance moved by cells in 24 hours in scratch-wounding assays as calculated from phase-contrast images. In each experiment, three wound locations were chosen for each of three biological replicates and images were taken every 15 minutes for 24 hours. Error bars represent the standard error calculated from the biological replicates. There is a statistically significant difference between the distance moved by SW480/lamA and SW480/cntl cells in 24 hours (* = $p<0.05$) using a paired t-test. SW480/lamA cells moved 20% further than SW480/cntl cells in 24 hours.

2.3.3. Optimisation of biochemical fractionation protocol

To discover why expression of lamin A in colorectal cancer cells leads to increased cell motility, the cytoskeletons of SW480/lamA and SW480/cntl cells were investigated. A protocol to isolate the cytoskeleton in these cell lines was optimised, so that the differences in cytoskeletal protein expression could be determined using 2D DIGE. The advantage of running the cytoskeletal fraction on 2D gels rather than the whole cell extract is that the interpretation of results should in principle be easier, as the gel should be less crowded, allowing for higher resolution of proteins. The cytoskeleton was chosen for analysis as previous studies had implicated cytoskeleton proteins as determinants of altered cell motility in SW480/lamA cells (Willis et al., 2008).

The aim of the biochemical fractionation process was to isolate the cytoskeleton with a high yield and as few non-cytoskeletal proteins present as possible. It is important that the cytoskeleton is as structurally and functionally intact as is possible, with the minimum of protein denaturation. However, it must be noted that it is impossible to isolate the cytoskeleton in a completely natural state, as the cellular environment changes dramatically in a fractionation process and proteins may adhere to the cytoskeleton during homogenisation.

The original protocol used was an extraction protocol modified from Dyer et al (1997) (Section 2.2.3.1). Cells were grown to 70% confluency before undergoing a sequential extraction with CSK, CSK/TritonX-100 to remove membrane lipids and the soluble components of the cell, Dig/DNase to digest chromatin, and a final extraction with 0.25M ammonium sulphate to terminate DNase digestion (Fey et al., 1986; Zhai et al., 1987). The last insoluble fraction (P4) should contain the cytoskeleton and the nuclear matrix.

The first problem encountered was that in some immunoblots, two protein bands were seen very close together where just one band was expected, for example in Figure 2.4A there appears to be a double band for lamin C in the lanes containing P3 and P4. This may have been due to oxidation of the proteins, despite the presence of DTT in the buffers. Subsequently, DTT was replaced by 0.04M NEM in every 1ml of buffer in an attempt to prevent oxidation. This appeared to be much more effective (Figure 2.4B) as there were no double bands seen in subsequent immunoblots. The pellets and supernatants were also snap frozen in liquid nitrogen once they had been produced, to reduce the risk of protein degradation during the remainder of the procedure.

In some immunoblots, there was little or no detection of some proteins in the first insoluble fraction, P1 (Figure 2.4A). P1 is a whole cell extract therefore the proteins are not as effectively extracted in this fraction compared to the other fractions. Subsequently, to ensure efficient protein extraction, P1 was homogenised using a Dounce homogeniser before the addition of 2x sample buffer. The immunoblot in Figure 2.4B shows that bands in P1 representing A-type lamins became much more prominent; therefore it appeared that homogenising P1 was successful in extracting the proteins.

To further reduce the number of variable factors in the experiments, fractionation of both SW480/lamA and SW480/cntl cells was performed at the same time. The fractionation procedure was carried out immediately after cell harvesting. To allow comparisons to be made between the solubility of proteins in cells in confluent and non-confluent states (Section 2.3.4), cells were seeded on day 1 and extracted from flasks of both cell lines at the same time on day 2 (subconfluent cells) and day 4 (confluent cells). Cells were counted and the same number of cells was used for all four fractionations.

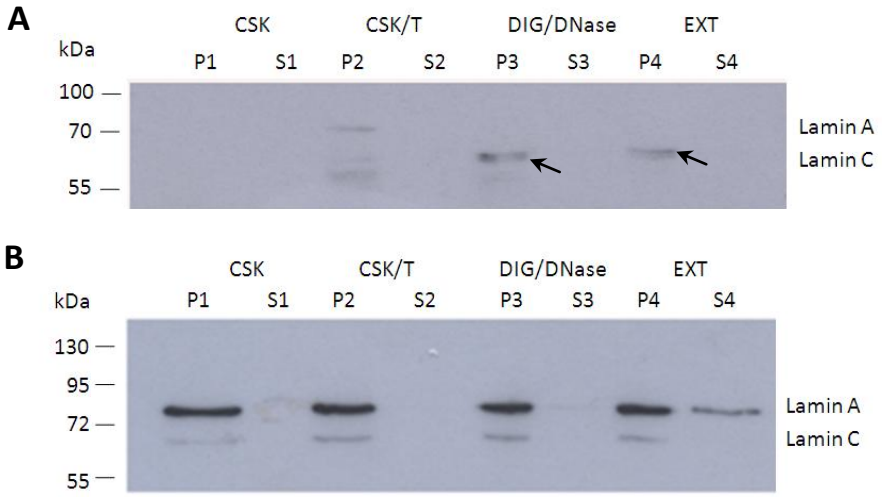

Figure 2.4: Optimisation of biochemical fractionation protocol

A Pellets and supernatants from biochemical fractionation of SW480/cntl cells were resolved on 10% SDS-PAGE gels, transferred to nitrocellulose and probed with Jol2 (anti-lamin A/C) antibody. DTT was added to samples to reduce protein oxidation, however double bands for lamin C can be seen in P3 and P4 fractions (arrows).

B Pellets and supernatants from biochemical fractionation of SW480/cntl cells were resolved on 10% SDS-PAGE gels, transferred to nitrocellulose and probed with Jol2 (anti-lamin A/C) antibody. NEM was added to samples to reduce protein oxidation and P1 was homogenised with a Dounce homogeniser to allow more efficient extraction of proteins.

2.3.4. Confluent and subconfluent SW480 cells show differences in solubility of α-tubulin, β-actin and lamin C

Cell density is known to affect protein expression, cytoskeletal dynamics, cell motility, cell signalling and cell-cell/cell-matrix interactions. With this in mind, biochemical fractionations were performed on cells that had been harvested when subconfluent (40-50% confluent) or confluent (95-100% confluent).

Figure 2.5 shows that, as expected, A-type lamins were present after each extraction step. Small amounts of lamin A and C were visible in some of the soluble fractions, particularly after ammonium sulphate extraction (S4). The ratio of lamin C: lamin A was greater in the insoluble fractions of subconfluent cells than in confluent cells.

Actin was present in all of the soluble and insoluble fractions studied. In SW480/cntl cells, there was less insoluble actin in subconfluent than in confluent cells. In SW480/lamA cells, there was less actin in the soluble fraction S2 of subconfluent cells than of confluent cells.

α-tubulin was present in all of the insoluble fractions of both confluent and subconfluent cells. A small amount of α-tubulin was visible in the first soluble fraction (S1) of confluent cells and very little/none was seen in subconfluent cells. No differences were observed in expression of α-tubulin between the two cell lines.

It is therefore important to ensure the cells are harvested when at the same confluency when preparing pellets for 2D DIGE analysis. 70% confluency was selected for further analysis, as this was the confluency used in previous experiments in our lab to analyse differences between SW480/lamA and SW480/cntl.

2.3.5. Cells expressing GFP-lamin A show changes in protein expression

The levels of retention of lamin A, lamin C and α-tubulin were broadly similar in SW480/cntl and SW480/lamA fractions (Figure 2.5). GFP-lamin A was present in SW480/lamA cells and not in SW480/cntl cells as expected.

In confluent cells, there was less insoluble actin in P1-3 of SW480/lamA cells compared to SW480/cntl cells. The profiles of actin retention were broadly similar in subconfluent cells, although there appeared to be more soluble actin in SW480/cntl compared to SW480/lamA in the first two fractionation steps.

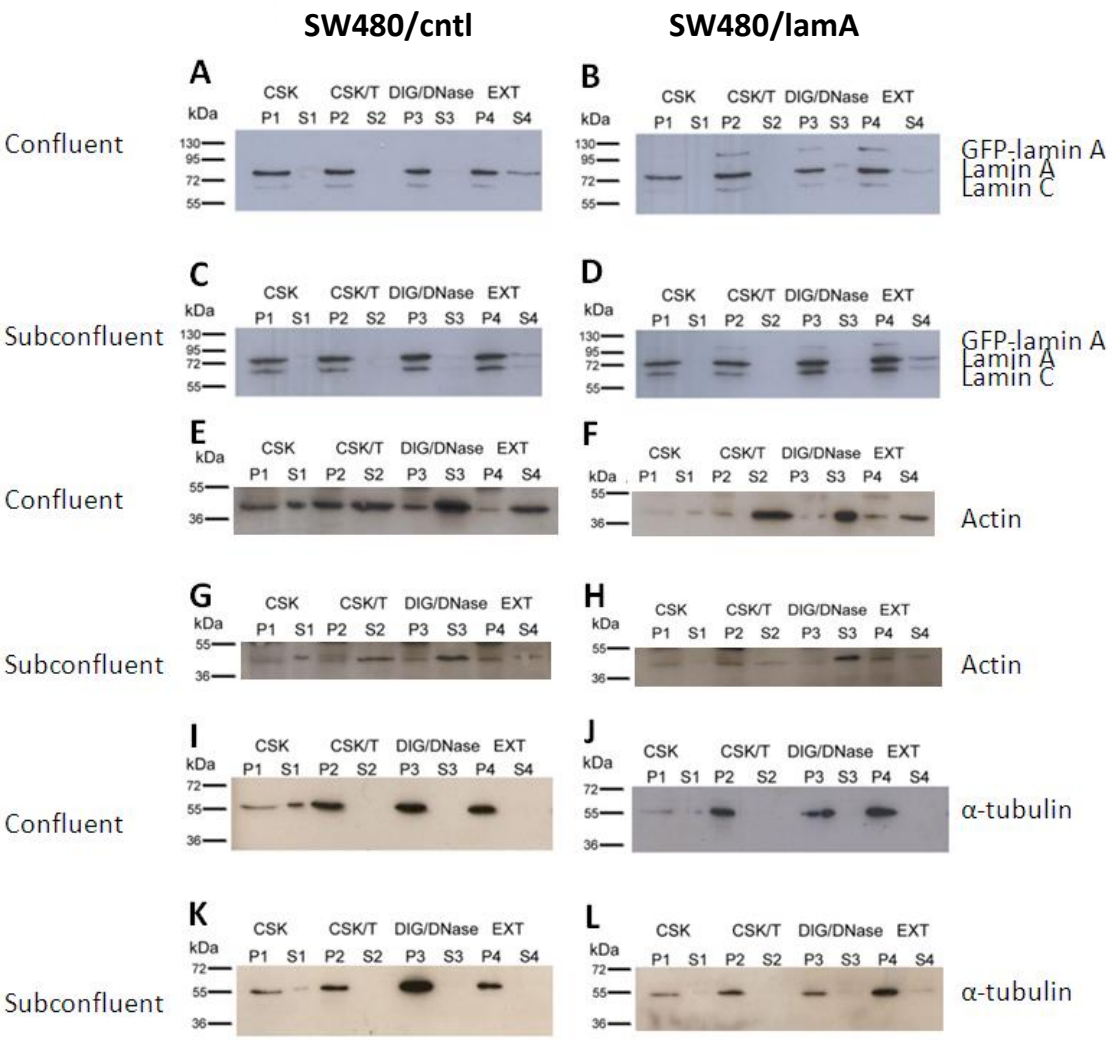

Figure 2.5: The effect of cell confluency and expression of lamin A on protein expression in colorectal cancer cells

Pellets and supernatants from biochemical fractionation of SW480/lamA and SW480/cntl cells were resolved on 12% SDS-PAGE gels and transferred to nitrocellulose. Blots were probed with Jol2 (anti-lamin A/C) **(A-D)**, anti-actin **(E-H)** or anti-α-tubulin **(I-L)** antibodies. 'Confluent' cells were harvested at 95-100% confluency and 'subconfluent' cells were harvested at 40-50% confluency.

2.3.6. Confirmation that insoluble fraction P4 contains the detergent/high salt resistant cytoskeleton

The immunoblots in Figure 2.5 show that A-type lamins, actin and α-tubulin are all present in the insoluble fraction P4 in both SW480/lamA and SW480/cntl cells. Figure 2.6 shows that keratin 18 is also present in P4 in both cell types. These results together demonstrate that the final insoluble pellet contains the detergent and high salt resistant nucleo/cytoskeletal (N/CSK) proteins.

To confirm that some proteins had been removed in the fractionation process, the expression of the membrane-bound protein vinculin was analysed using immunoblotting (Figure 2.6). Vinculin was mostly solubilised in the Triton X-100 extraction, as it is primarily present in the soluble fraction S2. A small amount of vinculin was still present in the insoluble pellet P4. Although vinculin is localised to the plasma membrane, it may be present in small amounts in P4 as it is known to bind to actin (Jockusch and Isenberg, 1981).

The final insoluble pellet P4 was therefore used in 2D DIGE analysis to investigate the effect of over-expression of lamin A in SW480 colorectal cancer cells on cytoskeleton organisation (Section 2.3.8).

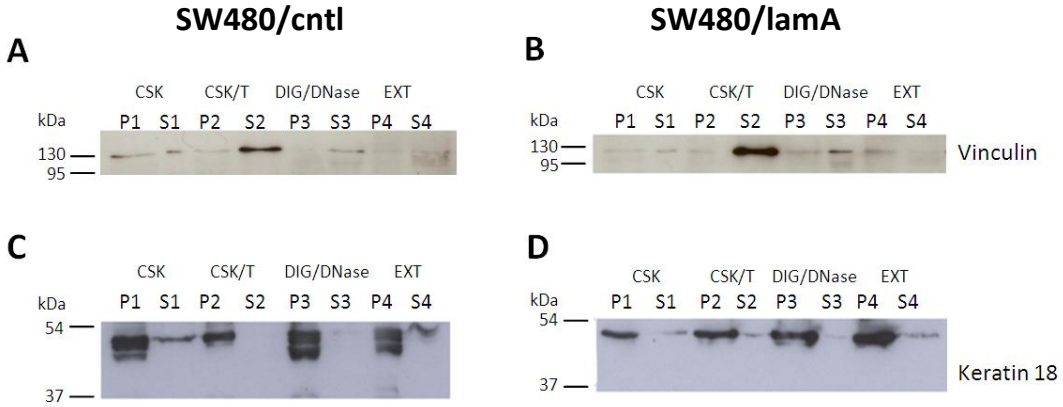

Figure 2.6: The membrane-bound protein vinculin is lost from detergent/high salt resistant N/CSK during biochemical fractionation of SW480 colorectal cancer cells, whereas keratin 18 remains mostly insoluble

Pellets and supernatants from biochemical fractionation of SW480/lamA and SW480/cntl cells were resolved on 12% SDS-PAGE gels and transferred to nitrocellulose. Blots were probed with anti-vinculin **(A, B)** or anti-keratin 18 **(C, D)** antibodies. Cells in blots A and B were harvested at 90-100% confluency and cells in blots C and D were harvested at 70-80% confluency.

2.3.7. Optimisation of 2D electrophoresis (2-DE)

2-DE (O'Farrell, 1975) allows the separation of a complex mixture of proteins in two dimensions. Proteins are first separated by their isoelectric points (pI) using isoelectric focusing and then according to their molecular weights using SDS-PAGE. 2-DE can be used to detect differences in protein expression between different samples and can also detect post- and co-translational modifications.

To prepare samples for 2-DE, proteins were precipitated with 80% (v/v) acetone and re-solubilised in lysis buffer [9M urea, 2M thiourea and 4% (w/v) CHAPS]. A modified Bradford assay was used to determine protein concentration (see Section 2.2.7.1). It is important to accurately quantify the amount of protein in each sample, particularly in 2D DIGE analysis, so that identical amounts of protein can be added to each gel to allow quantitative comparisons between samples.

IPG strips of different lengths were used in the 2-DE analysis. Initially, mini-format 2-DE gels were run with 7cm IPG strips, to quickly screen the samples in order to identify the correct pH range to be used and to ensure the biological replicates were reproducible. Large-format 2-DE gels were run with 24cm IPG strips for 2D DIGE analysis and to make preparative gels, from which samples were taken for mass spectrometry analysis. The longer IPG strips allow higher loading capacity and detection of more protein spots, therefore allowing easier identification of proteins.

Firstly, detergent/high salt resistant N/CSK, isolated from SW480/lamA and SW480/cntl cells were analysed using broad range (pH 3-10) IPG strips. 50µg of protein was loaded using in-gel rehydration into 7cm IPG strips. Proteins were resolved in the first dimension using isoelectric focusing. IPG strips were equilibrated and proteins were resolved in the second dimension using 12% mini-format SDS-PAGE gels. The resolved proteins were visualised using Coomassie Blue.

A number of proteins resolved well on the 2D gels. Most proteins appeared to be acidic and resolved within a pH range of 4-7. (Figure 2.7: A, B) To improve protein resolution and minimise the possibility that different proteins may migrate to the same position on the 2-DE gel, the same samples were run as described above, but using narrow range IPG strips (pH4-7) (Figure 2.7: C, D) Protein spots seen on both pH3-10 and pH4-7 gels were more clearly separated on pH 4-7 gels, demonstrating increased resolution.

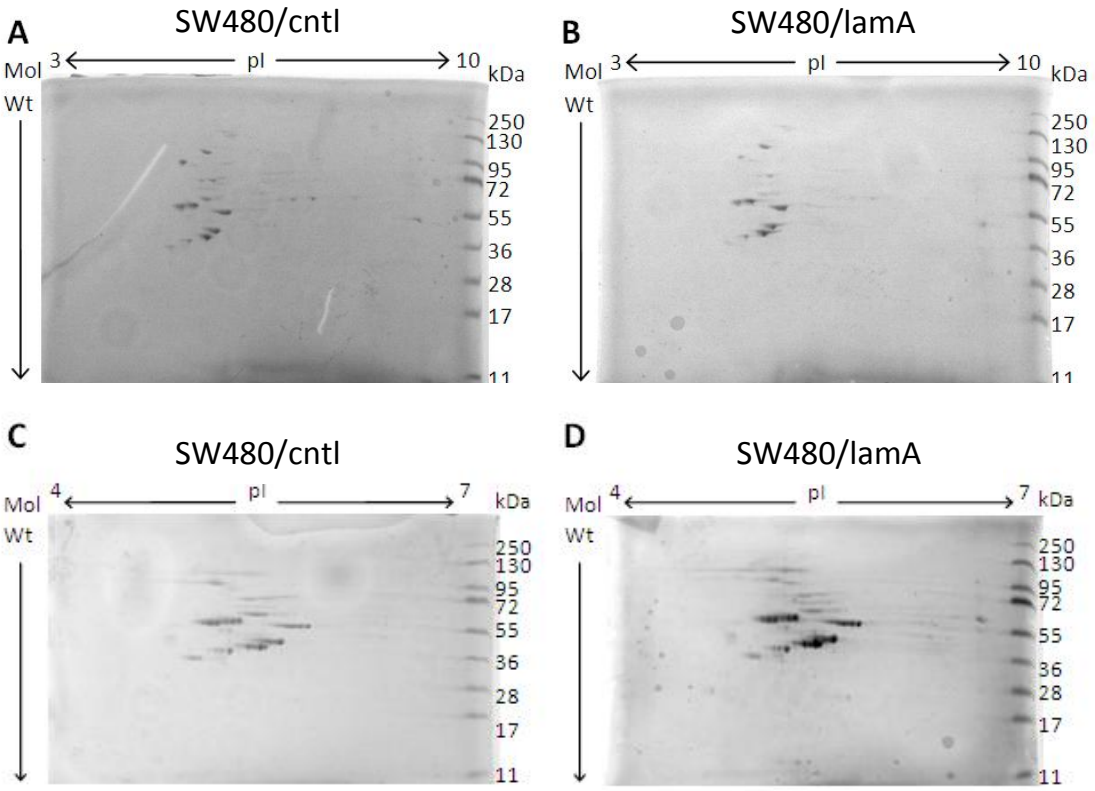

Figure 2.7: Optimisation of 2-DE protocol

Detergent/high salt resistant N/CSKs were isolated from SW480/lamA and SW480/cntl cells. Samples were acetone precipitated and resolubilised in lysis buffer.

A, B: 50µg of protein was loaded using in-gel rehydration into 7cm pH 3-10 IPG strips. Proteins were resolved in the first dimension using isoelectric focusing and in the second dimension using 12% mini-format SDS-PAGE gels. The resolved proteins were visualised using Coomassie blue staining. Images show mini-format gels run with replicate samples from SW480/cntl cells **(A)** and from SW480/lamA cells **(B)**.

C, D: 2-DE was performed as described above, with pH4-7 IPG strips and 100µg protein. Images show mini-format gels run with replicate samples from SW480/cntl cells **(C)** and from SW480/lamA cells **(D)**.

It is important to study biological replicates to increase confidence that any differences found between samples are due to a genuine biological difference. Proteomic analysis of the differences between SW480/lamA and SW480/cntl requires the biological replicates to be highly reproducible so that quantitative comparisons can be made. To ensure the protein profiles of biological replicates were reproducible, detergent/high salt resistant N/CSKs were isolated from SW480/lamA and SW480/cntl cells in six independent experiments. A 12% 1D SDS-PAGE gel was run with 20µg protein from each of the biological replicates from both cell types and stained using Coomassie blue (Figure 2.8). This showed that the biological replicates were reproducible and that the determination of concentration using the modified Bradford assay was accurate. It was also evident that there is very little obvious difference between the two samples and therefore a quantitative approach such as 2-D DIGE would be necessary to accurately determine the differences.

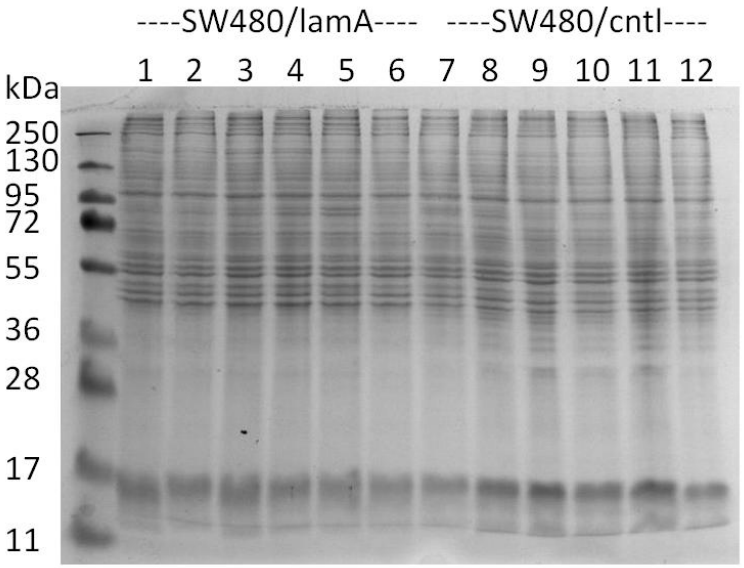

Figure 2.8: 1D gel shows reproducibility of samples for 2D DIGE

Detergent/high salt resistant N/CSKs were isolated from SW480/lamA and SW480/cntl cells in five further independent experiments. Samples were acetone precipitated and re-solubilised in lysis buffer. 20µg protein was added to each well of a 12% SDS-PAGE gel which was stained with Coomassie Blue after electrophoresis.

Each biological replicate was then run on a mini-format 2-DE gel to discover if the 2D gel profiles were reproducible (Figure 2.9). 100µg of protein was loaded using in-gel rehydration into 7cm pH 4-7 IPG strips. Proteins were resolved in the first dimension using isoelectric focusing. IPG strips were equilibrated and proteins were resolved in the second dimension using 10% mini-format SDS-PAGE gels. The resolved proteins were visualised using Coomassie Blue. The images show that the biological replicates are reproducible.

It was thought that a 10% gel might increase the separation of high molecular weight proteins; however the visible protein spots were closer together on the 10% gels than in the 12% gels. Hence, 12% gels were used in subsequent experiments.

As the 1D gel (Figure 2.8) revealed many high molecular weight proteins not seen on the mini 2D gels (Figure 2.9), a large format 2D gel was run and stained with SYPRO Ruby to discover whether or not the profile was more complicated than it appeared with Coomassie blue staining. 200µg of protein was loaded using anodic cups into 24cm pH 4-7 IPG strips. Proteins were resolved in the first dimension using isoelectric focusing. IPG strips were equilibrated and proteins were resolved in the second dimension using 12% large format SDS-PAGE gels (Figure 2.10). These gels revealed that more high molecular weight protein spots were visible than on the mini-format 2D gels stained with Coomassie blue.

Figure 2.9: 2D mini-format gels confirm reproducibility of replicate samples of detergent/high salt resistant N/CSKs and demonstrate that a pH range of 4-7 is appropriate for 2D DIGE

Detergent/high salt resistant N/CSKs were isolated from SW480/lamA and SW480/cntl cells in six independent experiments. Samples were acetone precipitated and resolubilised in lysis buffer. 100µg of protein was loaded using in-gel rehydration into 7cm pH 4-7 IPG strips. Proteins were resolved in the first dimension using isoelectric focusing and in the second dimension using 10% mini-format SDS-PAGE gels.

The resolved proteins were visualised using Coomassie blue staining. Images show mini-format gels run with replicate samples from SW480/cntl cells (**A, C, E, G, I, K)** and from SW480/lamA cells **(B, D, F, H, J, L)**.

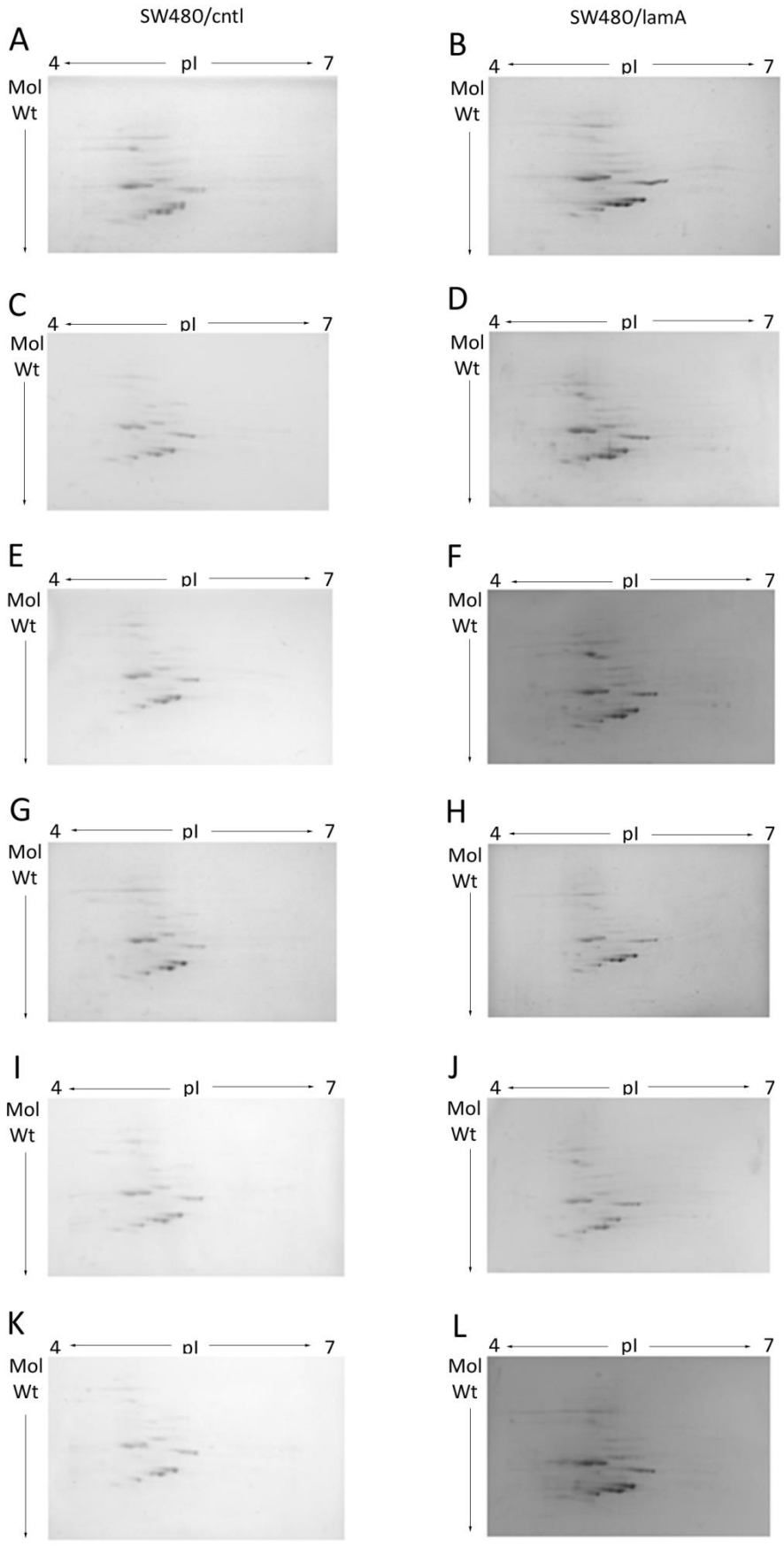
SW480/cntl
SW480/lamA
A
B
C
D
E
F
G
H
I
J
K
L
4
pI
7
Mol
Wt

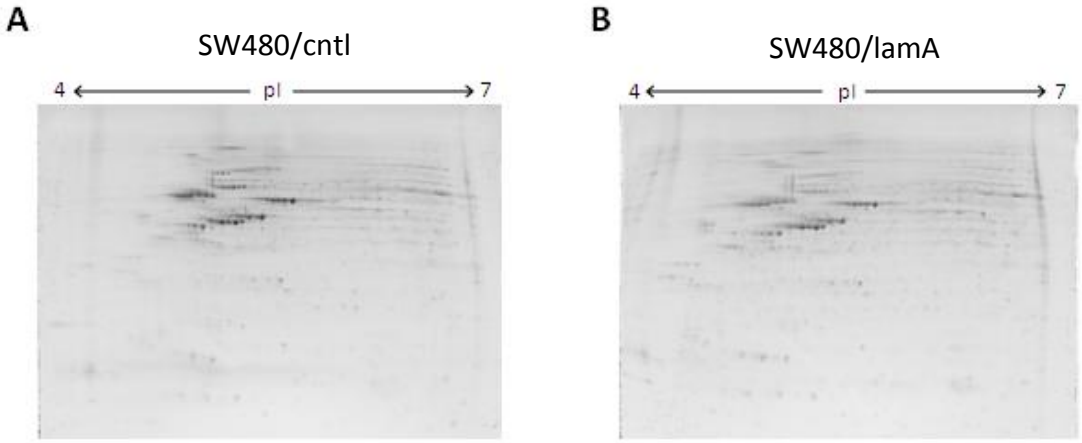

Figure 2.10: 2D large-format gels stained with SYPRO Ruby

Detergent/high salt resistant N/CSKs were isolated from SW480/lamA and SW480/cntl cells in six independent experiments. Samples were acetone precipitated and resolubilised in lysis buffer. 200ug of protein from the third replicate of each cell type was loaded using in-gel rehydration into 24cm pH 4-7 IPG strips. Proteins were resolved in the first dimension using isoelectric focusing and in the second dimension using 10% large-format SDS-PAGE gels. The resolved proteins were visualised using SYPRO Ruby staining. Images show large-format gels run with replicate 3 from SW480/cntl cells (**A)** and from SW480/lamA cells **(B).**

2.3.8. 2D difference in-gel electrophoresis (2D DIGE)

2D DIGE (Unlu et al., 1997) allows differences in protein expression between samples to be accurately detected by labelling samples with CyDyes before electrophoresis. CyDyes are mass and charge matched so that identical proteins labelled with any CyDye will migrate to identical locations on a 2D gel. An internal standard is included on every gel to remove the effects of inter-gel variation, and is produced by mixing together aliquots of all the samples in the experiment. This allows quantitative comparisons to be made between gels, based on the ratio of the protein abundance in the sample compared to the standard. Statistical methods can then be employed to analyse changes in protein abundance between different samples.

Six biological replicates were originally produced, but replicate 2 from both SW480/lamA and SW480/cntl cells was discarded as the cells had been isolated at a slightly lower cell density than the other five replicates.

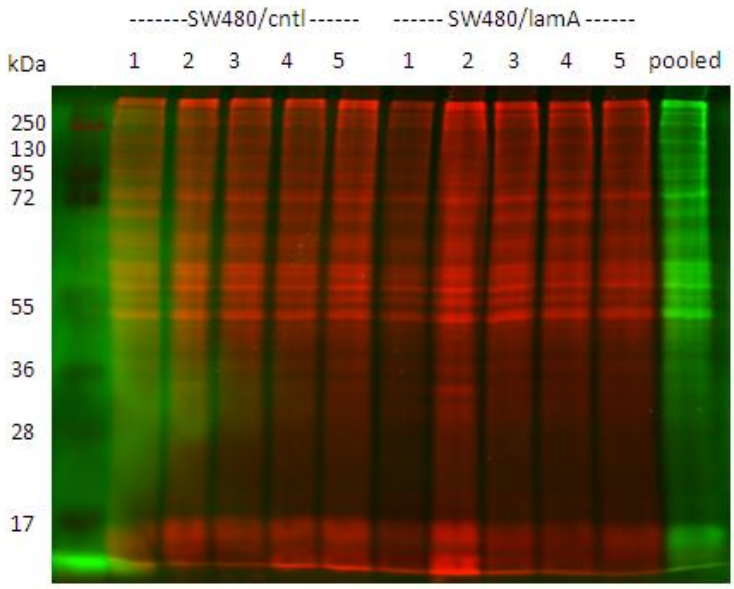

Figure 2.11: Samples for 2D DIGE analysis labelled with Cy3 and Cy5

Detergent/high salt resistant N/CSKs isolated from SW480/lamA and SW480/cntl cells were labelled with Cy5 and a pooled internal standard was labelled with Cy3. 4µg of each labelled sample was run on a 12% SDS-PAGE gel and visualised with a Typhoon Variable Mode Imager.

For each sample, 1µl of CyDye was added to 50µg protein (prepared as for 2-DE) in 38µl Tris-urea labelling buffer. SW480/lamA and SW480/cntl samples were both labelled with Cy5, and the pooled internal standard was labelled with Cy3. CyDye labelling was confirmed by running 4µg of each labelled sample on a 12% SDS-PAGE gel (Figure 2.11).

Samples were loaded using anodic cups into 24cm pH 4-7 IPG strips. Proteins were resolved in the first dimension using isoelectric focusing. IPG strips were equilibrated and proteins were resolved in the second dimension using 12% large format SDS-PAGE gels. Gels were scanned using a Typhoon Variable Mode Imager and the images were processed using Progenesis Samespots. Gel images were aligned in automatic model then checked manually. Only four replicates of SW480/lamA were used in the final 2D DIGE analysis as the principle components analysis showed that one of the replicates (replicate 1) was anomalous. An Anova test was performed, and spots with a p-value of <0.05 and a power of >0.7 were chosen to be identified by mass spectrometry. This list of 64 spots was further reduced to a list of 29 spots which were confirmed by eye to be likely to contain sufficient protein for mass spectrometry analysis (Figure 2.12).

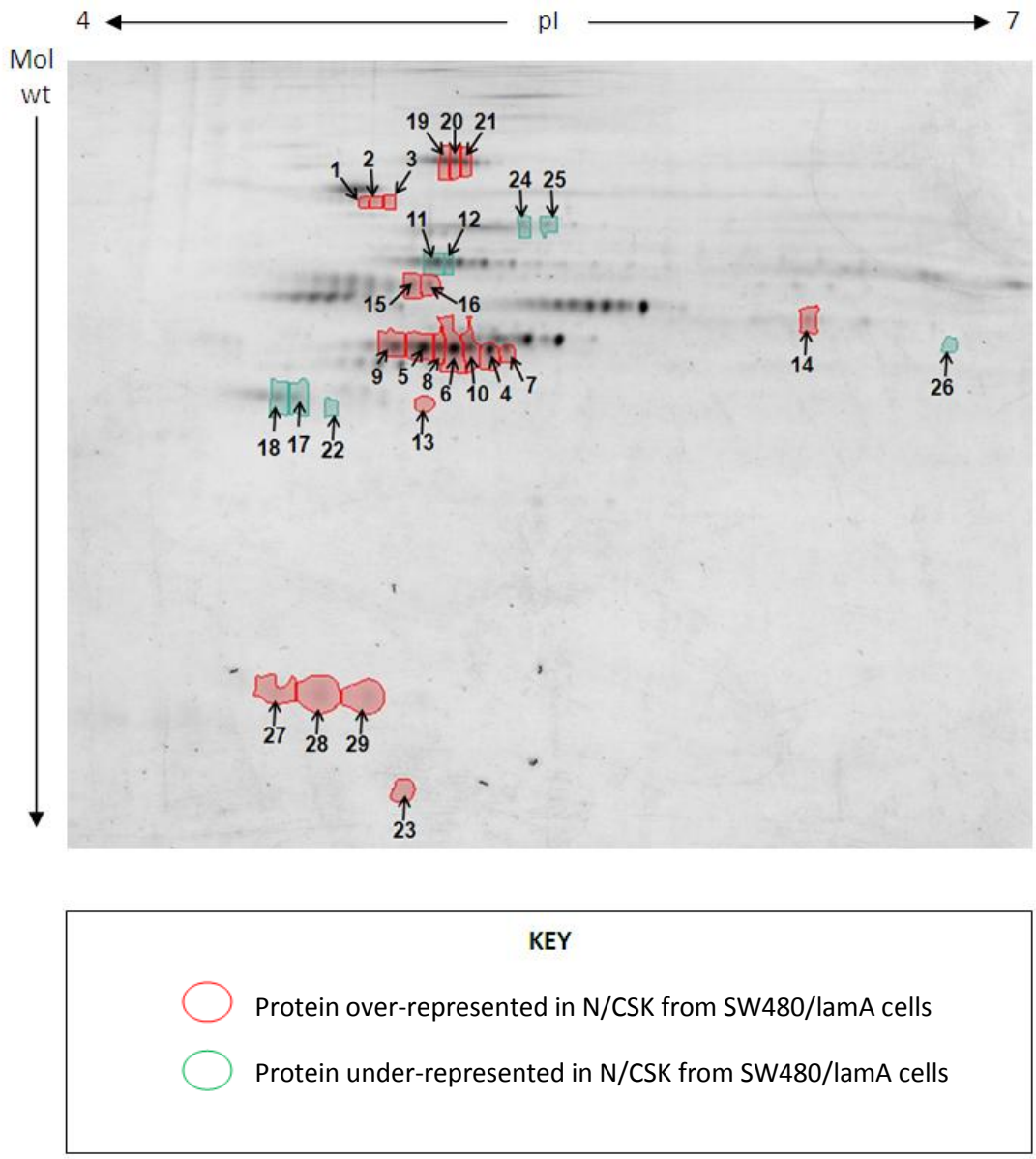

Figure 2.12: 2D DIGE reveals differences in protein abundances of detergent/ high salt resistant N/CSK from SW480/lamA and SW480/cntl cells

2D DIGE gel comparing detergent/ high salt resistant N/CSK from SW480/lamA and SW480/cntl cells. Arrows represent protein spots selected for analysis by MALDI-ToF-ToF

In order to identify the protein present in each spot, 2-DE preparative gels were run with 500µg protein. Protein samples were loaded using anodic cups into 24cm pH 4-7 IPG strips and proteins were resolved in the first dimension using isoelectric focusing. IPG strips were equilibrated and proteins were resolved in the second dimension using 12% large format SDS-PAGE gels. The 29 protein spots identified by 2D DIGE analysis were removed from the gel using a Genomic Solutions ProGest robot and subjected to tryptic digestion. MALDI ToF-ToF analysis was performed on the samples and combined lists of MS and MS-MS data were matched to theoretical trypsin digests of proteins from the NCBInr database (www.ncbi.nlm.nih.gov) using the MASCOT software (v2.2, Matrix Science) at a mass accuracy of 50ppm. The proteins identified are detailed in Figures 2.13 and 2.14. Proteins identified with a MOWSE score higher than 82 were considered significant.

Eight proteins were over-represented in the cytoskeletal fraction of SW480 cells expressing lamin A: transglutaminase 2, β-actin, eIF2α, EF-1γ, vimentin, actinin α4, histone cluster 2 H4b and eIF5A. Five proteins were under-represented in the cytoskeletal fraction of SW480/lamA cells: Hsp60, nucleophosmin, EF-1δ, mortalin and EF-Tu.

Many of the proteins (transglutaminase 2, Hsp60, vimentin, nucleophosmin, actinin α4, mortalin and eIF5A) migrated as a train of two or three distinct spots with similar M_r but differing pI values. The largest number of mobility forms was observed for β-actin which was identified in a train of seven spots. The spots found in trains of mobility forms were discovered to have very similar fold change values, with a range of no more than 0.2.

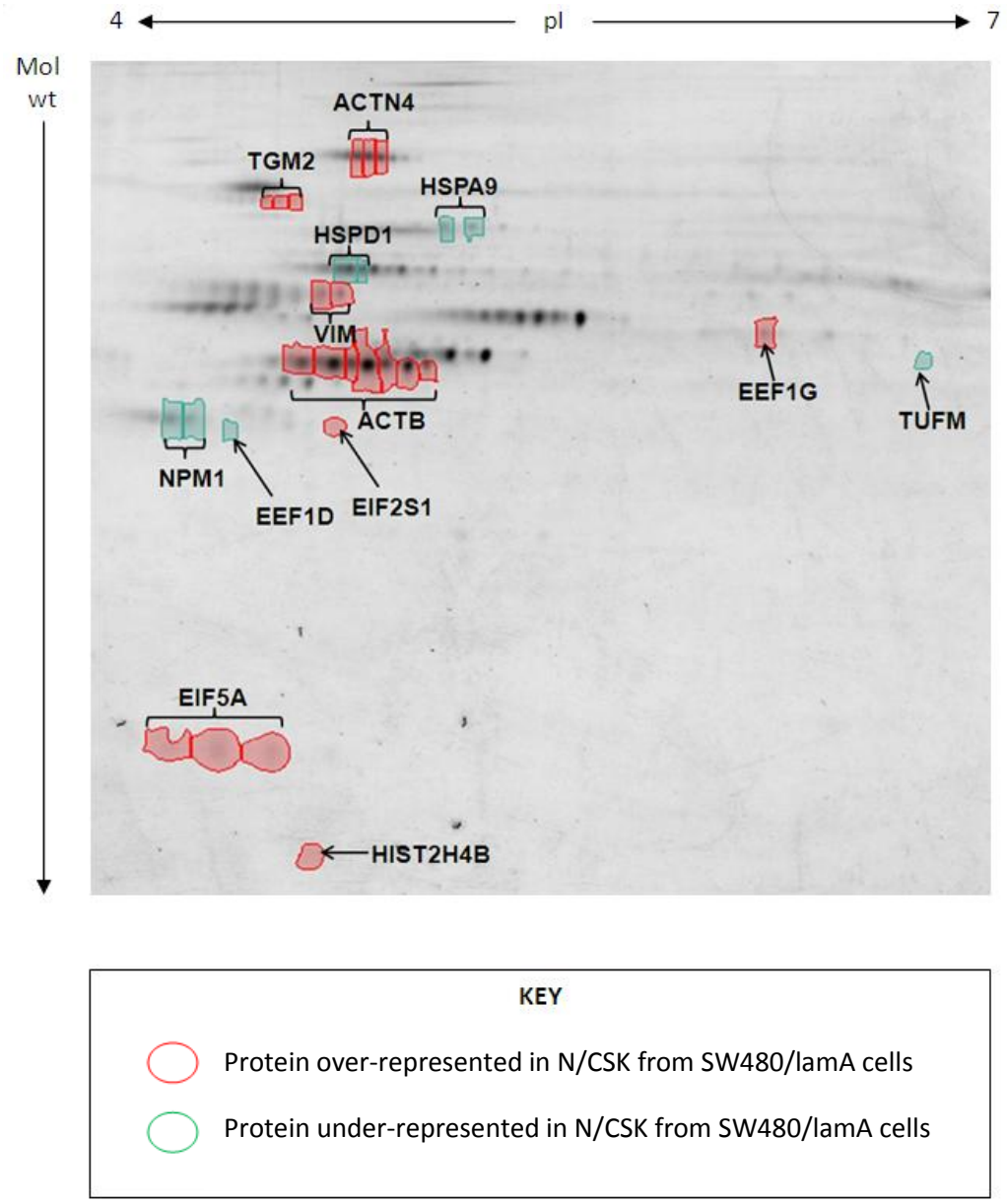

Figure 2.13: 2D DIGE and MALDI-ToF-ToF mass spectrometry reveal differences in protein abundances of detergent/ high salt resistant N/CSK from SW480/lamA and SW480/cntl cells

2-D DIGE gel comparing detergent/ high salt resistant N/CSK from SW480/lamA and SW480/cntl cells, annotated to show the identities of the proteins determined by MALDI-ToF-ToF

Table 2.8: Protein spots from Figure 2.11A identified using mass spectrometry					
Spot no.	**Gene symbol**	**Gene name**	**MS only protein score**	**MOWSE score**	**Fold change**
1	TGM2	Transglutaminase 2	63	108	3.3
2	TGM2	Transglutaminase 2	88	180	3.5
3	TGM2	Transglutaminase 2	73	102	3.3
4	ACTB	Beta actin	170	766	1.6
5	ACTB	Beta actin	183	592	1.6
6	ACTB	Beta actin	212	791	1.6
7	ACTB	Beta actin	190	680	1.5
8	ACTB	Beta actin	136	398	1.5
9	ACTB	Beta actin	132	273	1.5
10	ACTB	Beta actin	203	656	1.4
11	HSPD1	Heat shock 60kDa protein 1 (chaperonin)	81	148	1.5
12	HSPD1	Heat shock 60kDa protein 1 (chaperonin)	164	345	1.5
13	EIF2S1	Eukaryotic translation initiation factor 2, subunit 1 alpha, 35kDa		56	1.4
14	EEF1G	Eukaryotic translation elongation factor 1 gamma	173	446	1.4
15	VIM	Vimentin	373	422	1.3
16	VIM	Vimentin	174	233	1.4
17	NPM1	Nucleophosmin	60	166	1.3
18	NPM1	Nucleophosmin	118	164	1.4
19	ACTN4	Actinin, alpha 4	401	722	1.2
20	ACTN4	Actinin, alpha 4	374	683	1.2
21	ACTN4	Actinin, alpha 4	383	698	1.2
22	EEF1D	Eukaryotic translation elongation factor 1 delta	145	294	1.7
23	HIST2H4B	Histone cluster 2, H4b		117	2.1
24	HSPA9	Heat shock 70kDa protein 9 (mortalin)	335	701	1.5
25	HSPA9	Heat shock 70kDa protein 9 (mortalin)	348	701	1.7
26	TUFM	Tu translation elongation factor, mitochondrial		166	1.6
27	EIF5A	Eukaryotic translation initiation factor 5A		166	1.6
28	EIF5A	Eukaryotic translation initiation factor 5A		127	1.6
29	EIF5A	Eukaryotic translation initiation factor 5A		215	1.6

Tables 2.8-2.10 reveal the identities of the proteins highlighted in the 2D DIGE experiment, their MS only and MOWSE scores and their fold changes

Table 2.9: Proteins over-represented in N/CSK of SW480/lamA cells				
Spot Number(s)	**Gene Symbol**	**Protein Name**	**MOWSE score**	**Fold change**
1-3	**TGM2**	Transglutaminase 2	102 - 180	3.3-3.5
4-10	**ACTB**	β-actin	273 - 791	1.4-1.6
13	**EIF2S1**	Eukaryotic translation initiation factor 2, subunit 1 alpha, 35kDa	56	1.4
14	**EEF1G**	Eukaryotic translation elongation factor 1 gamma	446	1.4
15-16	**VIM**	Vimentin	233 - 422	1.3-1.4
19-21	**ACTN4**	Actinin, α4	683-722	1.2
23	**HIST2H4B**	Histone cluster 2, H4b	117	2.1
27-29	**EIF5A**	Eukaryotic translation initiation factor 5A	127-215	1.6

Table 2.10: Proteins under-represented in N/CSK of SW480/lamA cells				
Spot Number(s)	**Gene Symbol**	**Protein Name**	**MOWSE score**	**Fold change**
11-12	**HSPD1**	Heat shock 60kDa protein 1 (chaperonin)	148 - 345	1.5
17-18	**NPM1**	Nucleophosmin	164-166	1.3
22	**EEF1D**	Eukaryotic translation elongation factor 1 delta	294	1.7
24-25	**HSPA9**	Heat shock 70kDa protein 9 (mortalin)	701	1.5-1.7
26	**TUFM**	Tu translation elongation factor, mitochondrial	166	1.6

2.4. Discussion

The aim of this study was to investigate the changes induced in the insoluble cytoskeleton when lamin A is over-expressed in colon carcinoma cells, leading to increased cell motility. We used biochemical fractionation to isolate a cytoskeletal fraction from SW480/lamA and SW480/cntl cells and then performed 2D DIGE to analyse the changes in abundance of proteins in this fraction. It is important to note that we were not comparing differences in protein expression between the two cell types, rather the changes in abundance of proteins associated with the cytoskeleton. Previous studies have used quantitative proteomics to investigate changes in cancer cell motility; however this is the first study to focus on a cytoskeletal fraction.

Proteomic analysis using 2D DIGE requires the biological replicates to be highly reproducible so that quantitative comparisons can be made, in order to increase confidence that any differences found between samples are due to a genuine difference in protein abundance. Immunoblots comparing protein expression in confluent and subconfluent cells revealed that there were differences in the solubility of A-type lamins and α-tubulin. Hence, cells were always harvested when 70% confluent, to keep the cell density constant between biological replicates. 2D gels resolving the proteins present in the last insoluble pellet (P4), which contained cytoskeletal-related proteins, were shown to be highly reproducible. In conclusion, we were very satisfied that the methodologies used were reliable and the biological replicates produced were reproducible.

Spots present on all the 2D DIGE gels were subjected to an Anova test and 64 spots had a p-value of <0.05 and power of >0.7 and were considered to be significantly differentially expressed. 29 out of the 64 spots were considered likely to contain sufficient protein for mass spectrometry analysis and these spots were analysed by MALDI ToF-ToF. The strict statistical criteria used to define proteins that were differentially expressed gives further confidence in the reliability of the data.

We found that most of the 29 spots analysed represented multiple isoforms of a set of 13 proteins. If this is also true of the 35 spots not subjected to MALDI ToF-ToF analysis, it is possible that as few as 30 salt and detergent resistant proteins are needed to modify the cytoskeleton in order to promote increased cell motility. Many of the proteins (transglutaminase 2, Hsp60, vimentin, nucleophosmin, actinin α4, mortalin, eIF5A and β-actin) migrated as a train of between two and seven distinct spots with similar M_r but differing pI values. Interestingly, the spots found in trains of mobility forms were

discovered to have very similar fold change values, with a range of no more than 0.2. This gives further confidence that the fold changes identified are reliable. The gel mobility isoforms may represent post-translational modifications such as phosphorylation and acetylation (Anderson et al., 2010; Coulonval et al., 2003; Halligan et al., 2004).

MALDI ToF-ToF analysis identified eight proteins that were over-represented in the cytoskeletal fraction of SW480 cells expressing lamin A: transglutaminase 2, β-actin, eIF2α, EF-1γ, vimentin, actinin α4, histone cluster 2 H4b and eIF5A. Five proteins were identified that were under-represented in the cytoskeletal fraction of SW480/lamA cells: Hsp60, nucleophosmin, EF-1δ, mortalin and EF-Tu. Twelve out of these thirteen proteins fall into three distinct categories: components/modifiers of the CSK, protein chaperones and translation initiation/elongation proteins.

eIF5α, EF-1γ and EF-1δ are all involved in translation elongation and EF-1γ and EF-1δ are both subunits of the elongation factor 1 complex (Riis et al., 1990; Saini et al., 2009). EF-Tu is involved in protein synthesis in mitochondria, where it drives the cycle of peptide elongation and eIF2α is a subunit of eIF2, which catalyses the first regulated step of protein synthesis initiation (Sonenberg and Dever, 2003).

Most of these proteins have known roles in cancer. eIF5A is a regulator of p53, p53-dependent apoptosis and TNF-alpha-mediated apoptosis and over-expression of eIF5A has been shown to induce apoptosis in colon cancer cells (Taylor et al., 2007). eIF2α is over-expressed in many tumour types, including gastrointestinal carcinoma (Lobo et al., 2000; Rosenwald et al., 2001; Wang et al., 2001; Wang et al., 1999). High levels of Ef-1γ have been seen in many tumour types, including colon tumours, compared to their normal counterparts (Chi et al., 1992; Lew et al., 1992; Mathur et al., 1998). Over-expression of EF-1γ mRNA in gastric and oesophageal carcinomas was correlated with tumour aggressiveness (Mimori et al., 1996; Mimori et al., 1995). EF-1δ mRNA and/or cDNA expression was higher in some cancer cells and tumours compared to their normal counterparts (Kolettas et al., 1998; Ogawa et al., 2004; Shuda et al., 2000). EF-1δ mRNA expression was correlated with lymph node metastases and poorer prognosis in oesophageal cancer (Ogawa et al., 2004). However, the effect of EF-1δ in colon carcinoma has not yet been studied and the effects of EF-1δ on tumours may be cell-type specific. Down-regulation of EF-Tu is associated with human colonic epithelial ageing (Yi et al., 2010). Although high levels of EF-Tu were found in tumour tissue compared to normal tissue (Koch et al., 1990), little is known about the role of the protein in cancer.

The changes seen in the retention of translation factors may reflect an association between transcriptional machinery and the cytoskeleton or the nuclear matrix. The cytoskeleton is known to be a site for targeted protein synthesis, and EF1α co-localises with F- and β-actin mRNA at cell protrusions of crawling cells (Bassell and Singer, 1997; Bassell et al., 1994; Liu et al., 2002; Singer, 1992; Yang et al., 1990). The findings might reflect the hypothesis that there is a trans-cellular network which physically links the interior of the nucleus via the lamins and the cytoskeleton to the extracellular matrix, allowing signalling between the outside of the cell and the interior of the nucleus.

Histone cluster 2 H4b was over-represented in the cytoskeletal fraction of SW480 cells expressing lamin A. Histone cluster 2 H4b has only recently been found at the protein level (Jufvas et al., 2011) and its function is as yet unknown. Lamins have been shown to bind to histones (Mattout et al., 2007; Taniura et al., 1995), therefore the change in the abundance of histone cluster 2 H4b may reflect changes in the organisation of chromatin associated with lamin A expression.

Three of the five proteins that were under-represented in the cytoskeletal fraction of SW480/lamA cells (Hsp60, mortalin and nucleophosmin) are protein chaperones. All three are implicated in cancer (Cappello et al., 2005a; Dundas et al., 2005; Lim and Wang, 2006) and are known to bind to CSK proteins or influence CSK dynamics and organisation (Kuwabara et al., 2006; Sandsmark et al., 2007; Staubach et al., 2009).

Nucleophosmin (B23) is a nucleolar phosphoprotein that shuttles between the nucleus and the cytoplasm. It has been suggested that nucleophosmin can act as both an oncogene and a tumour suppressor gene (Lim and Wang, 2006). It regulates tumour suppressors such as p53 and ARF (Gjerset, 2006). The role of nucleophosmin in regulation of the cytoskeleton and cell motility is also complex. It is involved in regulating centrosome duplication (Okuda et al., 2000; Tokuyama et al., 2001) and maintaining the correct organisation of the microtubule network (Wang et al., 2010). HeLa cells lacking nucleophosmin were found to have a disrupted microtubule network, with less polymerised tubulin (Wang et al., 2010). Recently, knockdown of nucleophosmin has been shown to cause distortion of α-tubulin and β-actin structure, resulting from defects in centrosomal microtubule nucleation (Amin et al., 2008). Nucleophosmin is a regulator of actin cytoskeleton dynamics. In astrocytes, increased expression of nucleophosmin led to decreased actin stress fiber formation and inhibition of nucleophosmin shuttling caused increased cell motility (Sandsmark et al., 2007). It is possible that the decreased association of nucleophosmin with the cytoskeleton

in SW480/lamA cells is linked to increased actin dynamics or increased actin stress fibre formation, which is often found in invasive cells (Miettinen et al., 1994; Zavadil et al., 2001).

Hsp60 is a molecular chaperone found mostly in the mitochondria, but also in the cytosol, cell surface, extracellular space and peripheral blood (Cappello et al., 2008). Many studies have investigated the role of Hsp60 in cancer. Hsp60 levels are often increased in colorectal tumours when compared to normal cells and tissues (Cappello et al., 2003; Cappello et al., 2005a; He et al., 2007; Mori et al., 2005). Elevated Hsp60 levels were found to correlate with high tumour grade and high occurrence of lymph node metastases in large bowel carcinomas (Cappello et al., 2005a). However, Hsp60 expression is not always elevated in cancer cells (Cappello et al., 2005b; Lebret et al., 2003) and Hsp60 may both promote and prevent apoptosis in tumour cells (Chandra et al., 2007; Kirchhoff et al., 2002; Lin et al., 2001; Samali et al., 1999; Xanthoudakis et al., 1999). In HUVECs (human umbilical vein endothelial cells) treated with digoxin to induce apoptosis, lamin A was up-regulated and HSP60 was down-regulated, and overexpression of Hsp60 led to decreased apoptosis (Qiu et al., 2008). There is no consistent effect of Hsp60 expression on prognosis between or even within cancer subtypes (Chaiyarit et al., 1999; Kimura et al., 1993; Lebret et al., 2003; Schneider et al., 1999; Thomas et al., 2005).

Mortalin is a member of the Hsp70 family and, like Hsp60, is a chaperone protein found primarily in the mitochondria but also in other cellular locations such as the plasma membrane, endoplasmic reticulum, cytoplasmic vesicles and the cytosol (Ran et al., 2000; Singh et al., 1997). Some members of the Hsp70 family of proteins have been shown to bind tubulin (Gache et al., 2005; Sanchez et al., 1994; Williams and Nelsen, 1997) and mortalin is known to bind the microtubule protein RHAMM (receptor for hyaluronan mediated motility) (Kuwabara et al., 2006). Mortalin expression is elevated in many, but not all, cancer cells and tissues (Dundas et al., 2005; Wadhwa et al., 2006). Dundas *et al.* showed that mortalin is over-expressed in colorectal tumours. High levels of mortalin correlated with poor prognosis independent of Dukes stage (Dundas et al., 2005).

The final part of this discussion will focus on the final four proteins which were over-represented in the cytoskeletal fraction of SW480/lamA cells: tranglutaminase 2, β-actin, actinin α4 and vimentin.

β-actin is one of six different actin proteins and is one of the two non-muscle cytoskeletal actins (Vandekerckhove and Weber, 1978). Actin proteins are vital for cells to be able to

move, divide and maintain their shape and they are found as globular G-actin monomers or filamentous F-actin. All known forms of migration require the reorganisation of the actin cytoskeleton. It is widely known that migration occurs through actin polymerisation at the leading edge of the cell and contraction at the sides and rear of the cell, generated by actin-myosin filaments. β-actin is present at the leading edge of the cell and in actin bundles such as stress fibres, filopodia and at cell-to-cell contacts (Dugina et al., 2009; Hoock et al., 1991). Depletion of β-actin by siRNA causes fibroblasts to move more slowly than controls (Dugina et al., 2009). It appears that the links between actin polymerisation, cell motility and metastasis are complex. Over-expression of β-actin in myoblasts caused increased cell motility, although this did not result from an increase in the rate of actin polymerisation (Peckham et al., 2001). However, an increase in the F:G actin ratio was found in the cytosol of three metastatic colon adenocarcinoma cell lines compared to a non-metastatic control, suggesting actin polymerisation is increased in metastatic cells (Nowak et al., 2002). In invasive carcinoma cells from mammary tumours, the genes coding for genes that regulate β-actin polymerisation, such as the cofilin capping protein and Arp2/3 pathways were up-regulated (Wang et al., 2004).

Actinin α4 is an F-actin cross-linking protein and a member of the spectrin gene superfamily (Honda et al., 1998). It also acts as a nucleocytoplasmic shuttling molecule and may be involved in regulation of gene expression (Kumeta et al., 2010). Actinin α4 is known to be associated with invasion and metastasis in many cancers, including CRC (Honda et al., 1998; Honda et al., 2005; Kikuchi et al., 2008; Yamamoto et al., 2009). Actinin α4 is enriched at the leading edges of invasive cells (Honda et al., 1998) and has been shown to increase cell motility in CRC (Honda et al., 2005). Down-regulation of actinin α4 reduces cell motility in glioblastoma and lung fibroblasts (Sen et al., 2009; Shao et al., 2010a). In cells stimulated with EGF, actinin α4 is phosphorylated and dissociated from actin filaments (Shao et al., 2010b). High total or cytoplasmic expression of actinin α4 is significantly associated with poor survival in breast, pancreatic and ovarian cancer (Honda et al., 1998; Kikuchi et al., 2008; Yamamoto et al., 2007).

Tissue transglutaminase (tTG, TG2) is a ubiquitously expressed multifunctional protein. It has both intracellular and extracellular functions, and can be found localised to the cytosol, plasma membrane, nucleus or ECM. TG2 contains a Ca2+ regulated transamidase active site and cross-links proteins through catalysing the formation of a ε-(γ-glutamyl) lysine isopeptide bond. TG2 is thought to play a role in the organisation of the cytoskeleton, as actin, α-actinin, tubulin, myosin, cofilin and Hsp27 protein 1 are all TG2 substrates (Nemes

et al., 1997; Orru et al., 2003; Puszkin and Raghuraman, 1985; Robinson et al., 2007). TG2 is also known to co-localise with stress fibres in human umbilical vein endothelial cells (Chowdhury et al., 1997). Interestingly, TG2 substrates identified in colon cancer cells include EF-1α, EF-1γ, Hsp60 and members of the Hsp70 family (Orru et al., 2003).

TG2 expression is associated with increased cell adhesion an TG2 is known to bind fibronectin and has been shown to be an adhesion co-receptor of β1 and β3 integrins (Akimov et al., 2000; Cai et al., 1991; Gaudry et al., 1999; Gentile et al., 1992; Jones et al., 1997). TG2 is involved in wound healing (Verderio et al., 2004) and down-regulation of TG2 causes a significant decrease in migration and adhesion of monocytic cells on fibronectin (Akimov and Belkin, 2001). TG2 is also an activator of RhoA, which is involved in cytoskeletal rearrangement, a process required for cell migration (Ridley and Hall, 1992; Singh et al., 2003b).

Increased expression of TG2 has been demonstrated in many types of tumours and cancer cells when compared to normal counterparts and expression of TG2 in colorectal cancer, breast cancer, malignant melanoma and ovarian carcinoma was higher in metastatic tumours than in primary tumours (Fok et al., 2006; Hwang et al., 2008; Mehta et al., 2004; Miyoshi et al., 2010; Verma et al., 2006). Down-regulation of TG2 by siRNA was shown to inhibit metastasis (Hwang et al., 2008; Verma et al., 2008). TG2 activity and expression is sometimes found to be lower in tumour tissues than normal tissues (Barnes et al., 1985; Birckbichler et al., 2000). Expression of TG2 in cancer cells is often associated with decreased prognosis (Hwang et al., 2008; Miyoshi et al., 2010) however intra-tumoural injection with TG2 was shown to increase survival (Jones et al., 2006). Colorectal cancer patients with high expression of TG2 have a poorer rate of overall survival than those with low TG2 expression ($P = 0.001$) (Miyoshi et al., 2010). The effect of TG2 expression therefore may depend on the type and stage of the cancer, or on the cellular localisation of TG2 (Mehta et al., 2010).

One substrate of TG2 that was also over-represented in the SW480/lamA cytoskeletal fraction is vimentin (Clement et al., 1998; Gupta et al., 2007). Vimentin is a type III intermediate filament protein and a marker of mesenchymal cells, which organises many proteins involved with cell adhesion, signalling and migration. Vimentin polymers are motile and highly dynamic and there is subunit exchange between the different forms, which include non-filamentous particles, short filaments known as ‘squiggles’ and long ‘mature’ intermediate filaments (Chou et al., 2007). Our results demonstrate that there is

more insoluble vimentin in SW480/lamA cells compared to control cells, which could reflect the organisation of the different vimentin forms in these cells.

Vimentin regulates the function of integrins, which are transmembrane cell adhesion receptors. Integrins connect the ECM to the actin cytoskeleton and convert signals from the ECM into cellular responses such as changes in cell morphology, proliferation and migration (Brakebusch and Fassler, 2003). Fibroblasts derived from vimentin null mice show defects in cell migration (Eckes et al., 1998) and down-regulation of vimentin expression in SW480 cells results in impaired migration and invasion (McInroy and Maatta, 2007). Vimentin expression was higher in CRC when compared to normal tissue, along with β-actin and Hsp60 (Alfonso et al., 2005). Expression of vimentin in cancers has been linked to enhanced invasiveness and aggressiveness of cancers (Nagaraja et al., 2006; Singh et al., 2003a; Zajchowski et al., 2001). Vimentin expression in the tumour stroma of CRC was associated with poor prognosis (Ngan et al., 2007).

It is possible that the changes observed in the cytoskeleton are a result of TG2 cross-linking actin, vimentin and α4-actinin to other cytoskeleton proteins. The under-representation of chaperonin proteins in the cytoskeletal fraction may also be explained by altered regulation of the cross-linking of these proteins to the cytoskeleton by TG2. The reduced association, particularly of B23, within the cytoskeleton might alter the balance between stress fibre formation and other forms of filamentous actin, a hallmark of invasive cells (Miettinen et al., 1994; Zavadil et al., 2001).

Another process which might be involved in the observed changes is the epithelial-mesenchymal transition (EMT) as vimentin, TG2 and actin are known to be involved in EMT. EMT is a well-known process in development and wound healing, in which epithelial cells convert to mesenchymal cells. Epithelial cells are tightly packed cells which line body cavities and surfaces and are connected by adherens junctions, tight junctions and desmosomes; mesenchymal cells are highly mobile and invasive with an elongated morphology and front end-back end polarity. EMT also occurs in cancer, and provides a mechanism by which tumour cells can leave the primary tumour and metastasise. Molecules that induce EMT in development are also known to induce EMT in cancer, such as TGF-β, Wnt and Snail/Slug (Cui et al., 1996; Huber et al., 2005; Kim et al., 2002; Savagner et al., 1997; Zavadil and Bottinger, 2005). The hallmarks of EMT are downregulation of epithelial markers such as E-cadherin, upregulation of mesenchymal markers, typically

vimentin or fibronectin, increased cell migration and invasion and a fibroblast-like cell morphology.

TG2 expression was shown to induce an epithelial-mesenchymal transition (EMT) in ovarian cancer cells (Shao et al., 2009) leading to increased cell invasiveness and metastasis. TG2 was also shown to induce EMT in mammary epithelial cells (Kumar et al., 2010). In these studies, expression of TG2 caused the loss of E-cadherin and up-regulation of mesenchymal markers such as vimentin, fibronectin and N-cadherin, and transcriptional repressors such as Snail1, Slug, Zeb1 and Zeb2.

Remodelling of the actin cytoskeleton is a pre-requisite for EMT, whereby intercellular junctions are dissociated and cortical actin is reorganised into actin stress fibres (Miettinen et al., 1994; Zavadil et al., 2001). In EMT, TGFβ targets guanine nucleotide exchange factors, which activate Rho GTPases, which lead to formation of actin stress fibres (Bhowmick et al., 2001; Ridley and Hall, 1992; Shen et al., 2001). Actin filaments in stress fibres are held together by α-actinin (Lazarides and Burridge, 1975). There is no information in the published literature about the role of actinin α4 in EMT of cancer cells, however it may have a role to play in this process as it is known that α-actinin is up-regulated in mouse mammary gland epithelial cells in response to TGFβ (Xie et al., 2003).

In the following chapters we will investigate expression of genes and proteins to explore further the possible mechanisms, including EMT, by which the colon carcinoma cells over-expressing lamin A become more motile.

CHAPTER THREE

The identification of a network of changes in gene expression induced by over-expression of lamin A

3.1. Introduction

Cancer cells progress from normal to transformed to metastatic as a result of many genetic alterations (Hanahan and Weinberg, 2000). Understanding the motility of cancer cells is important in order to improve diagnosis and prognosis of cancer and to develop therapeutic approaches to control metastasis. In the previous chapter, changes in the cytoskeleton and its associated proteins were investigated when lamin A was over-expressed in colon carcinoma cells. To further elucidate the mechanism leading to increased cell motility in these cells, we decided to study the results of a DNA microarray analysis comparing genome-wide expression levels of genes in SW480/lamA and SW480/cntl cells. Our aim was to use bioinformatic approaches to find groups of genes with common functions which were differentially expressed in these cells and to highlight potential candidates for future analysis.

Over the last two decades, genome-wide gene expression profiling has become an invaluable tool in understanding cancer initiation and progression. DNA microarrays are the most commonly used method for large scale whole genome experiments as expression levels of genes across the entire human genome can be quantified in a single experiment. Applications of DNA microarrays include the identification of diagnostic and prognostic biomarkers, therapeutic targets, genetic signatures of tumours and responses to chemotherapy (Beane et al., 2009; Heller, 2002).

In this study, the Affymetrix GeneChip® Human Genome U133 (HG-U133) Plus 2.0 Array was used, which allows the analysis of the entire human genome. On this microarray, each gene or sequence is represented by a probe set comprising eleven probe pairs, which are 25 bases long and span a target sequence of around 600 bases. The probe pairs comprise Perfect Match (PM) and Mismatch (MM) probes and contain identical oligonucleotide sequences, except for the central base in the MM probe which is mismatched. The MM probes are used as a control for non-specific hybridisation and the eleven probe pairs provide independent measurements for every transcript. Probe sets corresponding to

constitutively expressed human maintenance genes are present on the microarray, to be used as normalisation controls (http://www.ohsu.edu/xd/research/research-cores/gmsr /project-design/array-technology/affymetrix-genechip-arrays.cfm).

Results produced from microarray experiments present challenges for data analysis, as it is difficult to identify the relevant biological processes from the large quantity of information generated. Hence, it is necessary to use applications that can give an overview of the biological processes implicated in the dataset and collate the data into clusters of known biological function. IPA® (Ingenuity® Systems, www.ingenuity.com) is a web-based software application which can be used to analyse data from experiments such as microarrays and metabolomic and proteomic experiments. The IPA software contains the Ingenuity® Knowledge Base, a database of biological interactions derived from millions of individually modelled relationships between proteins, genes, complexes, cells, tissues, drugs, and diseases. The database is curated by content and modelling experts, and contains data from over 200,000 peer-reviewed publications (Calvano et al., 2005). From this information, a molecular network, known as an 'interactome', has been generated, in which molecules are linked due to known direct physical, transcriptional and enzymatic interactions. The interactome allows new experimental data to be examined in the context of existing knowledge of genome-wide interactions. In this study, IPA was used to construct interaction networks highlighting the biological processes that are over-represented in the microarray data.

Microarray datasets should be validated by an alternative quantitative method of measuring gene expression, in order to have confidence in the datasets. Real time Q-PCR (Chiang et al., 1996; Gibson et al., 1996; Heid et al., 1996; Higuchi et al., 1993) is the gold standard technique for quantitative transcriptome analysis and is a method commonly used to validate microarray data. It allows gene expression to be quantified precisely, even from very small starting amounts of cDNA.

In real time Q-PCR, nucleic acid sequences are simultaneously amplified and quantified throughout the PCR reaction. A thermocycler is used to measure molecules that give a fluorescent signal as a result of probe hydrolysis (TaqMan, Applied Biosystems); probe hybridisation (LightCycler, Roche); hairpin probe hybridisation (LUX, Invitrogen); hairpin-loop hybridisation (Molecular Beacons, Sigma) or binding to double stranded DNA (SYBR Green) (VanGuilder et al., 2008). In this study, SYBR green detection was chosen due to the expertise in our lab and its relative cost and ease of use. SYBR green-based detection is not

sequence specific and thus the presence of primer-dimers and amplification errors will give erroneous fluorescence readings. Hence, primers were checked carefully for sequence specificity and a lack of self-complementarity. In a real time Q-PCR reaction, the fluorescence signal is measured during the exponential amplification phase. C_T (cycle threshold) numbers are generated which denote the amplification cycle at which the fluorescent signal exceeds a threshold above the background fluorescence (baseline). Therefore, the higher the C_T value, the lower the gene expression.

Q-PCR data can be analysed by absolute quantification, through calculating the number of copies of a specific RNA, or relative quantification, through comparing the gene expression in two or more samples. In this study I used relative quantification as I wanted to compare gene expression in SW480/lamA and SW480/cntl cells. I used the $2^{-\Delta\Delta CT}$ method (Livak and Schmittgen, 2001) as this is the most common method for relative quantification of real time Q-PCR results. This method calculates the fold change in expression based on the C_T values of the two samples to be compared, normalised to an endogenous control gene which is expressed at a constant level in each sample.

In summary, it was hoped that IPA-based analysis of microarray data comparing gene expression in SW480/lamA and SW480/cntl cells and validation by Q-PCR would shed light on the mechanisms underlying the increased cell motility seen in colon carcinoma cells over-expressing lamin A.

3.2. Materials and Methods

3.2.1. Microarray

The microarray experiment was performed by Dr. N. Willis (Durham University) and Dr. H. Peters (Newcastle University). Briefly, SW480/lamA and SW480/cntl cells were cultured as described in Section 2.2.2. Total RNA was extracted from cells at 70-80% confluency with TRI Reagent™, according to the manufacturer's instructions. Genome-wide microarray analysis was performed using a Human Genome U133 Plus 2.0 high density oligonucleotide Affymetrix GeneChip Array (Affymetrix, Santa Clara, CA, USA).

3.2.2. Analysis of microarray dataset

The microarray dataset analysis was a collaboration with Dr. D. Swan, Newcastle University. *.CEL (Cell Intensity) files containing the results of the intensity calculations on the pixel values from the microarray experiment were loaded into GeneSpring GX10 (Agilent). The data was processed with the MAS5 algorithm (Hubbell et al., 2002) to produce Present (if the transcript was detected), Marginal (if the transcript was at the limit of detection) and Absent (if the transcript was undetected) flag data for the probesets. Probesets with 1 or more Present or Marginal calls were selected for further analysis and Affymetrix control probesets were removed. The data was renormalized using GCRMA (Guanine Cytosine Robust Multi-Array Analysis)(Wu et al., 2003) to produce intensity values for the probesets. Probesets were considered differentially expressed if there was a fold change of greater than 2 between genes from SW480/lamA cells and SW480/cntl cells.

The data set was then uploaded into Ingenuity Pathways Analysis (IPA) to compute functional analysis of probesets. Each identifier was mapped to its corresponding object in the Ingenuity Pathways Knowledge Base. A cut-off of 2.5 fold was set to identify genes whose expression was significantly differentially regulated. These Network Eligible molecules were overlaid onto a global molecular network developed from information contained in the Ingenuity Pathways Knowledge Base. Networks of Network Eligible Molecules were then algorithmically generated based on their connectivity. IPA analysis was performed using standard settings to examine significance against biological functions and disease and canonical pathways (using Fischer Exact tests and a p value of <0.05). The interaction networks produced indicate literature-curated interactions with other molecules. Each network was given a score, calculated by IPA according to the number of Network Eligible Molecules in the network, the network's size, the total number of Network Eligible Molecules analysed and the total number of molecules in IPA's knowledge base that could be included in networks (www.ingenuity.com). The network score is based

on the hypergeometric distribution and is calculated using a right-tailed Fisher's Exact Test, with the score being the negative log of the p-value. This score is used to rank the networks.

3.2.3. Molecular biology

To prevent RNase degradation, all molecular biology techniques were carried out in RNase-free conditions. RNase Away spray (Fisher Scientific, Loughborough, UK) was used to clean surfaces. Ethanol was of molecular biology grade and RNase-free pipette tips and nuclease-free water (Ambion, Austin, TX, USA) were used. The validation of the microarray data using Q-PCR was carried out in collaboration with Miss. D. Battle, Durham University.

3.2.3.1. Primer Design

The expression levels of thirteen genes from the microarray dataset were assessed by Q-PCR analysis to validate the microarray dataset and GAPDH was used as the endogenous control gene.

Affymetrix Probe Set IDs corresponding to genes of interest were identified from the microarray dataset which contained the results for genes with an expression change of at least two fold when comparing expression in SW80/cntl and SW480/lamA cell lines. A NetAffx™ Query (http://www.affymetrix.com/analysis/index.affx) was performed for each Probe Set ID to determine the target sequence and relevant RefSeq transcript IDs. The Probe Set IDs were found to detect all splice variants of *BMP4, COL18A1, EIF4E, IGF2* and *ZEB1*. Only one splice variant of *EGFR* (NM_005228) was detected. All splice variants of *FN1* except NM_054034 were detected and the remaining genes (*AREG, CDH1, EREG, SERPINE1, SNAI2* and *TGFBI*) are not alternatively spliced.

The PrimerBank database (Spandidos et al., 2010; Wang and Seed, 2003) was then used to search for Q-PCR primers corresponding to the genes of interest, taking into account (if relevant) which transcript variants were detected in the microarray analysis. PrimerBank is a public database containing over 300,000 mouse and human primer pairs for PCR analysis, designed by a computer algorithm. The primers are designed to meet the following criteria (Wang and Seed, 2003):

a) Primers should be 19-23 nucleotides in length, which is long enough to be gene-specific, but minimises the potential for primers to cross-react

b) GC contents (35-65%) should be similar to guarantee uniform priming

c) ΔG threshold value of -9 kcal/mol for the last five residues at the 3' end, to minimise non-specific primer extension

d) T_m values of between 60-63^{o}C such that they will function at a high annealing temperature of 60^{o}C which reduces non-specific amplification

e) Amplicons of 150-350bp (or 100-800bp if necessary) for maximum PCR efficiency

f) Minimised primer cross-reactivity by rejection of primers containing non-unique 15mers and rejection of primers with a BLAST score of less than 30

g) Rejection of primers that would lead to secondary structures forming in the target or primer, to maximise PCR efficiency.

h) Rejection of primers that would form primer dimers – those that contain four residues at the 3' end, which can be found in the complementary sequence - as this can lead to reduced PCR yield because free primers are low.

N.B. The primers used to detect *CDH1* were not taken from the PrimerBank database, but had been used previously in our laboratory.

Primer pairs were analysed using Gene Runner (©Hastings Software Inc.) to check for possible secondary structure formation between and within primer pairs. Primers were occasionally optimised by removing one or two nucleotides from the start or end of the sequence, or adding an extra nucleotide to the end of the sequence. The final primer sequences used in this chapter are detailed in Table 3.1. 50nmol primers were synthesised by Invitrogen. Primers were diluted to produce a 10µmole working solution.

Table 3.1: Primer Sequences used in Q-PCR analysis

Gene	Forward Primer Sequence	Reverse Primer Sequence
AREG	CCCAAAACAAGACGGAAAGTGA	GCTGACATTTGCATGTTACTG
BMP4	TGGTCTTGAGTATCCTGAGCG	CTGAGGTTAAAGAGGAAACGA
CDH1	TCTTCCCCGCCCTGCC	CTAGCAGCTTCGGAACCGC
COL18A1	GGCTGGCCTACGTCTTTGG	CGGATGTGGAACAGCAGTGAG
EGFR	AAGGAAATCCTCGATGAAGCCT	TGTCTTTGTGTTCCCGGACATA
EIF4E	AGGATGGTATTGAGCCTATGTGG	CACAGAAGTGTCTCTAGCCAAAA
EREG	GCTCTGACATGAATGGCTATTGT	TGTTCACATCGGACACCAGTAT
FN1	GGCCTGGAACCGGGAACCGA	AGGGTGGGTGACGAAAGGGGT
GAPDH	CATGAGAAGTATGACAACAGCCT	AGTCCTTCCACGATACCAAAGT
IGF2	CCTCCAGTTCGTCTGTGGG	CACGTCCCTCTCGGACTTG
SERPINE1	CATCCCCCATCCTACGTG	CCCCATAGGGTGAGAAAACC
SNAI2	ATACCACAACCAGAGATCCTCA	GACTCACTCGCCCCAAAGATG
TGFBI	CACTCTCAAACCTTTACGAGACC	CGTTGCTAGGGGCGAAGATG
ZEB1	GATGATGAATGCGAGTCAGATGC	ACAGCAGTGTCTTGTTGTTGTAG

3.2.3.2. RNA extraction

SW480/lamA and SW480/cntl cells were grown to 70% confluency and RNA was isolated according to the RNeasy mini kit (Qiagen) protocol. Briefly, cells grown in T75 cell culture flasks were washed in versene, trypsinised and centrifuged as described in Section 2.2.2. Cells were resuspended and washed in 4ml PBS before centrifugation at 200g for 10 minutes (Eppendorf 5810R). After the supernatant was removed, cells were snap frozen in liquid nitrogen and stored at -80^{o}C. When required, cell pellets were thawed and resuspended in 600µl Buffer RLT. The lysates were homogenised by vortexing for 1 minute. 600µl 70% ethanol (molecular biology grade) was added to each homogenised lysate and pipette mixed. The samples were transferred to an RNeasy spin column in a 2ml collection tube and centrifuged for 15s at 8,000g. 700µl Buffer RW1 was added to the spin column and centrifuged for 15s at 8,000g. 500µl Buffer RPE was then added to the spin column and centrifuged for 15s at 8,000g before another 500µl Buffer RPE was added to the spin column and centrifuged for 2 minutes at 8,000g to dry the spin column membrane. The spin column was then placed in a new 2ml collection tube and centrifuged at 16,000g for 1 minute to minimise any carryover of buffer RPE. The spin column was placed in a new

1.5ml collection tube and 30µl RNase-free water was added. The sample was centrifuged at 10,000rpm for 1 minute to elute the RNA. Purified RNA was stored at -80^{o}C.

3.2.3.3. Quantitation and purity of RNA

A NanoDrop spectrophotometer (Thermo Fisher Scientific, UK) was used to assess the concentration and purity of RNA, according to the manufacturer's instructions. 1µl of sample was loaded onto the optical pedestal and the absorbance at 260nm and 280nm and the concentration of RNA was calculated. The A_{260}:A_{280} ratio was used to assess RNA purity, as a value of 1.7-2.0 indicated a pure sample.

3.2.3.4. cDNA synthesis

cDNA synthesis was performed using the iScript cDNA synthesis kit (BioRad), according to the manufacturer's instructions. Briefly, 4µl 5x iScript buffer, 1µl iScript reverse transcriptase and 11µl nuclease-free water were added to 2µg of isolated RNA in 0.5ml PCR tubes. The reaction mixtures were incubated at 25^{o}C for 5 minutes, 42^{o}C for 30 minutes and then 85^{o}C for 5 minutes to heat inactivate the reverse transcriptase. 80µl RNAse-free water was added to the synthesised cDNA such that the final concentration of cDNA was 20ng/µl. Aliquots were stored at -80^{o}C.

3.2.3.5. Testing Q-PCR primers

The $2^{-\Delta\Delta CT}$ method is based on the assumption that the amplification efficiencies of the gene of interest and endogenous control gene (in this study, *GAPDH*) are approximately equal (Livak and Schmittgen, 2001). To assess the efficiency of the amplicons, a Q-PCR experiment was performed to analyse the C_T values produced from a cDNA dilution series. This dilution series included cDNA concentrations ranging from 0.1 – 100ng.

Q- PCR was carried out in MicroAmp® optical 96 well reaction plates (Applied Biosystems). 1.5µl cDNA, 9µl DNase/RNase-free water, 12.5µl Fast SYBR ®Green Master Mix (Applied Biosystems), 1µl forward primer (1000µmole) and 1µl reverse primer (1000µmole) were added to each well. A no template control (containing no cDNA) was run for each primer used. MicroAmp® optical adhesive film (Applied Biosystems) was placed on the top of the 96 well reaction plate to reduce well-well contamination and evaporation. The plate was spun down in a bench-top centrifuge until any bubbles had been removed. A 7500 Fast Real-Time PCR System (Applied Biosciences) was used to perform Q-PCR. Samples were denatured at 95^{o}C for 20 seconds, before 40 cycles of melting for 3 seconds at 95^{o}C followed by annealing and extending at 60^{o}C for 30 seconds. This was followed by a melt curve stage in which the samples were heated to 95^{o}C for 15 seconds, cooled to 60^{o}C for 1

minute and subjected to a slow continuous temperature increase to 95°C, before being cooled to 65°C for 15 seconds. The baseline and threshold values were detected automatically, and checked manually. The baseline should be wide enough to eliminate the background fluorescence from the early cycles of amplification but should not overlap the exponential growth region of the amplification curve. The threshold should be as close as possible to the base of the exponential phase, but above the baseline.

Graphs were plotted displaying log10[cDNA] on the X axis and C_T values on the Y axis. Primers were acceptable for use in Q-PCR experiments if the gradient of the graph was between -3 and -3.6, as this means the efficiency of the genes is similar enough for the $2^{-\Delta\Delta Ct}$ calculation to be valid. A gradient of -3.3 represents an efficiency of 100%.

3.2.3.6. Q- PCR

Once the efficiency of the primers had been assessed, Q-PCR was carried out with as described above with 30ng (1.5µl) cDNA added to each experimental well. A no template control containing no cDNA was also run for each primer used. Three technical replicates were performed in each plate, and three biological replicates were run in separate plates. The C_T values produced were used to calculate relative changes in gene expression using the $2^{-\Delta\Delta CT}$ method (Livak and Schmittgen, 2001), where:

$$\Delta\Delta C_T = (C_{T,GOI} - C_{T,\ GAPDH})_{SW480/lamA} - (C_{T,GOI} - C_{T,\ GAPDH})_{SW480/cntl}$$

The upper and lower error limits were calculated as follows:

$$\text{Lower error limit} = 2^{-(\text{mean } \Delta\Delta CT + SE)}$$

$$\text{Upper error limit} = 2^{-(\text{mean } \Delta\Delta CT - SE)}$$

The standard error of the mean (SE) was calculated as follows, where n = number of biological replicates:

$$SE = \text{standard deviation of mean } \Delta C_T / \sqrt{n}$$

A two-tailed student t test was used to determine whether or not there was a statistically significant difference between gene expression in SW480/lamA and SW480/cntl cells for each gene studied.

3.3. Results

3.3.1. Microarray analysis reveals changes in gene expression between SW480/lamA and SW480/cntl cells

To understand the genome-wide transcriptional responses to over-expression of lamin A in SW480 colon carcinoma cells, a microarray experiment was performed using Human Genome U133 Plus 2.0 high density oligonucleotide Affymetrix GeneChip Arrays (Affymetrix, Santa Clara, CA, USA) to compare gene expression in SW480/lamA and SW480/cntl cells. 1211 probesets were considered to be differentially expressed as there was a fold change of greater than 2 between expression of genes from SW480/lamA cells and SW480/cntl cells.

3.3.2. Analysis of microarray data using IPA

To identify significant biological processes perturbed in response to over-expression of lamin A, we used IPA to examine our data in the context of existing knowledge of genome-wide interactions. The microarray data set containing probesets showing greater than 2.5 fold differential expression between genes from SW480/lamA cells and SW480/cntl cells was uploaded into IPA, which built interaction networks using the Ingenuity Knowledge Base. Genes that were not part of the dataset but that were biologically relevant to the network were added by IPA to give a total of approximately 35 molecules in each network. The algorithm used to create the networks ensures that as many genes from the dataset are included as is possible. The interaction networks produced (Figures 3.1-3.2; Appendix) display individual molecules as nodes connected by edges representing the relationships between the nodes. Scores (discussed in Section 3.2.2) calculated by IPA were used to rank the networks, where scores of 2 or higher have a p value of at least 0.01. Network 1 (Tables 3.2-3.4) contains 35 genes, therefore a score of 44 reveals that there is a 1 in $1x10^{44}$ chance that a network containing at least the same number of Network Eligible Molecules will be picked by chance when randomly selecting 35 genes from the IPA knowledge base. The scores ranged from 44 (Network 1) to 11 (Network 10), which suggests that every network is linked to biological processes which are affected when lamin A is over-expressed in colon cancer cells.

Of the highest scoring ten networks identified (Table 3.5), three were linked to molecules involved in cancer and three were linked to cell movement, and Network 1, the most significant network, was linked to cancer, cellular movement and cellular growth and proliferation. Figure 3.3 shows known interactions between the genes in Network 1,

derived from information contained in the Ingenuity Knowledge Base. The genes implicated in this network and the known interactions between them may give insight into the mechanisms involved in the change in motility seen when lamin A is expressed in SW480 colon carcinoma cells.

In vivo, biological pathways interact with each other rather than functioning independently. To explore the relationships between the networks, molecules that were common to two or more networks were identified (Figure 3.4). Ten genes were found to be common to two or more networks, four of which were derived from the microarray dataset, but six of which were added by IPA. Seven of the networks were found to form a large cluster, including networks linked to cancer (Networks 1, 3 and 7), cellular movement (Networks 1 and 7), cellular growth and proliferation (Networks 1, 3 and 4) and cell-cell signalling and interaction/cell signalling (Networks 4, 5 and 8). Networks 3, 4 and 7 formed the centre of this cluster, as each had links to three other networks. Networks 2 and 10 had ACTN2 in common. Although network 9 had no genes in common with other networks, it contained genes linked to cellular movement, akin to networks 1 and 7.

Figure 3.1: Network 1 produced by IPA
Affymetrix microarray data comparing SW480/cntl and SW480/lamA cell lines was analysed using IPA. Interaction networks were produced from probesets displaying greater than 2.5 fold differential expression and show known literature curated interactions with other molecules. The networks were analysed for significance against known biological functions. Networks are ranked by their 'Score', which is calculated by IPA and described in more detail in Section 3.2.2. The network with the highest score, 'Network 1', is shown in this figure.

The number of 'Focus molecules' indicates the number of genes in each network that were present in the microarray probe set. These genes are circled in the diagrams: genes in red circles were up-regulated in SW480/lamA when compared to SW480/cntl and genes with blue circles were down-regulated.

Network 1

Cancer, Cellular Movement,
Cellular Growth and Proliferation

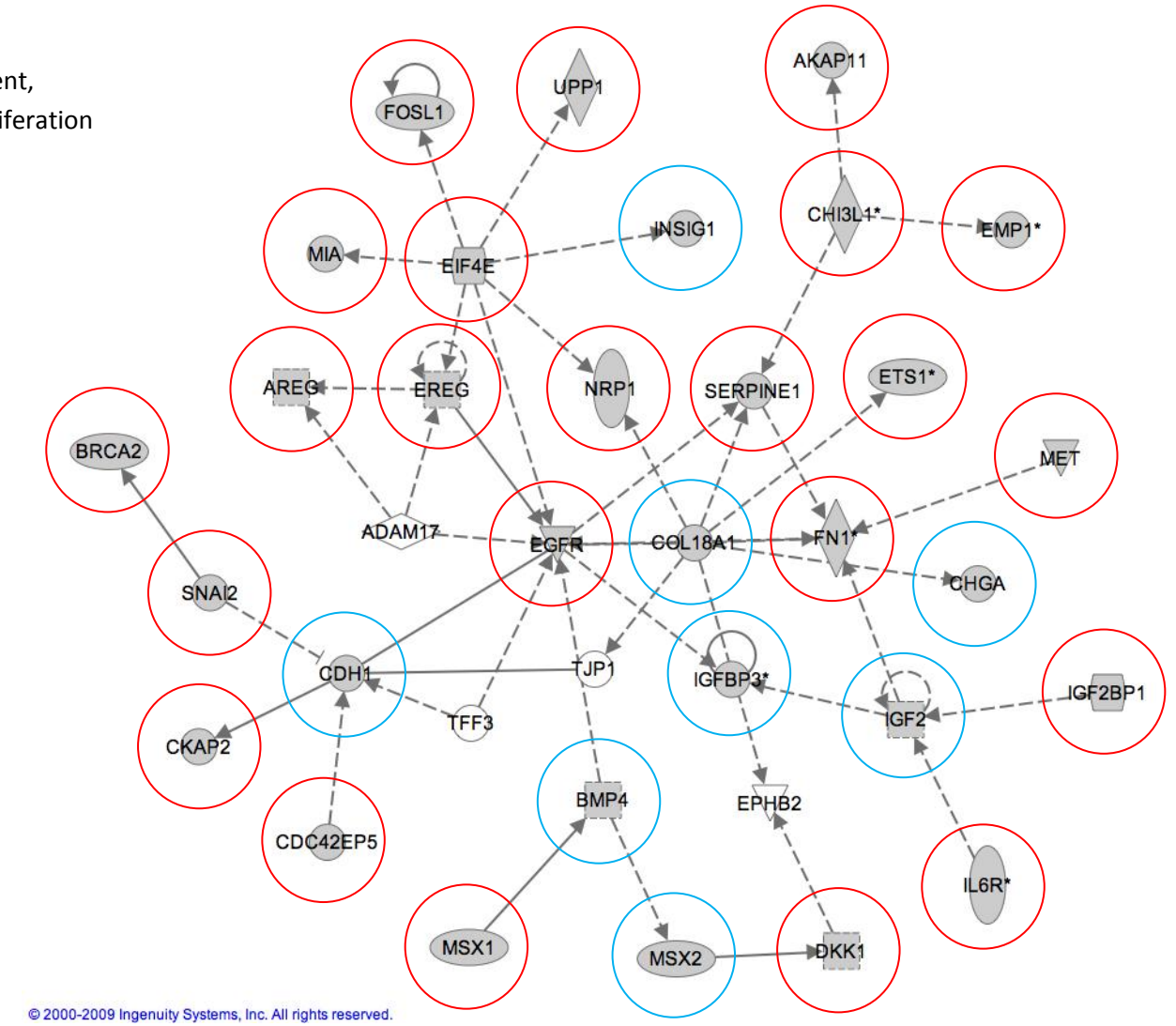

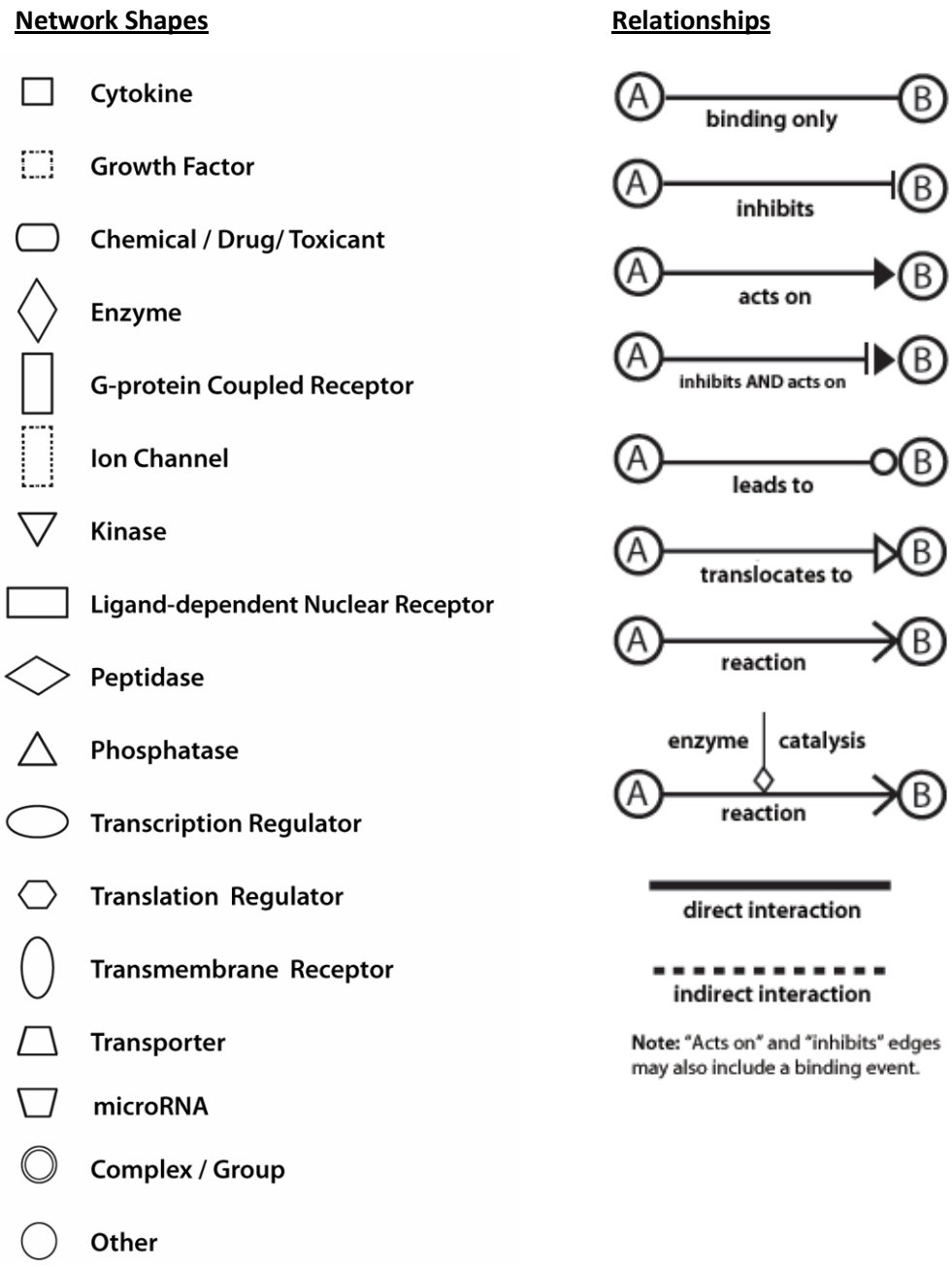

Figure 3.2: The types of molecules and interactions represented by shapes and arrows in IPA Networks

The shape surrounding the gene name denotes the type of molecule that the gene encodes. Lines (known as edges) that link genes indicate known interactions and a dotted line indicates an inferred or indirect interaction. The arrowheads indicate directionality and lines without an arrowhead refer to a binding interaction. Curved arrows designate self-regulation.

Table 3.2: Genes up-regulated in SW480/lamA cells		
Symbol	**Fold Change**	**Entrez Gene Name**
AKAP11	3.18	A kinase (PRKA) anchor protein 11
AREG	5.22	amphiregulin
BRCA2	2.29, 2.93	breast cancer 2, early onset
CDC42EP5	3.43	CDC42 effector protein (Rho GTPase binding) 5
CHI3L1	2.56, 4.65	chitinase 3-like 1 (cartilage glycoprotein-39)
CKAP2	2.78	cytoskeleton associated protein 2
DKK1	6.3	dickkopf homolog 1 (Xenopus laevis)
EGFR	2.13, 2.99	epidermal growth factor receptor
EIF4E	3.15	eukaryotic translation initiation factor 4E
EMP1	6.40, 8.84, 9.47	epithelial membrane protein 1
EREG	5.73	epiregulin
ETS1	2.77, 3.61	v-ets erythroblastosis virus E26 oncogene homolog 1 (avian)
FN1	3.31, 3.77, 3.93, 4.01	fibronectin 1
FOSL1	4.04	FOS-like antigen 1
IGF2BP1	2.68	insulin-like growth factor 2 mRNA binding protein 1
IL6R	3.82, 3.97	interleukin 6 receptor
MET	2.81	met proto-oncogene (hepatocyte growth factor receptor)
MIA	4.95	melanoma inhibitory activity
MSX1	3.54	msh homeobox 1
NRP1	2.75	neuropilin 1
SERPINE1	3.81	serpin peptidase inhibitor, clade E, member 1
SNAI2	4.05	snail homolog 2 (Drosophila)
UPP1	2.78	uridine phosphorylase 1

Table 3.3: Genes down-regulated in SW480/lamA cells		
Symbol	**Fold Change**	**Entrez Gene Name**
BMP4	7.19	bone morphogenetic protein 4
CDH1	3.43	cadherin 1, type 1, E-cadherin (epithelial)
CHGA	4.8	chromogranin A (parathyroid secretory protein 1)
COL18A1	2.7	collagen, type XVIII, alpha 1
IGFBP3	2.79, 2.92	insulin-like growth factor binding protein 3
IGF2	8.61	insulin-like growth factor 2 (somatomedin A)
INSIG1	2.27, 2.41, 2.81	insulin induced gene 1
MSX2	2.23, 2.89	msh homeobox 2

Table 3.4: Genes added by IPA	
Symbol	**Entrez Gene Name**
ADAM17	ADAM metallopeptidase domain 17
TFF3	trefoil factor 3 (intestinal)
TJP1	tight junction protein 1 (zona occludens 1)
EPHB2	EPH receptor B2

Tables 3.2-3.4 – Genes included in Network 1

These tables display the genes included in Network 1, whether they were present in the microarray dataset or added by IPA and the fold changes revealed by the microarray analysis.

Network	Top Functions	Score	Focus Molecules
1	Cancer, Cellular Movement, Cellular Growth and Proliferation	44	31
2	Cell-To-Cell Signalling and Interaction, Cellular Assembly and Organization, Nervous System Development and Function	20	19
3	Cancer, Cellular Growth and Proliferation, Cell Death	16	16
4	Cellular Growth and Proliferation, Cell-To-Cell Signalling and Interaction, Cellular Function and Maintenance	14	15
5	Cell Signalling, Small Molecule Biochemistry, Immunological Disease	14	15
6	Lipid Metabolism, Small Molecule Biochemistry, Molecular Transport	14	15
7	Cellular Movement, Connective Tissue Development and Function, Cancer	14	14
8	Cell-To-Cell Signalling and Interaction, Haematological System Development and Function, Immune Cell Trafficking	11	13
9	Cell Death, Cellular Movement, Cell Cycle	11	13
10	Neurological Disease, Psychological Disorders, Cell-To-Cell Signalling and Interaction	11	13

Table 3.5: IPA Networks 1-10

This table displays the top functions of the genes included in Networks 1-10, the network scores and the number of focus molecules in each Network.

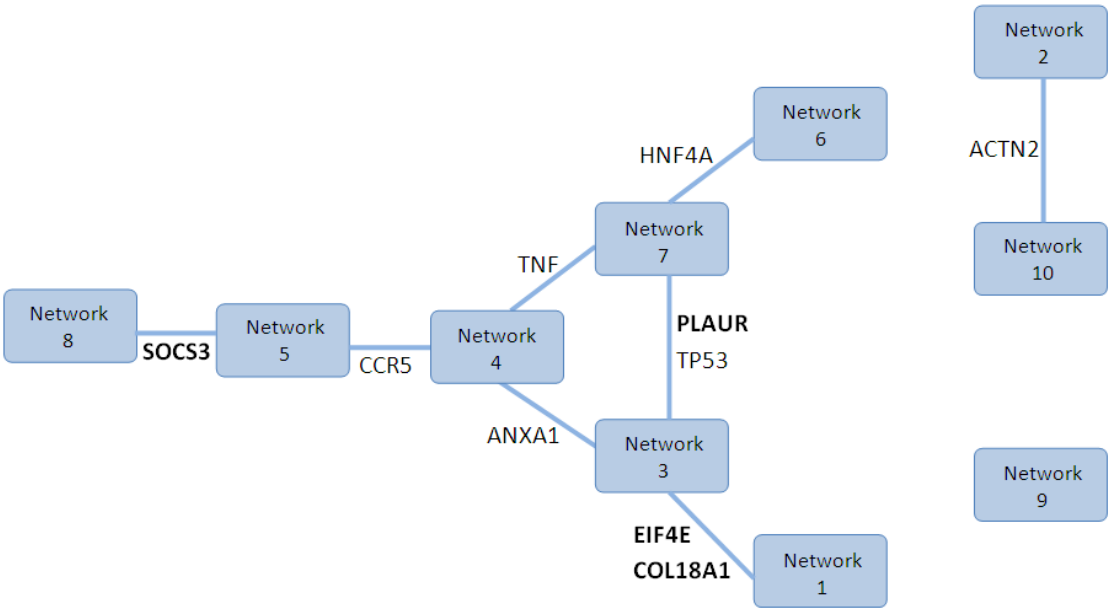

Figure 3.3: Interactions between Networks 1-10

This diagram shows which genes feature in more than one Network. Each Network has between 0-5 genes in common with other Networks. Genes in bold type are those present in the microarray dataset; those in normal type are genes added by IPA to complete the networks.

Further analysis of the IPA-generated networks indicated that two molecules previously considered to be implicated in the mechanism by which over-expression of lamin A in colon carcinoma cells leads to an increase in cell motility were present in Networks 1-10. *TGM2* is present in Network 5, which links together molecules involved in Cell Signalling, Small Molecule Biochemistry and Immunological Disease. *PLS3* is in Network 10, which contains molecules linked to Neurological Disease, Psychological Disorders and Cell-To-Cell Signalling and Interaction.

3.3.3. Validation of microarray data using Q-PCR

As discussed in the introduction to this chapter, real time Q-PCR is the gold standard technique for validation of microarray data sets. It is particularly important to validate the microarray dataset in this particular study, as although eleven technical replicates were incorporated into each probeset, no biological replicates were investigated. Eleven genes were selected for real time Q-PCR analysis, which were nodes in Network 1 (*AREG, BMP4, CDH1, COL18A1, EGFR, EIF4E, EREG, FN1, IGF2, SERPINE1* and *SNAI2*) that connected to between two and nine other genes in the network.

The $2^{-\Delta\Delta CT}$ method, used to quantify the relative expression change between samples, is based on the assumption that the amplification efficiencies of the gene of interest and endogenous control gene are approximately equal. To assess the efficiency of the amplicons, a Q-PCR experiment was performed to analyse the C_T values produced from a cDNA dilution series. This dilution series included cDNA concentrations ranging from 0.1 – 100ng. Graphs were plotted displaying log10[cDNA] on the X axis and C_T values on the Y axis. A gradient of -3.3 represents an efficiency of 100%. All the primers tested were acceptable for use in Q-PCR experiments because the gradient of the graphs were between -3 and -3.6, which means the efficiencies of the genes were similar enough for the $2^{-\Delta\Delta Ct}$ calculation to be valid.

As SYBR Green binds all double stranded DNA, it was important to perform melt curve analysis to confirm the integrity of the PCR product. After PCR cycling, the temperature was raised slowly from 65^{o}C to 95^{o}C and the 7500 Software v2.0.5 (Applied Biosystems) plotted graphs of the derivative reporter (–Rn') against temperature (^{o}C). The increase in temperature causes PCR products to denature, which leads to a decrease in fluorescence. In these graphs, a single peak represents the decreased fluorescence at the melting point of the PCR products. The presence of additional peaks can indicate that primer-dimers or non-specific products are formed. An extra peak was occasionally seen in 'no template control' experiments, where no cDNA was added. However, we are confident that primer-dimers and non-specific products did not influence our data, as only single peaks were found in graphs representing experiments containing cDNA. A representative melt curve graph is shown in Figure 3.4.

Due to the large amounts of data produced from the Q-PCR experiments, all the amplification plots produced are not shown; instead a representative amplification plot is shown in Figure 3.4. The combined data showing the relative expression of all 13 genes analysed in SW480/lamA and SW480/cntl cells, from three biological replicates, each with three technical replicates, can be seen in Figure 3.5.

The amplification plot in Figure 3.4 detailing the amplification of *EREG* in the SW480/lamA and SW480/cntl cell lines shows the progression of the real time Q-PCR reaction. ΔRn is plotted on the Y-axis and cycle number is plotted on the X-axis. ΔRn is calculated using the following equation:

$$\Delta Rn = (ROX™ \text{ fluorescence} / SYBR \text{ Green fluorescence}) - \text{baseline}$$

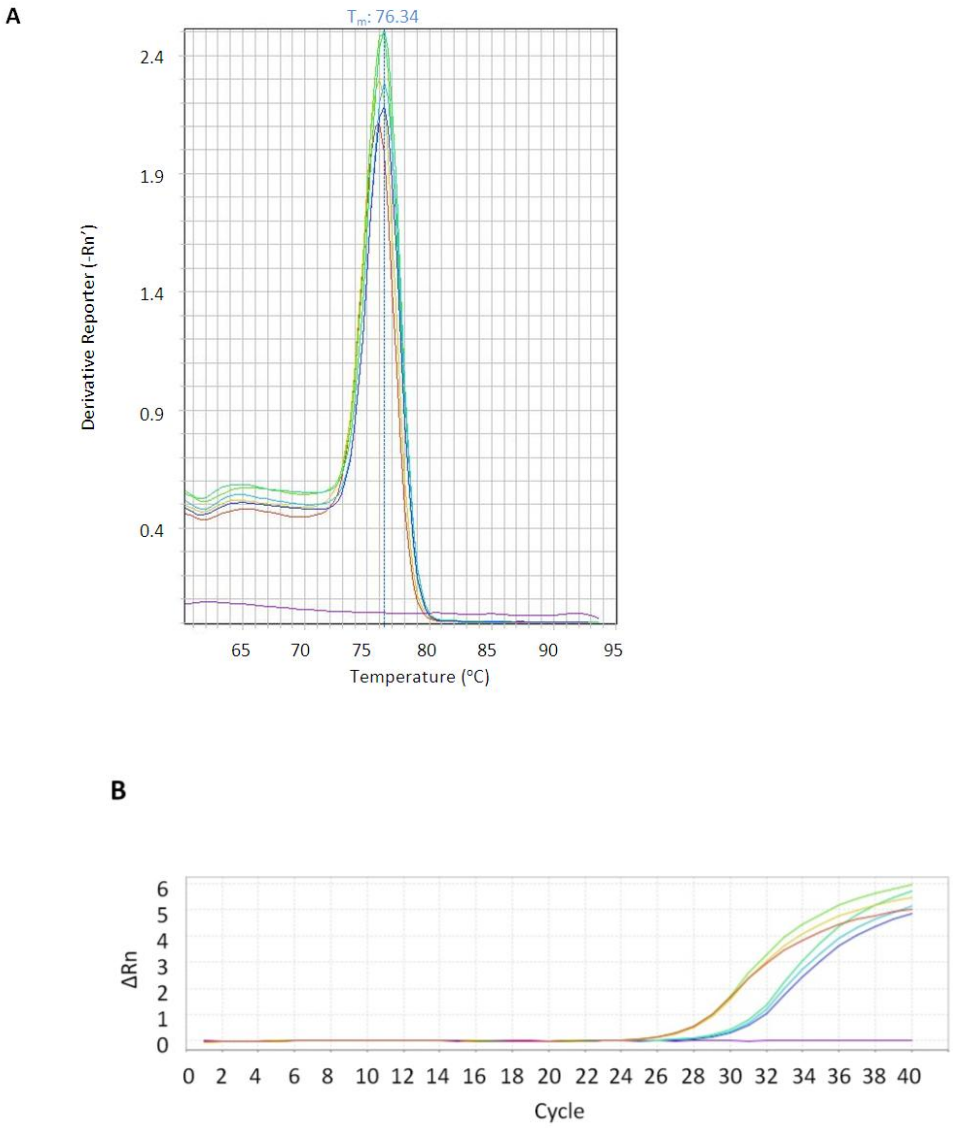

Figure 3.4: Representative graphs generated from real time Q-PCR experiments

Both graphs are taken from the real time Q-PCR analysis of *EREG* expression in SW480/lamA and SW480/cntl cells and are representative of other graphs generated in the experiment.

A Melt curve displaying single peaks which correspond to the point at which the PCR product has melted. The purple line indicates the 'no template control'.

B A real time Q-PCR amplification plot showing the changes in SYBR green fluorescence during the reaction. The red, yellow and green lines represent the technical replicates from the SW480/lamA sample and the blue and purple lines represent the technical replicates from the SW480/cntl sample.

ROX™ is a passive reference dye present in the SYBR green mastermix that provides an internal fluorescence reference to which the SYBR green signal can be normalised. The baseline is defined by the initial cycles of QPCR in which there is little change in fluorescence. From this graph, the C_T values can be determined, which denote the cycle number at which the amplification of a PCR product is first detected above the background fluorescence, passing the threshold. The threshold is a level of ΔRn that is above the baseline but low enough to be within the exponential growth region on the amplification plot. The higher the starting amount of target, the lower the C_T value. From the graphs in Figure 3.4, it can be seen that EREG expression is higher in SW480/lamA cells than in SW480/cntl cells, as the SW480/lamA sample has a lower C_T value.

Figure 3.5 shows the differences in expression of selected genes when comparing SW480/lamA and SW480/cntl cells. Of the genes present in Network 1, eight changes in gene expression identified in the microarray analysis were confirmed by Q-PCR (*BMP4, CDH1, COL18A1, EGFR, EIF4E, FN1, IGF2,* and *SERPINE1*), two changes in gene expression identified in the microarray analysis were not statistically significant (*AREG* and *EREG*) and Q-PCR analysis did not confirm the change in gene expression of *SNAI2* identified in the microarray analysis (Figure 3.6). As over 70% of the genes investigated confirmed the change in expression identified in the microarray analysis, it was concluded that there was enough evidence from the QPCR experiment to have confidence in the microarray data.

Figure 3.5: Quantitative real time PCR shows changes in gene expression between SW480/lamA and SW480/cntl cells

Q-PCR was carried out in 96 well plates with 30ng (1.5µl) cDNA added to each experimental well. A no template control (containing no cDNA) was also run for each primer used. Three technical replicates were performed in each plate, and three-five biological replicates were run in separate plates. The C_T values produced were used to calculate relative changes in gene expression using the $2^{-\Delta\Delta CT}$ method (Livak and Schmittgen, 2001), with *GAPDH* as the normalisation control gene.

A two-tailed student t test was used to determine whether or not there was a statistically significant difference between gene expression in SW480/lamA and SW480/cntl cells for each gene studied (* = $p<0.05$, ** = $p<0.01$, *** = $p<0.005$).

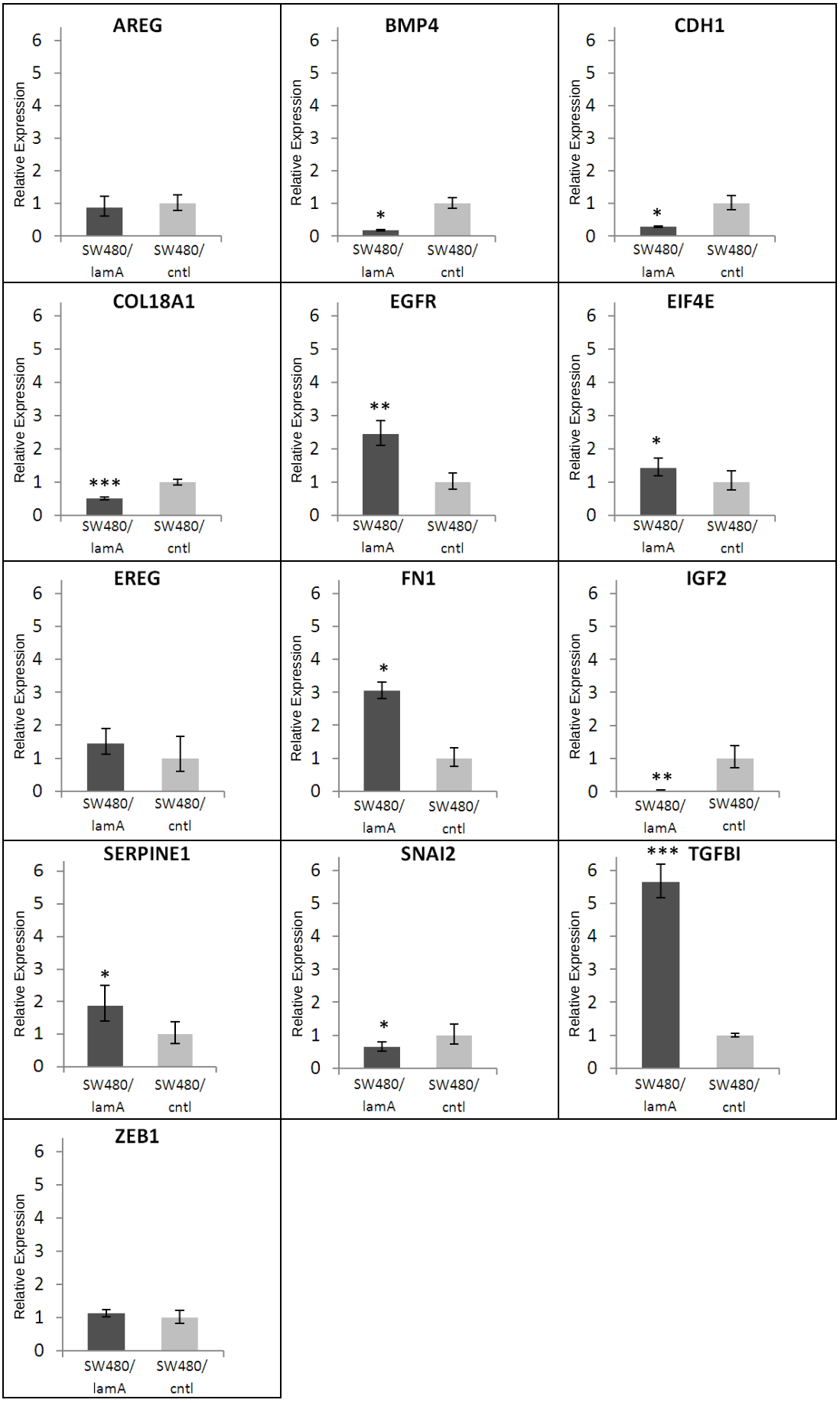
AREG
BMP4
CDH1
COL18A1
EGFR
EIF4E
EREG
FN1
IGF2
SERPINE1
SNAI2
TGFBI
ZEB1
Relative Expression
SW480/ lamA
SW480/ cntl
*
**
***

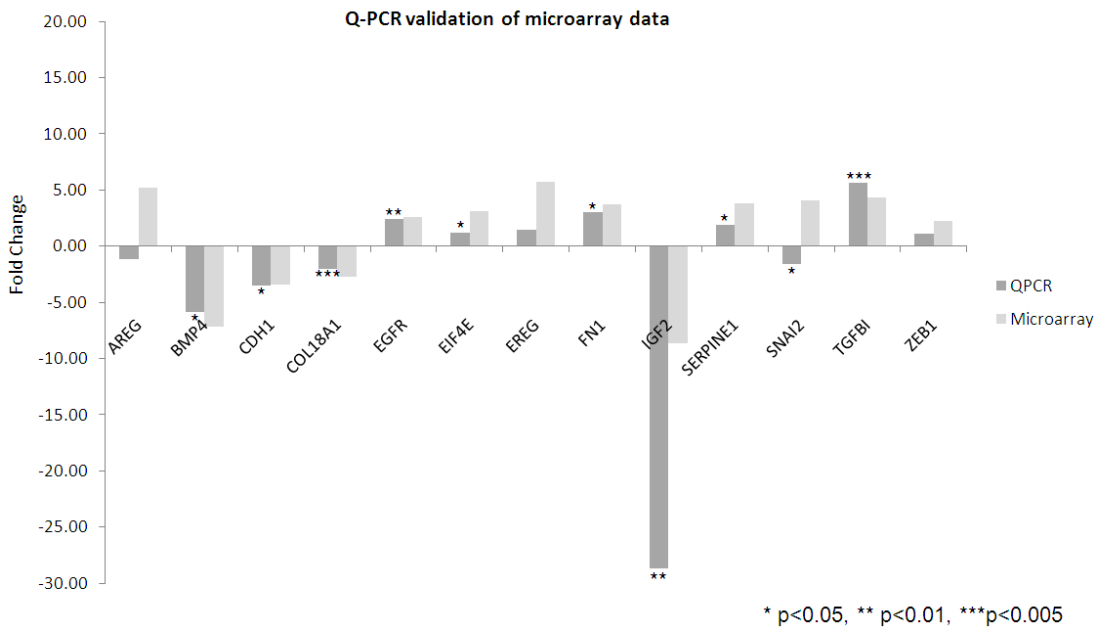

Figure 3.6: Validation of microarray data by real time Q-PCR

This graph shows the relative fold change of gene expression in SW480/lamA cells when compared to SW480/cntl cells. The dark grey bars represent the real time Q-PCR data, and the grey bars represent the microarray data. Statistical significance of real time Q-PCR data, determined by a two-tailed student t test, is denoted by asterisks (* = $p<0.05$, ** = $p<0.01$, *** = $p<0.005$).

3.3.4. Epithelial Mesenchymal Transition

In the previous chapter, it was noted that several of the proteins highlighted in the 2D DIGE results are involved in EMT. To discover whether EMT is a significant process implicated in the changes in gene expression between SW480/lamA and SW480/cntl, gene lists generated from the microarray data were compared to gene lists linked to EMT generated by IPA - 'Epithelial-Mesenchymal Transition of Epithelial Cells' (Table 3.6) and 'Epithelial-Mesenchymal Transition of Cells' (Table 3.7). There was a statistically significant overlap between the IPA-generated 'Epithelial-Mesenchymal Transition of Epithelial Cells' list and the microarray-generated 2.5 fold change list ($p=2.16x10^{-2}$) and the 2 fold change list ($p=6.73x10^{-3}$). Statistical significance was determined by a Fisher's exact (hypergeometric) test within IPA against the reference set of 'all genes'. There was also a statistically significant overlap between the IPA-generated 'Epithelial-Mesenchymal Transition of Cells' list and the microarray-generated 2.5 fold change list ($p=7.12x10^{-2}$) and the 2 fold change list ($p=1.35x10^{-3}$).

Expression levels of two genes (*ZEB1* and *TGFBI*) which were present in the microarray dataset and known to be linked to TGFβ were also analysed by Q-PCR. *ZEB1*, which was

found to be 2.25 fold up-regulated in SW480/lamA cells compared to the control cells in the microarray experiment, was chosen because like SNAI2, it is a repressor of E-cadherin, and has been shown to induce EMT in tumour cells (Eger et al., 2005). *TGFBI*, one of the genes from Network 9, was selected because it is known to promote metastasis when overexpressed in SW480 cells (Ma et al., 2008) and because it is induced by TGFβ, an inducer of EMT (Cui et al., 1996; Skonier et al., 1992). *TGFBI* was up-regulated 4.3 fold in SW480/lamA cells compared to the control cells in the microarray experiment.

Q-PCR analysis revealed that *TGFBI* was statistically significantly up-regulated in SW480/lamA compared to SW480/cntl cells, verifying the microarray data (Figures 3.5 and 3.6). *ZEB1* was also up-regulated in the cells over-expressing lamin A, consistent with the microarray data, but the differences determined by Q-PCR were not statistically significant.

Molecule	Fold change	Up/down regulated in SW480/lamA compared to SW480/cntl
BMP7		
CDC42		
CDH1	3.43	down
EGF		
LEF1	2.07	up
MST1R		
S100A4		
SMAD3		
SNAI1		
SNAI2	4.05	up
TGFB1		
TWIST1		
ZEB1	2.25	up

Table 3.6: Identities of genes in the IPA 'Epithelial-Mesenchymal Transition of Epithelial Cells' list and the fold changes of the genes present in the microarray dataset

The microarray 2 and 2.5 fold change datasets were searched for genes which appear in the IPA 'Epithelial-Mesenchymal Transition of Epithelial Cells' list and the fold changes between SW480/cntl and SW480/lamA cells were recorded.

Molecule	Fold change	Up/down regulated in SW480/lamA compared to SW480/cntl
ABL1		
AKT1		
AKT2		
BMP7		
CAV1		
CDC42		
CDH1	3.43	down
EGF		
FGF1		
FOXC2		
FOXO1		
GSC		
HNF4A		
HNRNPAB		
ID1		
IGF1R	2.12	down
IRS1	2.37	up
JAG1		
KLF8		
LEF1	2.07	up
MIR200A (includes EG:406983)		
MIR200B (includes EG:406984)		
MIR200C (includes EG:406985)		
MST1R		
NFYB		
PAX3		
PLAU		
PLAUR	2.39, 2.72, 2.73	up
PP1		
PTPN14		
S100A4		
SMAD3		
SMAD4		
SNAI1		
SNAI2	4.05	up
SP1		
TGFB1		
TGFB3		
TWIST1		
ZEB1	2.25	up
ZEB2		

Table 3.7: Identities of genes in the IPA 'Epithelial-Mesenchymal Transition of Cells' list and the fold changes of the genes present in the microarray dataset

The microarray 2 and 2.5 fold change datasets were searched for genes which appear in the IPA 'Epithelial-Mesenchymal Transition of Cells' list and the fold changes between SW480/cntl and SW480/lamA cells were recorded.

3.3.5. Comparison of 2D DIGE data with microarray data

The microarray data was then interrogated to discover if any of the genes encoding the twelve proteins identified in the 2D DIGE analysis comparing detergent/ high salt resistant N/CSK from SW480/lamA and SW480/cntl cells (Section 2.3.8) were present. *TGM2* expression was higher in SW480/lamA compared to control cells, with a 2.65 fold change in expression. *HSPD1* expression was lower in SW480/lamA cells compared to control cells, with a fold change of 2.60. In these cases, higher expression of the gene in SW480/lamA cells correlated with increased association of the protein with the cytoskeleton, and vice versa. The 2D DIGE data revealed that TGM2 was over-represented in the cytoskeletal fraction of SW480/lamA cells compared to control cells, with a 3.3-3.5 fold change, and HSPD1 protein expression was under-represented in the cytoskeletal fraction of SW480/lamA cells, with a 1.5 fold change.

3.4. Discussion

3.4.1. Validation of microarray results

We have previously shown that over-expression of lamin A in colon cancer cells leads to increased cell motility and a poor prognosis for patients. In this chapter, a genome-wide expression study was analysed in order to identify genes and pathways that are affected by lamin A expression. Expression of lamin A led to large-scale changes in gene expression, as over 1200 probesets were differentially expressed. Further analysis with IPA revealed that many of the genes highlighted were known to have functions in cell migration and EMT.

Q-PCR expression data for 9 out of 13 genes examined correlated closely with data from the microarray, and showed statistically significant differences in gene expression. This indicated that data obtained from the microarray analysis could reliably be used as the basis for further experiments.

Of the four genes investigated that did not have reproducible changes in gene expression when examined by microarray and Q-PCR analysis, three (*AREG, EREG* and *ZEB1*) which were differentially expressed in the microarray analysis showed no significant difference in gene expression in Q-PCR experiments and *SNAI2* expression was significantly lower in SW480/lamA cells in Q-PCR experiments, contrary to the results of the microarray analysis. There are a number of possible reasons for the variability in our data.

Firstly, it is possible that there are genuine biological differences in the cells, as the RNA samples for the microarray and the QPCR experiments, although isolated from the same cell line, were isolated many years apart. Many colorectal cancer cells are genetically unstable, and the SW480 cell line in particular is known to be chromosomally unstable (Camps et al., 2005; Lengauer et al., 1997; Ribas et al., 2003). Hence, there may be differences between RNA isolated for the microarray experiment, when the cell lines were first established compared to the RNA recently isolated for the Q-PCR analysis.

Differences in expression of *SNAI2* and *ZEB1* may be due to variability of transcription factor expression throughout EMT. It is thought that EMT may consist of discrete phases, with differences in gene expression occurring during transition between the different stages of EMT (Savagner et al., 1997; Vetter et al., 2009). Some studies have also shown that several transcription factors, including Twist and Zeb1, are upregulated following loss of E-cadherin. It is thought that this creates a feed-forward loop of E-cadherin repression which may lead to stabilisation of the mesenchymal state in EMT (Onder et al., 2008).

Hence, transcription factors such as Snail may initiate the repression of epithelial genes, whereas other transcription factors such as Zeb1 may act later in EMT to prolong the repression (Guaita et al., 2002; Peinado et al., 2007).

Regulation of the expression levels of Snai2 and Zeb1 is complex and is controlled by a number of different factors which may be responsible for the differences in expression between the microarray and Q-PCR data: E2A-HLF and Mitf regulate SNAI2 (Inukai et al., 1999; Sanchez-Martin et al., 2002) and IGF-1, Snail1 and Twist regulate Zeb1 (Dave et al., 2011; Graham et al., 2008). Also, Snai2 expression is not always accompanied by down-regulation of *CDH1* (Savagner et al., 1997; Uchikado et al., 2011) and TG2-induced EMT showed down-regulation of both *CDH1* and *SNAI2* (Kumar et al., 2010) so it is not necessarily inconsistent that both *SNAI2* and *CDH1* are down-regulated in cells expressing lamin A.

The proteins encoded by *AREG* and *EREG*, amphiregulin (AR) and epiregulin (EPI), are members of the epidermal growth factor family which can bind the epidermal growth factor receptor (EGFR) and are known to stimulate proliferation of some cell types, but inhibit growth of others (Plowman et al., 1990; Toyoda et al., 1995). Expression of EPI and AR can be regulated by toll-like receptor 4 (TLR4) (Hsu et al., 2010), which was found to be up-regulated by 2.09 in SW480/lamA cells in the microarray analysis. It is possible that no significant changes in EPI and AR expression were found in the Q-PCR analysis because TLR4 or another protein which regulates EPI and AR was not significantly changed in expression in the cells at the time of RNA extraction for Q-PCR analysis.

The microarray chip contains internal controls, whereby some genes have more than one corresponding probeset. *AREG* and *EREG* both had two corresponding probesets, where one probeset showed up-regulation of the gene, whereas the other probeset did not. *ZEB1* had four corresponding probesets, three of which were up-regulated by 1.29, 1.49 and 2.25 fold respectively, and one of which showed no change. *SNAI2* was only represented by one probeset. Therefore some of the non-reproducible changes in gene expression may due to problems such as errors in hybridisation efficiency in the microarray experiment.

3.4.2. Expression of lamin A in colon carcinoma cells causes changes in expression of genes linked to cell motility and EMT

Genes highlighted in the microarray dataset were clustered into networks by IPA on the basis of the known functions of their gene products. The ten most significant networks

produced all had highly significant scores of at least 11, indicating that each of these networks is linked to biological processes which are affected when lamin A is over-expressed in colon cancer cells. The most significant network, Network 1, had a score of 44 and contained 31 genes from the microarray dataset and 4 genes which were added by IPA. This network linked together molecules involved in cancer, cellular movement and cellular growth and proliferation.

A-type lamins are known to regulate cell proliferation, as normal and tumour cells with low expression levels of A-type lamins display high proliferative capacity (Broers et al., 1997; Rober et al., 1989; Van Berlo et al., 2005; Venables et al., 2001). However, we have previously shown that there is no difference in cell proliferation between SW480/lamA and SW480/cntl cells (Willis et al., 2008). Hence, I have concentrated on exploring the links between the genes of Network 1 and cell motility.

The aim of this chapter was to use IPA to highlight genes that might be involved in the mechanism that causes increased cell motility when lamin A is over-expressed in colon carcinoma cells. Therefore, it is extremely interesting that Network 1 includes genes linked to cell motility and that there is a statistically significant overlap between IPA lists of genes linked to EMT and the microarray dataset. It can be postulated that expression of lamin A in colorectal cancer cells causes an increase in cell motility through inducing an epithelial-mesenchymal transition.

Many of the genes in Network 1 encode proteins which are known to induce EMT or EMT-like responses, including *SNAI2* (Hajra et al., 2002; Savagner et al., 1997), *BMP4* (Hamada et al., 2007; Molloy et al., 2008), *MSX2* (Hamada et al., 2007; Satoh et al., 2008), *EIF4E* (Ghosh et al., 2009) and *EGFR* (Lo et al., 2007).

One of the hallmarks of EMT is down-regulation of the cell adhesion molecule E-cadherin. Loss of E-cadherin expression is one of the most common alterations in cancer cells and abolition of E-cadherin function is a critical step in the acquisition of invasive properties. The gene that encodes E-cadherin, *CDH1*, is one of the nodes found in Network 1, and was found to be down-regulated in SW480/lamA cells in both microarray and Q-PCR analysis. This is particularly interesting because our lab has previously shown that the increased cell motility of SW480/lamA cells is in part due to up-regulation of the actin bundling protein T-plastin, which causes down-regulation of E-cadherin (Willis et al., 2008). The gene for T-plastin, *PLS3*, which the microarray showed to be up-regulated by 19.06 in SW480/lamA cells, is in Network 10 which contains molecules linked to Neurological Disease,

Psychological Disorders and Cell-To-Cell Signalling and Interaction. Plastins control the organisation of the actin cytoskeleton through crosslinking actin filaments into tight bundles. Expression of L-plastin, an isoform of T-plastin, has been linked to increased invasiveness in cancer (Al Tanoury et al., 2010; Klemke et al., 2007). T-plastin expression is increased in cisplatin-resistant cancer cells, in comparison to cisplatin-sensitive cells (Hisano et al., 1996), which suggests that T-plastin may be up-regulated in more aggressive tumours. No links have yet been reported between T-plastin and EMT.

A number of proteins encoded by genes in Network 1 are involved in cell adhesion in addition to E-cadherin, including fibronectin, SERPINE1, MIA and CHGA. CHGA (chromogranin A) and SERPINE1 modulate cell adhesion and can exhibit either pro- or anti-adhesive activity (Durand et al., 2004; Gasparri et al., 1997). Both fibronectin and MIA are involved in cell-matrix attachments. Fibronectin is a ligand for many members of the integrin family, which link the ECM with the cytoskeleton. MIA is a protein expressed in primary and metastatic malignant melanomas but not in normal tissue (Blesch et al., 1994; Bosserhoff et al., 1996) which promotes metastasis through the regulation of cell-matrix attachments. It binds to fibronectin and laminin, preventing cells from binding the ECM, leading to invasion and metastasis (Bosserhoff et al., 1998).

Along with down-regulation of E-cadherin and changes in cell adhesion, EMT involves up-regulation of mesenchymal markers, extensive reorganisation of the actin and intermediate filament cytoskeleton and increased cell motility. We observed that many genes in Network 1 were linked to these processes:

A number of the genes in Network 1 encode proteins known to be associated with the cytoskeleton, including *IGFBP1, CDC42EP5* and *CKAP2*. CDC42 effector protein 5 is a CDC42 binding protein that induces the assembly of actin filaments, leading to changes in cell shape (Hirsch et al., 2001). In fibroblasts, ectopic expression of CDC42EP5 led to loss of stress fibres and extension of protrusive lamellipodia (Joberty et al., 1999). IGF2BP1 binds β-actin mRNA, preventing its translation until the complex reaches the periphery of the cell (Huttelmaier et al., 2005; Ross et al., 1997), localizing it to sites of active actin polymerisation, where it modulates cell migration. Cytoskeleton-associated protein 2 is known to associate with the microtubule-organising centre and microtubules (Bae et al., 2003; Maouche-Chretien et al., 1998; Seki and Fang, 2007). SERPINE1 and fibronectin expression and EGFR transactivation are sensitive to disruption of the cytoskeleton

(Providence et al., 1999; Samarakoon et al., 2009; Samarakoon and Higgins, 2002; Varedi et al., 1997).

One of the main processes linked to the proteins encoded by the genes in Network 1 is cellular motility. *FN1, EIF4E, NRP1* and *EGFR*, which were up-regulated in the microarray dataset are known to encode proteins which are expressed in highly motile and invasive cancer cells. Fibronectin is a typical mesenchymal marker and has been shown to promote cancer cell migration and invasion (Meng et al., 2009; Shibata et al., 1997). Down-regulation of fibronectin in SPC-A-1sci lung cancer cells caused decreased metastasis both in vitro and in vivo (Jia et al., 2010). eIF4E, a component of the translation initiation complex, is essential for pseudopod protrusion and tumour cell migration and invasion (Shankar et al., 2010). Knockdown of eIF4E in metastatic cells results in an MET and reduced actin cytoskeleton dynamics (Shankar et al., 2010). NRP1 is up-regulated in metastatic cells compared to non-metastatic cell lines and tumours (Miao et al., 2000). Over-expression of EGFR is linked to increased cell motility, invasion and metastasis (Kruger and Reddy, 2003; Thomas et al., 2003; Verbeek et al., 1998). SERPINE1, which was also up-regulated, has both pro- and anti- migration and invasion roles in cancer, depending on its level of expression, the composition of the ECM and expression levels of associated proteins (Dellas and Loskutoff, 2005; Durand et al., 2004). Decreased EMP1, which was down-regulated in our microarray dataset, is known to be correlated with lymph node metastasis in patients with oral squamous cell carcinoma (Zhang et al., 2011).

It is possible that expression levels of lamin A influence TGFβ-mediated EMT. A-type lamins are known to be involved in regulating gene activity downstream of TGFβ, as A-type lamins modulate responses to TGFβ signalling in mesenchymal cells through regulation of transcription factors such as pRB and SMADs (Van Berlo et al., 2005). MAN1, a lamin A-interacting protein, is also known to regulate TGFβ signalling through binding to R-Smads (Lin et al., 2005; Osada et al., 2003).

Many of the genes in Network 1 are linked to TGFβ signalling. BMP4 is a member of the TGFβ superfamily. *SERPINE1* and *SNAI2* are up-regulated by TGFβ and *AREG* is downregulated by TGFβ (Akiyoshi et al., 2001; Choi et al., 2007; Joseph et al., 2009). eIF4E is linked to TGFβ-mediated EMT, as TGFβ activates mTOR, inducing the phosphorylation of 4E-BP1, which causes dissociation of eIF4E from 4E-BP1, increasing protein synthesis (Hay and Sonenberg, 2004; Lamouille and Derynck, 2007).

It should be noted that the IPA analysis did not highlight EMT in Networks 1-10. Taking this into consideration along with the finding that the changes in *SNAI2, ZEB1, AREG* and *EREG* expression were inconsistent, it is possible that the changes seen in our system represent a novel pathway that is similar to EMT but not a classical EMT.

3.4.3. Conclusion

In conclusion, our data indicate that lamin A expression in colon carcinoma cells may cause an EMT-like response resulting in cells with a more aggressive phenotype, leading to poor survival for the patient. This is a novel finding, as currently nothing is published about the relationship between lamin A expression and EMT. The differences between SW480/lamA and SW480/cntl cell lines may be mediated through the TGFβ signalling pathway, changes in the organisation of the cytoskeleton or by increasing the level of transcription factors.

CHAPTER FOUR
The effects of siRNA knockdown of lamin A on gene and protein expression and cell motility

4.1. Introduction

In the previous chapter we showed that lamin A expression in colon carcinoma cells increases cell motility and causes an EMT-like process most likely through activating a predicted pathway (Network 1) that may be controlled by TGFβ signalling. Here, I test this hypothesis by using siRNA to knockdown lamin A and subsequently to investigate which genes in Network 1 change in response.

In Chapter 3 it was postulated that expression levels of lamin A may influence TGFβ-mediated signalling, as A-type lamins are known to be involved in regulating gene activity downstream of TGFβ. A-type lamins modulate responses to TGFβ signalling in mouse embryonic fibroblasts through regulation of transcription factors such as pRB and SMADs (Van Berlo et al., 2005; Worman, 2006).

The four genes initially selected for analysis were *CDH1, FN1, TGFBI* and *TGM2* as their expression is known to be regulated by TGFβ (Cui et al., 1996; Ignotz and Massague, 1986; Shin et al., 2008; Skonier et al., 1992; Xu et al., 2009). *CDH1* and *FN1* were both present in Network 1 and have previously been implicated in cell motility changes during metastasis (Meng et al., 2009; Perl et al., 1998; Shibata et al., 1997; Willis et al., 2008). *TGFBI* was identified as being differentially expressed in the microarray analysis (Chapter 3) and TG2 was highlighted in the 2D DIGE analysis (Chapter 2).

Expression levels of *SNAI2* and *ZEB1*, which are both also regulated by TGFβ, were also analysed because whilst they were shown to be upregulated in SW480/lamA cells in the microarray analysis this was not confirmed in the QPCR analysis. It is thought that EMT may consist of discrete phases, each with different gene expression profiles (Savagner et al., 1997; Vetter et al., 2009), whereby transcription factors such as Snail initiate the repression of epithelial genes, whereas other transcription factors such as Zeb1 act later in EMT to prolong the repression (Guaita et al., 2002; Peinado et al., 2007). Therefore, it is possible that expression levels of *SNAI2* and *ZEB1* differ throughout the EMT response, warranting further study.

There are many different ways in which TGFβ can induce EMT in cancer cells: through SMAD-dependent pathways and through SMAD-independent pathways which involve activation of signalling systems such as Ras/MAP kinase, Wnt/β-catenin, PI3K/AKT, NF-κB, Rho/ROCK, Jagged/Notch, and MDM2/p53 (Tian et al., 2011).

In EMT, TGFβ can induce expression of Snail and ZEB families of transcription factors which then activate expression of mesenchymal genes such as fibronectin and repress expression of epithelial markers such as E-cadherin (Medici et al., 2008; Xu et al., 2009). TGFBI is also induced by TGFβ (Cui et al., 1996; Skonier et al., 1992) and is known to promote metastasis when overexpressed in SW480 cells (Ma et al., 2008).

In a recent paper, TG2 was shown to induce EMT, causing increased expression of E-cadherin repressors such as Zeb1, downregulation of E-cadherin and upregulation of fibronectin (Kumar et al., 2010). TG2 was found to be required for TGFβ-induced EMT, and is thought to be a downstream effector of TGFβ (Kumar et al., 2010). It was also found that TG2 expression conferred a stem-cell like phenotype along with induction of EMT (Kumar et al., 2010).

Therefore, it was hypothesised that knockdown of lamin A by siRNA would lead to an MET in which decreased expression of *TGM2* and *TGFBI* was followed by decreased expression of *SNAI2* and *ZEB1*, which would cause increased expression of *CDH1* and decreased expression of *FN1*. Finally, it was expected that the changes in gene expression would lead to a decrease in cell motility compared to control cells.

4.2. Materials and Methods

4.2.1. siRNA knockdown

4.2.1.1. siRNA sequences used

The Silencer® Select Custom Designed siRNA (Ambion) sequences targeted sequences in exons 11 or 12 of *LMNA*, and were therefore specific for lamin A but not lamin C (Table 4.1). Silencer® Select Negative Control #1 siRNA (si-c) was used as a negative control.

Table 4.1: siRNA sequences targeting lamin A

Name	ID	Sequence (5'-3')
Si-1	s238117	Sense: UCAUCUAUCUCAAUCCUAAtt Antisense: UUAGGAUUGAGAUAGAUGAga
Si-2	s238118	Sense: GGCCUGCUGUGAUUCCACUtt Antisense: AGUGGAAUCACAGCAGGCCaa

4.2.1.2. siRNA transfection in T-25 tissue culture flasks

24 hours before transfection, SW480/lamA cells were seeded at a density of $2.5x10^5$ cells per flask. Cell media was changed immediately preceding transfection, and L-15 media containing FBS but no antibiotics was added. Cells were treated with a transfection mixture containing 400µl serum-free L-15 medium, 20µl Oligofectamine reagent (Invitrogen) and 30µl Lamin A siRNA [20µM] (ID#s238117 or #s238118, Ambion) or scrambled siRNA [20µM] (Ambion). Media was changed after 24 hours. Cells were processed for protein or RNA extraction between 24 and 48 hours post-transfection.

4.2.1.3. siRNA transfection in 6 well plates

In the experiments shown in Figure 4.3, cells were seeded at a density of $1.0x10^5$ cells per well 24 hours before transfection. In all other experiments, cells were seeded at a density of $4.0x10^5$ cells per well 24 hours before transfection. Cell media was changed immediately preceding transfection, and L-15 media containing FBS but no antibiotics was added. Cells were treated with a transfection mixture containing 200µl serum-free L-15 medium, 10µl Oligofectamine reagent (Invitrogen) and 10µl Lamin A siRNA [20µM] (ID#s238117 Ambion), 10µl scrambled siRNA [20µM] (Ambion) or 10µl nuclease free water. Media was changed after 24 hours. Cells were processed for protein/RNA extraction or wounding assays between 24 and 120 hours post-transfection.

4.2.2. Wounding assays

Differences in cell motility were measured using scratch wound assays. SW480/lamA cells were seeded at $4.0x10^5$ cells per well in a 6 well plate and transfected with siRNA as described in Section 4.2.1. After either 72 or 96 hours, the cell media was removed and wounds were made using a 10µl pipette tip (Star Lab, UK). The cell media was changed two times to remove floating cells. The wound area was visualized using a live cell imaging phase contrast microscope (Zeiss) at X10 magnification, and photographs of the cells were taken in confluent areas. Images were captured every 15minutes for 24 hours in identical wound locations. Three wound locations were chosen per well.

The width of the wound at the start (0hr) and end (24hr) of the experiment was measured six times for each wound at 100µm intervals using Axiovision Rel. 4.8 (Zeiss). The mean distance the cells moved in 24hours was calculated and standard errors were calculated from the biological replicates. A paired student t-test was used to test for statistical significance.

Photographs of the cells were taken with the live cell imaging phase contrast microscope (Zeiss) at X10 magnification before the wounding assay started, in order to compare the morphology of the cells.

4.2.3. Q-PCR

Q-PCR was carried out as described in Section 3.2.3. RNA was isolated from the cells at 36, 48, 60, 72, 84 and 96 hours post-transfection. Primers specific for *CDH1, FN1, SNAI2, TGFBI* and *ZEB1*, described in Section 3.2.3, were used in Q-PCR analysis. Primers were also designed to target *TGM2*, with the following sequences: forward primer sequence: AGCGTTCCTCTTTGCATCCTC and reverse primer sequence: GTAGCTGTTGATAACTGGCTCC.

4.2.4. One dimensional SDS-PAGE and immunoblotting

1D SDS-PAGE and immunoblotting were performed as described in Section 2.2.5. The mouse polyclonal anti-TGFBI antibody (ab89062) was sourced from Abcam and was used at a dilution of 1:250.

4.3. Results

4.3.1. Selection of siRNA construct for efficient down-regulation of lamin A

It was first necessary to investigate the efficiency of the siRNA constructs in knocking down expression of lamin A in SW480/cntl cells. The cells were transfected with two different siRNA constructs and a scrambled negative control siRNA. Cells were harvested 24, 36 and 48 hours after transfection and the efficiency of knockdown was analysed through immunoblotting (Figure 4.1).

siRNA ID s238117 (si-1) was much more effective at knocking down lamin A than siRNA ID s238118 (si-2) (Figure 4.1). si-1 knocked down lamin A by over 60% after 48hours. Neither of the siRNAs knocked down GFP-lamin A expression at the timepoints assayed. At some timepoints GFP-lamin A and/or endogenous lamin A expression was higher in control cells than in si-lamin A treated cells. To ensure that the scrambled siRNA control did not have any effect on expression of lamin A, control transfections were performed using water (NTC) instead of siRNA (Figure 4.2 A). Expression of lamin A was assessed at 48, 72 and 96 hours after transfection. No difference was seen between expression of lamin A in the scrambled siRNA control and the NTC, demonstrating that si-control is a suitable control.

As knockdown of lamin A was highest 48hrs after transfection, expression of lamin A was assessed at 24 hour time points up to 120 hours post-transfection (Figure 4.2 B). si-1 was shown to consistently knock down endogenous lamin A at 24, 48, 72, 96 and 120 hour time points, and endogenous lamin A was knocked down by over 95% at 120 hours post-transfection (Figure 4.2 B,D).

GFP-lamin A was knocked down by over 50% at the 24 and 120 hour timepoints (Figure 4.2 B,D), whereas expression in si-cntl cells was approximately the same, or higher, at the 48-96 hour timepoints.

These experiments show that si-1 can efficiently knockdown endogenous lamin A for at least 120 hours post-transfection, and that GFP-laminA expression is also reduced at 120 hours post-transfection. si-1 was therefore used in further experiments, and is henceforth referred to as si-laminA.

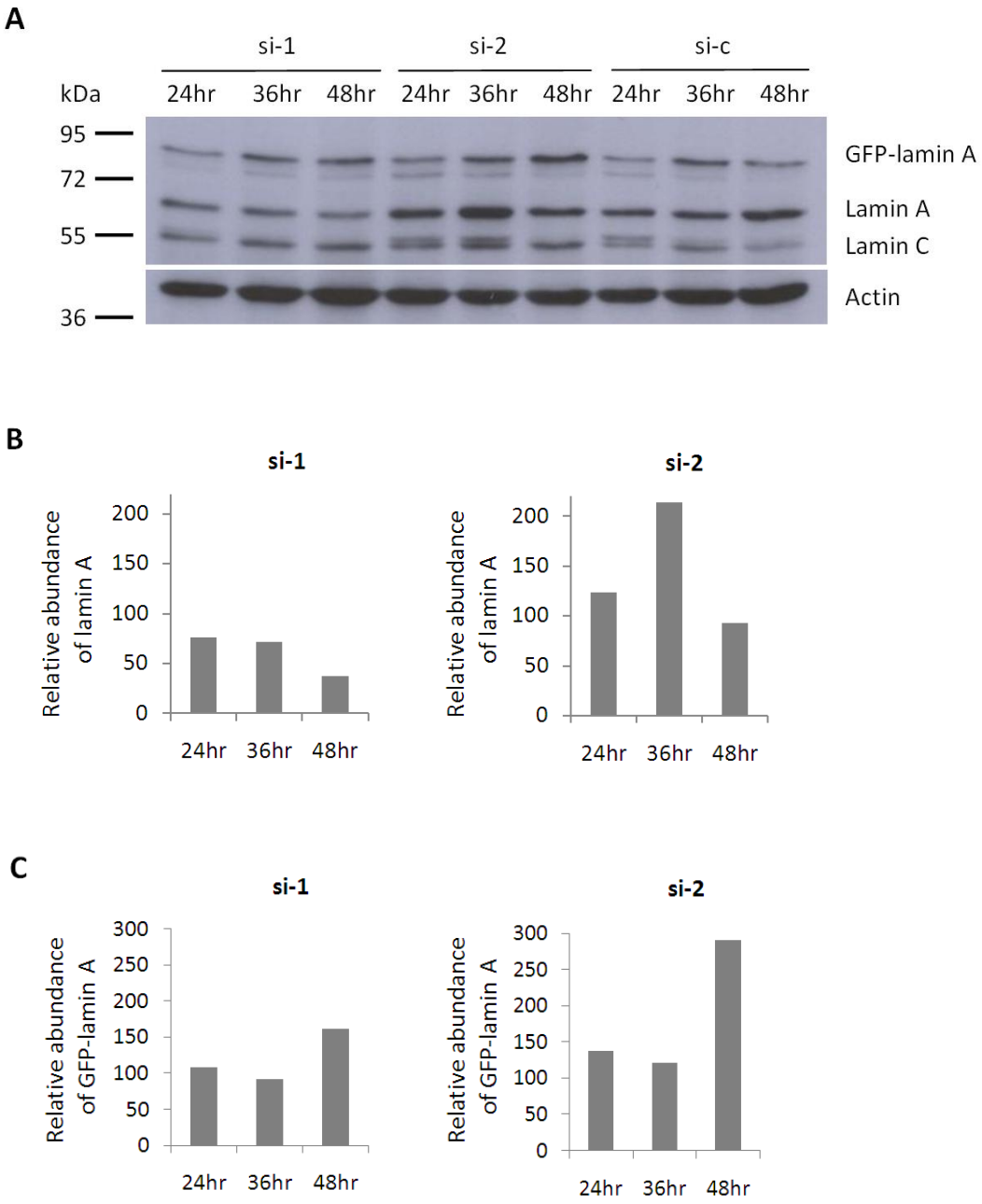

Figure 4.1: Analysis of different siRNA oligonucleotides shows that si-1 is more effective than si-2 at knocking down lamin A expression

A Immunoblot of whole cell extracts from SW480/lam A cells transfected with lamin A siRNA ID s238117 (si-1), ID s238118 (si-2) or scrambled negative control (si-c), resolved on a 10% SDS-PAGE gel and probed with Jol2 antibody. Actin was used as a loading control. Cell pellets were harvested at 24, 36 and 48 hours post transfection with siRNA.

B Densitometric analysis of endogenous lamin A expression at each time point in cells transfected with si-1 or si-2, relative to si-c. Images were taken with Fujifilm Intelligent Dark Box II and relative densities were measured with Image J software.

C Densitometric analysis of GFP-lamin A expression at each time point in cells transfected with si-1 or si-2, relative to si-c as described above.

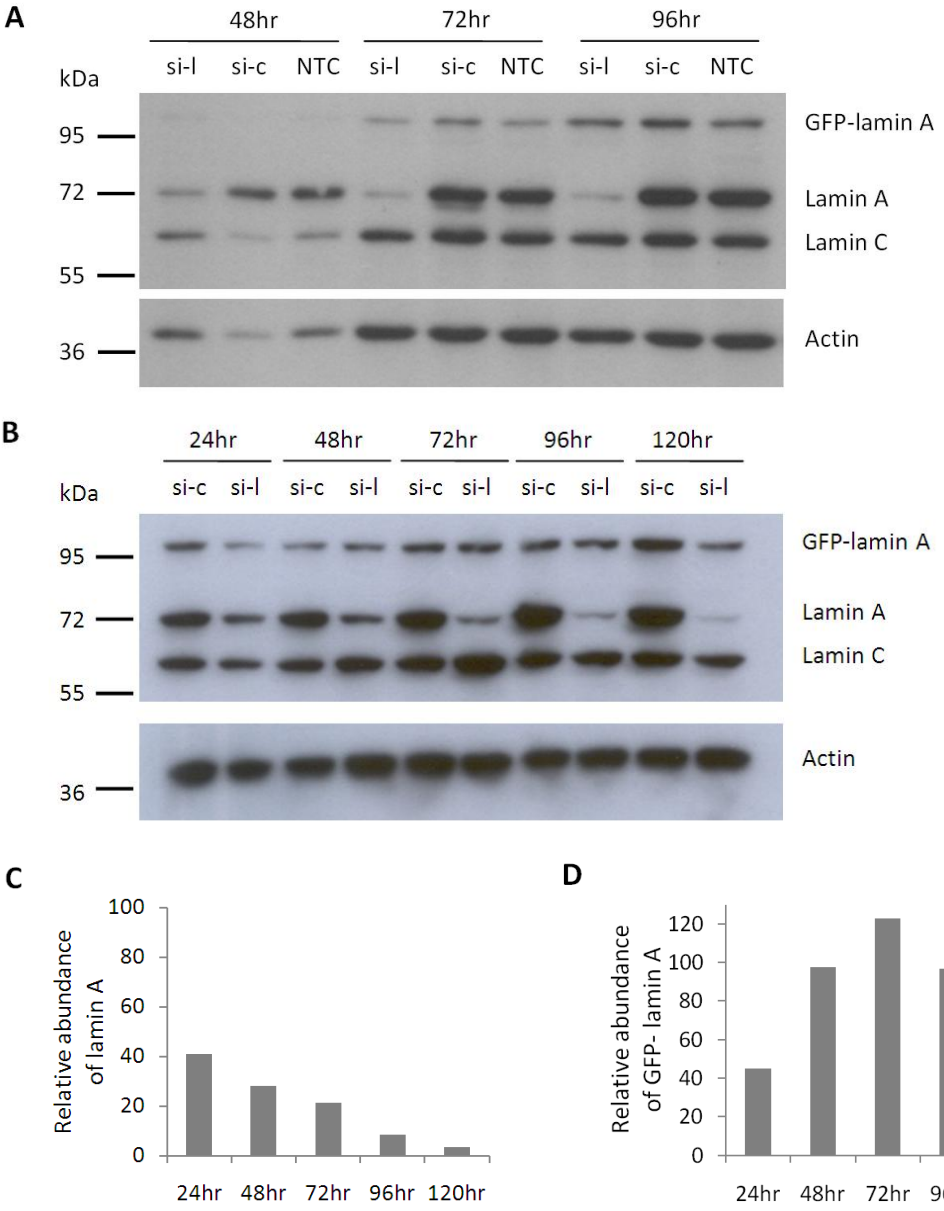

Figure 4.2: SW480/lamA cells transfected with lamin A siRNA show reduced lamin A expression when compared to control cells

A Immunoblot of whole cell extracts from SW480/lam A cells transfected with si-laminA ID s238117 (si-l), scrambled negative control siRNA (si-c) or no si-RNA (NTC), resolved on a 10% SDS-PAGE gel and probed with Jol2 antibody. Actin was used as a loading control. Cell pellets were harvested at 48, 72 and 96 hours post transfection with siRNA.

B Immunoblot of whole cell extracts from SW480/lam A cells transfected with si-laminA ID s238117 (si-l) or scrambled negative control siRNA (si-c), resolved on a 10% SDS-PAGE gel and probed with Jol2 antibody. Actin was used as a loading control. Cell pellets were harvested at 24, 48, 72, 96 and 120 hours post transfection with siRNA.

C Densitometric analysis of endogenous lamin A expression in SW480/lamA cells transfected with si-lamin A compared to those transfected with si-control. Images were taken with Fujifilm Intelligent Dark Box II and relative densities were measured with Image J software.

D Densitometric analysis of GFP-lamin A expression in SW480/lamA cells transfected with si-lamin A compared to those transfected with si-control, as described above

4.3.2. Down-regulation of lamin A by siRNA transfection causes decreased cell motility

Scratch wound assays were used to investigate the effect of knockdown of lamin A on cell motility. Cells were seeded in 6 well plates and were transfected with either si-laminA or si-control 24 hours after seeding. Cells reached 100% confluency at 72 hours post-transfection. Scratches were made either 72 hours or 96 hours post-transfection, and the distance moved by cells in 24 hours was calculated from phase-contrast images (Figure 4.3). Three scratches were made in each well, enabling at least three technical replicates and three biological replicates of each experimental condition to be analysed per plate. There was no statistically significant difference between si-control and si-lamin A cell motility between 72 and 96 hours post siRNA transfection. However, there was a statistically significant difference between the distance moved by si-control and si-lamin A cells between 96 and 120 hours post siRNA transfection ($p<0.001$) whereby si-control cells moved 1.3 times further than si-lamin A cells.

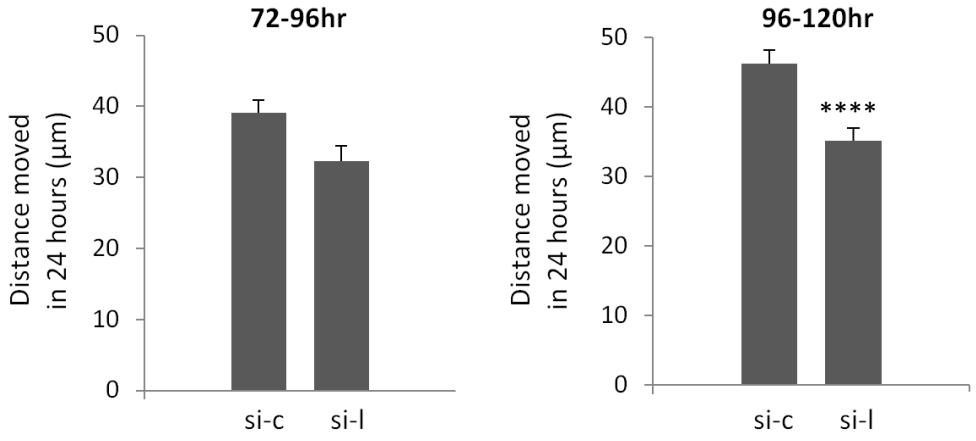

Figure 4.3: SW480/lamA cells transfected with lamin A siRNA show reduced cell motility when compared to control cells

The mean distance moved by cells in 24 hours as calculated from phase-contrast images. In each experiment, three locations were chosen for each of three biological replicates and images were taken every 15 minutes for 24 hours. Error bars represent the standard error calculated from the biological replicates.

There was no statistically significant difference between si-control and si-lamin A cell motility measured between 72-96 hours post siRNA transfection. However, there was a statistically significant difference between the distance moved by si-control and si-lamin A cells between 96 and 120 hours post siRNA transfection ($p<0.001$; ****). Si-control cells moved 1.3 times further than si-lamin A cells.

4.3.3. Down-regulation of lamin A by siRNA transfection causes changes in gene expression over time

We next wanted to investigate whether or not changes in expression of genes implicated in cell motility in general, or more specifically in EMT, occurred between the time at which knockdown of lamin A was first observed, and the change in cell motility seen at 96 hours post-transfection. To do this, SW480/lamA cells were seeded in 6 well plates and transfected with either si-laminA or si-control 24 hours after seeding. Cells were processed for RNA extraction every 12 hours between the 60 hour and 96 hour time points. To confirm knockdown of lamin A, cells were processed for protein extraction every 24 hours between the 24 hour and 120 hour time points. To confirm the change in motility, a scratch wound assay was performed between 96 and 120 hours post-transfection. The whole experiment was repeated independently three times.

Knockdown of endogenous lamin A in si-laminA transfected SW480/lamA cells could be seen at all timepoints from 24-120 hours and the band for lamin A in the immunoblot was barely visible by 120 hours (Figure 4.2B). GFP-lamin A expression was also reduced by 60% in si-lamin A cells at the 120 hour timepoint. The scratch wound assay (Figure 4.4 B,C) confirmed that si-laminA transfected cells were less motile than si-control transfected cells ($p<0.0005$), as si-cntl cells moved 40% further than si-laminA cells.

Changes in expression of *CDH1, FN1, SNAI2, TGFBI, TGM2* and *ZEB1* over time were determined by Q-PCR, using the RNA isolated from si-laminA and si-control treated SW480/lamA cells (Figure 4.5). Data was obtained from three independent RNA extractions and three technical replicates for each gene at each time point.

There was often large variation between samples (see error bars in Figure 4.5A), resulting in few results that were statistically significant (Table 4.2). However, statistically significant differences in expression between SW480/lamA cells transfected with si-lamin A and si-control were seen at 72hr (*TGFBI*), 84hr (*SNAI2, TGFBI*) and 96hr (*ZEB1*) post-transcription.

TGFBI expression was consistently lower in si-lamin A transfected cells. The difference was statistically significant at the 72hr ($p<0.05$) and 84hr ($p<0.005$) timepoints. This is consistent with the microarray and QPCR data, in which *TGFBI* expression was up-regulated in SW480/lamA cells. We would expect *TGFBI* expression to be reduced in SW480/lamA cells transfected with si-lamin A which show reduced cell motility, as *TGFBI* is known to promote metastasis when overexpressed in SW480 cells (Ma et al., 2008).

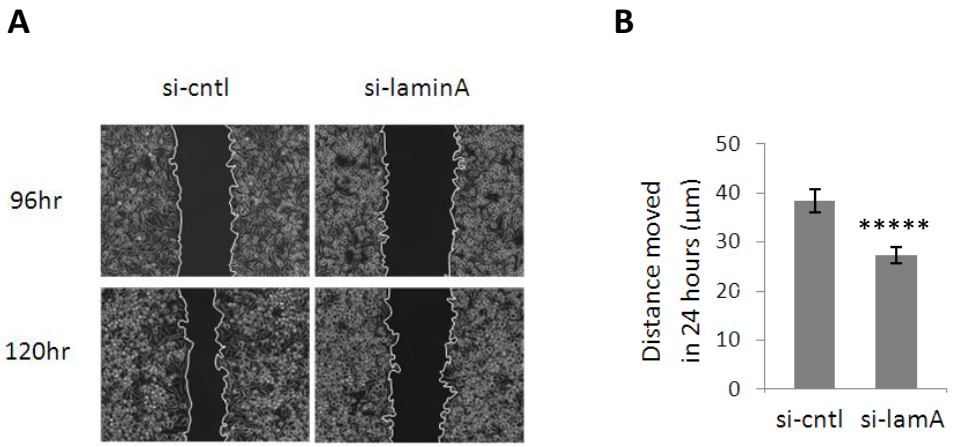

Figure 4.4: siRNA knockdown of lamin A causes decreased cell motility in SW480 colorectal cancer cells

A Representative phase-contrast images of the start and end time points of the cell wounding assay. Cells were grown in 6-well plates and wounded at 96 hours post-transfection with si-lamin A or si-cntl. Scale bars = 50µm.

B The mean distance moved by cells in 24 hours was calculated from the phase-contrast images. In each experiment, four locations were chosen for each of three biological replicates and images were taken every 15 minutes for 24 hours. The experiment was performed on three separate occasions. Error bars represent the standard error calculated from the nine biological replicates performed for each siRNA type. Si-cntl cells moved 40% further than si-laminA cells ($p<0.0005$; *****).

Figure 4.5: siRNA knockdown of lamin A causes changes in gene expression in SW480 colorectal cancer cells over time

A Quantitative real time PCR was used to measure the expression of *CDH1, FN1, SNAI2, TGFBI, TGM2* and *ZEB1* at 60, 72, 84 and 96 hours post siRNA transfection. The data was analysed using the ddCt method, wherein expression levels were normalised to *GAPDH*. Biological triplicates were analysed and technical triplicates were performed for each sample. Error bars show standard errors of biological replicates. * = $p<0.05$, *** = $p<0.005$

B As above, however, in this graph expression levels of each gene in si-laminA treated cells are shown as relative to those in si-control treated cells. Relative differences in gene expression were measured using the log10 of the mean 2^{-ddCt}. * = $p<0.05$, *** = $p<0.005$

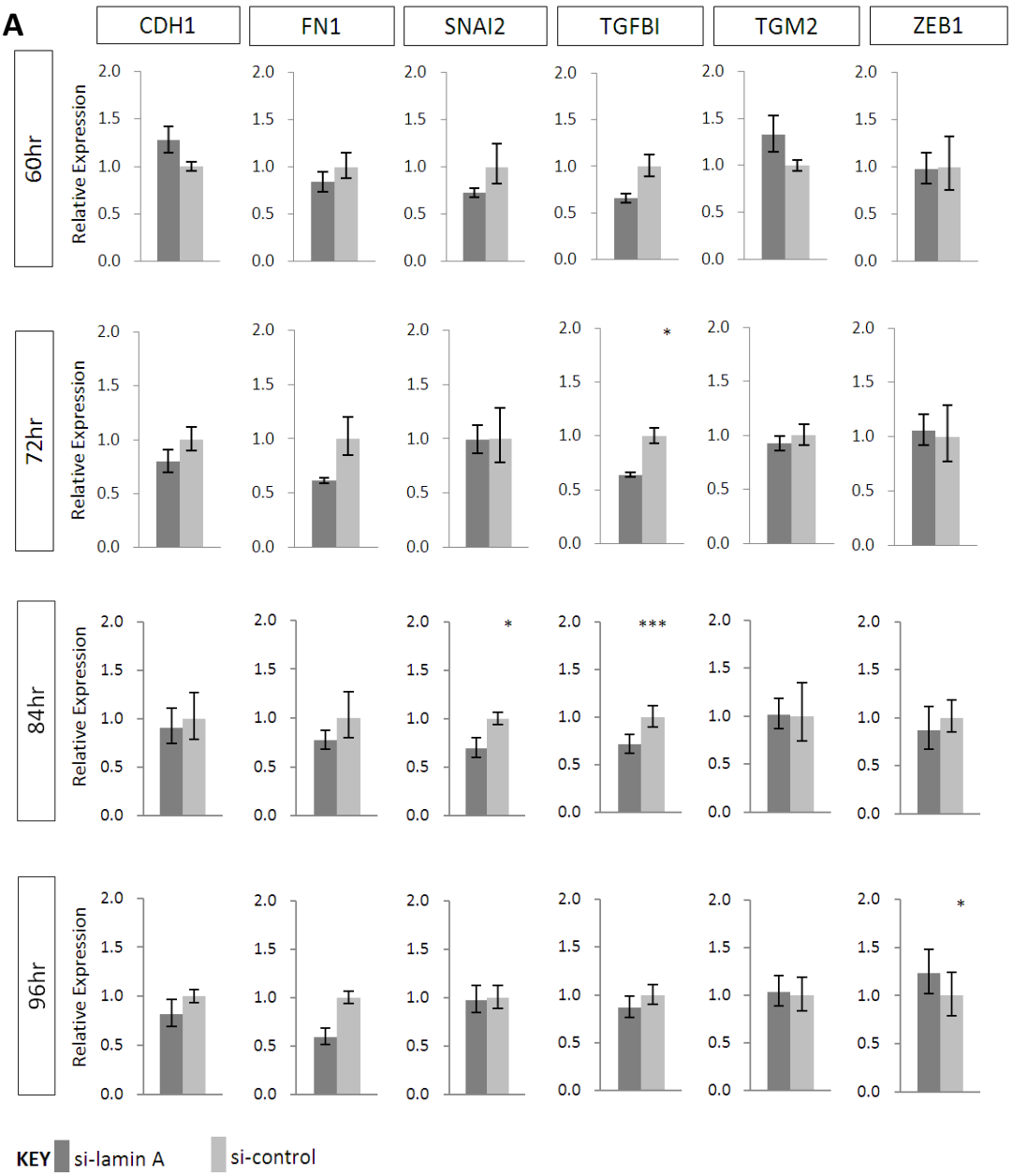
A
CDH1
FN1
SNAI2
TGFBI
TGM2
ZEB1
60hr
72hr
84hr
96hr
Relative Expression
2.0
1.5
1.0
0.5
0.0
*
***
KEY
si-lamin A
si-control

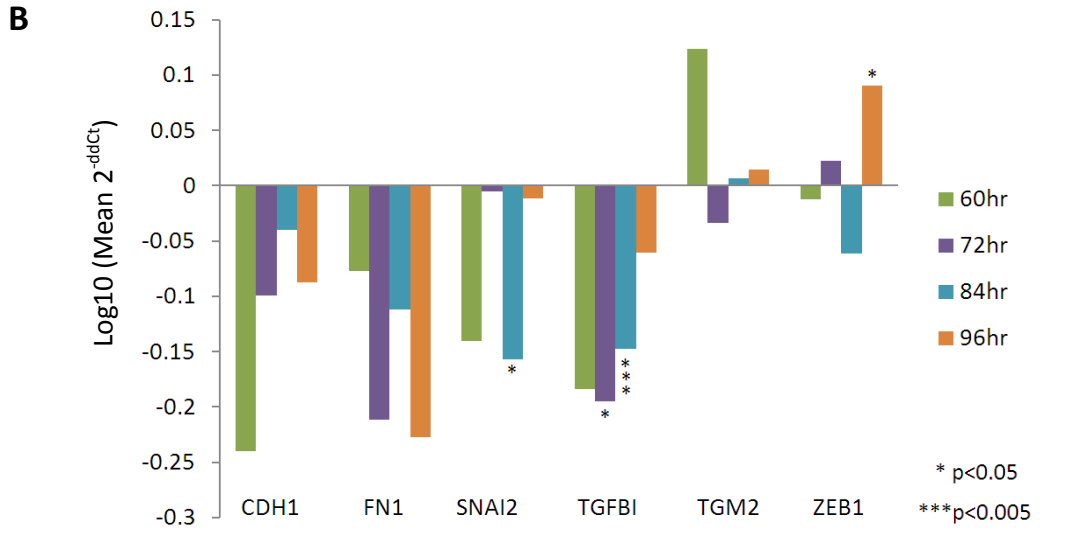
B
Log10 (Mean 2-ddCt)
0.15
0.1
0.05
0
-0.05
-0.1
-0.15
-0.2
-0.25
-0.3
CDH1
FN1
SNAI2
TGFBI
TGM2
ZEB1
60hr
72hr
84hr
96hr
* p<0.05
***p<0.005

Table 4.2: P values for the differences in gene expression between si-lamin A and si-cntl treated SW480/lamA cells

	CDH1	*FN1*	*SNAI2*	*TGFBI*	*TGM2*	*ZEB1*
60hr	0.107	0.599	0.337	0.151	0.153	0.901
72hr	0.137	0.265	0.933	**0.048**	0.244	0.681
84hr	0.746	0.544	**0.047**	**0.003**	0.965	0.306
96hr	0.188	0.055	0.662	0.244	0.812	**0.023**

P values calculated using a 1 sample T test, showing the statistical significance of the difference in expression levels of target genes measured in SW480/lamA cells treated with si-lamin A or si-cntl.

There were no statistically significant differences found in *FN1* expression, however, *FN1* expression was lower in si-lamin A treated cells at the 96hr timepoint with a p value of 0.055, which was almost statistically significant. We would expect *FN1* expression to be lower in si-lamin A treated cells, as *FN1* expression was increased in SW480/lamA cells in the microarray and Q-PCR data.

In previous experiments, levels of expression of *SNAI2* were not consistent, as expression was higher in SW480/lamA cells in the microarray, but lower in SW480/lamA cells in the QPCR data. In this experiment, expression levels of *SNAI2* were not significantly different at most of the timepoints assayed, however *SNAI2* expression was downregulated in si-lamin A cells at the 84hr timepoint ($p<0.05$).

In the microarray experiment, *ZEB1* expression was higher in SW480/lamA cells; however no statistically significant changes were seen in *ZEB1* expression when comparing SW480/lamA and SW480/cntl cells using QPCR. Expression levels of *ZEB1* were not significantly different in cells transfected with si-lamin A and si-control at most of the timepoints assayed, however *ZEB1* expression was upregulated in si-lamin A cells at the 96hr timepoint ($p<0.05$). This is inconsistent with the findings from the microarray experiment.

As TG2 is known to induce EMT, was up-regulated 2.64 fold in SW480/lamA cells in the microarray experiment, and was shown to be overrepresented in the cytoskeletal fraction of SW480/lamA cells, we hypothesised that *TGM2* would be down-regulated in cells transfected with si-lamin A. However, contrary to our expectations, *TGM2* expression levels were not significantly different.

4.3.4. The effect of down-regulation of lamin A by siRNA transfection on TGFBI protein expression over time

Lastly, we wanted to investigate whether changes in expression of TGFBI occurred between transfection of siRNA causing a knockdown of lamin A, and the change in cell motility measured between 96-120 hours post-transfection. Immunoblots were used to assay the expression of TGFBI every 24 hours between 48-120hours post-transfection with either si-lamin A or si-control. It is apparent that expression levels of TGFBI in both si-laminA and si-control transfected cells increase over time, as the cells become more confluent. Expression of TGFBI was approximately equal compared to control cells between 48-120 hours after transfection (Figure 4.6).

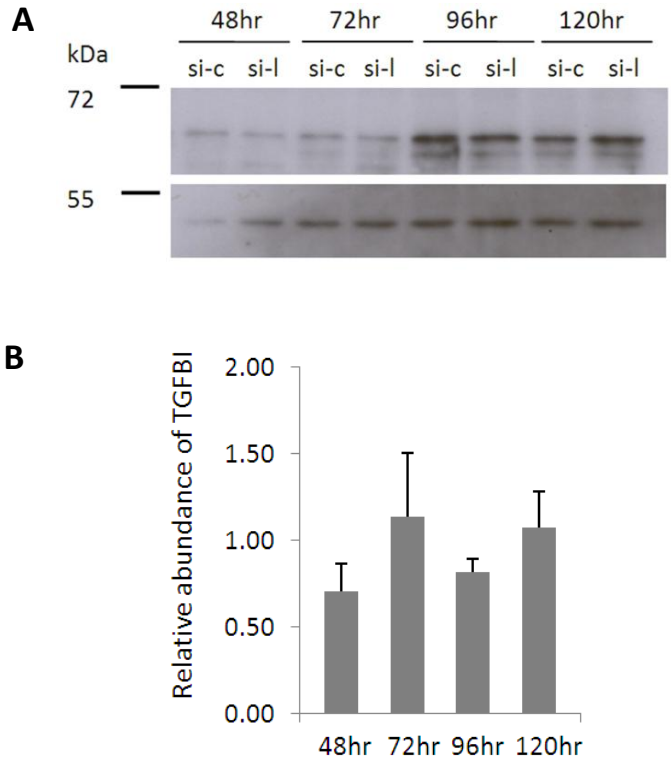

Figure 4.6: The effect of siRNA knockdown of lamin A on expression of TGFBI

A Immunoblot of whole cell extracts from SW480/lam A cells transfected with si-laminA or si-control resolved on a 10% SDS-PAGE gel and probed with anti-TGFBI antibody. Actin was used as a loading control. Cell pellets were harvested at 48, 72, 96 and 120 hours post transfection with siRNA.

B Densitometric analysis of TGFBI expression in SW480/lamA cells transfected with si-lamin A compared to those transfected with si-control. Images were taken with Fujifilm Intelligent Dark Box II and relative densities were measured with Image J software. Error bars represent standard error of three biological replicates.

4.4. Discussion

In this chapter siRNA was used to downregulate expression of lamin A and GFP-lamin A to confirm that the motility changes shown in Chapter 2 were a direct consequence of expression of lamin A, and to assess the effect of downregulation of lamin A on gene and protein expression over time.

Knockdown of endogenous lamin A was highly successful, with a decrease in protein expression evident from 24 hours after transfection and over 95% reduction in expression by 120 hours after transfection. Expression of GFP-lamin A was reduced by over 50% 120 hours after transfection. The wound closure rate was not significantly slower in si-lamin A treated cells compared to control cells 72-96 hours after transfection, however si-lamin A cells moved over 40% more slowly than control cells when assayed 96-120 hours post-transfection. These findings confirm our previous finding that upregulation of lamin A in SW480 CRC cells causes increased cell motility.

To test the hypothesis that knockdown of lamin A would lead to changes in expression of TGFβ-regulated genes previously identified in this investigation, we analysed the expression of *CDH1, FN1, TGFBI, SNAI2, TGM2* and *ZEB1* at 12 hour timepoints after the knockdown of lamin A and before the observed change in cell motility. We hypothesised that siRNA knockdown of lamin A would lead to an MET in which decreased expression of *TGM2* and *TGFBI* would be followed by decreased expression of *SNAI2* and *ZEB1* and subsequent increased expression of *CDH1* and decreased expression of *FN1*.

In partial accordance with this hypothesis, there was decreased expression of *TGFBI* at the 72hr ($p<0.05$) and 84hr ($p<0.005$) timepoints and decreased *SNAI2* expression at the 84hr timepoint ($p<0.05$) in si-lamin A transfected cells compared to control cells.

Although the decrease in cell motility in cells transfected with si-lamin A compared to control cells was extremely reproducible ($p<0.0005$), when assaying gene expression using Q-PCR there was often large variation between the three replicate samples, resulting in few results that were statistically significant. Increasing the number of biological replicates may give a more accurate representation of the changes occurring in the cells and may increase the number of statistically significant changes seen.

Unexpectedly, *ZEB1* expression was higher in si-lamin A cells 96hrs after transfection ($p<0.05$). Expression levels of *ZEB1* in SW480/lamA cells have been inconsistent throughout this study. In the microarray experiment, *ZEB1* expression was higher in SW480/lamA cells,

yet no statistically significant changes were seen in *ZEB1* expression when comparing SW480/lamA and SW480/cntl cells using QPCR. It is possible that changes in *ZEB1* expression occur predominantly at the leading edge of the cell. Invasive cells that have undergone EMT are typically found at the invasion front of CRCs, whereas the central cells of the tumour have more characteristics of epithelial cells (Brabletz et al., 2001; Hlubek et al., 2007). Repressors of E-cadherin such as *ZEB1* have been shown to be highly expressed and E-cadherin expression reduced at the invasive front of cancers (Hlubek et al., 2007; Huszar et al., 2010; Spaderna et al., 2006). Migrating cells at the invasive front of a tumour contain membrane protrusions that form a leading edge. Some proteins such as GPR56, APC and phospho-β-catenin have been shown to accumulate at the leading edge of migrating cells (Faux et al., 2010; Shashidhar et al., 2005). The change in expression of *ZEB1* and other genes of interest may therefore be seen most predominantly in the protein expression at the leading edge of the cell. Future experiments will include examining the expression and distribution of the proteins encoded by the genes of interest.

The results suggest that a change in total expression levels of *TGM2, CDH1* and *FN1* is not required to mediate the effects of lamin A expression on cell motility. However, these genes may regulate lamin A-mediated cell motility through changes in the levels of TG2, E-cadherin and fibronectin protein expression, or in the distribution of these proteins within the cell. It is also possible that expression of these genes is regulated by lamin A expression but does not have an effect on cell motility in the SW480 cell line.

The most significant change in gene expression was that of *TGFBI*, which was consistently lower in si-lamin A transfected cells compared to control cells. This is consistent with the microarray and QPCR data, in which *TGFBI* expression was up-regulated in SW480/lamA cells and with previous studies, in which *TGFBI* was shown to promote metastasis when overexpressed in SW480 cells (Ma et al., 2008). However, expression of TGFBI protein was approximately equal compared to control cells between 48-120 hours post-transfection. Expression levels of TGFBI protein in both si-laminA and si-control transfected cells increased over time, as the cells became more confluent. It is possible that the effect of the density of cells on TGFBI expression is masking any differences between TGFBI expression in SW480/lamA and SW480/cntl cells. TGFBI expression has been shown to be density dependent in human corneal epithelial cells (Wang et al., 2002); however in this study the transcript levels reduced as the cell density increased. Expression levels of proteins encoded by some of the other genes investigated in this study, such as *CDH1* and *SNAI2*, are also known to be affected by cell density. Levels of E-cadherin increase as the cell

density increases (Maeda et al., 2005) and Snai2 has been shown to regulate E-cadherin in SW480 cells in a cell density dependent manner (Conacci-Sorrell et al., 2003). However, it must be noted that the effects of cell density on protein expression may not affect comparisons between si-lamin A and si-control transfected cells, as all the cells were at equal density at each timepoint assayed.

TGFBI encodes an extracellular matrix protein which is induced by TGFβ and is ubiquitously expressed in most normal human tissues, apart from in the brain (Skonier et al., 1992; Thapa et al., 2007; Zhao et al., 2002). It associates with many other ECM proteins including fibronectin, integrins and collagens (Bae et al., 2002; Billings et al., 2002). TGFBI is thought to mediate cell motility and adhesion through its interaction with integrins (Bae et al., 2002; Kim et al., 2003). Reduced expression of TGFBI has been found in some human cancer cell lines and tumours (Calaf et al., 2008; Zhao et al., 2006; Zhao et al., 2002) and elevated expression has been found in some colorectal tumour samples (Agrawal et al., 2002; Buckhaults et al., 2001; Kitahara et al., 2001; Notterman et al., 2001). Like TGFβ, the function of TGFBI in cancer cells is complex, as TGFBI can either promote cancer progression or act as a tumour suppressor (Ma et al., 2008; Zhang et al., 2009). Interestingly, the untransfected SW480 cell line contains very low levels of TGFBI protein, whereas the cell line SW620, derived from a lymph node metastasis from the same patient, expresses much higher levels of TGFBI protein (Leibovitz et al., 1976; Ma et al., 2008).

SNAI2 expression was also decreased 84 hours after transfection ($p<0.05$) in si-lamin A transfected cells compared to control cells. Snai2 is a member of the Snail family of zinc transcription factors. It is a well known inducer of EMT (Hajra et al., 2002; Savagner et al., 1997), a downstream mediator of TGFβ (Choi et al., 2007; Joseph et al., 2009) and is known to promote cell motility and invasion in cancer cells (Joseph et al., 2009; Katafiasz et al., 2011). The relationship between expression of lamin A and expression of SNAI2 has not been consistent in this study. In the microarray experiment, *SNAI2* was found to be 4.05 fold up-regulated in SW480/lamA cells compared to control cells, however *SNAI2* expression was significantly lower in SW480/lamA cells as assessed by Q-PCR.

As has been suggested for *ZEB1*, the change in expression of *SNAI2* and *TGFBI* may be seen predominantly in a change of Snai2 and TGFBI protein expression at the leading edge of the cell. Future experiments using immunofluorescence in combination with wounding assays will seek to test this hypothesis.

The data suggest that knockdown of lamin A forms in SW480/lamA cells leads to a decrease in expression of *TGFBI* and *SNAI2*, followed by a decrease in cell motility. It is unclear from the data gathered so far whether or not this change in cell motility is caused by an MET. The observed decrease in cell motility may be also caused in part by other genes in Network1 that we did not assess, or by other signalling systems regulated by TGFβ. In future experiments, I would examine expression of the remaining genes in Network 1 after siRNA knockdown of lamin A. Nothing is yet known about a potential link between *TGFBI* and *SNAI2* expression. Further experiments are required to assess if *TGFBI* and *SNAI2* are directly causing the change in cell motility. This could be achieved by measuring the rate of cell motility after either overexpressing the genes in SW480/cntl cells or using siRNA to knockdown gene expression in SW480/lamA cells.

CHAPTER FIVE
General Discussion

5.1 Background and aims of thesis

Lamins are multifunctional proteins that are often aberrantly expressed in tumours. Many studies show lamin A/C to be down-regulated in tumour cells, but expression is also frequently increased or up-regulated (Foster et al., 2010). Often expression levels vary dramatically even within cancer subtypes; for example, in CRC and basal cell carcinomas, A-type lamin expression can be positive, reduced or negative (Moss et al., 1999; Tilli et al., 2003; Venables et al., 2001; Willis et al., 2008).

Expression of lamin A in CRC cells promotes increased cell motility (Willis et al., 2008). In wounding assays, wound closure was significantly faster in CRC cells transfected with GFP–lamin A compared with control cells transfected with GFP alone. The same study revealed that patients with CRC tumours expressing A-type lamins were almost twice as likely to die from their disease compared with clinicopathologically identical patients whose tumours were negative for expression of A-type lamins (Willis et al., 2008). A-type lamins are therefore potential biomarkers for poor prognosis in CRC.

The central aim of this thesis was to investigate the mechanisms by which over-expression of lamin A in CRC cells causes increased cell motility, leading to a poor prognosis for patients. The findings of Willis *et al.* suggest that lamin A may influence cell motility through the regulation of actin dynamics and cell adhesion, as GFP-lamin A expression was shown to control a pathway in which up-regulated expression of the actin bundling protein T plastin led to down-regulated expression of the cell adhesion molecule E-cadherin (Willis et al., 2008). My aim was to investigate these findings further by using both quantitative proteomics and genomics. As initial approaches, a proteomic study was used to assess the organisation of the cytoskeleton, and a microarray experiment was used to examine genome wide changes induced in response to lamin A over-expression.

5.2 Over-expression of lamin A causes changes in the organisation of the cytoskeleton

To investigate cytoskeletal organisation in this study, it was necessary to use a highly reproducible procedure to isolate the cytoskeleton for analysis with 2D DIGE so that quantitative comparisons could be made. To do this, I optimised a biochemical

fractionation protocol for the preparation of cytoskeletal fractions, and this technique was shown to produce extremely reproducible profiles of protein expression in 2D gels. This protocol has been shared with investigators in Spain who wish to analyse the cytoskeleton in their work, and has recently been published (Foster et al., 2011). This protocol should therefore be a useful tool for those who wish to investigate aspects of the cytoskeleton.

This study is the first to use quantitative proteomics to investigate changes linked to cancer cell motility in a cytoskeletal fraction. Using 2D DIGE, 64 protein spots showed changes in representation within the cytoskeleton of SW480/lamA cells compared to SW480/cntl cells, and there was a large enough amount of protein in 29 of these spots for them to be identified using mass spectrometry. In future experiments, to identify the remaining proteins in this fraction, we could use SILAC (stable isotope labelling with amino acids in cell culture) technology, which is thought to provide highly sensitive detection of protein changes (Boisvert and Lamond, 2010; Ong et al., 2002). In this procedure, cells of interest would be labelled with amino acids containing stable isotopes such as deuterium or ^{13}C, and comparisons would be made with control cells containing non-labelled amino acids.

The majority of proteins identified in the 2D DIGE investigation were either components/ cross-linkers of the cytoskeleton, protein chaperones or translation initiation/elongation factors. The finding that tissue transglutaminase (TG2) was highly over-represented in the cytoskeleton fraction of SW480/lamA cells is very interesting, as TG2 may cause some of the changes in protein association with the cytoskeleton found in these cells. TG2 forms intramolecular and intermolecular crosslinks by catalysing the formation of ε-(γ-glutamyl) lysine isopeptide bonds between proteins. Many of the proteins identified in this study, such as actin, α-actinin, EF-1α, EF-1γ, Hsp60 and members of the Hsp70 family are known to be TG2 substrates, and other substrates include the cytoskeletal proteins tubulin, myosin and cofilin (Nemes et al., 1997; Orru et al., 2003; Puszkin and Raghuraman, 1985; Robinson et al., 2007). The changes observed in the cytoskeleton may be a result of TG2 crosslinking actin, vimentin and α-actinin to other cytoskeleton proteins. The under-representation of chaperonin proteins in the cytoskeletal fraction may also be explained by altered regulation of the cross-linking of these proteins to the cytoskeleton by TG2. Further experiments to determine the differences between TG2 crosslinking activity in SW480/lamA and SW480/cntl cells would be very informative. Affinity isolation combined with SILAC technology could be used to identify TG2 binding partners and to assess any differences between the cell types. Double-immunofluorescence staining could also be used to visualise potential TG2 co-localisation with proteins of interest in CRC cells.

Five translation initiation/elongation factors, many of which have known roles in cancer, were shown to be over or under-represented in the cytoskeletal fraction of SW480/lamA cells. This may reflect an association between transcriptional machinery and the cytoskeleton or nuclear matrix. Future work should focus on using immunofluorescence to visualise the intracellular distribution of these proteins and to assess their association with different cytoskeletal proteins.

To further elucidate the mechanism leading to increased cell motility in these cells, IPA was used to analyse a genome-wide DNA microarray experiment which compared gene expression in SW480/lamA and SW480/cntl cells. Over-expression of lamin A led to large scale changes in gene expression; over 1200 probesets were differentially expressed. The most significant interaction network identified by IPA highlighted genes linked to cancer, cellular movement and cellular growth and proliferation. This network had a highly significant score of 44 and 31 out of the 35 genes included were taken from the microarray dataset. To validate the microarray data, expression of a subset of eight out of eleven Network 1 genes examined was independently confirmed using Q-PCR. This network therefore contained over 30 genes which may be involved in the mechanism that causes increased cell motility in cells over-expressing lamin A.

The data from the genomic and proteomic studies, coupled with the finding that expression of lamin A causes increased expression of the actin bundling protein T-plastin (Willis et al., 2008), suggest that lamin A expression causes changes in the organisation of the actin cytoskeleton. Different forms of filamentous actin are found in cells, including stress fibres comprising contractile bundles of actin typically held together by α-actinin, actin meshworks in the cell cortex and lamellipodia and highly oriented, polarised cables in filopodia. In the proteomics study, cells over-expressing lamin A were found to have higher levels of insoluble β-actin and increased association of the actin cross-linking protein α-actinin with the cytoskeleton compared to control cells. A number of the genes in Network 1 also encode proteins known to be associated with the actin cytoskeleton, including IGF2BP1 and CDC42EP5. CDC42 effector protein 5 induces the assembly of actin filaments (Hirsch et al., 2001) and ectopic expression of CDC42EP5 in fibroblasts has been shown to cause loss of stress fibres and extension of protrusive lamellipodia (Joberty et al., 1999). IGF2BP1 binds β-actin mRNA, localizing it to sites of active actin polymerisation, where it modulates cell migration (Huttelmaier et al., 2005; Ross et al., 1997).

The reduced association of chaperonin proteins, particularly of nucleophosmin, within the cytoskeleton might alter the balance between different forms of actin. Nucleophosmin is thought to mediate changes in actin cytoskeleton dynamics, as increased expression of nucleophosmin has been shown to lead to decreased stress fibre formation (Sandsmark et al., 2007). EMT induced by TGFβ results in the reorganisation of cortical actin into longitudinal stress fibres (Miettinen et al., 1994; Piek et al., 1999; Zavadil et al., 2001). In EMT, TGFβ targets guanine nucleotide exchange factors, which activate Rho GTPases, which lead to formation of actin stress fibres (Bhowmick et al., 2001; Ridley and Hall, 1992; Shen et al., 2001). TG2 is also known to co-localise with stress fibres in human umbilical vein endothelial cells (Chowdhury et al., 1997). It would be interesting to investigate the structure of actin filaments in SW480/lamA and SW480/cntl cells using immunofluorescence with fluorescently tagged phalloidin, a toxin that binds to filamentous actin.

5.3 Over-expression of lamin A in CRC cells may cause an epithelial-mesenchymal transition

It was postulated that the observed change in cell motility may arise through an EMT or an EMT-like process, as Network 1 contained genes encoding epithelial markers such as *CDH1* which were down-regulated and mesenchymal markers such as *FN1* which were up-regulated in SW480/lamA cells. There was also found to be a statistically significant overlap between IPA lists of genes linked to EMT and the microarray dataset. Three of the proteins identified in the 2D DIGE experiment are known to be involved with this process: vimentin is a typical mesenchymal marker (Ivaska, 2011), TG2 is known to induce EMT (Kumar et al., 2010; Shao et al., 2009) and rearrangement of the actin cytoskeleton is a hallmark of EMT (Yilmaz and Christofori, 2009). Many of the genes in Network 1 encode proteins which are known to induce EMT or EMT-like responses, including *SNAI2* (Hajra et al., 2002; Savagner et al., 1997), *BMP4* (Hamada et al., 2007; Molloy et al., 2008), *MSX2* (Hamada et al., 2007; Satoh et al., 2008), *EIF4E* (Ghosh et al., 2009) and *EGFR* (Lo et al., 2007).

It is possible that expression levels of lamin A influence TGFβ-mediated EMT. A-type lamins are known to be involved in regulating gene activity downstream of TGFβ, as A-type lamins modulate responses to TGFβ signalling in mesenchymal cells through regulation of transcription factors such as pRB and SMADs (Van Berlo et al., 2005). MAN1, a lamin A-interacting protein, is also known to regulate TGFβ signalling through binding to R-Smads (Lin et al., 2005; Osada et al., 2003).

Many of the genes highlighted in Network 1 and in the 2D DIGE analysis are linked to TGFβ signalling. BMP4 is a member of the TGFβ superfamily. *SERPINE1* and *SNAI2* are up-regulated by TGFβ and *AREG* is downregulated by TGFβ (Akiyoshi et al., 2001; Choi et al., 2007; Joseph et al., 2009). eIF4E is linked to TGFβ-mediated EMT, as TGFβ activates mTOR, inducing the phosphorylation of 4E-BP1, which causes dissociation of EIF4E from 4E-BP1, increasing protein synthesis (Hay and Sonenberg, 2004; Lamouille and Derynck, 2007). TGFβ and TG2 interact cooperatively, as TG2 expression is regulated by TGFβ and TG2 is involved in the ECM storage and activation of latent TGFβ (LTGFβ) (Kojima et al., 1993; Ritter and Davies, 1998; Telci et al., 2009; Verderio et al., 1999). BMP4 is also involved in regulation of TG2 gene expression (Ritter and Davies, 1998).

Currently there are no published findings about the relationship between lamin A expression and EMT, therefore the suggestion that lamin A may cause an EMT or an EMT-like process is novel.

5.4 siRNA knockdown of lamin A leads to down-regulation of *TGFBI* and *SNAI2* expression followed by reduced cell motility

In the final chapter of this thesis, the effect of siRNA knock down of lamin A on genes involved in TGFβ signalling was investigated. The aim was to understand which of the genes known to be regulated by lamin A expression are responsible for causing the changes in cell motility.

Transfection of si-lamin A resulted in a reduction of endogenous lamin A expression by over 95% and a reduction of GFP-lamin A expression by over 50% by 120 hours after transfection. Cells transfected with si-lamin A were less motile than control cells, confirming that the increased cell motility shown in Chapter 2 was a direct consequence of the over-expression of lamin A. Reduced cell motility in si-lamin A transfected cells was preceded by decreased expression of *TGFBI* and *SNAI2*. These findings are consistent with the microarray and QPCR data, in which *TGFBI* expression was up-regulated in SW480/lamA cells and with previous studies, in which TGFBI was shown to promote metastasis when overexpressed in SW480 cells (Ma et al., 2008). However, expression of TGFBI protein was similar in si-lamin A and si-control cells between 48-120 hours post-transfection. As migrating cells at the invasive front of a tumour have been shown have different protein expression compared to the cells away from the invasive front (Hlubek et al., 2007; Huszar et al., 2010; Spaderna et al., 2006), it is possible that changes in expression of *SNAI2* and *TGFBI* may be seen predominantly in a change of Snai2 and TGFBI protein expression at the

leading edge of the cell. Future experiments using immunofluorescence in combination with wounding assays will seek to test this hypothesis.

TGFBI is induced by TGFβ (Skonier et al., 1992) and is thought to mediate cell motility and adhesion through its interaction with integrins (Bae et al., 2002; Kim et al., 2003). Its expression is reduced in some cancer cell lines and tumours and elevated in others (Agrawal et al., 2002; Buckhaults et al., 2001; Calaf et al., 2008; Kitahara et al., 2001; Notterman et al., 2001; Zhao et al., 2006; Zhao et al., 2002). TGFBI can either act as a tumour suppressor or a promoter of cancer progression (Ma et al., 2008; Zhang et al., 2009). Interestingly, the untransfected SW480 cell line contains very low levels of TGFBI protein, whereas its metastatic counterpart SW620 expresses much higher levels of TGFBI protein (Leibovitz et al., 1976; Ma et al., 2008).

Snai2 is a member of the Snail family of zinc transcription factors. Also known as Slug, it is a well known inducer of EMT (Hajra et al., 2002; Savagner et al., 1997), a downstream mediator of TGFβ (Choi et al., 2007; Joseph et al., 2009) and is known to promote cell motility and invasion in cancer cells (Joseph et al., 2009; Katafiasz et al., 2011). In the microarray experiment, SNAI2 was found to be 4.05 fold up-regulated in SW480/lamA cells compared to control cells, however SNAI2 expression was significantly lower in SW480/lamA cells as assessed by Q-PCR.

In future experiments, to assess whether *TGFBI* and *SNAI2* are directly causing the change in cell motility, the genes could be overexpressed in SW480/cntl cells or knocked down in SW480/lamA cells followed by assessment of cell motility using wounding assays. As the expression levels of genes using Q-PCR were very variable between replicates in this experiment, it would also be useful to repeat the assessment of gene expression with a larger number of biological repeats. This may give a more accurate representation of the changes occurring in the cells.

5.5 Conclusions

It is unclear from the data gathered so far whether or not the change in cell motility induced by lamin A over-expression is caused by an EMT. It should be noted that the IPA analysis did not highlight EMT in Networks 1-10 and changes in microarray and Q-PCR assessments of expression of *SNAI2, ZEB1, AREG* and *EREG* were inconsistent. In Chapter 4, no significant differences were seen in *CDH1, FN1* or *TGM2* expression between 60-96 hours post transfection with si-laminA and *ZEB1* expression was unexpectedly higher 96 hours after transfection.

It is possible that the changes seen in our system represent a novel pathway that is similar to EMT but not a classical EMT. Many of the genes and proteins identified in this thesis are known to affect cell motility. *FN1, EIF4E, NRP1, EGFR* and *SERPINE1*, which were all upregulated in SW480/lamA cells, all encode proteins which have been found to be expressed in highly motile and invasive cancer cells (Chazaud et al., 2002; Miao et al., 2000; Shankar et al., 2010; Shibata et al., 1997; Verbeek et al., 1998). Decreased expression levels of *EMP1*, which was downregulated in SW480/lamA cells, are known to correlate with metastatic cells (Zhang et al., 2011). Inhibition of nucleophosmin shuttling can cause increased cell motility (Sandsmark et al., 2007) and elevated Hsp60 levels correlate with high occurrence of lymph node metastases in large bowel carcinomas (Cappello et al., 2005a). Actinin α4 is enriched at the leading edges of invasive cells (Honda et al., 1998) and has been shown to increase cell motility in CRC (Honda et al., 2005). Down-regulation of actinin α4 reduces cell motility in glioblastoma and lung fibroblasts (Sen et al., 2009; Shao et al., 2010a).

Experiments following on from this study should focus on identifying which genes and proteins are required for increased cell motility to occur following over-expression of lamin A in CRC cells. The data in this thesis is an excellent resource for work in this area, as the proteomics study revealed 13 proteins and Network 1 contains 35 genes which may be necessary in this process. Networks 2-10 were also all shown by IPA to be statistically significant, indicating that these networks would also be a valuable resource for future work. Both *TGFB1* and *TGFBI* are present in Networks 1-10: *TGFB1* is a node in Network 7 and *TGFBI* is present in Network 9. As both Networks 7 and 9 are linked to cellular motility, these would be ideal starting points for future work. In addition, components of the canonical and non-canonical TGFβ pathways should be studied. siRNA knockdown of proteins of interest followed by wounding assays will be vital to assess the effect of individual proteins on cell motility. It is hoped that a mechanism will eventually be discovered which describes the order of events which follow a change in expression of lamin A, leading to a change in cell motility. Once the mechanism has been revealed, other cancer cell lines and tumours should be examined, to discover if the findings are applicable to tumours originating from other locations.

A number of the proteins and genes identified in this study, including EF-1δ, mortalin, Hsp60, actinin α4, TG2, E-cadherin, Snai2 and vimentin are known to be linked to cancer prognosis. It would be interesting to assess the effect of expression of these proteins on prognosis of CRC. This could be done using a tissue bank such as the Netherlands Cohort

Study on Diet and Cancer (NLCS), a prospective cohort study which contains tissue samples linked to clinicopathological data. There is also another tissue array bank, located in Western Australia, which is larger than the NLCS and contains several thousand tissue samples. This databank could be used to assess the use of proteins of interest as predictive markers to determine whether expression of these proteins influences the response of tumours to adjuvant therapies. Expression of TGFBI, for example, has already shown to be associated with response to chemotherapy in lung cancer (Irigoyen et al., 2010). Although lamin A is already known to be a prognostic biomarker for CRC, it would be more useful to identify a panel of biomarkers which could be used as a prognostic tool for CRC. A panel of biomarkers would be expected to allow clinicians to make more accurate predictions of prognosis compared to predictions based on the current Dukes and TNM classification systems or a single biomarker.

In conclusion, the data described in this thesis suggest that expression of lamin A in CRC cells causes changes in the organisation of the actin cytoskeleton and in TGF-β signalling, potentially involving an epithelial to mesenchymal transition, leading to increased cell motility and an increased risk of death from cancer.

Appendix

Network diagrams 2-10 produced by IPA

Affymetrix microarray data comparing RNA from SW480/cntl and SW480/lamA cell lines was analysed using IPA. Interaction networks were produced from probesets displaying greater than 2.5 fold differential expression and show known literature curated interactions with other molecules. The networks were analysed for significance against known biological functions. Networks are ranked by their 'Score', which is calculated by IPA, and takes into account the number of network eligible molecules in the network, its size, the total number of network eligible molecules analysed and the total number of molecules in the knowledge base.

The number of 'Focus molecules' indicates the number of genes in each network that were present in the microarray probeset. These genes are circled in the diagrams: genes in red circles were up-regulated in SW480/lamA when compared to SW480/cntl and genes with blue circles were down-regulated. Each network clustered together genes with particular functions:

Network 2: Cell-To-Cell Signalling and Interaction, Cellular Assembly and Organization, Nervous System Development and Function

Network 3: Cancer, Cellular Growth and Proliferation, Cell Death

Network 4: Cellular Growth and Proliferation, Cell-To-Cell Signalling and Interaction, Cellular Function and Maintenance

Network 5: Cell Signalling, Small Molecule Biochemistry, Immunological Disease

Network 6: Lipid Metabolism, Small Molecule Biochemistry, Molecular Transport

Network 7: Cellular Movement, Connective Tissue Development and Function, Cancer

Network 8: Cell-To-Cell Signalling and Interaction, Haematological System Development and Function, Immune Cell Trafficking

Network 9: Cell Death, Cellular Movement, Cell Cycle

Network 10: Neurological Disease, Psychological Disorders, Cell-To-Cell Signalling and Interaction

Network 2

Cell-To-Cell Signalling and Interaction, Cellular Assembly and Organisation, Nervous System Development and Function

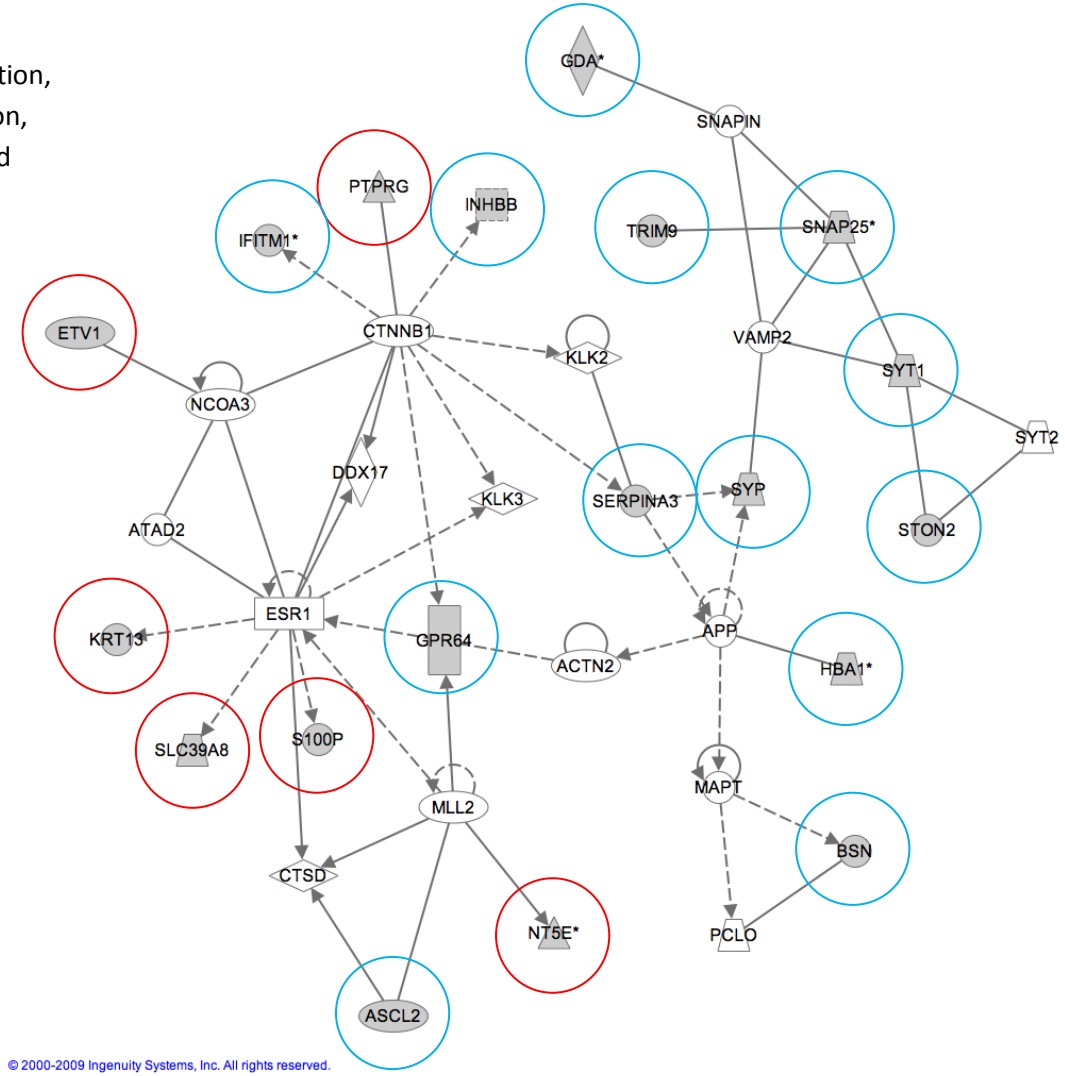

Up-regulated in SW480/lamA

Down-regulated in SW480/lamA

Network 2: Cell-To-Cell Signalling and Interaction, Cellular Assembly and Organization, Nervous System Development and Function

Score: 20 Focus molecules: 19

Genes up-regulated in SW480/lamA cells		
Symbol	**Fold Change**	**Entrez Gene Name**
ETV1	8.59	ets variant gene 1
KRT13	11.3	keratin 13
NT5E	4.84, 6.48, 11.28, 26.97	5'-nucleotidase, ecto (CD73)
PTPRG	5.19	protein tyrosine phosphatase, receptor type, G
S100P	7.61	S100 calcium binding protein P
SLC39A8	2.38, 4.25	solute carrier family 39 (zinc transporter), member 8

Genes down-regulated in SW480/lamA cells		
Symbol	**Fold Change**	**Entrez Gene Name**
ASCL2	2.98	achaete-scute complex homolog 2 (Drosophila)
BSN	2.76	bassoon (presynaptic cytomatrix protein)
GDA	3.09, 30.96	guanine deaminase
GPR64	4.08	G protein-coupled receptor 64
HBA1	2.77, 2.85, 2.85, 3.02, 3.50, 3.96	hemoglobin, alpha 1
IFITM1	4.94, 6.38	interferon induced transmembrane protein 1 (9-27)
INHBB	2.99	inhibin, beta B
SERPINA3	2.63	serpin peptidase inhibitor, clade A, member 3
SNAP25	4.49, 7.66, 10.44	synaptosomal-associated protein, 25kDa
STON2	2.51	stonin2
SYP	2.78	synaptophysin
SYT1	2.43, 2.88	synaptotagmin I
TRIM9	2.65	tripartite motif-containing 9

Genes added by IPA	
Symbol	**Entrez Gene Name**
ACTN2	actinin, alpha 2
APP	amyloid beta (A4) precursor protein
ATAD2	ATPase family, AAA domain containing 2
CTNNB1	catenin (cadherin-associated protein), beta 1, 88kDa
CTSD	cathepsin D
DDX17	DEAD (Asp-Glu-Ala-Asp) box polypeptide 17
ESR1	estrogen receptor 1
KLK2	kallikrein-related peptidase 2
KLK3	kallikrein-related peptidase 3
MAPT	microtubule-associated protein tau
MLL2	myeloid/lymphoid or mixed-lineage leukemia 2
NCOA3	nuclear receptor coactivator 3
PCLO	piccolo (presynaptic cytomatrix protein)
SNAPIN	SNAP-associated protein
SYT2	synaptotagmin II
VAMP2	vesicle-associated membrane protein 2 (synaptobrevin 2)

Network 3:
Cancer,
Cellular Growth and Proliferation,
Cell Death

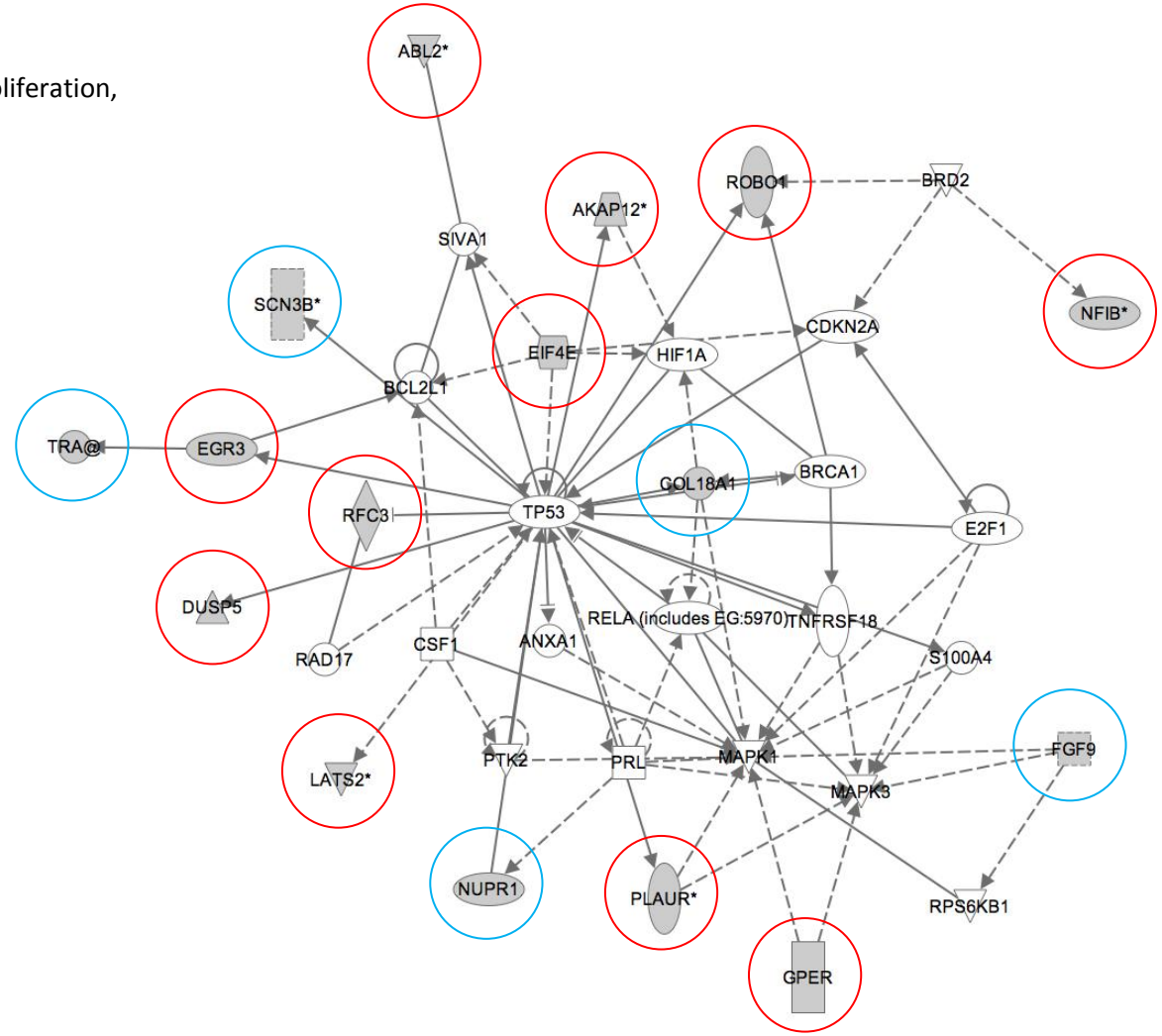

Up-regulated in SW480/lamA

Down-regulated in SW480/lamA

Network 3: Cancer, Cellular Growth and Proliferation, Cell Death
Score: 16 Focus molecules: 16

Genes up-regulated in SW480/lamA cells		
Symbol	**Fold Change**	**Entrez Gene Name**
ABL2	2.65, 3.07	v-abl Abelson murine leukemia viral oncogene homolog 2
AKAP12	7.47, 9.11, 12.86	A kinase (PRKA) anchor protein (gravin) 12
DUSP5	4.16	dual specificity phosphatase 5
EGR3	3.6	early growth response 3
EIF4E	3.15	eukaryotic translation initiation factor 4E
GPER	45.56	G protein-coupled estrogen receptor 1
LATS2	4.17, 4.51	LATS, large tumor suppressor, homolog 2 (Drosophila)
NFIB	2.02, 3.99, 5.61	nuclear factor I/B
PLAUR	2.39, 2.72, 2.73	plasminogen activator, urokinase receptor
RFC3	2.43, 2.51	replication factor C (activator 1) 3, 38kDa
ROBO1	4.84	roundabout, axon guidance receptor, homolog 1 (Drosophila)

Genes down-regulated in SW480/lamA cells		
Symbol	**Fold Change**	**Entrez Gene Name**
COL18A1	2.7	collagen, type XVIII, alpha 1
FGF9	2.76	fibroblast growth factor 9 (glia-activating factor)
NUPR1	3.48	nuclear protein 1
SCN3B	6.63, 11.39	sodium channel, voltage-gated, type III, beta
TRA@	3.26	T cell receptor alpha locus

Genes added by IPA	
Symbol	**Entrez Gene Name**
ANXA1	annexin A1
BCL2L1	BCL2-like 1
BRCA1	breast cancer 1, early onset
BRD2	bromodomain containing 2
CDKN2A	cyclin-dependent kinase inhibitor 2A
CSF1	colony stimulating factor 1 (macrophage)
E2F1	E2F transcription factor 1
HIF1A	hypoxia inducible factor 1, alpha subunit
MAPK1	mitogen-activated protein kinase 1
MAPK3	mitogen-activated protein kinase 3
PRL	prolactin
PTK2	PTK2 protein tyrosine kinase 2
RAD17	RAD17 homolog (S. pombe)
RELA	v-rel reticuloendotheliosis viral oncogene homolog A (avian)
RPS6KB1	ribosomal protein S6 kinase, 70kDa, polypeptide 1
S100A4	S100 calcium binding protein A4
SIVA1	SIVA1, apoptosis-inducing factor
TNFRSF18	tumor necrosis factor receptor superfamily, member 18
TP53	tumor protein p53

Network 4:
Cellular Growth and Proliferation,
Cell-To-Cell Signalling and Interaction,
Cellular Function and Maintenance

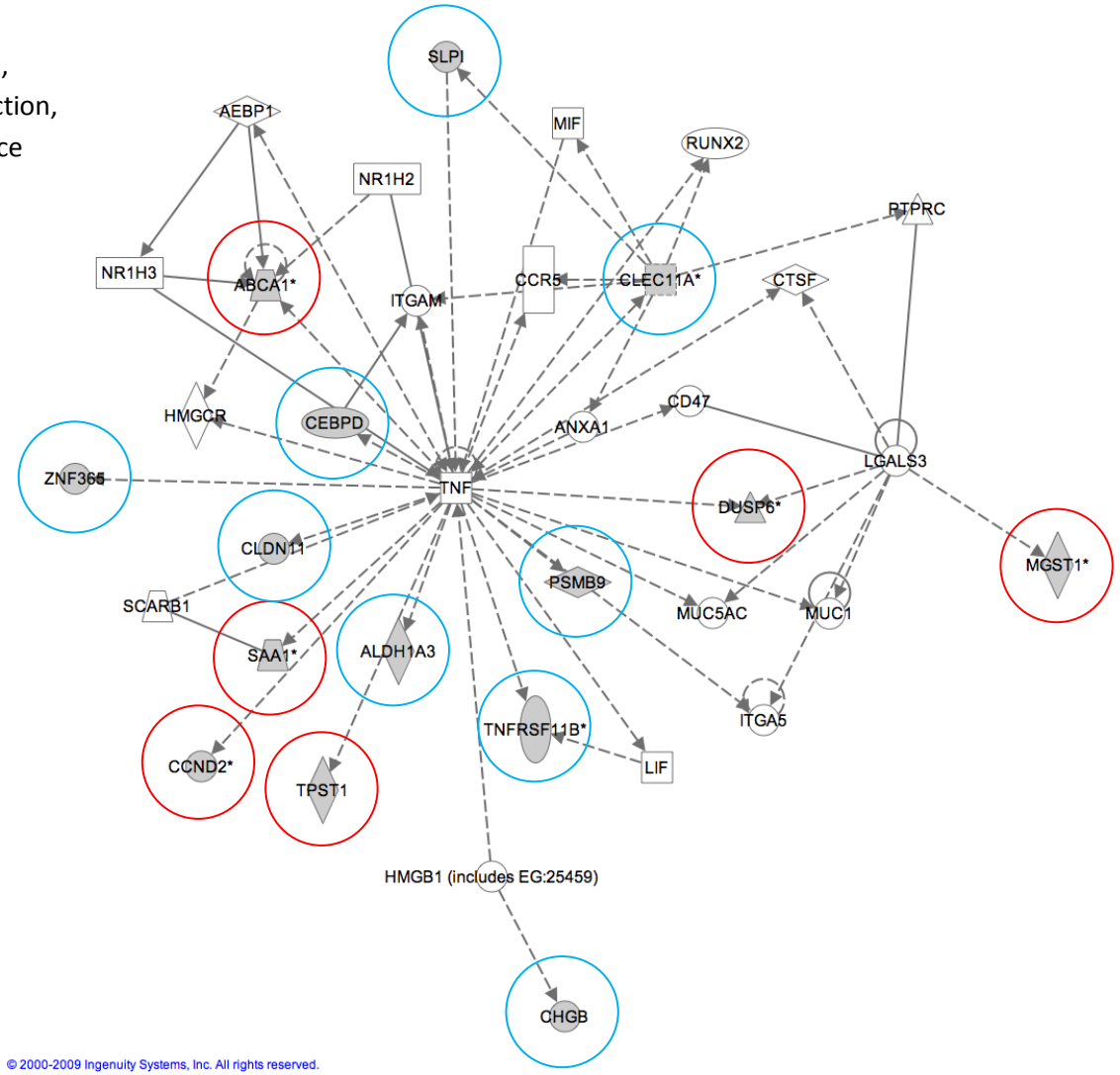

Up-regulated in SW480/lamA

Down-regulated in SW480/lamA

Network 4: Cellular Growth and Proliferation, Cell-To-Cell Signalling and Interaction, Cellular Function and Maintenance
Score: 14 Focus Molecules: 15

Genes up-regulated in SW480/lamA cells		
Symbol	**Fold Change**	**Entrez Gene Name**
ABCA1	2.58, 2.96	ATP-binding cassette, sub-family A (ABC1), member 1
CCND2	3.12, 5.19	cyclin D2
DUSP6	2.98, 2.99, 3.36	dual specificity phosphatase 6
MGST1	2.36, 2.81, 3.64	microsomal glutathione S-transferase 1
SAA1	3.29, 6.66	serum amyloid A1
TPST1	2.98	tyrosylprotein sulfotransferase 1

Genes down-regulated in SW480/lamA cells		
Symbol	**Fold Change**	**Entrez Gene Name**
ALDH1A3	4.87	aldehyde dehydrogenase 1 family, member A3
CEBPD	2.58	CCAAT/enhancer binding protein (C/EBP), delta
CHGB	11.5	chromogranin B (secretogranin 1)
CLDN11	2.85	claudin 11 (oligodendrocyte transmembrane protein)
CLEC11A	3.04, 3.73	C-type lectin domain family 11, member A
PSMB9	2.58	proteasome (prosome, macropain) subunit, beta type, 9 (large multifunctional peptidase 2)
SLPI	2.51	secretory leukocyte peptidase inhibitor
TNFRSF11B	3.76, 4.30	tumor necrosis factor receptor superfamily, member 11b (osteoprotegerin)
ZNF365	4.09	zinc finger protein 365

Genes added by IPA	
Symbol	**Entrez Gene Name**
AEBP1	AE binding protein 1
ANXA1	annexin A1
CCR5	chemokine (C-C motif) receptor 5
CD47	CD47 molecule
CTSF	cathepsin F
HMGB1	high-mobility group box 1
HMGCR	3-hydroxy-3-methylglutaryl-CoA reductase
ITGA5	integrin, alpha 5 (fibronectin receptor, alpha polypeptide)
ITGAM	integrin, alpha M
LGALS3	lectin, galactoside-binding, soluble, 3
LIF	leukemia inhibitory factor (cholinergic differentiation factor)
MIF	macrophage migration inhibitory factor (glycosylation-inhibiting factor)
MUC1	mucin 1, cell surface associated
MUC5AC	mucin 5AC, oligomeric mucus/gel-forming
NR1H2	nuclear receptor subfamily 1, group H, member 2
NR1H3	nuclear receptor subfamily 1, group H, member 3
PTPRC	protein tyrosine phosphatase, receptor type, C
RUNX2	runt-related transcription factor 2
SCARB1	scavenger receptor class B, member 1

Network 5:

Cell Signalling,
Small Molecule Biochemistry,
Immunological Disease

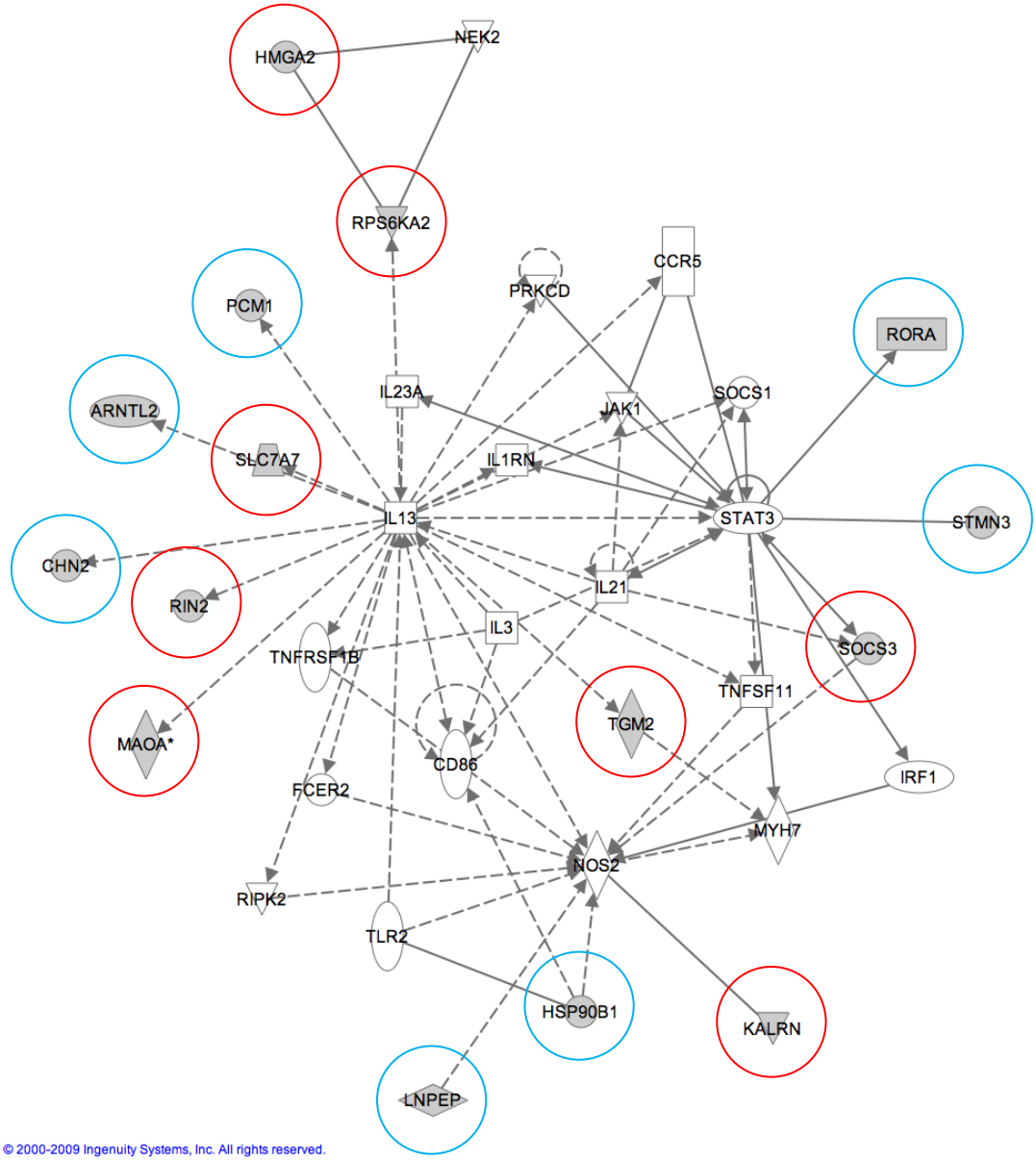

Up-regulated in SW480/lamA

Down-regulated in SW480/lamA

Network 5: Cell Signalling, Small Molecule Biochemistry, Immunological Disease
Score: 14 Focus Molecules: 15

Genes up-regulated in SW480/lamA cells		
Symbol	**Fold Change**	**Entrez Gene Name**
HMGA2	4.1	high mobility group AT-hook 2
KALRN	2.87	kalirin, RhoGEF kinase
MAOA	6.22, 8.07, 12.08	monoamine oxidase A
RIN2	28	Ras and Rab interactor 2
RPS6KA2	2.51	ribosomal protein S6 kinase, 90kDa, polypeptide 2
SLC7A7	2.69	solute carrier family 7 (cationic amino acid transporter, y+ system), member 7
SOCS3	2.73	suppressor of cytokine signaling 3
TGM2	2.65	transglutaminase 2 (C polypeptide, protein-glutamine-gamma-glutamyltransferase)

Genes down-regulated in SW480/lamA cells		
Symbol	**Fold Change**	**Entrez Gene Name**
ARNTL2	2.69	aryl hydrocarbon receptor nuclear translocator-like 2
CHN2	2.79	chimerin (chimaerin) 2
HSP90B1	2.69	heat shock protein 90kDa beta (Grp94), member 1
LNPEP	2.37, 2.58	leucyl/cystinyl aminopeptidase
PCM1	3.09	pericentriolar material 1
RORA	2.24	RAR-related orphan receptor A
STMN3	2.66	stathmin-like 3

Genes added by IPA	
Symbol	**Entrez Gene Name**
CCR5	chemokine (C-C motif) receptor 5
CD86	CD86 molecule
FCER2	Fc fragment of IgE, low affinity II, receptor for (CD23)
IL3	interleukin 3 (colony-stimulating factor, multiple)
IL13	interleukin 13
IL21	interleukin 21
IL1RN	interleukin 1 receptor antagonist
IL23A	interleukin 23, alpha subunit p19
IRF1	interferon regulatory factor 1
JAK1	Janus kinase 1
MYH7	myosin, heavy chain 7, cardiac muscle, beta
NEK2	NIMA (never in mitosis gene a)-related kinase 2
NOS2	nitric oxide synthase 2, inducible
PRKCD	protein kinase C, delta
RIPK2	receptor-interacting serine-threonine kinase 2
SOCS1	suppressor of cytokine signaling 1
STAT3	signal transducer and activator of transcription 3
TLR2	toll-like receptor 2
TNFRSF1B	tumor necrosis factor receptor superfamily, member 1B
TNFSF11	tumor necrosis factor (ligand) superfamily, member 11

Network 6
Lipid Metabolism,
Small Molecule Biochemistry,
Molecular Transport

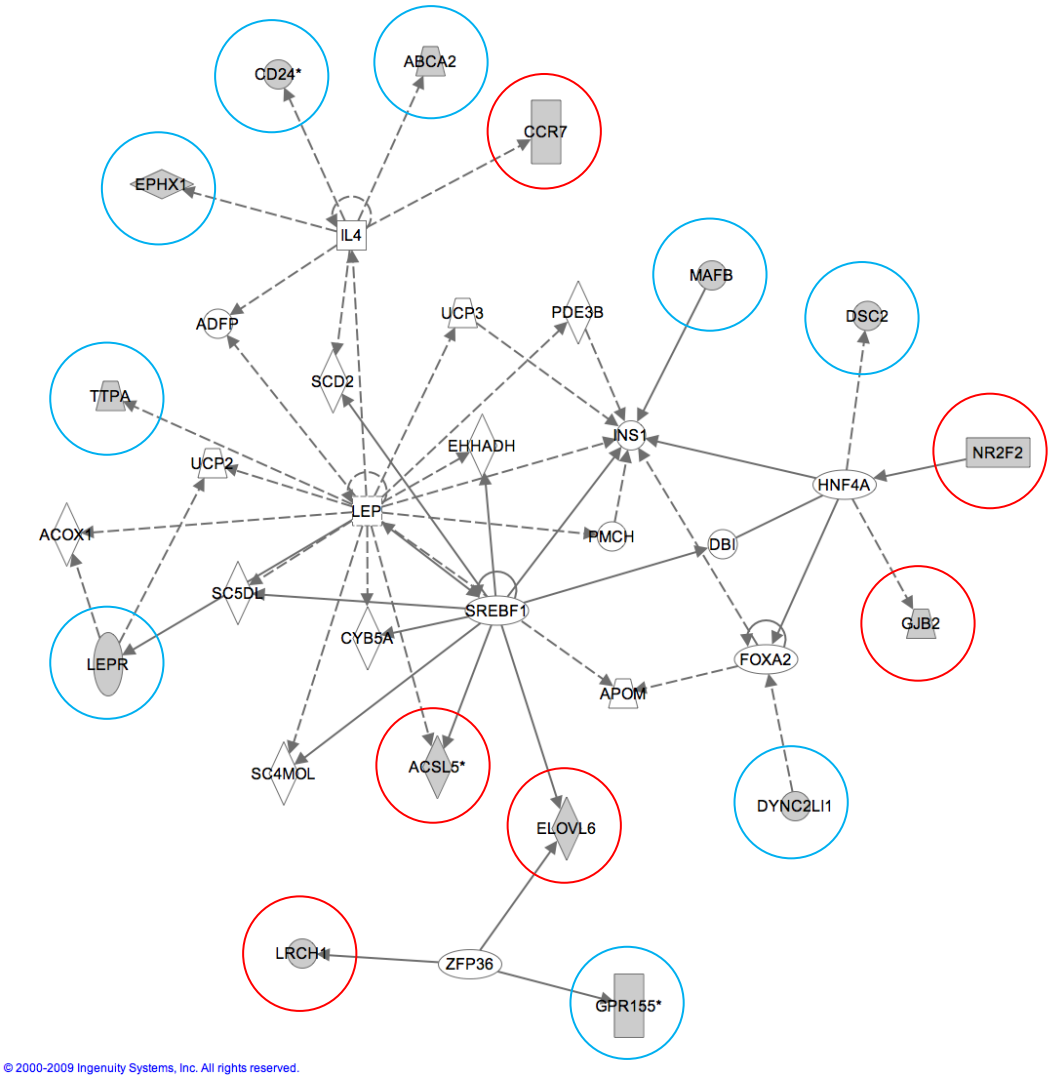

Up-regulated in SW480/lamA

Down-regulated in SW480/lamA

Network 6: Lipid Metabolism, Small Molecule Biochemistry, Molecular Transport
Score: 14 Focus Molecules: 15

Genes up-regulated in SW480/lamA cells		
Symbol	**Fold Change**	**Entrez Gene Name**
ACSL5	2.67, 3.66	acyl-CoA synthetase long-chain family member 5
CCR7	3.83	chemokine (C-C motif) receptor 7
ELOVL6	2.5, 2.93	ELOVL family member 6, elongation of long chain fatty acids
GJB2	20.67	gap junction protein, beta 2, 26kDa
LRCH1	2.62	leucine-rich repeats and calponin homology (CH) domain containing 1
NR2F2	2.98	nuclear receptor subfamily 2, group F, member 2

Genes down-regulated in SW480/lamA cells		
Symbol	**Fold Change**	**Entrez Gene Name**
ABCA2	2.55	ATP-binding cassette, sub-family A (ABC1), member 2
CD24	2.96, 3.36, 5.89, 6.32, 7.00, 7.02	CD24 molecule
DSC2	2.94	desmocollin 2
DYNC2LI1	2.5	dynein, cytoplasmic 2, light intermediate chain 1
EPHX1	3.18	epoxide hydrolase 1, microsomal (xenobiotic)
GPR155	4.82, 5.04	G protein-coupled receptor 155
LEPR	2.83	leptin receptor
MAFB	2.25, 3.91	v-maf musculoaponeurotic fibrosarcoma oncogene homolog B (avian)
TTPA	3.57	tocopherol (alpha) transfer protein

Genes added by IPA	
Symbol	**Entrez Gene Name**
ACOX1	acyl-CoA oxidase 1, palmitoyl
ADFP	perilipin 2
APOM	apolipoprotein M
CYB5A	cytochrome b5 type A
DBI	diazepam binding inhibitor (GABA receptor modulator, acyl-CoA binding protein)
EHHADH	enoyl-CoA, hydratase/3-hydroxyacyl CoA dehydrogenase
FOXA2	forkhead box A2
HNF4A	hepatocyte nuclear factor 4, alpha
IL4	interleukin 4
INS1	forkhead box M1
LEP	leptin
PDE3B	phosphodiesterase 3B, cGMP-inhibited
PMCH	pro-melanin-concentrating hormone
SC4MOL	sterol-C4-methyl oxidase-like
SC5DL	sterol-C5-desaturase-like
SCD2	stearoyl-CoA desaturase 5
SREBF1	sterol regulatory element binding transcription factor 1
UCP2	uncoupling protein 2 (mitochondrial, proton carrier)
UCP3	uncoupling protein 3 (mitochondrial, proton carrier)
ZFP36	zinc finger protein 36, C3H type, homolog (mouse)

Network 7

Cellular Movement, Connective Tissue Development and Function, Cancer

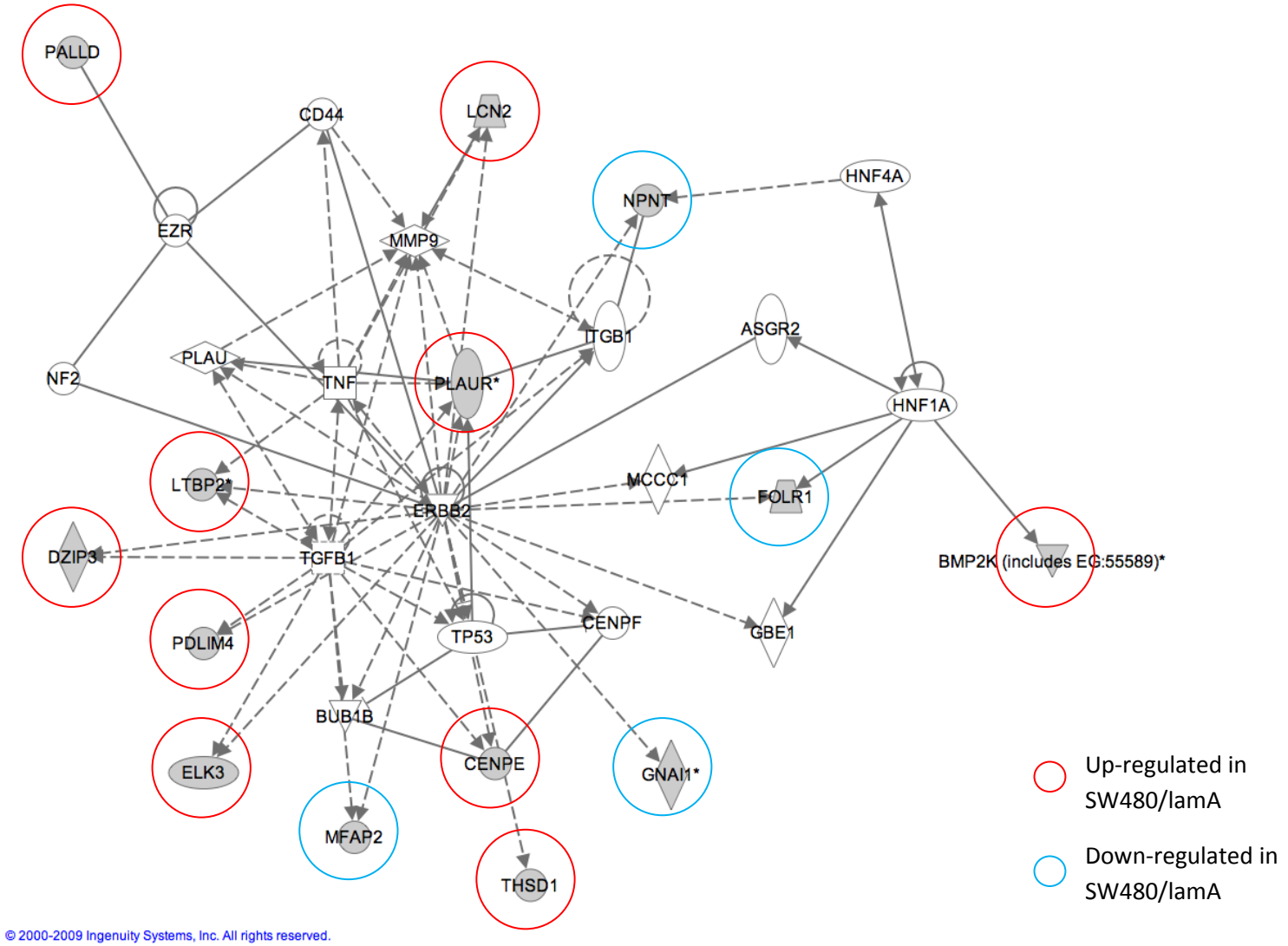

Network 7: Cellular Movement, Connective Tissue Development and Function, Cancer
Score: 14 Focus Molecules: 14

Genes up-regulated in SW480/lamA cells		
Symbol	**Fold Change**	**Entrez Gene Name**
BMP2K	2.11, 3.17, 4.95	BMP2 inducible kinase
CENPE	3.26	centromere protein E, 312kDa
DZIP3	3.25	DAZ interacting protein 3, zinc finger
ELK3	3.89	ELK3, ETS-domain protein (SRF accessory protein 2)
LCN2	2.72	lipocalin 2
LTBP2	3.89, 4.34	latent transforming growth factor beta binding protein 2
PALLD	2.32, 2.56	palladin, cytoskeletal associated protein
PDLIM4	4.04	PDZ and LIM domain 4
PLAUR	2.39, 2.72, 2.73	plasminogen activator, urokinase receptor
THSD1	2.92	thrombospondin, type I, domain containing 1

Genes down-regulated in SW480/lamA cells		
Symbol	**Fold Change**	**Entrez Gene Name**
FOLR1	4.69	folate receptor 1 (adult)
GNAI1	10.03, 12.68	guanine nucleotide binding protein (G protein), alpha inhibiting activity polypeptide 1
MFAP2	2.77	microfibrillar-associated protein 2
NPNT	5.92	nephronectin

Genes added by IPA	
Symbol	**Entrez Gene Name**
ASGR2	asialoglycoprotein receptor 2
BUB1B	budding uninhibited by benzimidazoles 1 homolog beta (yeast)
CD44	CD44 molecule (Indian blood group)
CENPF	centromere protein F, 350/400kDa (mitosin)
ERBB2	v-erb-b2 erythroblastic leukemia viral oncogene homolog 2, neuro/glioblastoma derived oncogene homolog (avian)
EZR	ezrin
GBE1	glucan (1,4-alpha-), branching enzyme 1
HNF1A	HNF1 homeobox A
HNF4A	hepatocyte nuclear factor 4, alpha
ITGB1	integrin, beta 1 (fibronectin receptor, beta polypeptide, antigen CD29 includes MDF2, MSK12)
MCCC1	methylcrotonoyl-CoA carboxylase 1 (alpha)
MMP9	matrix metallopeptidase 9
NF2	neurofibromin 2 (merlin)
PLAU	plasminogen activator, urokinase
TGFB1	transforming growth factor, beta 1
TNF	tumor necrosis factor
TP53	tumor protein p53

Network 8

Cell-To-Cell Signalling and Interaction,
Haematological System Development and Function,
Immune Cell Trafficking

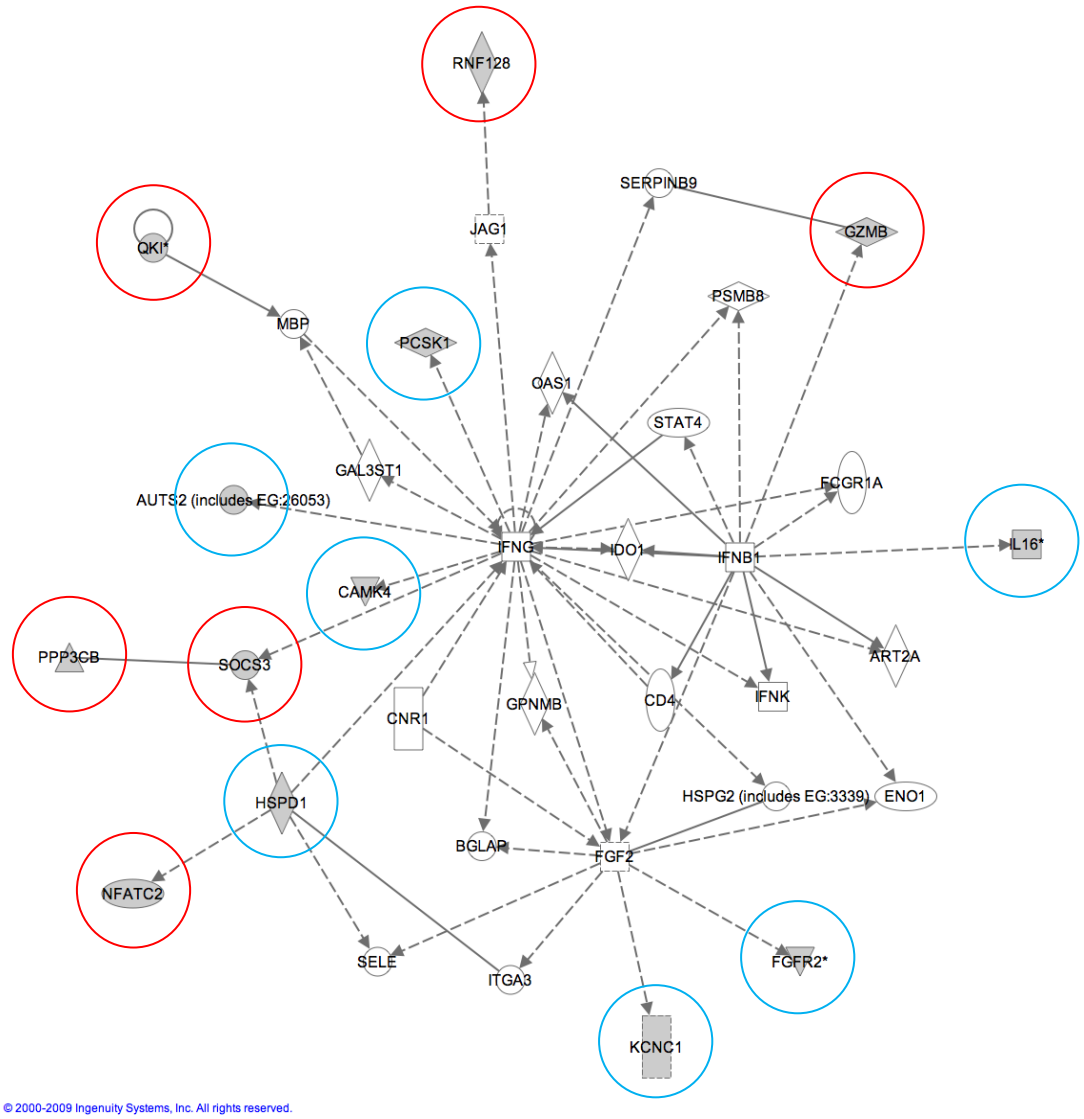

Up-regulated in SW480/lamA

Down-regulated in SW480/lamA

Network 8: Cell-To-Cell Signalling and Interaction, Haematological System Development and Function, Immune Cell Trafficking

Score: 11 Focus Molecules: 13

Genes up-regulated in SW480/lamA cells		
Symbol	**Fold Change**	**Entrez Gene Name**
GZMB	3.22	granzyme B
NFATC2	2.61	Nuclear factor of activated T-cells, cytoplasmic, calcineurin-dependent 2
PPP3CB	3.2	protein phosphatase 3 (formerly 2B), catalytic subunit, beta isoform
QKI	2.16, 2.24, 2.74, 3.31	quaking homolog, KH domain RNA binding (mouse)
RNF128	29.38	ring finger protein 128
SOCS3	2.73	suppressor of cytokine signaling 3

Genes down-regulated in SW480/lamA cells		
Symbol	**Fold Change**	**Entrez Gene Name**
AUTS2	4.16	autism susceptibility candidate 2
CAMK4	2.98	calcium/calmodulin-dependent protein kinase IV
FGFR2	2.50, 2.65	fibroblast growth factor receptor 2
HSPD1	2.6	heat shock 60kDa protein 1 (chaperonin)
IL16	2.64, 4.28	interleukin 16 (lymphocyte chemoattractant factor)
KCNC1	4.12	potassium voltage-gated channel, Shaw-related subfamily, 1
PCSK1	49.8	proprotein convertase subtilisin/kexin type 1

Genes added by IPA	
Symbol	**Entrez Gene Name**
ART2A	ADP-ribosyltransferase 2a
BGLAP	bone gamma-carboxyglutamate (gla) protein
CD4	CD4 molecule
CNR1	cannabinoid receptor 1 (brain)
ENO1	enolase 1, (alpha)
FCGR1A	Fc fragment of IgG, high affinity Ia, receptor (CD64)
FGF2	fibroblast growth factor 2 (basic)
GAL3ST1	galactose-3-O-sulfotransferase 1
GPNMB	glycoprotein (transmembrane) nmb
HSPG2	heparan sulfate proteoglycan 2
IDO1	indoleamine 2,3-dioxygenase 1
IFNB1	interferon, beta 1, fibroblast
IFNG	interferon, gamma
IFNK	interferon, kappa
ITGA3	integrin, alpha 3
JAG1	jagged 1
MBP	myelin basic protein
OAS1	2',5'-oligoadenylate synthetase 1, 40/46kDa
PSMB8	proteasome (prosome, macropain) subunit, beta type, 8
SELE	selectin E
SERPINB9	serpin peptidase inhibitor, clade B (ovalbumin), member 9
STAT4	signal transducer and activator of transcription 4

Network 9

Cell Death,
Cellular Movement,
Cell Cycle

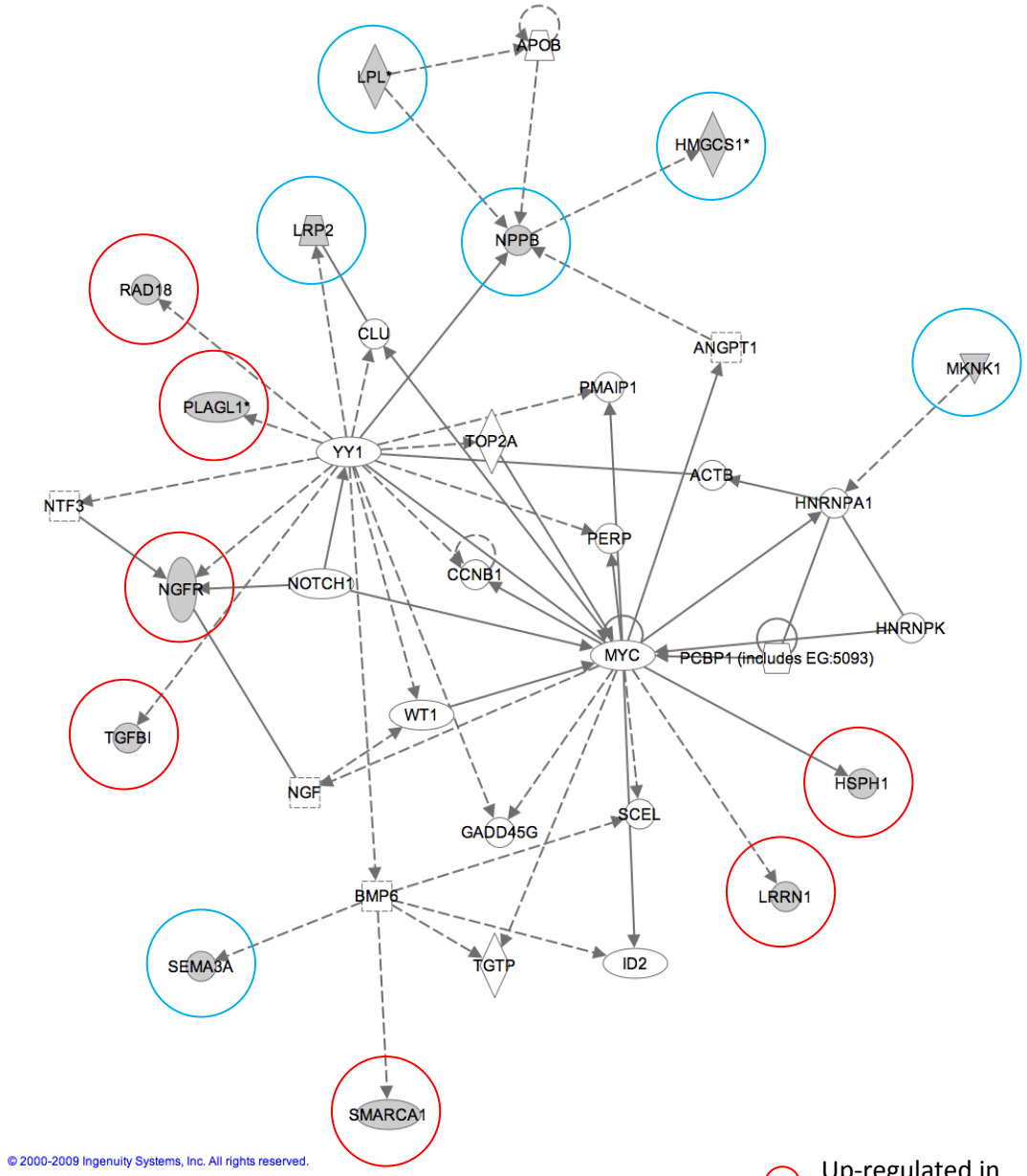

Up-regulated in SW480/lamA

Down-regulated in SW480/lamA

Network 9: Cell Death, Cellular Movement, Cell Cycle

Score: 11 Focus Molecules: 13

Genes up-regulated in SW480/lamA cells		
Symbol	**Fold Change**	**Entrez Gene Name**
HSPH1	2.48, 2.80, 2.81	general transcription factor IIF, polypeptide 2, 30kDa
LRRN1	3.22	leucine rich repeat neuronal 1
NGFR	2.98	nerve growth factor receptor (TNFR superfamily, member 16)
PLAGL1	2.54, 2.62	pleiomorphic adenoma gene-like 1
RAD18	2.59	RAD18 homolog (S. cerevisiae)
SMARCA1	2.55	SWI/SNF related, matrix associated, actin dependent regulator of chromatin, subfamily a, member 1
TGFBI	4.3	transforming growth factor, beta-induced, 68kDa

Genes down-regulated in SW480/lamA cells		
Symbol	**Fold Change**	**Entrez Gene Name**
HMGCS1	2.82, 4.25	3-hydroxy-3-methylglutaryl-Coenzyme A synthase 1 (soluble)
LPL	2.89, 3.32	lipoprotein lipase
LRP2	3.64	low density lipoprotein-related protein 2
MKNK1	3.15	MAP kinase interacting serine/threonine kinase 1
NPPB	3.54	natriuretic peptide precursor B
SEMA3A	3.86	sema domain, immunoglobulin domain (Ig), short basic domain, secreted, (semaphorin) 3A

Genes added by IPA	
Symbol	**Entrez Gene Name**
ACTB	actin, beta
ANGPT1	angiopoietin 1
APOB	apolipoprotein B (including Ag(x) antigen)
BMP6	bone morphogenetic protein 6
CCNB1	cyclin B1
CLU	clusterin
GADD45G	growth arrest and DNA-damage-inducible, gamma
HNRNPA1	heterogeneous nuclear ribonucleoprotein A1
HNRNPK	heterogeneous nuclear ribonucleoprotein K
ID2	inhibitor of DNA binding 2, dominant negative helix-loop-helix protein
MYC	v-myc myelocytomatosis viral oncogene homolog (avian)
NGF	nerve growth factor (beta polypeptide)
NOTCH1	notch 1
NTF3	neurotrophin 3
PCBP1	poly(rC) binding protein 1
PERP	PERP, TP53 apoptosis effector
PMAIP1	phorbol-12-myristate-13-acetate-induced protein 1
SCEL	sciellin
TGTP	T-cell specific GTPase 1
TOP2A	topoisomerase (DNA) II alpha 170kDa
WT1	Wilms tumor 1
YY1	YY1 transcription factor

Network 10

Neurological Disease,
Psychological Disorders,
Cell-To-Cell Signalling and Interaction

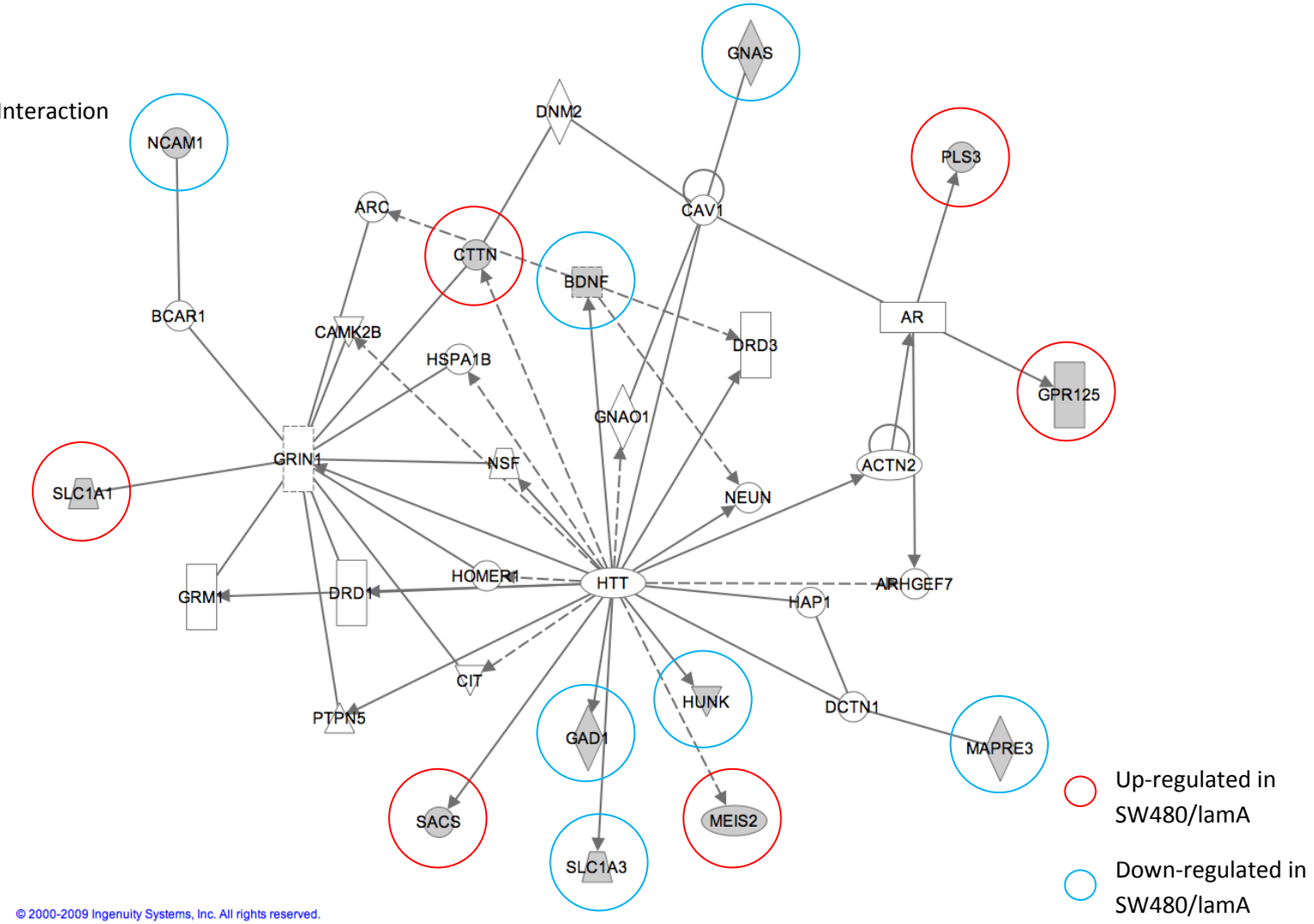

Network 10: Neurological Disease, Psychological Disorders, Cell-To-Cell Signalling and Interaction

Score: 11 Focus Molecules: 13

Genes up-regulated in SW480/lamA cells		
Symbol	**Fold Change**	**Entrez Gene Name**
CTTN	2.55	cortactin
GPR125	3.02	G protein-coupled receptor 125
MEIS2	3.56	Meis homeobox 2
PLS3	19.06	plastin 3 (T isoform)
SACS	3.29	spastic ataxia of Charlevoix-Saguenay (sacsin)
SLC1A1	2.76	solute carrier family 1, member 1

Genes down-regulated in SW480/lamA cells		
Symbol	**Fold Change**	**Entrez Gene Name**
BDNF	5.38	brain-derived neurotrophic factor
GAD1	2.68	glutamate decarboxylase 1 (brain, 67kDa)
GNAS	4.22	GNAS complex locus
HUNK	4.16	hormonally upregulated Neu-associated kinase
MAPRE3	2.75	microtubule-associated protein, RP/EB family, member 3
NCAM1	3.34	neural cell adhesion molecule 1
SLC1A3	2.83	solute carrier family 1 (glial high affinity glutamate transporter), member 3

Genes added by IPA	
Symbol	**Entrez Gene Name**
ACTN2	actinin, alpha 2
AR	androgen receptor
ARC	activity-regulated cytoskeleton-associated protein
ARHGEF7	Rho guanine nucleotide exchange factor (GEF) 7
BCAR1	breast cancer anti-estrogen resistance 1
CAMK2B	calcium/calmodulin-dependent protein kinase II beta
CAV1	caveolin 1, caveolae protein, 22kDa
CIT	citron (rho-interacting, serine/threonine kinase 21)
DCTN1	dynactin 1
DNM2	dynamin 2
DRD1	dopamine receptor D1
DRD3	dopamine receptor D3
GNAO1	guanine nucleotide binding protein (G protein), alpha activating activity polypeptide O
GRIN1	glutamate receptor, ionotropic, N-methyl D-aspartate 1
GRM1	glutamate receptor, metabotropic 1
HAP1	huntingtin-associated protein 1
HOMER1	homer homolog 1 (Drosophila)
HSPA1B	heat shock 70kDa protein 1B
HTT	huntingtin
NEUN	RNA binding protein, fox-1 homolog (C. elegans) 3
NSF	N-ethylmaleimide-sensitive factor
PTPN5	protein tyrosine phosphatase, non-receptor type 5

References

Aebi, U., Cohn, J., Buhle, L., and Gerace, L. (1986). The nuclear lamina is a meshwork of intermediate-type filaments. Nature *323*, 560-564.

Agrawal, D., Chen, T., Irby, R., Quackenbush, J., Chambers, A.F., Szabo, M., Cantor, A., Coppola, D., and Yeatman, T.J. (2002). Osteopontin identified as lead marker of colon cancer progression, using pooled sample expression profiling. J Natl Cancer Inst *94*, 513-521.

Agrelo, R., Setien, F., Espada, J., Artiga, M.J., Rodriguez, M., Perez-Rosado, A., Sanchez-Aguilera, A., Fraga, M.F., Piris, M.A., and Esteller, M. (2005). Inactivation of the lamin A/C gene by CpG island promoter hypermethylation in hematologic malignancies, and its association with poor survival in nodal diffuse large B-cell lymphoma. J Clin Oncol *23*, 3940-3947.

Ahnen, D.J. (1999). Tissue markers of colon cancer risk. Gastrointest Endosc *49*, S50-59.

Akimov, S.S., and Belkin, A.M. (2001). Cell surface tissue transglutaminase is involved in adhesion and migration of monocytic cells on fibronectin. Blood *98*, 1567-1576.

Akimov, S.S., Krylov, D., Fleischman, L.F., and Belkin, A.M. (2000). Tissue transglutaminase is an integrin-binding adhesion coreceptor for fibronectin. J Cell Biol *148*, 825-838.

Akiyoshi, S., Ishii, M., Nemoto, N., Kawabata, M., Aburatani, H., and Miyazono, K. (2001). Targets of transcriptional regulation by transforming growth factor-beta: expression profile analysis using oligonucleotide arrays. Jpn J Cancer Res *92*, 257-268.

Al-Hajj, M., Wicha, M.S., Benito-Hernandez, A., Morrison, S.J., and Clarke, M.F. (2003). Prospective identification of tumorigenic breast cancer cells. Proc Natl Acad Sci U S A *100*, 3983-3988.

Al Tanoury, Z., Schaffner-Reckinger, E., Halavatyi, A., Hoffmann, C., Moes, M., Hadzic, E., Catillon, M., Yatskou, M., and Friederich, E. (2010). Quantitative kinetic study of the actin-bundling protein L-plastin and of its impact on actin turn-over. PLoS One *5*, e9210.

Albanes, D., and Winick, M. (1988). Are cell number and cell proliferation risk factors for cancer? J Natl Cancer Inst *80*, 772-774.

Alfonso, P., Nunez, A., Madoz-Gurpide, J., Lombardia, L., Sanchez, L., and Casal, J.I. (2005). Proteomic expression analysis of colorectal cancer by two-dimensional differential gel electrophoresis. Proteomics *5*, 2602-2611.

Allegra, C.J., Paik, S., Colangelo, L.H., Parr, A.L., Kirsch, I., Kim, G., Klein, P., Johnston, P.G., Wolmark, N., and Wieand, H.S. (2003). Prognostic value of thymidylate synthase, Ki-67, and p53 in patients with Dukes' B and C colon cancer: a National Cancer Institute-National Surgical Adjuvant Breast and Bowel Project collaborative study. J Clin Oncol *21*, 241-250.

Amin, M.A., Matsunaga, S., Uchiyama, S., and Fukui, K. (2008). Nucleophosmin is required for chromosome congression, proper mitotic spindle formation, and kinetochore-microtubule attachment in HeLa cells. FEBS Lett *582*, 3839-3844.

Anderson, D.C., Green, G.R., Smith, K., and Selker, E.U. (2010). Extensive and varied modifications in histone H2B of wild-type and histone deacetylase 1 mutant Neurospora crassa. Biochemistry *49*, 5244-5257.

Andre, T., Boni, C., Navarro, M., Tabernero, J., Hickish, T., Topham, C., Bonetti, A., Clingan, P., Bridgewater, J., Rivera, F.*, et al.* (2009). Improved overall survival with oxaliplatin, fluorouracil, and leucovorin as adjuvant treatment in stage II or III colon cancer in the MOSAIC trial. J Clin Oncol *27*, 3109-3116.

Astler, V.B., and Coller, F.A. (1954). The prognostic significance of direct extension of carcinoma of the colon and rectum. Ann Surg *139*, 846-852.

Atkin, W.S., Edwards, R., Kralj-Hans, I., Wooldrage, K., Hart, A.R., Northover, J.M., Parkin, D.M., Wardle, J., Duffy, S.W., and Cuzick, J. (2010). Once-only flexible sigmoidoscopy screening in prevention of colorectal cancer: a multicentre randomised controlled trial. Lancet *375*, 1624-1633.

Avivi-Green, C., Polak-Charcon, S., Madar, Z., and Schwartz, B. (2000). Apoptosis cascade proteins are regulated in vivo by high intracolonic butyrate concentration: correlation with colon cancer inhibition. Oncol Res *12*, 83-95.

Bae, C.D., Sung, Y.S., Jeon, S.M., Suh, Y., Yang, H.K., Kim, Y.I., Park, K.H., Choi, J., Ahn, G., and Park, J. (2003). Up-regulation of cytoskeletal-associated protein 2 in primary human gastric adenocarcinomas. J Cancer Res Clin Oncol *129*, 621-630.

Bae, J.S., Lee, S.H., Kim, J.E., Choi, J.Y., Park, R.W., Yong Park, J., Park, H.S., Sohn, Y.S., Lee, D.S., Bae Lee, E.*, et al.* (2002). Betaig-h3 supports keratinocyte adhesion, migration, and proliferation through alpha3beta1 integrin. Biochem Biophys Res Commun *294*, 940-948.

Baker, S.J., Preisinger, A.C., Jessup, J.M., Paraskeva, C., Markowitz, S., Willson, J.K., Hamilton, S., and Vogelstein, B. (1990). p53 gene mutations occur in combination with 17p allelic deletions as late events in colorectal tumorigenesis. Cancer Res *50*, 7717-7722.

Barnes, R.N., Bungay, P.J., Elliott, B.M., Walton, P.L., and Griffin, M. (1985). Alterations in the distribution and activity of transglutaminase during tumour growth and metastasis. Carcinogenesis *6*, 459-463.

Bassell, G., and Singer, R.H. (1997). mRNA and cytoskeletal filaments. Curr Opin Cell Biol *9*, 109-115.

Bassell, G.J., Powers, C.M., Taneja, K.L., and Singer, R.H. (1994). Single mRNAs visualized by ultrastructural in situ hybridization are principally localized at actin filament intersections in fibroblasts. J Cell Biol *126*, 863-876.

Batlle, E., Henderson, J.T., Beghtel, H., van den Born, M.M.W., Sancho, E., Huls, G., Meeldijk, J., Robertson, J., van de Wetering, M., Pawson, T.*, et al.* (2002). [beta]-Catenin and TCF Mediate Cell Positioning in the Intestinal Epithelium by Controlling the Expression of EphB/EphrinB. Cell *111*, 251-263.

Beane, J., Spira, A., and Lenburg, M.E. (2009). Clinical impact of high-throughput gene expression studies in lung cancer. J Thorac Oncol *4*, 109-118.

Benedix, F., Kube, R., Meyer, F., Schmidt, U., Gastinger, I., and Lippert, H. (2010). Comparison of 17,641 patients with right- and left-sided colon cancer: differences in epidemiology, perioperative course, histology, and survival. Dis Colon Rectum *53*, 57-64.

Bergo, M.O., Gavino, B., Ross, J., Schmidt, W.K., Hong, C., Kendall, L.V., Mohr, A., Meta, M., Genant, H., Jiang, Y.*, et al.* (2002). Zmpste24 deficiency in mice causes spontaneous bone fractures, muscle weakness, and a prelamin A processing defect. Proc Natl Acad Sci U S A *99*, 13049-13054.

Bernstein, H., Bernstein, C., Payne, C.M., Dvorakova, K., and Garewal, H. (2005). Bile acids as carcinogens in human gastrointestinal cancers. Mutat Res *589*, 47-65.

Bhowmick, N.A., Ghiassi, M., Bakin, A., Aakre, M., Lundquist, C.A., Engel, M.E., Arteaga, C.L., and Moses, H.L. (2001). Transforming growth factor-beta1 mediates epithelial to mesenchymal transdifferentiation through a RhoA-dependent mechanism. Mol Biol Cell *12*, 27-36.

Biamonti, G., Giacca, M., Perini, G., Contreas, G., Zentilin, L., Weighardt, F., Guerra, M., Della Valle, G., Saccone, S., and Riva, S. (1992). The gene for a novel human lamin maps at a highly transcribed locus of chromosome 19 which replicates at the onset of S-phase. Mol Cell Biol *12*, 3499-3506.

Billings, P.C., Whitbeck, J.C., Adams, C.S., Abrams, W.R., Cohen, A.J., Engelsberg, B.N., Howard, P.S., and Rosenbloom, J. (2002). The transforming growth factor-beta-inducible matrix protein (beta)ig-h3 interacts with fibronectin. J Biol Chem *277*, 28003-28009.

Birckbichler, P.J., Bonner, R.B., Hurst, R.E., Bane, B.L., Pitha, J.V., and Hemstreet, G.P., 3rd (2000). Loss of tissue transglutaminase as a biomarker for prostate adenocarcinoma. Cancer *89*, 412-423.

Blesch, A., Bosserhoff, A.K., Apfel, R., Behl, C., Hessdoerfer, B., Schmitt, A., Jachimczak, P., Lottspeich, F., Buettner, R., and Bogdahn, U. (1994). Cloning of a novel malignant melanoma-derived growth-regulatory protein, MIA. Cancer Res *54*, 5695-5701.

Boisvert, F.M., and Lamond, A.I. (2010). p53-Dependent subcellular proteome localization following DNA damage. Proteomics *10*, 4087-4097.

Bosserhoff, A.K., Golob, M., Buettner, R., Landthaler, M., and Hein, R. (1998). [MIA ("melanoma inhibitory activity"). Biological functions and clinical relevance in malignant melanoma]. Hautarzt *49*, 762-769.

Bosserhoff, A.K., Hein, R., Bogdahn, U., and Buettner, R. (1996). Structure and promoter analysis of the gene encoding the human melanoma-inhibiting protein MIA. J Biol Chem *271*, 490-495.

Brabletz, T., Jung, A., Reu, S., Porzner, M., Hlubek, F., Kunz-Schughart, L.A., Knuechel, R., and Kirchner, T. (2001). Variable beta-catenin expression in colorectal cancers indicates tumor progression driven by the tumor environment. Proc Natl Acad Sci U S A *98*, 10356-10361.

Brakebusch, C., and Fassler, R. (2003). The integrin-actin connection, an eternal love affair. EMBO J *22*, 2324-2333.

Bray, F., Sankila, R., Ferlay, J., and Parkin, D.M. (2002). Estimates of cancer incidence and mortality in Europe in 1995. Eur J Cancer *38*, 99-166.

Broers, J.L., Kuijpers, H.J., Ostlund, C., Worman, H.J., Endert, J., and Ramaekers, F.C. (2005). Both lamin A and lamin C mutations cause lamina instability as well as loss of internal nuclear lamin organization. Exp Cell Res *304*, 582-592.

Broers, J.L., Machiels, B.M., Kuijpers, H.J., Smedts, F., van den Kieboom, R., Raymond, Y., and Ramaekers, F.C. (1997). A- and B-type lamins are differentially expressed in normal human tissues. Histochem Cell Biol *107*, 505-517.

Broers, J.L., Peeters, E.A., Kuijpers, H.J., Endert, J., Bouten, C.V., Oomens, C.W., Baaijens, F.P., and Ramaekers, F.C. (2004). Decreased mechanical stiffness in LMNA-/- cells is caused by defective nucleo-cytoskeletal integrity: implications for the development of laminopathies. Hum Mol Genet *13*, 2567-2580.

Broers, J.L., Ramaekers, F.C., Bonne, G., Yaou, R.B., and Hutchison, C.J. (2006). Nuclear lamins: laminopathies and their role in premature ageing. Physiol Rev *86*, 967-1008.

Broers, J.L., Raymond, Y., Rot, M.K., Kuijpers, H., Wagenaar, S.S., and Ramaekers, F.C. (1993). Nuclear A-type lamins are differentially expressed in human lung cancer subtypes. Am J Pathol *143*, 211-220.

Buckhaults, P., Rago, C., St Croix, B., Romans, K.E., Saha, S., Zhang, L., Vogelstein, B., and Kinzler, K.W. (2001). Secreted and cell surface genes expressed in benign and malignant colorectal tumors. Cancer Res *61*, 6996-7001.

Bufill, J.A. (1990). Colorectal cancer: evidence for distinct genetic categories based on proximal or distal tumor location. Ann Intern Med *113*, 779-788.

Burkitt, D.P. (1971). Epidemiology of cancer of the colon and rectum. Cancer *28*, 3-13.

Cai, D., Ben, T., and De Luca, L.M. (1991). Retinoids induce tissue transglutaminase in NIH-3T3 cells. Biochem Biophys Res Commun *175*, 1119-1124.

Calaf, G.M., Echiburu-Chau, C., Zhao, Y.L., and Hei, T.K. (2008). BigH3 protein expression as a marker for breast cancer. Int J Mol Med *21*, 561-568.

Calvano, S.E., Xiao, W., Richards, D.R., Felciano, R.M., Baker, H.V., Cho, R.J., Chen, R.O., Brownstein, B.H., Cobb, J.P., Tschoeke, S.K*., et al.* (2005). A network-based analysis of systemic inflammation in humans. Nature *437*, 1032-1037.

Camps, J., Ponsa, I., Ribas, M., Prat, E., Egozcue, J., Peinado, M.A., and Miro, R. (2005). Comprehensive measurement of chromosomal instability in cancer cells: combination of fluorescence in situ hybridization and cytokinesis-block micronucleus assay. FASEB J *19*, 828-830.

Capell, B.C., and Collins, F.S. (2006). Human laminopathies: nuclei gone genetically awry. Nat Rev Genet *7*, 940-952.

Cappello, F., Bellafiore, M., Palma, A., David, S., Marciano, V., Bartolotta, T., Sciume, C., Modica, G., Farina, F., Zummo, G*., et al.* (2003). 60KDa chaperonin (HSP60) is over-expressed during colorectal carcinogenesis. Eur J Histochem *47*, 105-110.

Cappello, F., Conway de Macario, E., Marasa, L., Zummo, G., and Macario, A.J. (2008). Hsp60 expression, new locations, functions and perspectives for cancer diagnosis and therapy. Cancer Biol Ther *7*, 801-809.

Cappello, F., David, S., Rappa, F., Bucchieri, F., Marasa, L., Bartolotta, T.E., Farina, F., and Zummo, G. (2005a). The expression of HSP60 and HSP10 in large bowel carcinomas with lymph node metastase. BMC Cancer *5*, 139.

Cappello, F., Di Stefano, A., D'Anna, S.E., Donner, C.F., and Zummo, G. (2005b). Immunopositivity of heat shock protein 60 as a biomarker of bronchial carcinogenesis. Lancet Oncol *6*, 816.

Carson, J.D., Van Aller, G., Lehr, R., Sinnamon, R.H., Kirkpatrick, R.B., Auger, K.R., Dhanak, D., Copeland, R.A., Gontarek, R.R., Tummino, P.J.*, et al.* (2008). Effects of oncogenic p110alpha subunit mutations on the lipid kinase activity of phosphoinositide 3-kinase. Biochem J *409*, 519-524.

Chaiyarit, P., Kafrawy, A.H., Miles, D.A., Zunt, S.L., Van Dis, M.L., and Gregory, R.L. (1999). Oral lichen planus: an immunohistochemical study of heat shock proteins (HSPs) and cytokeratins (CKs) and a unifying hypothesis of pathogenesis. J Oral Pathol Med *28*, 210-215.

Chandra, D., Choy, G., and Tang, D.G. (2007). Cytosolic accumulation of HSP60 during apoptosis with or without apparent mitochondrial release: evidence that its pro-apoptotic or pro-survival functions involve differential interactions with caspase-3. J Biol Chem *282*, 31289-31301.

Charatan, F. (2004). Bowel cancer survival rates vary across England. BMJ *328*, 974.

Chazaud, B., Ricoux, R., Christov, C., Plonquet, A., Gherardi, R.K., and Barlovatz-Meimon, G. (2002). Promigratory effect of plasminogen activator inhibitor-1 on invasive breast cancer cell populations. Am J Pathol *160*, 237-246.

Chi, K., Jones, D.V., and Frazier, M.L. (1992). Expression of an elongation factor 1 gamma-related sequence in adenocarcinomas of the colon. Gastroenterology *103*, 98-102.

Chiang, P.W., Song, W.J., Wu, K.Y., Korenberg, J.R., Fogel, E.J., Van Keuren, M.L., Lashkari, D., and Kurnit, D.M. (1996). Use of a fluorescent-PCR reaction to detect genomic sequence copy number and transcriptional abundance. Genome Res *6*, 1013-1026.

Choi, J., Park, S.Y., and Joo, C.K. (2007). Transforming growth factor-beta1 represses E-cadherin production via slug expression in lens epithelial cells. Invest Ophthalmol Vis Sci *48*, 2708-2718.

Chou, Y.H., Flitney, F.W., Chang, L., Mendez, M., Grin, B., and Goldman, R.D. (2007). The motility and dynamic properties of intermediate filaments and their constituent proteins. Exp Cell Res *313*, 2236-2243.

Chowdhury, Z.A., Barsigian, C., Chalupowicz, G.D., Bach, T.L., Garcia-Manero, G., and Martinez, J. (1997). Colocalization of tissue transglutaminase and stress fibers in human vascular smooth muscle cells and human umbilical vein endothelial cells. Exp Cell Res *231*, 38-49.

Clement, S., Velasco, P.T., Murthy, S.N., Wilson, J.H., Lukas, T.J., Goldman, R.D., and Lorand, L. (1998). The intermediate filament protein, vimentin, in the lens is a target for cross-linking by transglutaminase. J Biol Chem *273*, 7604-7609.

Clements, L., Manilal, S., Love, D.R., and Morris, G.E. (2000). Direct interaction between emerin and lamin A. Biochem Biophys Res Commun *267*, 709-714.

Collas, P., Thompson, L., Fields, A.P., Poccia, D.L., and Courvalin, J.C. (1997). Protein kinase C-mediated interphase lamin B phosphorylation and solubilization. J Biol Chem *272*, 21274-21280.

Conacci-Sorrell, M., Simcha, I., Ben-Yedidia, T., Blechman, J., Savagner, P., and Ben-Ze'ev, A. (2003). Autoregulation of E-cadherin expression by cadherin-cadherin interactions: the roles of beta-catenin signaling, Slug, and MAPK. J Cell Biol *163*, 847-857.

Conway, J.F., and Parry, D.A. (1990). Structural features in the heptad substructure and longer range repeats of two-stranded alpha-fibrous proteins. Int J Biol Macromol *12*, 328-334.

Coradeghini, R., Barboro, P., Rubagotti, A., Boccardo, F., Parodi, S., Carmignani, G., D'Arrigo, C., Patrone, E., and Balbi, C. (2006). Differential expression of nuclear lamins in normal and cancerous prostate tissues. Oncol Rep *15*, 609-613.

Coulonval, K., Bockstaele, L., Paternot, S., and Roger, P.P. (2003). Phosphorylations of cyclin-dependent kinase 2 revisited using two-dimensional gel electrophoresis. J Biol Chem *278*, 52052-52060.

Crisp, M., Liu, Q., Roux, K., Rattner, J.B., Shanahan, C., Burke, B., Stahl, P.D., and Hodzic, D. (2006). Coupling of the nucleus and cytoplasm: role of the LINC complex. J Cell Biol *172*, 41-53.

Cross, A.J., Pollock, J.R., and Bingham, S.A. (2003). Haem, not protein or inorganic iron, is responsible for endogenous intestinal N-nitrosation arising from red meat. Cancer Res *63*, 2358-2360.

Cui, W., Fowlis, D.J., Bryson, S., Duffie, E., Ireland, H., Balmain, A., and Akhurst, R.J. (1996). TGFbeta1 inhibits the formation of benign skin tumors, but enhances progression to invasive spindle carcinomas in transgenic mice. Cell *86*, 531-542.

Curtin, K., Slattery, M.L., and Samowitz, W.S. (2011). CpG island methylation in colorectal cancer: past, present and future. Patholog Res Int *2011*, 902674.

Dave, N., Guaita-Esteruelas, S., Gutarra, S., Frias, A., Beltran, M., Peiro, S., and de Herreros, A.G. (2011). Functional Cooperation between Snail1 and Twist in the Regulation of ZEB1 Expression during Epithelial to Mesenchymal Transition. J Biol Chem *286*, 12024-12032.

Dellas, C., and Loskutoff, D.J. (2005). Historical analysis of PAI-1 from its discovery to its potential role in cell motility and disease. Thromb Haemost *93*, 631-640.

Derynck, R., and Zhang, Y.E. (2003). Smad-dependent and Smad-independent pathways in TGF-beta family signalling. Nature *425*, 577-584.

Despres, J.P. (1993). Abdominal obesity as important component of insulin-resistance syndrome. Nutrition *9*, 452-459.

Dick, J.E. (2003). Breast cancer stem cells revealed. Proc Natl Acad Sci U S A *100*, 3547-3549.

Dugina, V., Zwaenepoel, I., Gabbiani, G., Clement, S., and Chaponnier, C. (2009). Beta and gamma-cytoplasmic actins display distinct distribution and functional diversity. J Cell Sci *122*, 2980-2988.

Dukes, C.E. (1932). The classification of cancer of the rectum. The Journal of Pathology and Bacteriology *35*, 323-332.

Dukes, C.E. (1949). The Surgical Pathology of Rectal Cancer. J Clin Pathol *2*, 95-98.

Dukes, C.E., and Bussey, H.J. (1958). The spread of rectal cancer and its effect on prognosis. Br J Cancer *12*, 309-320.

Dundas, S.R., Lawrie, L.C., Rooney, P.H., and Murray, G.I. (2005). Mortalin is over-expressed by colorectal adenocarcinomas and correlates with poor survival. J Pathol *205*, 74-81.

Durand, M.K., Bodker, J.S., Christensen, A., Dupont, D.M., Hansen, M., Jensen, J.K., Kjelgaard, S., Mathiasen, L., Pedersen, K.E., Skeldal, S.*, et al.* (2004). Plasminogen activator inhibitor-I and tumour growth, invasion, and metastasis. Thromb Haemost *91*, 438-449.

Dwyer, N., and Blobel, G. (1976). A modified procedure for the isolation of a pore complex-lamina fraction from rat liver nuclei. The Journal of Cell Biology *70*, 581-591.

Dyer, J.A., Kill, I.R., Pugh, G., Quinlan, R.A., Lane, E.B., and Hutchison, C.J. (1997). Cell cycle changes in A-type lamin associations detected in human dermal fibroblasts using monoclonal antibodies. Chromosome Res *5*, 383-394.

Eckes, B., Dogic, D., Colucci-Guyon, E., Wang, N., Maniotis, A., Ingber, D., Merckling, A., Langa, F., Aumailley, M., Delouvee, A.*, et al.* (1998). Impaired mechanical stability, migration and contractile capacity in vimentin-deficient fibroblasts. J Cell Sci *111 (Pt 13)*, 1897-1907.

Edge, S. (2009). American Joint Committee on Cancer: AJCC Cancer Staging Manual, 7th edn (New York, Springer).

Eger, A., Aigner, K., Sonderegger, S., Dampier, B., Oehler, S., Schreiber, M., Berx, G., Cano, A., Beug, H., and Foisner, R. (2005). DeltaEF1 is a transcriptional repressor of E-cadherin and regulates epithelial plasticity in breast cancer cells. Oncogene *24*, 2375-2385.

Emerson, L.J., Holt, M.R., Wheeler, M.A., Wehnert, M., Parsons, M., and Ellis, J.A. (2009). Defects in cell spreading and ERK1/2 activation in fibroblasts with lamin A/C mutations. Biochim Biophys Acta *1792*, 810-821.

Eschrich, S., Yang, I., Bloom, G., Kwong, K.Y., Boulware, D., Cantor, A., Coppola, D., Kruhoffer, M., Aaltonen, L., Orntoft, T.F.*, et al.* (2005). Molecular staging for survival prediction of colorectal cancer patients. J Clin Oncol *23*, 3526-3535.

Fairley, E.A., Kendrick-Jones, J., and Ellis, J.A. (1999). The Emery-Dreifuss muscular dystrophy phenotype arises from aberrant targeting and binding of emerin at the inner nuclear membrane. J Cell Sci *112 (Pt 15)*, 2571-2582.

Fan, J., and Beck, K.A. (2004). A role for the spectrin superfamily member Syne-1 and kinesin II in cytokinesis. J Cell Sci *117*, 619-629.

Fantuzzi, G. (2005). Adipose tissue, adipokines, and inflammation. J Allergy Clin Immunol *115*, 911-919; 920.

Faux, M.C., Coates, J.L., Kershaw, N.J., Layton, M.J., and Burgess, A.W. (2010). Independent interactions of phosphorylated beta-catenin with E-cadherin at cell-cell contacts and APC at cell protrusions. PLoS One *5*, e14127.

Fearon, E.R. (2011). Molecular genetics of colorectal cancer. Annu Rev Pathol *6*, 479-507.

Fearon, E.R., and Vogelstein, B. (1990). A genetic model for colorectal tumorigenesis. Cell *61*, 759-767.

Ferlay, J., Parkin, D.M., and Steliarova-Foucher, E. (2010a). Estimates of cancer incidence and mortality in Europe in 2008. Eur J Cancer *46*, 765-781.

Ferlay, J., Shin, H.R., Bray, F., Forman, D., Mathers, C., and Parkin, D.M. (2010b). Estimates of worldwide burden of cancer in 2008: GLOBOCAN 2008. Int J Cancer *127*, 2893-2917.

Fey, E.G., Krochmalnic, G., and Penman, S. (1986). The nonchromatin substructures of the nucleus: the ribonucleoprotein (RNP)-containing and RNP-depleted matrices analyzed by sequential fractionation and resinless section electron microscopy. J Cell Biol *102*, 1654-1665.

Figueredo, A., Coombes, M.E., and Mukherjee, S. (2008). Adjuvant therapy for completely resected stage II colon cancer. Cochrane Database Syst Rev, CD005390.

Fisher, D.Z., Chaudhary, N., and Blobel, G. (1986). cDNA sequencing of nuclear lamins A and C reveals primary and secondary structural homology to intermediate filament proteins. Proceedings of the National Academy of Sciences *83*, 6450-6454.

Fok, J.Y., Ekmekcioglu, S., and Mehta, K. (2006). Implications of tissue transglutaminase expression in malignant melanoma. Mol Cancer Ther *5*, 1493-1503.

Foran, E., McWilliam, P., Kelleher, D., Croke, D.T., and Long, A. (2006). The leukocyte protein L-plastin induces proliferation, invasion and loss of E-cadherin expression in colon cancer cells. Int J Cancer *118*, 2098-2104.

Foster, C.R., Przyborski, S.A., Wilson, R.G., and Hutchison, C.J. (2010). Lamins as cancer biomarkers. Biochem Soc Trans *38*, 297-300.

Foster, C.R., Robson, J.L., Simon, W.J., Twigg, J., Cruikshank, D., Wilson, R.G., and Hutchison, C.J. (2011). The role of Lamin A in cytoskeleton organization in colorectal cancer cells: A proteomic investigation. Nucleus *2*, 434-443.

Fricker, M., Hollinshead, M., White, N., and Vaux, D. (1997). Interphase nuclei of many mammalian cell types contain deep, dynamic, tubular membrane-bound invaginations of the nuclear envelope. J Cell Biol *136*, 531-544.

Fukushima, H., Yamamoto, H., Itoh, F., Horiuchi, S., Min, Y., Iku, S., and Imai, K. (2001). Frequent alterations of the beta-catenin and TCF-4 genes, but not of the APC gene, in colon cancers with high-frequency microsatellite instability. J Exp Clin Cancer Res *20*, 553-559.

Furukawa, K. (1999). LAP2 binding protein 1 (L2BP1/BAF) is a candidate mediator of LAP2-chromatin interaction. J Cell Sci *112 (Pt 15)*, 2485-2492.

Furukawa, K., and Hotta, Y. (1993). cDNA cloning of a germ cell specific lamin B3 from mouse spermatocytes and analysis of its function by ectopic expression in somatic cells. EMBO J *12*, 97-106.

Furukawa, K., Inagaki, H., and Hotta, Y. (1994). Identification and Cloning of an mRNA Coding for a Germ Cell-Specific A-Type Lamin in Mice. Experimental Cell Research *212*, 426-430.

Furukawa, K., and Kondo, T. (1998). Identification of the lamina-associated-polypeptide-2-binding domain of B-type lamin. Eur J Biochem *251*, 729-733.

Gache, V., Louwagie, M., Garin, J., Caudron, N., Lafanechere, L., and Valiron, O. (2005). Identification of proteins binding the native tubulin dimer. Biochem Biophys Res Commun *327*, 35-42.

Gasparri, A., Sidoli, A., Sanchez, L.P., Longhi, R., Siccardi, A.G., Marchisio, P.C., and Corti, A. (1997). Chromogranin A fragments modulate cell adhesion. Identification and characterization of a pro-adhesive domain. J Biol Chem *272*, 20835-20843.

Gaudry, C.A., Verderio, E., Aeschlimann, D., Cox, A., Smith, C., and Griffin, M. (1999). Cell surface localization of tissue transglutaminase is dependent on a fibronectin-binding site in its N-terminal beta-sandwich domain. J Biol Chem *274*, 30707-30714.

Gentile, V., Thomazy, V., Piacentini, M., Fesus, L., and Davies, P.J. (1992). Expression of tissue transglutaminase in Balb-C 3T3 fibroblasts: effects on cellular morphology and adhesion. J Cell Biol *119*, 463-474.

Georgiades, I.B., Curtis, L.J., Morris, R.M., Bird, C.C., and Wyllie, A.H. (1999). Heterogeneity studies identify a subset of sporadic colorectal cancers without evidence for chromosomal or microsatellite instability. Oncogene *18*, 7933-7940.

Ghosh, B., Benyumov, A.O., Ghosh, P., Jia, Y., Avdulov, S., Dahlberg, P.S., Peterson, M., Smith, K., Polunovsky, V.A., Bitterman, P.B.*, et al.* (2009). Nontoxic chemical interdiction of the epithelial-to-mesenchymal transition by targeting cap-dependent translation. ACS Chem Biol *4*, 367-377.

Gibson, U.E., Heid, C.A., and Williams, P.M. (1996). A novel method for real time quantitative RT-PCR. Genome Res *6*, 995-1001.

Gill, S., Loprinzi, C.L., Sargent, D.J., Thome, S.D., Alberts, S.R., Haller, D.G., Benedetti, J., Francini, G., Shepherd, L.E., Francois Seitz, J.*, et al.* (2004). Pooled analysis of fluorouracil-based adjuvant therapy for stage II and III colon cancer: who benefits and by how much? J Clin Oncol *22*, 1797-1806.

Gjerset, R.A. (2006). DNA damage, p14ARF, nucleophosmin (NPM/B23), and cancer. J Mol Histol *37*, 239-251.

Goldman, A.E., Moir, R.D., Montag-Lowy, M., Stewart, M., and Goldman, R.D. (1992). Pathway of incorporation of microinjected lamin A into the nuclear envelope. J Cell Biol *119*, 725-735.

Goldman, R.D., Shumaker, D.K., Erdos, M.R., Eriksson, M., Goldman, A.E., Gordon, L.B., Gruenbaum, Y., Khuon, S., Mendez, M., Varga, R.*, et al.* (2004). Accumulation of mutant lamin A causes progressive changes in nuclear architecture in Hutchinson-Gilford progeria syndrome. Proc Natl Acad Sci U S A *101*, 8963-8968.

Gospodarowicz, M.K., Miller, D., Groome, P.A., Greene, F.L., Logan, P.A., and Sobin, L.H. (2004). The process for continuous improvement of the TNM classification. Cancer *100*, 1-5.

Graham, T.R., Zhau, H.E., Odero-Marah, V.A., Osunkoya, A.O., Kimbro, K.S., Tighiouart, M., Liu, T., Simons, J.W., and O'Regan, R.M. (2008). Insulin-like growth factor-I-dependent up-regulation of ZEB1 drives epithelial-to-mesenchymal transition in human prostate cancer cells. Cancer Res *68*, 2479-2488.

Greene, F.L., Page, D.L., Fleming, I.D., Fritz A.G., Balch, C.M., Haller, D.G., Morrow, M (2002). AJCC cancer staging manual, 6th edn (New York, Springer).

Groden, J., Thliveris, A., Samowitz, W., Carlson, M., Gelbert, L., Albertsen, H., Joslyn, G., Stevens, J., Spirio, L., Robertson, M.*, et al.* (1991). Identification and characterization of the familial adenomatous polyposis coli gene. Cell *66*, 589-600.

Guaita, S., Puig, I., Franci, C., Garrido, M., Dominguez, D., Batlle, E., Sancho, E., Dedhar, S., De Herreros, A.G., and Baulida, J. (2002). Snail induction of epithelial to mesenchymal transition in tumor cells is accompanied by MUC1 repression and ZEB1 expression. J Biol Chem *277*, 39209-39216.

Guelen, L., Pagie, L., Brasset, E., Meuleman, W., Faza, M.B., Talhout, W., Eussen, B.H., de Klein, A., Wessels, L., de Laat, W.*, et al.* (2008). Domain organization of human chromosomes revealed by mapping of nuclear lamina interactions. Nature *453*, 948-951.

Gunderson, L.L., and Sosin, H. (1974). Areas of failure found at reoperation (second or symptomatic look) following "curative surgery" for adenocarcinoma of the rectum. Clinicopathologic correlation and implications for adjuvant therapy. Cancer *34*, 1278-1292.

Gunnell, D., Okasha, M., Smith, G.D., Oliver, S.E., Sandhu, J., and Holly, J.M. (2001). Height, leg length, and cancer risk: a systematic review. Epidemiol Rev *23*, 313-342.

Gupta, M., Greenberg, C.S., Eckman, D.M., and Sane, D.C. (2007). Arterial vimentin is a transglutaminase substrate: a link between vasomotor activity and remodeling? J Vasc Res *44*, 339-344.

Hague, A., Manning, A.M., Hanlon, K.A., Huschtscha, L.I., Hart, D., and Paraskeva, C. (1993). Sodium butyrate induces apoptosis in human colonic tumour cell lines in a p53-independent pathway: implications for the possible role of dietary fibre in the prevention of large-bowel cancer. Int J Cancer *55*, 498-505.

Hajra, K.M., Chen, D.Y., and Fearon, E.R. (2002). The SLUG zinc-finger protein represses E-cadherin in breast cancer. Cancer Res *62*, 1613-1618.

Hale, C.M., Shrestha, A.L., Khatau, S.B., Stewart-Hutchinson, P.J., Hernandez, L., Stewart, C.L., Hodzic, D., and Wirtz, D. (2008). Dysfunctional connections between the nucleus and the actin and microtubule networks in laminopathic models. Biophys J *95*, 5462-5475.

Halligan, B.D., Ruotti, V., Jin, W., Laffoon, S., Twigger, S.N., and Dratz, E.A. (2004). ProMoST (Protein Modification Screening Tool): a web-based tool for mapping protein modifications on two-dimensional gels. Nucleic Acids Res *32*, 638-644.

Hamada, S., Satoh, K., Hirota, M., Kimura, K., Kanno, A., Masamune, A., and Shimosegawa, T. (2007). Bone morphogenetic protein 4 induces epithelial-mesenchymal transition through MSX2 induction on pancreatic cancer cell line. J Cell Physiol *213*, 768-774.

Hanahan, D., and Weinberg, R.A. (2000). The hallmarks of cancer. Cell *100*, 57-70.

Hanahan, D., and Weinberg, R.A. (2011). Hallmarks of cancer: the next generation. Cell *144*, 646-674.

Haque, F., Lloyd, D.J., Smallwood, D.T., Dent, C.L., Shanahan, C.M., Fry, A.M., Trembath, R.C., and Shackleton, S. (2006). SUN1 interacts with nuclear lamin A and cytoplasmic nesprins to provide a physical connection between the nuclear lamina and the cytoskeleton. Mol Cell Biol *26*, 3738-3751.

Haraguchi, T., Koujin, T., Segura-Totten, M., Lee, K.K., Matsuoka, Y., Yoneda, Y., Wilson, K.L., and Hiraoka, Y. (2001). BAF is required for emerin assembly into the reforming nuclear envelope. J Cell Sci *114*, 4575-4585.

Harborth, J., Elbashir, S.M., Bechert, K., Tuschl, T., and Weber, K. (2001). Identification of essential genes in cultured mammalian cells using small interfering RNAs. Journal of Cell Science *114*, 4557-4565.

Hardcastle, J.D., Chamberlain, J.O., Robinson, M.H., Moss, S.M., Amar, S.S., Balfour, T.W., James, P.D., and Mangham, C.M. (1996). Randomised controlled trial of faecal-occult-blood screening for colorectal cancer. Lancet *348*, 1472-1477.

Harriss, D.J., Cable, N.T., George, K., Reilly, T., Renehan, A.G., and Haboubi, N. (2007). Physical activity before and after diagnosis of colorectal cancer: disease risk, clinical outcomes, response pathways and biomarkers. Sports Med *37*, 947-960.

Hay, N., and Sonenberg, N. (2004). Upstream and downstream of mTOR. Genes Dev *18*, 1926-1945.

He, Y., Wu, Y., Mou, Z., Li, W., Zou, L., Fu, T., Zhang, A., Xiang, D., Xiao, H., and Wang, X. (2007). Proteomics-based identification of HSP60 as a tumor-associated antigen in colorectal cancer. Proteomics Clin Appl *1*, 336-342.

Heid, C.A., Stevens, J., Livak, K.J., and Williams, P.M. (1996). Real time quantitative PCR. Genome Res *6*, 986-994.

Heller, M.J. (2002). DNA microarray technology: devices, systems, and applications. Annu Rev Biomed Eng *4*, 129-153.

Higuchi, R., Fockler, C., Dollinger, G., and Watson, R. (1993). Kinetic PCR analysis: real-time monitoring of DNA amplification reactions. Biotechnology (N Y) *11*, 1026-1030.

Hirsch, D.S., Pirone, D.M., and Burbelo, P.D. (2001). A new family of Cdc42 effector proteins, CEPs, function in fibroblast and epithelial cell shape changes. J Biol Chem *276*, 875-883.

Hisano, T., Ono, M., Nakayama, M., Naito, S., Kuwano, M., and Wada, M. (1996). Increased expression of T-plastin gene in cisplatin-resistant human cancer cells: identification by mRNA differential display. FEBS Lett *397*, 101-107.

Hlubek, F., Brabletz, T., Budczies, J., Pfeiffer, S., Jung, A., and Kirchner, T. (2007). Heterogeneous expression of Wnt/beta-catenin target genes within colorectal cancer. Int J Cancer *121*, 1941-1948.

Hoger, T.H., Zatloukal, K., Waizenegger, I., and Krohne, G. (1990). Characterization of a second highly conserved B-type lamin present in cells previously thought to contain only a single B-type lamin. Chromosoma *100*, 67-69.

Holaska, J.M., Kowalski, A.K., and Wilson, K.L. (2004). Emerin caps the pointed end of actin filaments: evidence for an actin cortical network at the nuclear inner membrane. PLoS Biol *2*, E231.

Holaska, J.M., Lee, K.K., Kowalski, A.K., and Wilson, K.L. (2003). Transcriptional repressor germ cell-less (GCL) and barrier to autointegration factor (BAF) compete for binding to emerin in vitro. J Biol Chem *278*, 6969-6975.

Honda, K., Yamada, T., Endo, R., Ino, Y., Gotoh, M., Tsuda, H., Yamada, Y., Chiba, H., and Hirohashi, S. (1998). Actinin-4, a novel actin-bundling protein associated with cell motility and cancer invasion. J Cell Biol *140*, 1383-1393.

Honda, K., Yamada, T., Hayashida, Y., Idogawa, M., Sato, S., Hasegawa, F., Ino, Y., Ono, M., and Hirohashi, S. (2005). Actinin-4 increases cell motility and promotes lymph node metastasis of colorectal cancer. Gastroenterology *128*, 51-62.

Hoock, T.C., Newcomb, P.M., and Herman, I.M. (1991). Beta actin and its mRNA are localized at the plasma membrane and the regions of moving cytoplasm during the cellular response to injury. J Cell Biol *112*, 653-664.

Houben, F., Willems, C.H., Declercq, I.L., Hochstenbach, K., Kamps, M.A., Snoeckx, L.H., Ramaekers, F.C., and Broers, J.L. (2009). Disturbed nuclear orientation and cellular migration in A-type lamin deficient cells. Biochim Biophys Acta *1793*, 312-324.

Hsu, D., Fukata, M., Hernandez, Y.G., Sotolongo, J.P., Goo, T., Maki, J., Hayes, L.A., Ungaro, R.C., Chen, A., Breglio, K.J*., et al.* (2010). Toll-like receptor 4 differentially regulates epidermal growth factor-related growth factors in response to intestinal mucosal injury. Lab Invest *90*, 1295-1305.

Hsu, S., Huang, F., Hafez, M., Winawer, S., and Friedman, E. (1994). Colon carcinoma cells switch their response to transforming growth factor beta 1 with tumor progression. Cell Growth Differ *5*, 267-275.

Hubbell, E., Liu, W.M., and Mei, R. (2002). Robust estimators for expression analysis. Bioinformatics *18*, 1585-1592.

Huber, M.A., Kraut, N., and Beug, H. (2005). Molecular requirements for epithelial-mesenchymal transition during tumor progression. Curr Opin Cell Biol *17*, 548-558.

Hudson, M.E., Pozdnyakova, I., Haines, K., Mor, G., and Snyder, M. (2007). Identification of differentially expressed proteins in ovarian cancer using high-density protein microarrays. Proc Natl Acad Sci U S A *104*, 17494-17499.

Huszar, M., Pfeifer, M., Schirmer, U., Kiefel, H., Konecny, G.E., Ben-Arie, A., Edler, L., Munch, M., Muller-Holzner, E., Jerabek-Klestil, S*., et al.* (2010). Up-regulation of L1CAM is linked to loss of hormone receptors and E-cadherin in aggressive subtypes of endometrial carcinomas. J Pathol *220*, 551-561.

Huttelmaier, S., Zenklusen, D., Lederer, M., Dictenberg, J., Lorenz, M., Meng, X., Bassell, G.J., Condeelis, J., and Singer, R.H. (2005). Spatial regulation of beta-actin translation by Src-dependent phosphorylation of ZBP1. Nature *438*, 512-515.

Hwang, J.Y., Mangala, L.S., Fok, J.Y., Lin, Y.G., Merritt, W.M., Spannuth, W.A., Nick, A.M., Fiterman, D.J., Vivas-Mejia, P.E., Deavers, M.T*., et al.* (2008). Clinical and biological significance of tissue transglutaminase in ovarian carcinoma. Cancer Res *68*, 5849-5858.

Ignotz, R.A., and Massague, J. (1986). Transforming growth factor-beta stimulates the expression of fibronectin and collagen and their incorporation into the extracellular matrix. J Biol Chem *261*, 4337-4345.

Inukai, T., Inoue, A., Kurosawa, H., Goi, K., Shinjyo, T., Ozawa, K., Mao, M., Inaba, T., and Look, A.T. (1999). SLUG, a ces-1-related zinc finger transcription factor gene with

antiapoptotic activity, is a downstream target of the E2A-HLF oncoprotein. Mol Cell *4*, 343-352.

Irigoyen, M., Pajares, M.J., Agorreta, J., Ponz-Sarvise, M., Salvo, E., Lozano, M.D., Pio, R., Gil-Bazo, I., and Rouzaut, A. (2010). TGFBI expression is associated with a better response to chemotherapy in NSCLC. Mol Cancer *9*, 130.

Issa, J.P. (2008). Colon cancer: it's CIN or CIMP. Clin Cancer Res *14*, 5939-5940.

Ivaska, J. (2011). Vimentin: Central hub in EMT induction? Small Gtpases *2*, 51-53.

Ivorra, C., Kubicek, M., Gonzalez, J.M., Sanz-Gonzalez, S.M., Alvarez-Barrientos, A., O'Connor, L.E., Burke, B., and Andres, V. (2006). A mechanism of AP-1 suppression through interaction of c-Fos with lamin A/C. Genes Dev *20*, 307-320.

Jansen, M.P., Machiels, B.M., Hopman, A.H., Broers, J.L., Bot, F.J., Arends, J.W., Ramaekers, F.C., and Schouten, H.C. (1997). Comparison of A and B-type lamin expression in reactive lymph nodes and nodular sclerosing Hodgkin's disease. Histopathology *31*, 304-312.

Jass, J.R. (1991). Subsite distribution and incidence of colorectal cancer in New Zealand, 1974-1983. Dis Colon Rectum *34*, 56-59.

Jayne, D.G., Thorpe, H.C., Copeland, J., Quirke, P., Brown, J.M., and Guillou, P.J. (2010). Five-year follow-up of the Medical Research Council CLASICC trial of laparoscopically assisted versus open surgery for colorectal cancer. Br J Surg *97*, 1638-1645.

Jenkins, H., Holman, T., Lyon, C., Lane, B., Stick, R., and Hutchison, C. (1993). Nuclei that lack a lamina accumulate karyophilic proteins and assemble a nuclear matrix. J Cell Sci *106 (Pt 1)*, 275-285.

Jia, D., Yan, M., Wang, X., Hao, X., Liang, L., Liu, L., Kong, H., He, X., Li, J., and Yao, M. (2010). Development of a highly metastatic model that reveals a crucial role of fibronectin in lung cancer cell migration and invasion. BMC Cancer *10*, 364.

Joberty, G., Perlungher, R.R., and Macara, I.G. (1999). The Borgs, a new family of Cdc42 and TC10 GTPase-interacting proteins. Mol Cell Biol *19*, 6585-6597.

Jockusch, B.M., and Isenberg, G. (1981). Interaction of alpha-actinin and vinculin with actin: opposite effects on filament network formation. Proc Natl Acad Sci U S A *78*, 3005-3009.

Jones, R.A., Kotsakis, P., Johnson, T.S., Chau, D.Y., Ali, S., Melino, G., and Griffin, M. (2006). Matrix changes induced by transglutaminase 2 lead to inhibition of angiogenesis and tumor growth. Cell Death Differ *13*, 1442-1453.

Jones, R.A., Nicholas, B., Mian, S., Davies, P.J., and Griffin, M. (1997). Reduced expression of tissue transglutaminase in a human endothelial cell line leads to changes in cell spreading, cell adhesion and reduced polymerisation of fibronectin. J Cell Sci *110 (Pt 19)*, 2461-2472.

Joseph, M.J., Dangi-Garimella, S., Shields, M.A., Diamond, M.E., Sun, L., Koblinski, J.E., and Munshi, H.G. (2009). Slug is a downstream mediator of transforming growth factor-beta1-induced matrix metalloproteinase-9 expression and invasion of oral cancer cells. J Cell Biochem *108*, 726-736.

Jufvas, A., Stralfors, P., and Vener, A.V. (2011). Histone variants and their post-translational modifications in primary human fat cells. PLoS One *6*, e15960.

Katafiasz, D., Smith, L.M., and Wahl, J.K., 3rd (2011). Slug (SNAI2) expression in oral SCC cells results in altered cell-cell adhesion and increased motility. Cell Adh Migr *5*, 315-322.

Kewenter, J., Brevinge, H., Engaras, B., Haglind, E., and Ahren, C. (1994). Results of screening, rescreening, and follow-up in a prospective randomized study for detection of colorectal cancer by fecal occult blood testing. Results for 68,308 subjects. Scand J Gastroenterol *29*, 468-473.

Khatau, S.B., Hale, C.M., Stewart-Hutchinson, P.J., Patel, M.S., Stewart, C.L., Searson, P.C., Hodzic, D., and Wirtz, D. (2009). A perinuclear actin cap regulates nuclear shape. Proc Natl Acad Sci U S A *106*, 19017-19022.

Khatau, S.B., Kim, D.H., Hale, C.M., Bloom, R.J., and Wirtz, D. (2010). The perinuclear actin cap in health and disease. Nucleus *1*, 337-342.

Kikuchi, S., Honda, K., Tsuda, H., Hiraoka, N., Imoto, I., Kosuge, T., Umaki, T., Onozato, K., Shitashige, M., Yamaguchi, U.*, et al.* (2008). Expression and gene amplification of actinin-4 in invasive ductal carcinoma of the pancreas. Clin Cancer Res *14*, 5348-5356.

Kim, K., Lu, Z., and Hay, E.D. (2002). Direct evidence for a role of beta-catenin/LEF-1 signaling pathway in induction of EMT. Cell Biol Int *26*, 463-476.

Kim, M.O., Yun, S.J., Kim, I.S., Sohn, S., and Lee, E.H. (2003). Transforming growth factor-beta-inducible gene-h3 (beta(ig)-h3) promotes cell adhesion of human astrocytoma cells in vitro: implication of alpha6beta4 integrin. Neurosci Lett *336*, 93-96.

Kimura, E., Enns, R.E., Thiebaut, F., and Howell, S.B. (1993). Regulation of HSP60 mRNA expression in a human ovarian carcinoma cell line. Cancer Chemother Pharmacol *32*, 279-285.

Kinzler, K.W., Nilbert, M.C., Su, L.K., Vogelstein, B., Bryan, T.M., Levy, D.B., Smith, K.J., Preisinger, A.C., Hedge, P., McKechnie, D.*, et al.* (1991). Identification of FAP locus genes from chromosome 5q21. Science *253*, 661-665.

Kinzler, K.W., and Vogelstein, B. (1996). Lessons from hereditary colorectal cancer. Cell *87*, 159-170.

Kirchhoff, S.R., Gupta, S., and Knowlton, A.A. (2002). Cytosolic heat shock protein 60, apoptosis, and myocardial injury. Circulation *105*, 2899-2904.

Kirklin, J.W., Dockerty, M.B., and Waugh, J.M. (1949). The role of the peritoneal reflection in the prognosis of carcinoma of the rectum and sigmoid colon. Surg Gynecol Obstet *88*, 326-331.

Kitahara, O., Furukawa, Y., Tanaka, T., Kihara, C., Ono, K., Yanagawa, R., Nita, M.E., Takagi, T., Nakamura, Y., and Tsunoda, T. (2001). Alterations of gene expression during colorectal carcinogenesis revealed by cDNA microarrays after laser-capture microdissection of tumor tissues and normal epithelia. Cancer Res *61*, 3544-3549.

Kitten, G.T., and Nigg, E.A. (1991). The CaaX motif is required for isoprenylation, carboxyl methylation, and nuclear membrane association of lamin B2. The Journal of Cell Biology *113*, 13-23.

Klemke, M., Rafael, M.T., Wabnitz, G.H., Weschenfelder, T., Konstandin, M.H., Garbi, N., Autschbach, F., Hartschuh, W., and Samstag, Y. (2007). Phosphorylation of ectopically

expressed L-plastin enhances invasiveness of human melanoma cells. Int J Cancer *120*, 2590-2599.

Knudson, A.G., Jr. (1971). Mutation and cancer: statistical study of retinoblastoma. Proc Natl Acad Sci U S A *68*, 820-823.

Koch, I., Hofschneider, P.H., Lottspeich, F., Eckerskorn, C., and Koshy, R. (1990). Tumor-Related Expression of a Translation-Elongation Factor-Like Protein. Oncogene *5*, 839-843.

Kojima, S., Nara, K., and Rifkin, D.B. (1993). Requirement for transglutaminase in the activation of latent transforming growth factor-beta in bovine endothelial cells. J Cell Biol *121*, 439-448.

Kolettas, E., Lymboura, M., Khazaie, K., and Luqmani, Y. (1998). Modulation of elongation factor-1 delta (EF-1 delta) expression by oncogenes in human epithelial cells. Anticancer Res *18*, 385-392.

Kronborg, O., Fenger, C., Olsen, J., Jorgensen, O.D., and Sondergaard, O. (1996). Randomised study of screening for colorectal cancer with faecal-occult-blood test. Lancet *348*, 1467-1471.

Kruger, J.S., and Reddy, K.B. (2003). Distinct mechanisms mediate the initial and sustained phases of cell migration in epidermal growth factor receptor-overexpressing cells. Mol Cancer Res *1*, 801-809.

Kumar, A., Xu, J., Brady, S., Gao, H., Yu, D., Reuben, J., and Mehta, K. (2010). Tissue transglutaminase promotes drug resistance and invasion by inducing mesenchymal transition in mammary epithelial cells. PLoS One *5*, e13390.

Kumeta, M., Yoshimura, S.H., Harata, M., and Takeyasu, K. (2010). Molecular mechanisms underlying nucleocytoplasmic shuttling of actinin-4. J Cell Sci *123*, 1020-1030.

Kuwabara, H., Yoneda, M., Hayasaki, H., Nakamura, T., and Mori, H. (2006). Glucose regulated proteins 78 and 75 bind to the receptor for hyaluronan mediated motility in interphase microtubules. Biochem Biophys Res Commun *339*, 971-976.

Laemmli, U.K. (1970). Cleavage of structural proteins during the assembly of the head of bacteriophage T4. Nature *227*, 680-685.

Lammerding, J., Schulze, P.C., Takahashi, T., Kozlov, S., Sullivan, T., Kamm, R.D., Stewart, C.L., and Lee, R.T. (2004). Lamin A/C deficiency causes defective nuclear mechanics and mechanotransduction. J Clin Invest *113*, 370-378.

Lamouille, S., and Derynck, R. (2007). Cell size and invasion in TGF-beta-induced epithelial to mesenchymal transition is regulated by activation of the mTOR pathway. J Cell Biol *178*, 437-451.

Lattanzi, G., Cenni, V., Marmiroli, S., Capanni, C., Mattioli, E., Merlini, L., Squarzoni, S., and Maraldi, N.M. (2003). Association of emerin with nuclear and cytoplasmic actin is regulated in differentiating myoblasts. Biochem Biophys Res Commun *303*, 764-770.

Lazarides, E., and Burridge, K. (1975). Alpha-actinin: immunofluorescent localization of a muscle structural protein in nonmuscle cells. Cell *6*, 289-298.

Lebret, T., Watson, R.W., Molinie, V., O'Neill, A., Gabriel, C., Fitzpatrick, J.M., and Botto, H. (2003). Heat shock proteins HSP27, HSP60, HSP70, and HSP90: expression in bladder carcinoma. Cancer *98*, 970-977.

Lee, J.S., Hale, C.M., Panorchan, P., Khatau, S.B., George, J.P., Tseng, Y., Stewart, C.L., Hodzic, D., and Wirtz, D. (2007). Nuclear lamin A/C deficiency induces defects in cell mechanics, polarization, and migration. Biophys J *93*, 2542-2552.

Lee, K.K., Haraguchi, T., Lee, R.S., Koujin, T., Hiraoka, Y., and Wilson, K.L. (2001). Distinct functional domains in emerin bind lamin A and DNA-bridging protein BAF. J Cell Sci *114*, 4567-4573.

Leibovitz, A., Stinson, J.C., McCombs, W.B., 3rd, McCoy, C.E., Mazur, K.C., and Mabry, N.D. (1976). Classification of human colorectal adenocarcinoma cell lines. Cancer Res *36*, 4562-4569.

Lengauer, C., Kinzler, K.W., and Vogelstein, B. (1997). Genetic instability in colorectal cancers. Nature *386*, 623-627.

Levi, F., Randimbison, L., and La Vecchia, C. (1993). Trends in subsite distribution of colorectal cancers and polyps from the Vaud Cancer Registry. Cancer *72*, 46-50.

Lew, Y., Jones, D.V., Mars, W.M., Evans, D., Byrd, D., and Frazier, M.L. (1992). Expression of elongation factor-1 gamma-related sequence in human pancreatic cancer. Pancreas *7*, 144-152.

Liang, P.S., Chen, T.Y., and Giovannucci, E. (2009). Cigarette smoking and colorectal cancer incidence and mortality: systematic review and meta-analysis. Int J Cancer *124*, 2406-2415.

Libotte, T., Zaim, H., Abraham, S., Padmakumar, V.C., Schneider, M., Lu, W., Munck, M., Hutchison, C., Wehnert, M., Fahrenkrog, B.*, et al.* (2005). Lamin A/C-dependent localization of Nesprin-2, a giant scaffolder at the nuclear envelope. Mol Biol Cell *16*, 3411-3424.

Lim, M.J., and Wang, X.W. (2006). Nucleophosmin and human cancer. Cancer Detect Prev *30*, 481-490.

Lim, S.O., Park, S.J., Kim, W., Park, S.G., Kim, H.J., Kim, Y.I., Sohn, T.S., Noh, J.H., and Jung, G. (2002). Proteome analysis of hepatocellular carcinoma. Biochem Biophys Res Commun *291*, 1031-1037.

Lin, F., Morrison, J.M., Wu, W., and Worman, H.J. (2005). MAN1, an integral protein of the inner nuclear membrane, binds Smad2 and Smad3 and antagonizes transforming growth factor-beta signaling. Hum Mol Genet *14*, 437-445.

Lin, F., and Worman, H.J. (1993). Structural organization of the human gene encoding nuclear lamin A and nuclear lamin C. Journal of Biological Chemistry *268*, 16321-16326.

Lin, F., and Worman, H.J. (1995). Structural Organization of the Human Gene (LMNB1) Encoding Nuclear Lamin B1. Genomics *27*, 230-236.

Lin, K.M., Lin, B., Lian, I.Y., Mestril, R., Scheffler, I.E., and Dillmann, W.H. (2001). Combined and individual mitochondrial HSP60 and HSP10 expression in cardiac myocytes protects mitochondrial function and prevents apoptotic cell deaths induced by simulated ischemia-reoxygenation. Circulation *103*, 1787-1792.

Lipton, L., and Tomlinson, I. (2006). The genetics of FAP and FAP-like syndromes. Fam Cancer *5*, 221-226.

Liu, G., Grant, W.M., Persky, D., Latham, V.M., Jr., Singer, R.H., and Condeelis, J. (2002). Interactions of elongation factor 1alpha with F-actin and beta-actin mRNA: implications for anchoring mRNA in cell protrusions. Mol Biol Cell *13*, 579-592.

Liu, J., Rolef Ben-Shahar, T., Riemer, D., Treinin, M., Spann, P., Weber, K., Fire, A., and Gruenbaum, Y. (2000). Essential roles for Caenorhabditis elegans lamin gene in nuclear organization, cell cycle progression, and spatial organization of nuclear pore complexes. Mol Biol Cell *11*, 3937-3947.

Livak, K.J., and Schmittgen, T.D. (2001). Analysis of relative gene expression data using real-time quantitative PCR and the 2(-Delta Delta C(T)) Method. Methods *25*, 402-408.

Lloyd, D.J., Trembath, R.C., and Shackleton, S. (2002). A novel interaction between lamin A and SREBP1: implications for partial lipodystrophy and other laminopathies. Hum Mol Genet *11*, 769-777.

Lo, H.W., Hsu, S.C., Xia, W., Cao, X., Shih, J.Y., Wei, Y., Abbruzzese, J.L., Hortobagyi, G.N., and Hung, M.C. (2007). Epidermal growth factor receptor cooperates with signal transducer and activator of transcription 3 to induce epithelial-mesenchymal transition in cancer cells via up-regulation of TWIST gene expression. Cancer Res *67*, 9066-9076.

Lobo, M.V., Martin, M.E., Perez, M.I., Alonso, F.J., Redondo, C., Alvarez, M.I., and Salinas, M. (2000). Levels, phosphorylation status and cellular localization of translational factor eIF2 in gastrointestinal carcinomas. Histochem J *32*, 139-150.

Loewinger, L., and McKeon, F. (1988). Mutations in the nuclear lamin proteins resulting in their aberrant assembly in the cytoplasm. EMBO J *7*, 2301-2309.

Lu, Q.Y., Yang, Y., Jin, Y.S., Zhang, Z.F., Heber, D., Li, F.P., Dubinett, S.M., Sondej, M.A., Loo, J.A., and Rao, J.Y. (2009). Effects of green tea extract on lung cancer A549 cells: proteomic identification of proteins associated with cell migration. Proteomics *9*, 757-767.

Lupton, J.R., Steinbach, G., Chang, W.C., O'Brien, B.C., Wiese, S., Stoltzfus, C.L., Glober, G.A., Wargovich, M.J., McPherson, R.S., and Winn, R.J. (1996). Calcium supplementation modifies the relative amounts of bile acids in bile and affects key aspects of human colon physiology. J Nutr *126*, 1421-1428.

Ma, C., Rong, Y., Radiloff, D.R., Datto, M.B., Centeno, B., Bao, S., Cheng, A.W., Lin, F., Jiang, S., Yeatman, T.J*., et al.* (2008). Extracellular matrix protein betaig-h3/TGFBI promotes metastasis of colon cancer by enhancing cell extravasation. Genes Dev *22*, 308-321.

Machiels, B.M., Ramaekers, F.C., Kuijpers, H.J., Groenewoud, J.S., Oosterhuis, J.W., and Looijenga, L.H. (1997). Nuclear lamin expression in normal testis and testicular germ cell tumours of adolescents and adults. J Pathol *182*, 197-204.

Machiels, B.M., Zorenc, A.H.G., Endert, J.M., Kuijpers, H.J.H., van Eys, G.J.J.M., Ramaekers, F.C.S., and Broers, J.L.V. (1996). An Alternative Splicing Product of the Lamin A/C Gene Lacks Exon 10. Journal of Biological Chemistry *271*, 9249-9253.

Maeda, M., Johnson, K.R., and Wheelock, M.J. (2005). Cadherin switching: essential for behavioral but not morphological changes during an epithelium-to-mesenchyme transition. J Cell Sci *118*, 873-887.

Mancini, M.A., Shan, B., Nickerson, J.A., Penman, S., and Lee, W.H. (1994). The retinoblastoma gene product is a cell cycle-dependent, nuclear matrix-associated protein. Proc Natl Acad Sci U S A *91*, 418-422.

Mandel, J.S., Bond, J.H., Church, T.R., Snover, D.C., Bradley, G.M., Schuman, L.M., and Ederer, F. (1993). Reducing mortality from colorectal cancer by screening for fecal occult blood. Minnesota Colon Cancer Control Study. N Engl J Med *328*, 1365-1371.

Mansharamani, M., and Wilson, K.L. (2005). Direct binding of nuclear membrane protein MAN1 to emerin in vitro and two modes of binding to barrier-to-autointegration factor. J Biol Chem *280*, 13863-13870.

Maouche-Chretien, L., Deleu, N., Badoual, C., Fraissignes, P., Berger, R., Gaulard, P., Romeo, P.H., and Leroy-Viard, K. (1998). Identification of a novel cDNA, encoding a cytoskeletal associated protein, differentially expressed in diffuse large B cell lymphomas. Oncogene *17*, 1245-1251.

Markiewicz, E., Dechat, T., Foisner, R., Quinlan, R.A., and Hutchison, C.J. (2002). Lamin A/C binding protein LAP2alpha is required for nuclear anchorage of retinoblastoma protein. Mol Biol Cell *13*, 4401-4413.

Markiewicz, E., Tilgner, K., Barker, N., van de Wetering, M., Clevers, H., Dorobek, M., Hausmanowa-Petrusewicz, I., Ramaekers, F.C., Broers, J.L., Blankesteijn, W.M.*, et al.* (2006). The inner nuclear membrane protein emerin regulates beta-catenin activity by restricting its accumulation in the nucleus. EMBO J *25*, 3275-3285.

Markowitz, S., Wang, J., Myeroff, L., Parsons, R., Sun, L., Lutterbaugh, J., Fan, R.S., Zborowska, E., Kinzler, K.W., Vogelstein, B.*, et al.* (1995). Inactivation of the type II TGF-beta receptor in colon cancer cells with microsatellite instability. Science *268*, 1336-1338.

Markowitz, S.D., and Roberts, A.B. (1996). Tumor suppressor activity of the TGF-beta pathway in human cancers. Cytokine Growth Factor Rev *7*, 93-102.

Mathur, S., Cleary, K.R., Inamdar, N., Kim, Y.H., Steck, P., and Frazier, M.L. (1998). Overexpression of elongation factor-1gamma protein in colorectal carcinoma. Cancer *82*, 816-821.

Mattout, A., Goldberg, M., Tzur, Y., Margalit, A., and Gruenbaum, Y. (2007). Specific and conserved sequences in D. melanogaster and C. elegans lamins and histone H2A mediate the attachment of lamins to chromosomes. J Cell Sci *120*, 77-85.

McDonald, D., Carrero, G., Andrin, C., de Vries, G., and Hendzel, M.J. (2006). Nucleoplasmic beta-actin exists in a dynamic equilibrium between low-mobility polymeric species and rapidly diffusing populations. J Cell Biol *172*, 541-552.

McInroy, L., and Maatta, A. (2007). Down-regulation of vimentin expression inhibits carcinoma cell migration and adhesion. Biochem Biophys Res Commun *360*, 109-114.

McKeon, F.D., Kirschner, M.W., and Caput, D. (1986). Homologies in both primary and secondary structure between nuclear envelope and intermediate filament proteins. Nature *319*, 463-468.

Medici, D., Hay, E.D., and Olsen, B.R. (2008). Snail and Slug promote epithelial-mesenchymal transition through beta-catenin-T-cell factor-4-dependent expression of transforming growth factor-beta3. Mol Biol Cell *19*, 4875-4887.

Meguid, R.A., Slidell, M.B., Wolfgang, C.L., Chang, D.C., and Ahuja, N. (2008). Is there a difference in survival between right- versus left-sided colon cancers? Ann Surg Oncol *15*, 2388-2394.

Mehta, K., Fok, J., Miller, F.R., Koul, D., and Sahin, A.A. (2004). Prognostic significance of tissue transglutaminase in drug resistant and metastatic breast cancer. Clin Cancer Res *10*, 8068-8076.

Mehta, K., Kumar, A., and Kim, H.I. (2010). Transglutaminase 2: a multi-tasking protein in the complex circuitry of inflammation and cancer. Biochem Pharmacol *80*, 1921-1929.

Meng, X.N., Jin, Y., Yu, Y., Bai, J., Liu, G.Y., Zhu, J., Zhao, Y.Z., Wang, Z., Chen, F., Lee, K.Y.*, et al.* (2009). Characterisation of fibronectin-mediated FAK signalling pathways in lung cancer cell migration and invasion. Br J Cancer *101*, 327-334.

Miao, H.Q., Lee, P., Lin, H., Soker, S., and Klagsbrun, M. (2000). Neuropilin-1 expression by tumor cells promotes tumor angiogenesis and progression. FASEB J *14*, 2532-2539.

Midgley, R.S., Yanagisawa, Y., and Kerr, D.J. (2009). Evolution of nonsurgical therapy for colorectal cancer. Nat Clin Pract Gastroenterol Hepatol *6*, 108-120.

Miettinen, P.J., Ebner, R., Lopez, A.R., and Derynck, R. (1994). TGF-beta induced transdifferentiation of mammary epithelial cells to mesenchymal cells: involvement of type I receptors. J Cell Biol *127*, 2021-2036.

Mimori, K., Mori, M., Inoue, H., Ueo, H., Mafune, K., Akiyoshi, T., and Sugimachi, K. (1996). Elongation factor 1 gamma mRNA expression in oesophageal carcinoma. Gut *38*, 66-70.

Mimori, K., Mori, M., Tanaka, S., Akiyoshi, T., and Sugimachi, K. (1995). The overexpression of elongation factor 1 gamma mRNA in gastric carcinoma. Cancer *75*, 1446-1449.

Mislow, J.M., Holaska, J.M., Kim, M.S., Lee, K.K., Segura-Totten, M., Wilson, K.L., and McNally, E.M. (2002). Nesprin-1alpha self-associates and binds directly to emerin and lamin A in vitro. FEBS Lett *525*, 135-140.

Misteli, T. (2007). Beyond the sequence: cellular organization of genome function. Cell *128*, 787-800.

Miyoshi, N., Ishii, H., Mimori, K., Tanaka, F., Hitora, T., Tei, M., Sekimoto, M., Doki, Y., and Mori, M. (2010). TGM2 is a novel marker for prognosis and therapeutic target in colorectal cancer. Ann Surg Oncol *17*, 967-972.

Moir, R.D., Montag-Lowy, M., and Goldman, R.D. (1994). Dynamic properties of nuclear lamins: lamin B is associated with sites of DNA replication. J Cell Biol *125*, 1201-1212.

Molloy, E.L., Adams, A., Moore, J.B., Masterson, J.C., Madrigal-Estebas, L., Mahon, B.P., and O'Dea, S. (2008). BMP4 induces an epithelial-mesenchymal transition-like response in adult airway epithelial cells. Growth Factors *26*, 12-22.

Mori, D., Nakafusa, Y., Miyazaki, K., and Tokunaga, O. (2005). Differential expression of Janus kinase 3 (JAK3), matrix metalloproteinase 13 (MMP13), heat shock protein 60 (HSP60), and mouse double minute 2 (MDM2) in human colorectal cancer progression using human cancer cDNA microarrays. Pathol Res Pract *201*, 777-789.

Moss, S.F., Krivosheyev, V., de Souza, A., Chin, K., Gaetz, H.P., Chaudhary, N., Worman, H.J., and Holt, P.R. (1999). Decreased and aberrant nuclear lamin expression in gastrointestinal tract neoplasms. Gut *45*, 723-729.

Munemitsu, S., Albert, I., Souza, B., Rubinfeld, B., and Polakis, P. (1995). Regulation of intracellular beta-catenin levels by the adenomatous polyposis coli (APC) tumor-suppressor protein. Proc Natl Acad Sci U S A *92*, 3046-3050.

Nagaraja, G.M., Othman, M., Fox, B.P., Alsaber, R., Pellegrino, C.M., Zeng, Y., Khanna, R., Tamburini, P., Swaroop, A., and Kandpal, R.P. (2006). Gene expression signatures and biomarkers of noninvasive and invasive breast cancer cells: comprehensive profiles by representational difference analysis, microarrays and proteomics. Oncogene *25*, 2328-2338.

Nelson, R.L. (2001). Iron and colorectal cancer risk: human studies. Nutr Rev *59*, 140-148.

Nemes, Z., Jr., Adany, R., Balazs, M., Boross, P., and Fesus, L. (1997). Identification of cytoplasmic actin as an abundant glutaminyl substrate for tissue transglutaminase in HL-60 and U937 cells undergoing apoptosis. J Biol Chem *272*, 20577-20583.

Newland, R.C., Chapuis, P.H., Pheils, M.T., and MacPherson, J.G. (1981). The relationship of survival to staging and grading of colorectal carcinoma: a prospective study of 503 cases. Cancer *47*, 1424-1429.

Ngan, C.Y., Yamamoto, H., Seshimo, I., Tsujino, T., Man-i, M., Ikeda, J.I., Konishi, K., Takemasa, I., Ikeda, M., Sekimoto, M.*, et al.* (2007). Quantitative evaluation of vimentin expression in tumour stroma of colorectal cancer. Br J Cancer *96*, 986-992.

Ngo, S.N., Williams, D.B., Cobiac, L., and Head, R.J. (2007). Does garlic reduce risk of colorectal cancer? A systematic review. J Nutr *137*, 2264-2269.

Noel, J.K., Fahrbach, K., Estok, R., Cella, C., Frame, D., Linz, H., Cima, R.R., Dozois, E.J., and Senagore, A.J. (2007). Minimally invasive colorectal resection outcomes: short-term comparison with open procedures. J Am Coll Surg *204*, 291-307.

Norat, T.C., D.; Lau, R.; Aune, D.; Vieira, R. (2010). WCRF/AICR Systematic Literature Review Continuous Update Project Report. The Associations between Food, Nutrition and Physical Activity and the Risk of Colorectal Cancer.

Notterman, D.A., Alon, U., Sierk, A.J., and Levine, A.J. (2001). Transcriptional gene expression profiles of colorectal adenoma, adenocarcinoma, and normal tissue examined by oligonucleotide arrays. Cancer Res *61*, 3124-3130.

Nowak, D., Krawczenko, A., Dus, D., and Malicka-Blaszkiewicz, M. (2002). Actin in human colon adenocarcinoma cells with different metastatic potential. Acta Biochim Pol *49*, 823-828.

O'Brien, C.A., Pollett, A., Gallinger, S., and Dick, J.E. (2007). A human colon cancer cell capable of initiating tumour growth in immunodeficient mice. Nature *445*, 106-110.

O'Byrne, K.J., Dalgleish, A.G., Browning, M.J., Steward, W.P., and Harris, A.L. (2000). The relationship between angiogenesis and the immune response in carcinogenesis and the progression of malignant disease. Eur J Cancer *36*, 151-169.

O'Farrell, P.H. (1975). High resolution two-dimensional electrophoresis of proteins. J Biol Chem *250*, 4007-4021.

Obrand, D.I., and Gordon, P.H. (1998). Continued change in the distribution of colorectal carcinoma. Br J Surg *85*, 246-248.

Ogawa, K., Utsunomiya, T., Mimori, K., Tanaka, Y., Tanaka, F., Inoue, H., Murayama, S., and Mori, M. (2004). Clinical significance of elongation factor-1 delta mRNA expression in oesophageal carcinoma. Br J Cancer *91*, 282-286.

Oguchi, M., Sagara, J., Matsumoto, K., Saida, T., and Taniguchi, S. (2002). Expression of lamins depends on epidermal differentiation and transformation. Br J Dermatol *147*, 853-858.

Okuda, M., Horn, H.F., Tarapore, P., Tokuyama, Y., Smulian, A.G., Chan, P.K., Knudsen, E.S., Hofmann, I.A., Snyder, J.D., Bove, K.E*., et al.* (2000). Nucleophosmin/B23 is a target of CDK2/cyclin E in centrosome duplication. Cell *103*, 127-140.

Onder, T.T., Gupta, P.B., Mani, S.A., Yang, J., Lander, E.S., and Weinberg, R.A. (2008). Loss of E-cadherin promotes metastasis via multiple downstream transcriptional pathways. Cancer Res *68*, 3645-3654.

Ong, S.E., Blagoev, B., Kratchmarova, I., Kristensen, D.B., Steen, H., Pandey, A., and Mann, M. (2002). Stable isotope labeling by amino acids in cell culture, SILAC, as a simple and accurate approach to expression proteomics. Mol Cell Proteomics *1*, 376-386.

Orru, S., Caputo, I., D'Amato, A., Ruoppolo, M., and Esposito, C. (2003). Proteomics identification of acyl-acceptor and acyl-donor substrates for transglutaminase in a human intestinal epithelial cell line. Implications for celiac disease. J Biol Chem *278*, 31766-31773.

Osada, S., Ohmori, S.Y., and Taira, M. (2003). XMAN1, an inner nuclear membrane protein, antagonizes BMP signaling by interacting with Smad1 in Xenopus embryos. Development *130*, 1783-1794.

Ozaki, T., Saijo, M., Murakami, K., Enomoto, H., Taya, Y., and Sakiyama, S. (1994). Complex formation between lamin A and the retinoblastoma gene product: identification of the domain on lamin A required for its interaction. Oncogene *9*, 2649-2653.

Padmakumar, V.C., Abraham, S., Braune, S., Noegel, A.A., Tunggal, B., Karakesisoglou, I., and Korenbaum, E. (2004). Enaptin, a giant actin-binding protein, is an element of the nuclear membrane and the actin cytoskeleton. Exp Cell Res *295*, 330-339.

Padmakumar, V.C., Libotte, T., Lu, W., Zaim, H., Abraham, S., Noegel, A.A., Gotzmann, J., Foisner, R., and Karakesisoglou, I. (2005). The inner nuclear membrane protein Sun1 mediates the anchorage of Nesprin-2 to the nuclear envelope. J Cell Sci *118*, 3419-3430.

Pappas, G.D. (1956). THE FINE STRUCTURE OF THE NUCLEAR ENVELOPE OF AMOEBA PROTEUS. The Journal of Biophysical and Biochemical Cytology *2*, 431-434.

Pappin, D.J., Hojrup, P., and Bleasby, A.J. (1993). Rapid identification of proteins by peptide-mass fingerprinting. Curr Biol *3*, 327-332.

Peckham, M., Miller, G., Wells, C., Zicha, D., and Dunn, G.A. (2001). Specific changes to the mechanism of cell locomotion induced by overexpression of beta-actin. J Cell Sci *114*, 1367-1377.

Pederson, T. (2000). Half a century of "the nuclear matrix". Mol Biol Cell *11*, 799-805.

Pederson, T., and Aebi, U. (2002). Actin in the nucleus: what form and what for? J Struct Biol *140*, 3-9.

Pederson, T., and Aebi, U. (2005). Nuclear actin extends, with no contraction in sight. Mol Biol Cell *16*, 5055-5060.

Peinado, H., Olmeda, D., and Cano, A. (2007). Snail, Zeb and bHLH factors in tumour progression: an alliance against the epithelial phenotype? Nat Rev Cancer *7*, 415-428.

Pendas, A.M., Zhou, Z., Cadinanos, J., Freije, J.M., Wang, J., Hultenby, K., Astudillo, A., Wernerson, A., Rodriguez, F., Tryggvason, K.*, et al.* (2002). Defective prelamin A processing and muscular and adipocyte alterations in Zmpste24 metalloproteinase-deficient mice. Nat Genet *31*, 94-99.

Perl, A.K., Wilgenbus, P., Dahl, U., Semb, H., and Christofori, G. (1998). A causal role for E-cadherin in the transition from adenoma to carcinoma. Nature *392*, 190-193.

Pestic-Dragovich, L., Stojiljkovic, L., Philimonenko, A.A., Nowak, G., Ke, Y., Settlage, R.E., Shabanowitz, J., Hunt, D.F., Hozak, P., and de Lanerolle, P. (2000). A myosin I isoform in the nucleus. Science *290*, 337-341.

Peter, M., Heitlinger, E., Haner, M., Aebi, U., and Nigg, E.A. (1991). Disassembly of in vitro formed lamin head-to-tail polymers by CDC2 kinase. EMBO J *10*, 1535-1544.

Peter, M., Nakagawa, J., Doree, M., Labbe, J.C., and Nigg, E.A. (1990). In vitro disassembly of the nuclear lamina and M phase-specific phosphorylation of lamins by cdc2 kinase. Cell *61*, 591-602.

Piek, E., Moustakas, A., Kurisaki, A., Heldin, C.H., and ten Dijke, P. (1999). TGF-(beta) type I receptor/ALK-5 and Smad proteins mediate epithelial to mesenchymal transdifferentiation in NMuMG breast epithelial cells. J Cell Sci *112 (Pt 24)*, 4557-4568.

Pinto, D., and Clevers, H. (2005). Wnt, stem cells and cancer in the intestine. Biol Cell *97*, 185-196.

Plowman, G.D., Green, J.M., McDonald, V.L., Neubauer, M.G., Disteche, C.M., Todaro, G.J., and Shoyab, M. (1990). The amphiregulin gene encodes a novel epidermal growth factor-related protein with tumor-inhibitory activity. Mol Cell Biol *10*, 1969-1981.

Powell, S.M., Zilz, N., Beazer-Barclay, Y., Bryan, T.M., Hamilton, S.R., Thibodeau, S.N., Vogelstein, B., and Kinzler, K.W. (1992). APC mutations occur early during colorectal tumorigenesis. Nature *359*, 235-237.

Preston, S.L., Wong, W.M., Chan, A.O., Poulsom, R., Jeffery, R., Goodlad, R.A., Mandir, N., Elia, G., Novelli, M., Bodmer, W.F.*, et al.* (2003). Bottom-up histogenesis of colorectal adenomas: origin in the monocryptal adenoma and initial expansion by crypt fission. Cancer Res *63*, 3819-3825.

Providence, K.M., Kutz, S.M., and Higgins, P.J. (1999). Perturbation of the actin cytoskeleton induces PAI-1 gene expression in cultured epithelial cells independent of substrate anchorage. Cell Motil Cytoskeleton *42*, 218-229.

Puszkin, E.G., and Raghuraman, V. (1985). Catalytic properties of a calmodulin-regulated transglutaminase from human platelet and chicken gizzard. J Biol Chem *260*, 16012-16020.

Qiu, J., Gao, H.Q., Liang, Y., Yu, H., and Zhou, R.H. (2008). Comparative proteomics analysis reveals role of heat shock protein 60 in digoxin-induced toxicity in human endothelial cells. Biochim Biophys Acta *1784*, 1857-1864.

Quah, H.M., Chou, J.F., Gonen, M., Shia, J., Schrag, D., Landmann, R.G., Guillem, J.G., Paty, P.B., Temple, L.K., Wong, W.D.*, et al.* (2008). Identification of patients with high-risk stage II colon cancer for adjuvant therapy. Dis Colon Rectum *51*, 503-507.

Ramagli, L.S., and Rodriguez, L.V. (1985). Quantitation of microgram amounts of protein in two-dimensional polyacrylamide gel electrophoresis sample buffer. Electrophoresis *6*, 559-563.

Ran, Q., Wadhwa, R., Kawai, R., Kaul, S.C., Sifers, R.N., Bick, R.J., Smith, J.R., and Pereira-Smith, O.M. (2000). Extramitochondrial localization of mortalin/mthsp70/PBP74/GRP75. Biochem Biophys Res Commun *275*, 174-179.

Rando, O.J., Zhao, K., and Crabtree, G.R. (2000). Searching for a function for nuclear actin. Trends Cell Biol *10*, 92-97.

Raraty, M.G., and Winstanley, J.H. (1998). Variation in the staging of colorectal carcinomas: a survey of current practice. Ann R Coll Surg Engl *80*, 188-191.

Reddy, K.L., Zullo, J.M., Bertolino, E., and Singh, H. (2008). Transcriptional repression mediated by repositioning of genes to the nuclear lamina. Nature *452*, 243-247.

Ribas, M., Masramon, L., Aiza, G., Capella, G., Miro, R., and Peinado, M.A. (2003). The structural nature of chromosomal instability in colon cancer cells. FASEB J *17*, 289-291.

Ridley, A.J., and Hall, A. (1992). The small GTP-binding protein rho regulates the assembly of focal adhesions and actin stress fibers in response to growth factors. Cell *70*, 389-399.

Riis, B., Rattan, S.I., Clark, B.F., and Merrick, W.C. (1990). Eukaryotic protein elongation factors. Trends Biochem Sci *15*, 420-424.

Ritter, S.J., and Davies, P.J. (1998). Identification of a transforming growth factor-beta1/bone morphogenetic protein 4 (TGF-beta1/BMP4) response element within the mouse tissue transglutaminase gene promoter. J Biol Chem *273*, 12798-12806.

Rober, R.A., Weber, K., and Osborn, M. (1989). Differential timing of nuclear lamin A/C expression in the various organs of the mouse embryo and the young animal: a developmental study. Development *105*, 365-378.

Robinson, N.J., Baker, P.N., Jones, C.J., and Aplin, J.D. (2007). A role for tissue transglutaminase in stabilization of membrane-cytoskeletal particles shed from the human placenta. Biol Reprod *77*, 648-657.

Rosenwald, I.B., Pechet, L., Han, A., Lu, L., Pihan, G., Woda, B., Chen, J.J., and Szymanski, I. (2001). Expression of translation initiation factors eIF-4E and eIF-2alpha and a potential physiologic role of continuous protein synthesis in human platelets. Thromb Haemost *85*, 142-151.

Ross, A.F., Oleynikov, Y., Kislauskis, E.H., Taneja, K.L., and Singer, R.H. (1997). Characterization of a beta-actin mRNA zipcode-binding protein. Mol Cell Biol *17*, 2158-2165.

Roux, K.J., Crisp, M.L., Liu, Q., Kim, D., Kozlov, S., Stewart, C.L., and Burke, B. (2009). Nesprin 4 is an outer nuclear membrane protein that can induce kinesin-mediated cell polarization. Proc Natl Acad Sci U S A *106*, 2194-2199.

Rustgi, A.K. (2007). The genetics of hereditary colon cancer. Genes Dev *21*, 2525-2538.

Saini, P., Eyler, D.E., Green, R., and Dever, T.E. (2009). Hypusine-containing protein eIF5A promotes translation elongation. Nature *459*, 118-121.

Salahshor, S., and Woodgett, J.R. (2005). The links between axin and carcinogenesis. J Clin Pathol *58*, 225-236.

Salpingidou, G., Smertenko, A., Hausmanowa-Petrucewicz, I., Hussey, P.J., and Hutchison, C.J. (2007). A novel role for the nuclear membrane protein emerin in association of the centrosome to the outer nuclear membrane. J Cell Biol *178*, 897-904.

Samali, A., Cai, J., Zhivotovsky, B., Jones, D.P., and Orrenius, S. (1999). Presence of a pre-apoptotic complex of pro-caspase-3, Hsp60 and Hsp10 in the mitochondrial fraction of jurkat cells. EMBO J *18*, 2040-2048.

Samarakoon, R., Higgins, C.E., Higgins, S.P., and Higgins, P.J. (2009). TGF-beta1-Induced Expression of the Poor Prognosis SERPINE1/PAI-1 Gene Requires EGFR Signaling: A New Target for Anti-EGFR Therapy. J Oncol *2009*, 342391.

Samarakoon, R., and Higgins, P.J. (2002). MEK/ERK pathway mediates cell-shape-dependent plasminogen activator inhibitor type 1 gene expression upon drug-induced disruption of the microfilament and microtubule networks. J Cell Sci *115*, 3093-3103.

Samuels, Y., Wang, Z., Bardelli, A., Silliman, N., Ptak, J., Szabo, S., Yan, H., Gazdar, A., Powell, S.M., Riggins, G.J.*, et al.* (2004). High frequency of mutations of the PIK3CA gene in human cancers. Science *304*, 554.

Sanchez-Martin, M., Rodriguez-Garcia, A., Perez-Losada, J., Sagrera, A., Read, A.P., and Sanchez-Garcia, I. (2002). SLUG (SNAI2) deletions in patients with Waardenburg disease. Hum Mol Genet *11*, 3231-3236.

Sanchez, C., Padilla, R., Paciucci, R., Zabala, J.C., and Avila, J. (1994). Binding of heat-shock protein 70 (hsp70) to tubulin. Arch Biochem Biophys *310*, 428-432.

Sandsmark, D.K., Zhang, H., Hegedus, B., Pelletier, C.L., Weber, J.D., and Gutmann, D.H. (2007). Nucleophosmin mediates mammalian target of rapamycin-dependent actin cytoskeleton dynamics and proliferation in neurofibromin-deficient astrocytes. Cancer Res *67*, 4790-4799.

Sant, M., Aareleid, T., Berrino, F., Bielska Lasota, M., Carli, P.M., Faivre, J., Grosclaude, P., Hedelin, G., Matsuda, T., Moller, H.*, et al.* (2003). EUROCARE-3: survival of cancer patients diagnosed 1990-94--results and commentary. Ann Oncol *14 Suppl 5*, 61-118.

Sasseville, A.M., and Langelier, Y. (1998). In vitro interaction of the carboxy-terminal domain of lamin A with actin. FEBS Lett *425*, 485-489.

Sato, T., van Es, J.H., Snippert, H.J., Stange, D.E., Vries, R.G., van den Born, M., Barker, N., Shroyer, N.F., van de Wetering, M., and Clevers, H. (2011). Paneth cells constitute the niche for Lgr5 stem cells in intestinal crypts. Nature *469*, 415-418.

Satoh, K., Hamada, S., Kimura, K., Kanno, A., Hirota, M., Umino, J., Fujibuchi, W., Masamune, A., Tanaka, N., Miura, K.*, et al.* (2008). Up-regulation of MSX2 enhances the malignant phenotype and is associated with twist 1 expression in human pancreatic cancer cells. Am J Pathol *172*, 926-939.

Savagner, P., Yamada, K.M., and Thiery, J.P. (1997). The zinc-finger protein slug causes desmosome dissociation, an initial and necessary step for growth factor-induced epithelial-mesenchymal transition. J Cell Biol *137*, 1403-1419.

Scaffidi, P., and Misteli, T. (2005). Reversal of the cellular phenotype in the premature aging disease Hutchinson-Gilford progeria syndrome. Nat Med *11*, 440-445.

Schirmer, E.C., Florens, L., Guan, T., Yates, J.R., and Gerace, L. (2003). Nuclear Membrane Proteins with Potential Disease Links Found by Subtractive Proteomics. Science *301*, 1380-1382.

Schneider, J., Jimenez, E., Marenbach, K., Romero, H., Marx, D., and Meden, H. (1999). Immunohistochemical detection of HSP60-expression in human ovarian cancer. Correlation with survival in a series of 247 patients. Anticancer Res *19*, 2141-2146.

Schneider, M., Lu, W., Neumann, S., Brachner, A., Gotzmann, J., Noegel, A.A., and Karakesisoglou, I. (2011). Molecular mechanisms of centrosome and cytoskeleton anchorage at the nuclear envelope. Cell Mol Life Sci *68*, 1593-1610.

Scholefield, J.H., Moss, S., Sufi, F., Mangham, C.M., and Hardcastle, J.D. (2002). Effect of faecal occult blood screening on mortality from colorectal cancer: results from a randomised controlled trial. Gut *50*, 840-844.

Schroy, P., Rifkin, J., Coffey, R.J., Winawer, S., and Friedman, E. (1990). Role of transforming growth factor beta 1 in induction of colon carcinoma differentiation by hexamethylene bisacetamide. Cancer Res *50*, 261-265.

Schulze, S.R., Curio-Penny, B., Speese, S., Dialynas, G., Cryderman, D.E., McDonough, C.W., Nalbant, D., Petersen, M., Budnik, V., Geyer, P.K.*, et al.* (2009). A comparative study of Drosophila and human A-type lamins. PLoS One *4*, e7564.

Schurer, W., and Kanavos, P. (2010). Colorectal cancer management in the United Kingdom: current practice and challenges. Eur J Health Econ *10 Suppl 1*, S85-90.

Segura-Totten, M., Kowalski, A.K., Craigie, R., and Wilson, K.L. (2002). Barrier-to-autointegration factor: major roles in chromatin decondensation and nuclear assembly. J Cell Biol *158*, 475-485.

Seitz, H.K., and Stickel, F. (2007). Molecular mechanisms of alcohol-mediated carcinogenesis. Nat Rev Cancer *7*, 599-612.

Seki, A., and Fang, G. (2007). CKAP2 is a spindle-associated protein degraded by APC/C-Cdh1 during mitotic exit. J Biol Chem *282*, 15103-15113.

Sen, S., Dong, M., and Kumar, S. (2009). Isoform-specific contributions of alpha-actinin to glioma cell mechanobiology. PLoS One *4*, e8427.

Sengupta, N., Gill, K.A., MacFie, T.S., Lai, C.S., Suraweera, N., McDonald, S., and Silver, A. (2008). Management of colorectal cancer: a role for genetics in prevention and treatment? Pathol Res Pract *204*, 469-477.

Senior, A., and Gerace, L. (1988). Integral membrane proteins specific to the inner nuclear membrane and associated with the nuclear lamina. The Journal of Cell Biology *107*, 2029-2036.

Shankar, J., Messenberg, A., Chan, J., Underhill, T.M., Foster, L.J., and Nabi, I.R. (2010). Pseudopodial actin dynamics control epithelial-mesenchymal transition in metastatic cancer cells. Cancer Res *70*, 3780-3790.

Shao, H., Wang, J.H., Pollak, M.R., and Wells, A. (2010a). alpha-actinin-4 is essential for maintaining the spreading, motility and contractility of fibroblasts. PLoS One *5*, e13921.

Shao, H., Wu, C., and Wells, A. (2010b). Phosphorylation of alpha-actinin 4 upon epidermal growth factor exposure regulates its interaction with actin. J Biol Chem *285*, 2591-2600.

Shao, M., Cao, L., Shen, C., Satpathy, M., Chelladurai, B., Bigsby, R.M., Nakshatri, H., and Matei, D. (2009). Epithelial-to-mesenchymal transition and ovarian tumor progression induced by tissue transglutaminase. Cancer Res *69*, 9192-9201.

Shashidhar, S., Lorente, G., Nagavarapu, U., Nelson, A., Kuo, J., Cummins, J., Nikolich, K., Urfer, R., and Foehr, E.D. (2005). GPR56 is a GPCR that is overexpressed in gliomas and functions in tumor cell adhesion. Oncogene *24*, 1673-1682.

Shen, X., Li, J., Hu, P.P., Waddell, D., Zhang, J., and Wang, X.F. (2001). The activity of guanine exchange factor NET1 is essential for transforming growth factor-beta-mediated stress fiber formation. J Biol Chem *276*, 15362-15368.

Shibata, K., Kikkawa, F., Nawa, A., Suganuma, N., and Hamaguchi, M. (1997). Fibronectin secretion from human peritoneal tissue induces Mr 92,000 type IV collagenase expression and invasion in ovarian cancer cell lines. Cancer Res *57*, 5416-5420.

Shih, I.M., Wang, T.L., Traverso, G., Romans, K., Hamilton, S.R., Ben-Sasson, S., Kinzler, K.W., and Vogelstein, B. (2001). Top-down morphogenesis of colorectal tumors. Proc Natl Acad Sci U S A *98*, 2640-2645.

Shin, D.M., Jeon, J.H., Kim, C.W., Cho, S.Y., Lee, H.J., Jang, G.Y., Jeong, E.M., Lee, D.S., Kang, J.H., Melino, G*., et al.* (2008). TGFbeta mediates activation of transglutaminase 2 in response to oxidative stress that leads to protein aggregation. FASEB J *22*, 2498-2507.

Shuda, M., Kondoh, N., Tanaka, K., Ryo, A., Wakatsuki, T., Hada, A., Goseki, N., Igari, T., Hatsuse, K., Aihara, T*., et al.* (2000). Enhanced expression of translation factor mRNAs in hepatocellular carcinoma. Anticancer Res *20*, 2489-2494.

Shumaker, D.K., Lee, K.K., Tanhehco, Y.C., Craigie, R., and Wilson, K.L. (2001). LAP2 binds to BAF.DNA complexes: requirement for the LEM domain and modulation by variable regions. EMBO J *20*, 1754-1764.

Simon, D.N., Zastrow, M.S., and Wilson, K.L. (2010). Direct actin binding to A- and B-type lamin tails and actin filament bundling by the lamin A tail. Nucleus *1*, 264-272.

Singer, R.H. (1992). The cytoskeleton and mRNA localization. Curr Opin Cell Biol *4*, 15-19.

Singh, B., Soltys, B.J., Wu, Z.C., Patel, H.V., Freeman, K.B., and Gupta, R.S. (1997). Cloning and some novel characteristics of mitochondrial Hsp70 from Chinese hamster cells. Exp Cell Res *234*, 205-216.

Singh, S., Sadacharan, S., Su, S., Belldegrun, A., Persad, S., and Singh, G. (2003a). Overexpression of vimentin: role in the invasive phenotype in an androgen-independent model of prostate cancer. Cancer Res *63*, 2306-2311.

Singh, S.K., Hawkins, C., Clarke, I.D., Squire, J.A., Bayani, J., Hide, T., Henkelman, R.M., Cusimano, M.D., and Dirks, P.B. (2004). Identification of human brain tumour initiating cells. Nature *432*, 396-401.

Singh, U.S., Pan, J., Kao, Y.L., Joshi, S., Young, K.L., and Baker, K.M. (2003b). Tissue transglutaminase mediates activation of RhoA and MAP kinase pathways during retinoic acid-induced neuronal differentiation of SH-SY5Y cells. J Biol Chem *278*, 391-399.

Skonier, J., Neubauer, M., Madisen, L., Bennett, K., Plowman, G.D., and Purchio, A.F. (1992). cDNA cloning and sequence analysis of beta ig-h3, a novel gene induced in a human adenocarcinoma cell line after treatment with transforming growth factor-beta. DNA Cell Biol *11*, 511-522.

Sonenberg, N., and Dever, T.E. (2003). Eukaryotic translation initiation factors and regulators. Curr Opin Struct Biol *13*, 56-63.

Spaderna, S., Schmalhofer, O., Hlubek, F., Berx, G., Eger, A., Merkel, S., Jung, A., Kirchner, T., and Brabletz, T. (2006). A transient, EMT-linked loss of basement membranes indicates metastasis and poor survival in colorectal cancer. Gastroenterology *131*, 830-840.

Spandidos, A., Wang, X., Wang, H., and Seed, B. (2010). PrimerBank: a resource of human and mouse PCR primer pairs for gene expression detection and quantification. Nucleic Acids Res *38*, 792-799.

Sparks, A.B., Morin, P.J., Vogelstein, B., and Kinzler, K.W. (1998). Mutational analysis of the APC/beta-catenin/Tcf pathway in colorectal cancer. Cancer Res *58*, 1130-1134.

Starr, D.A., and Han, M. (2003). ANChors away: an actin based mechanism of nuclear positioning. J Cell Sci *116*, 211-216.

Staubach, S., Razawi, H., and Hanisch, F.G. (2009). Proteomics of MUC1-containing lipid rafts from plasma membranes and exosomes of human breast carcinoma cells MCF-7. Proteomics *9*, 2820-2835.

Stewart-Hutchinson, P.J., Hale, C.M., Wirtz, D., and Hodzic, D. (2008). Structural requirements for the assembly of LINC complexes and their function in cellular mechanical stiffness. Exp Cell Res *314*, 1892-1905.

Stierle, V., Couprie, J., Ostlund, C., Krimm, I., Zinn-Justin, S., Hossenlopp, P., Worman, H.J., Courvalin, J.C., and Duband-Goulet, I. (2003). The carboxyl-terminal region common to lamins A and C contains a DNA binding domain. Biochemistry *42*, 4819-4828.

Strelkov, S.V., Schumacher, J., Burkhard, P., Aebi, U., and Herrmann, H. (2004). Crystal Structure of the Human Lamin A Coil 2B Dimer: Implications for the Head-to-tail Association of Nuclear Lamins. Journal of Molecular Biology *343*, 1067-1080.

Stuurman, N. (1997). Identification of a conserved phosphorylation site modulating nuclear lamin polymerization. FEBS Lett *401*, 171-174.

Stuurman, N., Heins, S., and Aebi, U. (1998). Nuclear lamins: their structure, assembly, and interactions. J Struct Biol *122*, 42-66.

Sugimura, T., Wakabayashi, K., Nakagama, H., and Nagao, M. (2004). Heterocyclic amines: Mutagens/carcinogens produced during cooking of meat and fish. Cancer Sci *95*, 290-299.

Sullivan, T., Escalante-Alcalde, D., Bhatt, H., Anver, M., Bhat, N., Nagashima, K., Stewart, C.L., and Burke, B. (1999). Loss of A-type lamin expression compromises nuclear envelope integrity leading to muscular dystrophy. J Cell Biol *147*, 913-920.

Sun, S., Xu, M.Z., Poon, R.T., Day, P.J., and Luk, J.M. (2010). Circulating Lamin B1 (LMNB1) biomarker detects early stages of liver cancer in patients. J Proteome Res *9*, 70-78.

Tan, Y., Sangfelt, O., and Spruck, C. (2008). The Fbxw7/hCdc4 tumor suppressor in human cancer. Cancer Lett *271*, 1-12.

Taniura, H., Glass, C., and Gerace, L. (1995). A chromatin binding site in the tail domain of nuclear lamins that interacts with core histones. J Cell Biol *131*, 33-44.

Taylor, C.A., Sun, Z., Cliche, D.O., Ming, H., Eshaque, B., Jin, S., Hopkins, M.T., Thai, B., and Thompson, J.E. (2007). Eukaryotic translation initiation factor 5A induces apoptosis in colon cancer cells and associates with the nucleus in response to tumour necrosis factor alpha signalling. Exp Cell Res *313*, 437-449.

Tejpar, S. (2007). The multidisciplinary management of gastrointestinal cancer. The use of molecular markers in the diagnosis and treatment of colorectal cancer. Best Pract Res Clin Gastroenterol *21*, 1071-1087.

Telci, D., Collighan, R.J., Basaga, H., and Griffin, M. (2009). Increased TG2 expression can result in induction of transforming growth factor beta1, causing increased synthesis and deposition of matrix proteins, which can be regulated by nitric oxide. J Biol Chem *284*, 29547-29558.

Thapa, N., Lee, B.H., and Kim, I.S. (2007). TGFBIp/betaig-h3 protein: a versatile matrix molecule induced by TGF-beta. Int J Biochem Cell Biol *39*, 2183-2194.

Thomas, S.M., Coppelli, F.M., Wells, A., Gooding, W.E., Song, J., Kassis, J., Drenning, S.D., and Grandis, J.R. (2003). Epidermal growth factor receptor-stimulated activation of phospholipase Cgamma-1 promotes invasion of head and neck squamous cell carcinoma. Cancer Res *63*, 5629-5635.

Thomas, X., Campos, L., Mounier, C., Cornillon, J., Flandrin, P., Le, Q.H., Piselli, S., and Guyotat, D. (2005). Expression of heat-shock proteins is associated with major adverse prognostic factors in acute myeloid leukemia. Leuk Res *29*, 1049-1058.

Tian, M., Neil, J.R., and Schiemann, W.P. (2011). Transforming growth factor-beta and the hallmarks of cancer. Cell Signal *23*, 951-962.

Tilli, C.M., Ramaekers, F.C., Broers, J.L., Hutchison, C.J., and Neumann, H.A. (2003). Lamin expression in normal human skin, actinic keratosis, squamous cell carcinoma and basal cell carcinoma. Br J Dermatol *148*, 102-109.

Tokuyama, Y., Horn, H.F., Kawamura, K., Tarapore, P., and Fukasawa, K. (2001). Specific phosphorylation of nucleophosmin on Thr(199) by cyclin-dependent kinase 2-cyclin E and its role in centrosome duplication. J Biol Chem *276*, 21529-21537.

Towler, B., Irwig, L., Glasziou, P., Kewenter, J., Weller, D., and Silagy, C. (1998). A systematic review of the effects of screening for colorectal cancer using the faecal occult blood test, hemoccult. BMJ *317*, 559-565.

Toyoda, H., Komurasaki, T., Uchida, D., Takayama, Y., Isobe, T., Okuyama, T., and Hanada, K. (1995). Epiregulin. A novel epidermal growth factor with mitogenic activity for rat primary hepatocytes. J Biol Chem *270*, 7495-7500.

Toyota, M. (1999). CpG island methylator phenotype in colorectal cancer. Proc Natl Acad Sci USA *96*, 8681-8686.

Trevisan, M., Liu, J., Muti, P., Misciagna, G., Menotti, A., and Fucci, F. (2001). Markers of insulin resistance and colorectal cancer mortality. Cancer Epidemiol Biomarkers Prev *10*, 937-941.

Turnbull, R.B., Kyle, K., Watson, F.R., and Spratt, J. (1967). Cancer of Colon - Influence of No-Touch Isolation Technic on Survival Rates. Annals of Surgery *166*, 420-427.

Uchikado, Y., Okumura, H., Ishigami, S., Setoyama, T., Matsumoto, M., Owaki, T., Kita, Y., and Natsugoe, S. (2011). Increased Slug and decreased E-cadherin expression is related to poor prognosis in patients with gastric cancer. Gastric Cancer *14*, 41-49.

Unlu, M., Morgan, M.E., and Minden, J.S. (1997). Difference gel electrophoresis: a single gel method for detecting changes in protein extracts. Electrophoresis *18*, 2071-2077.

Van Berlo, J.H., Voncken, J.W., Kubben, N., Broers, J.L., Duisters, R., van Leeuwen, R.E., Crijns, H.J., Ramaekers, F.C., Hutchison, C.J., and Pinto, Y.M. (2005). A-type lamins are essential for TGF-beta1 induced PP2A to dephosphorylate transcription factors. Hum Mol Genet *14*, 2839-2849.

van de Wetering, M., Sancho, E., Verweij, C., de Lau, W., Oving, I., Hurlstone, A., van der Horn, K., Batlle, E., Coudreuse, D., Haramis, A.-P*., et al.* (2002). The [beta]-Catenin/TCF-4 Complex Imposes a Crypt Progenitor Phenotype on Colorectal Cancer Cells. Cell *111*, 241-250.

Vandekerckhove, J., and Weber, K. (1978). At least six different actins are expressed in a higher mammal: an analysis based on the amino acid sequence of the amino-terminal tryptic peptide. J Mol Biol *126*, 783-802.

VanGuilder, H.D., Vrana, K.E., and Freeman, W.M. (2008). Twenty-five years of quantitative PCR for gene expression analysis. Biotechniques *44*, 619-626.

Varedi, M., Ghahary, A., Scott, P.G., and Tredget, E.E. (1997). Cytoskeleton regulates expression of genes for transforming growth factor-beta 1 and extracellular matrix proteins in dermal fibroblasts. J Cell Physiol *172*, 192-199.

Vaughan, A., Alvarez-Reyes, M., Bridger, J.M., Broers, J.L., Ramaekers, F.C., Wehnert, M., Morris, G.E., Whitfield, W.G.F., and Hutchison, C.J. (2001). Both emerin and lamin C depend on lamin A for localization at the nuclear envelope. J Cell Sci *114*, 2577-2590.

Venables, R.S., McLean, S., Luny, D., Moteleb, E., Morley, S., Quinlan, R.A., Lane, E.B., and Hutchison, C.J. (2001). Expression of individual lamins in basal cell carcinomas of the skin. Br J Cancer *84*, 512-519.

Verbeek, B.S., Adriaansen-Slot, S.S., Vroom, T.M., Beckers, T., and Rijksen, G. (1998). Overexpression of EGFR and c-erbB2 causes enhanced cell migration in human breast cancer cells and NIH3T3 fibroblasts. FEBS Lett *425*, 145-150.

Verdecchia, A., Francisci, S., Brenner, H., Gatta, G., Micheli, A., Mangone, L., and Kunkler, I. (2007). Recent cancer survival in Europe: a 2000-02 period analysis of EUROCARE-4 data. Lancet Oncol *8*, 784-796.

Verderio, E., Gaudry, C., Gross, S., Smith, C., Downes, S., and Griffin, M. (1999). Regulation of cell surface tissue transglutaminase: effects on matrix storage of latent transforming growth factor-beta binding protein-1. J Histochem Cytochem *47*, 1417-1432.

Verderio, E.A., Johnson, T., and Griffin, M. (2004). Tissue transglutaminase in normal and abnormal wound healing: review article. Amino Acids *26*, 387-404.

Verma, A., Guha, S., Diagaradjane, P., Kunnumakkara, A.B., Sanguino, A.M., Lopez-Berestein, G., Sood, A.K., Aggarwal, B.B., Krishnan, S., Gelovani, J.G*., et al.* (2008). Therapeutic significance of elevated tissue transglutaminase expression in pancreatic cancer. Clin Cancer Res *14*, 2476-2483.

Verma, A., Wang, H., Manavathi, B., Fok, J.Y., Mann, A.P., Kumar, R., and Mehta, K. (2006). Increased expression of tissue transglutaminase in pancreatic ductal adenocarcinoma and its implications in drug resistance and metastasis. Cancer Res *66*, 10525-10533.

Vetter, G., Le Bechec, A., Muller, J., Muller, A., Moes, M., Yatskou, M., Al Tanoury, Z., Poch, O., Vallar, L., and Friederich, E. (2009). Time-resolved analysis of transcriptional events during SNAI1-triggered epithelial to mesenchymal transition. Biochem Biophys Res Commun *385*, 485-491.

Vogelstein, B., Fearon, E.R., Hamilton, S.R., Kern, S.E., Preisinger, A.C., Leppert, M., Nakamura, Y., White, R., Smits, A.M., and Bos, J.L. (1988). Genetic alterations during colorectal-tumor development. N Engl J Med *319*, 525-532.

Vorburger, K., Kitten, G.T., and Nigg, E.A. (1989). Modification of nuclear lamin proteins by a mevalonic acid derivative occurs in reticulocyte lysates and requires the cysteine residue of the C-terminal CXXM motif. EMBO J *8*, 4007-4013.

Wada, A., Fukuda, M., Mishima, M., and Nishida, E. (1998). Nuclear export of actin: a novel mechanism regulating the subcellular localization of a major cytoskeletal protein. EMBO J *17*, 1635-1641.

Wadhwa, R., Takano, S., Kaur, K., Deocaris, C.C., Pereira-Smith, O.M., Reddel, R.R., and Kaul, S.C. (2006). Upregulation of mortalin/mthsp70/Grp75 contributes to human carcinogenesis. Int J Cancer *118*, 2973-2980.

Wakefield, L.M., and Roberts, A.B. (2002). TGF-beta signaling: positive and negative effects on tumorigenesis. Curr Opin Genet Dev *12*, 22-29.

Wang, G., Gao, X., Huang, Y., Yao, Z., Shi, Q., and Wu, M. (2010). Nucleophosmin/B23 inhibits Eg5-mediated microtubule depolymerization by inactivating its ATPase activity. J Biol Chem *285*, 19060-19067.

Wang, M., Munier, F., Araki-Saski, K., and Schorderet, D. (2002). TGFBI gene transcript is transforming growth factor-beta1-responsive and cell density-dependent in a human corneal epithelial cell line. Ophthalmic Genet *23*, 237-245.

Wang, S., Lloyd, R.V., Hutzler, M.J., Rosenwald, I.B., Safran, M.S., Patwardhan, N.A., and Khan, A. (2001). Expression of eukaryotic translation initiation factors 4E and 2alpha correlates with the progression of thyroid carcinoma. Thyroid *11*, 1101-1107.

Wang, S., Rosenwald, I.B., Hutzler, M.J., Pihan, G.A., Savas, L., Chen, J.J., and Woda, B.A. (1999). Expression of the eukaryotic translation initiation factors 4E and 2alpha in non-Hodgkin's lymphomas. Am J Pathol *155*, 247-255.

Wang, W., Goswami, S., Lapidus, K., Wells, A.L., Wyckoff, J.B., Sahai, E., Singer, R.H., Segall, J.E., and Condeelis, J.S. (2004). Identification and testing of a gene expression signature of invasive carcinoma cells within primary mammary tumors. Cancer Res *64*, 8585-8594.

Wang, X., and Seed, B. (2003). A PCR primer bank for quantitative gene expression analysis. Nucleic Acids Res *31*, e154.

Ward, G.E., and Kirschner, M.W. (1990). Identification of cell cycle-regulated phosphorylation sites on nuclear lamin C. Cell *61*, 561-577.

Watanabe, M., Nishida, O., Kunii, Y., Kodaira, S., Takahashi, T., Tominaga, T., Hojyo, K., Kato, T., Niimoto, M., Kunitomo, K*., et al.* (2004). Randomized controlled trial of the efficacy of adjuvant immunochemotherapy and adjuvant chemotherapy for colorectal cancer, using different combinations of the intracutaneous streptococcal preparation OK-432 and the oral pyrimidines 1-hexylcarbamoyl-5-fluorouracil and uracil/tegafur. Int J Clin Oncol *9*, 98-106.

WCRF/AICR (2007). World Cancer Research Fund/ American Institute for Cancer Research. Food, Nutrition, Physical Activity and the Prevention of Cancer: a Global Perspective.

WCRF/AICR (2011). World Cancer Research Fund/ American Institute for Cancer Research. Continuous Update Project Interim Report Summary. Food, Nutrition, Physical Activity, and the Prevention of Colorectal Cancer.

Webster, M., Witkin, K.L., and Cohen-Fix, O. (2009). Sizing up the nucleus: nuclear shape, size and nuclear-envelope assembly. J Cell Sci *122*, 1477-1486.

Weitz, J., Koch, M., Debus, J., Hohler, T., Galle, P.R., and Buchler, M.W. (2005). Colorectal cancer. Lancet *365*, 153-165.

Wheeler, M.A., Davies, J.D., Zhang, Q., Emerson, L.J., Hunt, J., Shanahan, C.M., and Ellis, J.A. (2007). Distinct functional domains in nesprin-1alpha and nesprin-2beta bind directly to emerin and both interactions are disrupted in X-linked Emery-Dreifuss muscular dystrophy. Exp Cell Res *313*, 2845-2857.

Whitfield, J.F., Bird, R.P., Chakravarthy, B.R., Isaacs, R.J., and Morley, P. (1995). Calcium-cell cycle regulator, differentiator, killer, chemopreventor, and maybe, tumor promoter. J Cell Biochem Suppl *22*, 74-91.

Wilhelmsen, K., Litjens, S.H., Kuikman, I., Tshimbalanga, N., Janssen, H., van den Bout, I., Raymond, K., and Sonnenberg, A. (2005). Nesprin-3, a novel outer nuclear membrane protein, associates with the cytoskeletal linker protein plectin. J Cell Biol *171*, 799-810.

Williams, N.E., and Nelsen, E.M. (1997). HSP70 and HSP90 homologs are associated with tubulin in hetero-oligomeric complexes, cilia and the cortex of Tetrahymena. J Cell Sci *110 (Pt 14)*, 1665-1672.

Willis, N.D., Cox, T.R., Rahman-Casans, S.F., Smits, K., Przyborski, S.A., van den Brandt, P., van Engeland, M., Weijenberg, M., Wilson, R.G., de Bruine, A*., et al.* (2008). Lamin A/C is a risk biomarker in colorectal cancer. PLoS ONE *3*, e2988.

Wood, L.D., Parsons, D.W., Jones, S., Lin, J., Sjoblom, T., Leary, R.J., Shen, D., Boca, S.M., Barber, T., Ptak, J*., et al.* (2007). The genomic landscapes of human breast and colorectal cancers. Science *318*, 1108-1113.

Worman, H.J. (2006). Inner nuclear membrane and regulation of Smad-mediated signaling. Biochim Biophys Acta *1761*, 626-631.

Wu, Z., Irizarry, R., Gentleman, R., Murillo, F., and Spencer, F. (2003). A Model Based Background Adjustment for Oligonucleotide Expression Arrays. Technical Report, John Hopkins University, Department of Biostatistics Working Papers, Baltimore, MD

Wu, Z., Wu, L., Weng, D., Xu, D., Geng, J., and Zhao, F. (2009a). Reduced expression of lamin A/C correlates with poor histological differentiation and prognosis in primary gastric carcinoma. J Exp Clin Cancer Res *28*, 8.

Wu, Z.R., Wu, L.R., Weng, D.S., Xu, D.Z., Geng, J., and Zhao, F. (2009b). Reduced expression of lamin A/C correlates with poor histological differentiation and prognosis in primary gastric carcinoma. J Exp Clin Cancer Res *28*, 12.

Xanthoudakis, S., Roy, S., Rasper, D., Hennessey, T., Aubin, Y., Cassady, R., Tawa, P., Ruel, R., Rosen, A., and Nicholson, D.W. (1999). Hsp60 accelerates the maturation of pro-caspase-3 by upstream activator proteases during apoptosis. EMBO J *18*, 2049-2056.

Xie, L., Law, B.K., Aakre, M.E., Edgerton, M., Shyr, Y., Bhowmick, N.A., and Moses, H.L. (2003). Transforming growth factor beta-regulated gene expression in a mouse mammary gland epithelial cell line. Breast Cancer Res *5*, 187-198.

Xu, J., Lamouille, S., and Derynck, R. (2009). TGF-beta-induced epithelial to mesenchymal transition. Cell Res *19*, 156-172.

Yamamoto, S., Tsuda, H., Honda, K., Kita, T., Takano, M., Tamai, S., Inazawa, J., Yamada, T., and Matsubara, O. (2007). Actinin-4 expression in ovarian cancer: a novel prognostic indicator independent of clinical stage and histological type. Mod Pathol *20*, 1278-1285.

Yamamoto, S., Tsuda, H., Honda, K., Onozato, K., Takano, M., Tamai, S., Imoto, I., Inazawa, J., Yamada, T., and Matsubara, O. (2009). Actinin-4 gene amplification in ovarian cancer: a candidate oncogene associated with poor patient prognosis and tumor chemoresistance. Mod Pathol *22*, 499-507.

Yang, F., Demma, M., Warren, V., Dharmawardhane, S., and Condeelis, J. (1990). Identification of an actin-binding protein from Dictyostelium as elongation factor 1a. Nature *347*, 494-496.

Yang, L., Guan, T., and Gerace, L. (1997). Lamin-binding fragment of LAP2 inhibits increase in nuclear volume during the cell cycle and progression into S phase. J Cell Biol *139*, 1077-1087.

Yi, H., Li, X.H., Yi, B., Zheng, J., Zhu, G., Li, C., Li, M.Y., Zhang, P.F., Li, J.L., Chen, Z.C*., et al.* (2010). Identification of Rack1, EF-Tu and Rhodanese as aging-related proteins in human colonic epithelium by proteomic analysis. J Proteome Res *9*, 1416-1423.

Yilmaz, M., and Christofori, G. (2009). EMT, the cytoskeleton, and cancer cell invasion. Cancer Metastasis Rev *28*, 15-33.

Young, K.G., and Kothary, R. (2005). Spectrin repeat proteins in the nucleus. Bioessays *27*, 144-152.

Zajchowski, D.A., Bartholdi, M.F., Gong, Y., Webster, L., Liu, H.L., Munishkin, A., Beauheim, C., Harvey, S., Ethier, S.P., and Johnson, P.H. (2001). Identification of gene expression profiles that predict the aggressive behavior of breast cancer cells. Cancer Res *61*, 5168-5178.

Zavadil, J., Bitzer, M., Liang, D., Yang, Y.C., Massimi, A., Kneitz, S., Piek, E., and Bottinger, E.P. (2001). Genetic programs of epithelial cell plasticity directed by transforming growth factor-beta. Proc Natl Acad Sci U S A *98*, 6686-6691.

Zavadil, J., and Bottinger, E.P. (2005). TGF-beta and epithelial-to-mesenchymal transitions. Oncogene *24*, 5764-5774.

Zhai, Z.H., Nickerson, J.A., Krochmalnic, G., and Penman, S. (1987). Alterations in nuclear matrix structure after adenovirus infection. J Virol *61*, 1007-1018.

Zhang, J., Cao, W., Xu, Q., and Chen, W.T. (2011). The expression of EMP1 is downregulated in oral squamous cell carcinoma and possibly associated with tumour metastasis. J Clin Pathol *64*, 25-29.

Zhang, Y., Wen, G., Shao, G., Wang, C., Lin, C., Fang, H., Balajee, A.S., Bhagat, G., Hei, T.K., and Zhao, Y. (2009). TGFBI deficiency predisposes mice to spontaneous tumor development. Cancer Res *69*, 37-44.

Zhao, Y., El-Gabry, M., and Hei, T.K. (2006). Loss of Betaig-h3 protein is frequent in primary lung carcinoma and related to tumorigenic phenotype in lung cancer cells. Mol Carcinog *45*, 84-92.

Zhao, Y.L., Piao, C.Q., and Hei, T.K. (2002). Downregulation of Betaig-h3 gene is causally linked to tumorigenic phenotype in asbestos treated immortalized human bronchial epithelial cells. Oncogene *21*, 7471-7477.

Zhen, Y.Y., Libotte, T., Munck, M., Noegel, A.A., and Korenbaum, E. (2002). NUANCE, a giant protein connecting the nucleus and actin cytoskeleton. J Cell Sci *115*, 3207-3222.

Zheng, R., Ghirlando, R., Lee, M.S., Mizuuchi, K., Krause, M., and Craigie, R. (2000). Barrier-to-autointegration factor (BAF) bridges DNA in a discrete, higher-order nucleoprotein complex. Proc Natl Acad Sci U S A *97*, 8997-9002.

Zlobec, I., and Lugli, A. (2008). Prognostic and predictive factors in colorectal cancer. J Clin Pathol *61*, 561-569.